ANALYSIS AND CONTROL OF NON-AFFINE, NON-STANDARD, SINGULARLY PERTURBED SYSTEMS

A Dissertation

by

ANSHU NARANG

Submitted to the Office of Graduate Studies of
Texas A&M University
in partial fulfillment of the requirements for the degree of

DOCTOR OF PHILOSOPHY

Approved by:

Chair of Committee,	John Valasek
Committee Members,	Aniruddha Datta
	Helen L. Reed
	Srinivas Rao Vadali
Department Head,	Rodney D. W. Bowersox

December 2012

Major Subject: Aerospace Engineering

ABSTRACT

This dissertation addresses the control problem for the general class of control non-affine, non-standard singularly perturbed continuous-time systems. The problem of control for nonlinear multiple time scale systems is addressed here for the first time in a systematic manner. Toward this end, this dissertation develops the theory of feedback passivation for non-affine systems. This is done by generalizing the Kalman-Yakubovich-Popov lemma for non-affine systems. This generalization is used to identify conditions under which non-affine systems can be rendered passive. Asymptotic stabilization for non-affine systems is guaranteed by using these conditions along with well known passivity-based control methods. Unlike previous non-affine control approaches, the constructive static compensation technique derived here does not make any assumptions regarding the control influence on the nonlinear dynamical model. Along with these control laws, this dissertation presents novel hierarchical control design procedures to address the two major difficulties in control of multiple time scale systems: lack of an explicit small parameter that models the time scale separation and the complexity of constructing the slow manifold. These research issues are addressed by using insights from geometric singular perturbation theory and control laws are designed without making any assumptions regarding the construction of the slow manifold. The control schemes synthesized accomplish asymptotic slow state tracking for multiple time scale systems and simultaneous slow and fast state trajectory tracking for two time scale systems. The control laws are independent of the scalar perturbation parameter and an upper bound for it is determined such that closed-loop system stability is guaranteed.

Performance of these methods is validated in simulation for several problems

from science and engineering including the continuously stirred tank reactor, magnetic levitation, six degrees-of-freedom F-18/A Hornet model, non-minimum phase helicopter and conventional take-off and landing aircraft models. Results show that the proposed technique applies both to standard and non-standard forms of singularly perturbed systems and provides asymptotic tracking irrespective of the reference trajectory. This dissertation also shows that some benchmark non-minimum phase aerospace control problems can be posed as slow state tracking for multiple time scale systems and techniques developed here provide an alternate method for exact output tracking.

To dearest Ma, Papa, Amma and Appa

and my closest friend and husband, Siddarth

ACKNOWLEDGEMENTS

I am very grateful to my advisor Dr. John Valasek for his constant motivation, support and guidance during my doctorate study. Working with him I have had the opportunity to learn and experience the different aspects of academia that have helped shape my future career aspirations. I am indebted to Dr. Valasek for nominating me as an associate member of the AIAA Guidance, Navigation and Control Technical Committee. Thank you Sir.

A special thank you to Dr. Srinivas R. Vadali, Dr. Aniruddha Datta and Dr. Helen L. Reed for their critical reviews, feedbacks, and suggestions to improve the quality of my research work.

I would like to thank Dr. Suman Chakravorty for sharing his time and expertise through numerous group meetings and classroom discussions, and Dr. James D. Turner for sharing his insights during our discussions in the hallways. I would also like to thank Dr. John E. Hurtado for providing me a firm foundation in dynamical systems theory and giving me the opportunity to work in Land, Air and Space Robotics Laboratory.

I am thankful to my undergraduate advisor and mentor, Dr. S. N Saxena for his constant support in all my endeavors and motivating me to perform to the best of my capabilities.

My sincere thanks to Ms. Wanda Romero, Ms. Karen Knabe and Ms. Colleen Leatherman for going out of their way to help me throughout my graduate study.

I would like to thank the Zonta International Foundation for awarding me the Amelia Earhart Fellowship which was very helpful during my graduate study.

I am fortunate to have the friendship and support of Priyanka, Ryan and Neha

who have made life in College Station memorable. I cherish our long chats filled with crazy humor and serious discussions about everything under the sun.

It would have been impossible to come this far without the unconditional love and unwavering support of my family. My parents have always been my inspiration and without their motivation I would not have been able to work this far from home. I feel extremely fortunate to have parents whose love has made me what I am today. I am very grateful to Amma and Appa who have supported me and believed in me. No words can describe the influence Siddarth's love and constant words of motivation have had in my life. He has inspired me to excel and stood by me through both good and challenging times. I thank my sister Suruchi, Navin Jijaji, dearest Smridula and Pulkit for their continuous support and love. I feel blessed to be part of such a wonderful family and dedicate this work to them.

TABLE OF CONTENTS

LIST OF FIGURES

FIGURE Page

LIST OF TABLES

TABLE Page

1. INTRODUCTION

Feedback control is an integral part of most modern industrial processes and technological systems. Some of these applications are intrinsically unstable and hence their safe operation depends directly on control design. The design process usually involves defining desired specifications and requirements, mathematical modeling of the physical system, synthesizing a control law, analyzing the designed controller and evaluating the overall system performance. Among these the most fundamental task of the control engineer is to judiciously select control laws to achieve an acceptable performance and desired stability characteristics.

It is apparent that the complexity of the resultant controller and the selection process itself depend on the underlying description of the system being studied. It is for this reason that control design and analysis of systems with linear dynamics is well developed [1],[2]. Control law selection for linear systems is sequential in nature. It begins with appropriate gain selection whose effect on the system is analyzed using time-domain and/or frequency-domain techniques. Sometimes this is followed by a compensator design to meet the desired performance specifications. The above mentioned steps maybe repeated a few times to accomplish the desired stability properties.

On the contrary, design and analysis of feedback control for systems with non-linear dynamics is coupled. The control engineer selects a controller from available synthesis methods and proceeds to derive the specific form of the control law. This design is then analyzed using Lyapunov based methods, Jacobian linearization and/or numerical simulation. Often analysis concludes that the selected controller does not guarantee system stability and the engineer needs to adopt other control techniques

or use a combination of available methods. Once the control engineer is satisfied with a particular technique, acceptable domain of operation is determined through iterations. The limited number of available control approaches for addressing the nonlinearities in the system add to the demanding nature of this iterative process. *This restriction stems from the fact that unlike linear systems, no specific form of controller can be used to address all the different nonlinearities encountered in a system.* As a consequence nonlinear control theory for linear-in-control or control-affine systems has been extensively developed [3],[4] and the control of general nonlinear systems is an open research problem.

This dissertation considers the core problem of developing stabilizing controllers for *control non-affine* continuous-time systems and explores applications in science and engineering, especially physical systems that are singularly perturbed and exhibit multiple time scale behaviour. The motion of these dynamical systems is sometimes characterized by a small parameter multiplying the highest derivative. For example, in DC motors the small inductance acts as the perturbation parameter. In biochemical models the small "parasitic" parameter is the small quantity of an enzyme, in nuclear reactor models it is the fast neutrons and in most engineering systems the time constants of actuators characterize the small parameter. However, in some systems this parameter is not evident and is a function of several physical quantities. For example, in aerospace applications this small quantity varies with flight condition and does not multiply the highest derivative. Such dynamic equations are called *non-standard singularly perturbed systems* and are the focus of this research.

The presence of this small parameter is the cause of stiffness and higher order of dynamic equations. The system states whose velocity is associated with the small perturbation parameter evolve several times faster than the other system states. This causes the motion of the physical system to evolve on multiple time scales. Thus,

not all system states of a singularly perturbed system respond to the input signal at an equal rate. Unless this difference in response rates has been explicitly addressed during control synthesis, the magnitude of the corrective action from the controller will continue to increase. Consequently, this leads the system into saturation which is undesirable and sometimes dangerous.

This dissertation investigates feedback control methodologies and develops rigorous techniques to address the stabilization problem for control non-affine, non-standard singularly perturbed systems. Toward this end several fundamental research questions are addressed. The theory of *feedback passivation* is developed for constructing globally stabilizing static compensation control laws for non-affine-in-control systems. These control laws, along with insights from geometric singular perturbation theory [5], are employed to obtain a hierarchical design procedure to address the following two important control objectives for non-standard singularly perturbed systems.

1. The first control objective is to track a desired slow state reference trajectory while ensuring all the other system signals remain bounded.

2. The second objective requires simultaneous control of the slow and fast states of the system, as required by aerospace applications.

It is expected that the real-time implementable methods developed in this work will permeate numerous applications in control of nonlinear dynamics and multiple-time scale systems, several examples of which are described below.

- *Magnetic Levitation (Maglev) Systems*: An immediate application of non-affine-in-control system stabilization is the maglev system. Magnetic Levitation is a new form of transportation that suspends, guides and propels the vehicle

using electromagnets. The strength and the polarity of the electromagnetic field required to levitate a vehicle depends quadratically on the electric current. Since maglev does not have problems of friction, abrasion or lubrication, it is ideal to use in special environments such as wafer transportation, photo lithography, teleoperation, to lift test models in a wind tunnel and magnetic bearings. The Maglev train first introduced in Japan was shown to be 6 km/h (3.7 mph) faster than the conventional wheel-rail speed record. Maglev technologies are also being considered by NASAs Marshall Space Flight Center in Huntsville, Ala. to levitate and accelerate launch vehicles along a track at high speeds before it leaves the ground to reduce the spacecraft's weight at lift-off.

- *Control of Non-minimum Phase Systems*: Nonlinear control techniques such as feedback linearization and sliding mode control guarantee closed-loop stability and precise output tracking only for a specific class of nonlinear systems that are minimum phase and have outputs with a well-defined relative degree. But there are a number of important flight control problems such as acceleration control of tail-controlled missiles, control of planar Vertical Take-off and Landing (V/STOL) aircraft, Conventional Take-off and Landing (CTOL) aircraft and hover control of helicopter models that are characterized by unstable zero dynamics, thereby not satisfying the conditions listed above. The author of this work has shown that inherent multiple time scale behaviour is the cause of instability for a class of non-minimum phase systems and the problem can be equivalently converted into *stabilization problem of non-standard singularly perturbed system with non-affine controls* [6],[7].

- *Propulsion-Controlled Aircraft*: Research for throttle-only control was pioneered by NASA Dryden in order to provide an alternative method of con-

trol for aircraft that have lost their primary controls due to accident/wear and tear/malfunction. Propulsion-based control can be applied to any aircraft with two or more engines. It works on the principle that differential thrust creates a resultant yawing motion. Also, if the wing has a dihedral then this side force creates a net rolling moment. Past studies have used fault-tolerant schemes to determine the desired thrust profiles. However, compared to primary flight control surfaces the engines have slow response times. The Integrated Resilient Aircraft Control (IRAC) project of NASA Aviation safety relaxed the structural limits on fan speed and engine pressure ratio in emergency conditions to improve responsiveness and provide excess thrust. However, the over-thrust operation is potentially much more detrimental to engine life than fast response operation. The control technique proposed in Section 6 of this dissertation explicitly considers systems with slow actuators and is a potential candidate for propulsion-controlled aircraft.

- *Morphing Air Vehicles*: A stabilization controller designed for non-affine systems would find application for reconfigurable air-vehicles being considered for surveillance and multiple-mission performance. Recent fifth-generation fighters demonstrate some of these reconfigurable capabilities in the form of variable sweep, foldable wing tip sections, wing flaps, retractable landing gear and tail hooks. However, it is well known that linear control methods fail to apply to the flight regimes in which these air vehicles operate. Additionally, their dynamic behaviour is dominated by nonlinear phenomena that is a function of the vehicle states and control inputs and it also evolves at different response rates.

Besides the areas mentioned above, several important problems in science depend

nonlinearly on the control variable, e.g. concentration and temperature stabilization of continuously stirred reactors using coolant flow rate and circadian rhythm in the chemistry of eyes modeled as a van der pol oscillator [8]. The work in this dissertation primarily deals with the control problems of magnetic levitation, stabilization of continuously stirred reactor, non-minimum phase systems and highly nonlinear aircraft and helicopter models.

The remainder of this section is organized as follows. Formal definitions of standard and non-standard forms of singularly perturbed systems is presented in Section 1.1. Section 1.2 reviews the control approaches developed for standard singularly perturbed systems in the past. This section details the research issues associated with the control of non-standard singularly perturbed systems and specifies how it is related to control of general non-affine systems. Section 1.3 presents in detail the history of research in the field of control non-affine systems and identifies the open research issues.

1.1 Standard and Non-Standard Forms of Singularly Perturbed Systems

This dissertation considers a class of singularly perturbed systems that are modeled as ordinary differential equations with a small parameter, ϵ multiplying the derivatives of some of the states

$$\dot{\mathbf{x}} = \mathbf{f}(t, \mathbf{x}, \mathbf{z}, \mathbf{u}, \epsilon) \tag{1.1a}$$

$$\epsilon\dot{\mathbf{z}} = \mathbf{g}(t, \mathbf{x}, \mathbf{z}, \mathbf{u}, \epsilon) \tag{1.1b}$$

where $\mathbf{x} \in \mathbb{R}^m$ is the vector of slow variables, $\mathbf{z} \in \mathbb{R}^n$ is the vector of fast variables, $\mathbf{u} \in \mathbb{R}^p$ is the input vector and $\epsilon \in \mathbb{R}^+$ is the singular perturbation parameter that

satisfies $0 < \epsilon << 1$. The vector fields are assumed to be continuously differentiable. The presence of the singular perturbation parameter ϵ causes multiple time scale behaviour as the velocity $\dot{\mathbf{z}}$ evolves at $O(1/\epsilon)$. This behaviour forces the states $\mathbf{z}$ to evolve *faster* than the states $\mathbf{x}$ for a stable closed-loop system. Notice that in the limit $\epsilon \to 0$ the dimension of (1.1) reduces from $n + m$ to m because the resulting system becomes the differential-algebraic system

$$\dot{\mathbf{x}} = \mathbf{f}(t, \mathbf{x}, \mathbf{z}, \mathbf{u}, 0) \tag{1.2a}$$

$$\mathbf{0} = \mathbf{g}(t, \mathbf{x}, \mathbf{z}, \mathbf{u}, 0). \tag{1.2b}$$

The system (1.1) is in *standard form* if the algebraic equation of (1.2) has isolated real roots for the fast states in the domain of interest. This assumption results in a well-defined reduced-order model and (1.2) is called the *reduced-order slow system*.

The differential equation of the reduced-order slow system captures the dynamics of the slow states. In order to capture the transient response of the fast states, the full-order system is written in a different time scale $\tau = \frac{t-t_0}{\epsilon}$, also known as the fast time scale. Then in the limit $\epsilon \to 0$ the following *reduced-order fast system*

$$\mathbf{x}' = \mathbf{0} \tag{1.3a}$$

$$\mathbf{z}' = \mathbf{g}(t, \mathbf{x}, \mathbf{z}, \mathbf{u}, 0) \tag{1.3b}$$

captures the behaviour of the fast states. Notice that the fixed points of the reduced-order fast system are the isolated roots of the transcendental equations of the reduced-order slow system.

In general, *a dynamic model of any system obtained using Hamilton's principle or Newton's laws of motion is not in standard form*. There have been some techniques

in the literature that help to convert systems into standard forms [9][Ch 1, Sec 1.6] but it still remains an open problem and system dependent technique. In such cases, knowledge about the physical process is used and the small parameter is artificially introduced in front of the derivatives of the states that are known to respond fast. Formally, this process is called the forced-singular perturbation technique [10]. The dynamic model thus obtained violates the isolated root assumption and is in *non-standard* form.

1.2 Review of Stabilization Methods for Singularly Perturbed Systems

Feedback control design for standard singularly perturbed systems has received a lot of attention in the past [11],[12], [13],[14]. Most of these techniques were inspired by the solution forms obtained for open-loop full-order singularly perturbed systems [15]. It has been shown that the complete system behaviour can be approximated by the dynamics of the reduced-order slow system provided the reduced-order fast system is uniformly asymptotically stable about its isolated fixed point. This powerful result not only removes the numerical stiffness but also reduces the dimensionality of the resulting system. Figure 1.1 illustrates these results for an example two-dimensional system $\dot{x} = -x - z$; $\epsilon\dot{z} = -z$. Notice that the reduced-order slow system (broken lines) approximates the dominant solution of the complete system (solid lines), while the initial transient is captured by the reduced-order fast system (dotted lines).

Based on these analysis results, the typical control approach is to design two separate controllers for each of the two reduced-order systems and then apply their composite or sum to the full-order system. The stabilizing controller for the reduced-order slow system is designed first, assuming that the fast states have settled down onto the isolated roots. Next, the controller for the reduced-order fast system is

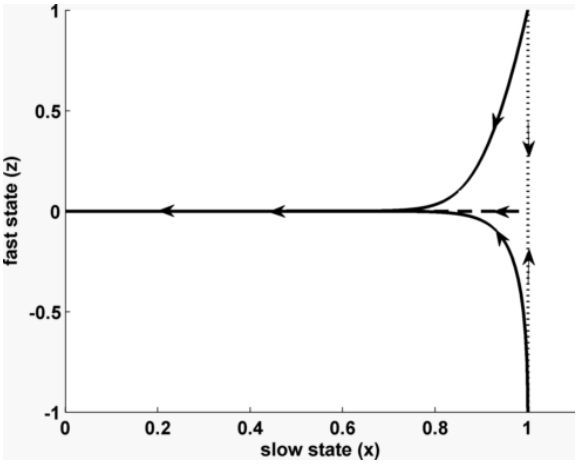

Figure 1.1: Trajectories of two-dimensional singularly perturbed system (solid lines) compared with reduced-order slow system (broken lines) and reduced-order fast system (dotted lines)

designed to ensure that this assumption holds. This two-stage approach was initiated by Suzuki and Miura [16] for linear time-invariant systems and since then has been extensively used for robust and optimal stabilization [17],[18] of linear singularly perturbed systems. This technique takes advantage of the fact that the reduced-order systems are represented as ordinary differential equations and stabilizers can be designed for each of these systems using any desired state-feedback control design technique. An example of sliding-mode control for linear systems was demonstrated by Heck [19]. The composite control technique proposed by Saberi and Khalil [20] extended the two-stage procedure for general class of singularly perturbed systems that are nonlinear in both the states and the control inputs. This approach uses Lyapunov-based control design and asymptotic stability is guaranteed for standard singularly perturbed systems.

The two-stage design procedure described above is applicable only to standard singularly perturbed systems. To enforce the isolated real root condition, previous studies in the literature have either

1. assumed that the system has a unique real root[21],[22] or

2. considered nonlinear systems that have unique roots. This condition is satisfied by multiple time scale systems that are nonlinear in the slow states and linear in the fast states [23],[24].

However, for general nonlinear systems the isolated roots of the algebraic equation are a set of fixed points of the fast dynamics and hence not always unique nor guaranteed to exist. Clearly, the existence of multiple roots hinders the decomposition of general nonlinear singularly perturbed systems into reduced-order slow and fast systems. A natural open problem is

Open Problem 1: *Assume the singularly perturbed system given in (1.1) is in non-standard form. Can reduced-order models be employed for stabilizing the system and/or asymptotically tracking a desired slow state?*

Khalil [25] proposed two techniques for linear non-standard singularly perturbed systems. In the first approach the control input was represented as a sum of linear fast state feedback and a translation vector. The feedback gain was chosen to transform the system into standard form. The translation vector acts as the control input for this resulting system, and the composite control technique is employed for stabilization. In the second approach, the standard form was obtained using a similarity transformation.

However, for nonlinear systems such as aircraft such a transformation is difficult to find. Thus an approximate approach that guarantees local bounded stability has been proposed. Menon [10] designed nonlinear flight test trajectories for velocity, angle-of-attack, sideslip angle and altitude by using the fast angular rates as the control variables while assuming the control surface deflections do not affect the slow states. This work was extended to over actuated systems by Snell [26] and

more recently employed to design longitudinal wind shear flight control laws [27]. However, studies [7],[28] show that the force contribution from the control surfaces in a helicopter is significant and cannot be neglected. Apart from these local results, there have been a few attempts in literature for optimal control [29] of non-standard systems but the feedback stabilization problem of non-standard singularly perturbed systems has not been considered.

All of the approaches discussed above demonstrate stabilization or slow state tracking either locally or globally by restricting the fast states. But for systems whose dynamics inherently possess different time scales, both the slow and the fast states constitute the output vector. For example, during air combat maneuvering an aircraft is typically required to track a fast moving target while regulating speed (slow variable) and/or one or more kinematic and aerodynamic angles. Such cases motivate following research question:

Open Problem 2: *Assume the singularly perturbed system given in (1.1) is in non-standard form. Can the reduced-order models be employed for simultaneous tracking of both the slow and the fast states of the system?*

It is clear that for simultaneous tracking, the fast states cannot be restricted to simply stabilize onto an isolated root. The reduced-order approach therefore appears to be inadequate for a general class of output tracking problem. Artstein [30] formulated optimal control laws to accomplish fast state tracking using invariant measures and the method of averaging for systems with oscillatory fast dynamics. Hastrudi-Zaad and Khorasani[31] used the integral manifold approach and the composite control technique to accomplish output tracking of linear singularly perturbed systems. The isolated root of the fast states and the control for the reduced-order slow system was approximated using straight-forward expansion, and the zero-order control and other correcting terms were computed to ensure the reduced-order slow

system output remains close to the desired output. Gliemlo [32] developed sufficient conditions for the general output feedback problem of standard singularly perturbed systems with exponentially stable fast dynamics, but the output feedback problem of non-standard singularly perturbed systems remains an open research problem. In this dissertation, a class of output tracking of non-standard singularly perturbed systems where both the slow and fast state constitute the output vector is considered. The objective is to employ reduced-order models and state-feedback control laws to accomplish asymptotic output tracking.

1.3 Review of Control Methodologies for Non-Affine in Control Nonlinear Systems

Two-stage design procedures for singularly perturbed system described in Section 1.2 reduce the control problem to stabilization of general nonlinear systems, the analysis of which has inspired researchers for decades. Early in the 1960s Balakrishnan [33] proved that any controllable nonlinear system could be transformed into the following *affine* form

$$\dot{\mathbf{x}} = \mathbf{f}(\mathbf{x}, \mathbf{u}) \equiv \mathbf{f}_1(\mathbf{x}) + \mathbf{f}_2(\mathbf{x})\mathbf{u}, \tag{1.4}$$

where $\mathbf{x} \in \mathbb{R}^n$ represents the state vector and $\mathbf{u} \in \mathbb{R}^m$ is the control input vector. This result inspired the plethora of nonlinear control techniques that we know today such as feedback linearization, gain-scheduling, sliding-mode control, backstepping and more recently forwarding. However, it is difficult to find a change of coordinates that leads to the linear form given in (1.4). Moreover if such a transformation exists, the resultant set of coordinates may be abstract mathematical quantities and/or lead to discontinuous vector fields and is not desirable from a control stand point.

The significant issue is that the notion of controllability is not well-defined for

general nonlinear systems. The notion of weak controllability is defined through the accessibility rank condition which tests whether a system can be driven locally in any arbitrary direction from a given state. If a system satisfies the accessibility rank condition then it is concluded that system has non-empty reachable and controllable sets. A fundamental result in [3][Ch.4, Sec4.3] shows that the accessibility rank condition reduces to the Kalman controllability condition for linear systems.

Although in theory the existence of a control can be tested by computing the accessibility of the system, in practice this computation is affected by the 'curse of dimensionality' [34][Ch.6, Sec.6.3]. Thus, in general the existence of continuous feedback laws in the nonlinear affine case are shown through existence of Lyapunov functions [3][Theorem 17]. This result was extended by Artstein [35] for continuous time-invariant non-affine systems of the form (1.4). It was proven that a stabilizable control exists if and only if the Lyapunov function $V(\mathbf{x})$ satisfies

$$\inf_{\mathbf{u}} \nabla V(\mathbf{x})\mathbf{f}(\mathbf{x},\mathbf{u}) < 0. \tag{1.5}$$

The intuitive idea behind this condition is that there exists some sort of 'energy' measure of the states that diminishes along suitably chosen paths and the control input is chosen to force the system to approach a minimal-energy configuration. This condition is a special case of the Hamilton-Jacobi-Bellman equation [34][Ch.6, Sec.6.3] with time-invariant objective function. It is well-known that this partial differential equation may not always have a solution. Moreover, if a solution exists, it may not be unique. This was discussed in Artstein's work and he suggested that non-affine systems in general cannot be stabilized with continuous feedback. Motivated by Artstein's conclusions, Jayawardhana [36] used pulse-width modulated control signals to stabilize non-interacting mechanical systems.

The fact that discontinuous control cannot be employed for most physical systems has motivated several researchers to explore other feedback solution methods for non-affine systems. Moulay [37] augmented convexity requirement on the argument of (1.5) to provide sufficiency conditions for existence of continuous stabilizing controls. Since the proof was non-constructive, a restricted class of single-input second and third order polynomial systems was studied. Assuming that a Lyapunov function exists, the control input was solved using analytic root solving techniques. Given $\dot{\mathbf{x}} = \mathbf{f}_0(\mathbf{x}) + \mathbf{f}_1(\mathbf{x})u + \mathbf{f}_2(\mathbf{x})u^2$ and Lyapunov function $V(\mathbf{x})$, the control input was solved such that

$$\dot{V}(\mathbf{x}) = \nabla V(\mathbf{x}) \left[\mathbf{f}_0(\mathbf{x}) + \mathbf{f}_1(\mathbf{x})u + \mathbf{f}_2(\mathbf{x})u^2\right] < 0. \tag{1.6}$$

The restrictions on analytical solutions for polynomial systems of degree four and higher hindered the extension of this approach for general non-affine systems.

Lin [38],[39] explored passivity-based methods for smooth open-loop Lyapunov stable non-affine systems. The central idea in this approach was to take advantage of smoothness and represent the nonlinear vector field as a linear combination of affine and non-affine parts

$$\dot{\mathbf{x}} = \mathbf{f}(\mathbf{x}, \mathbf{u}) \equiv \mathbf{f}_0(\mathbf{x}) + \mathbf{g}(\mathbf{x})\mathbf{u} + \mathbf{R}(\mathbf{x}, \mathbf{u}). \tag{1.7}$$

Upon doing so the controller was designed by assuming that the affine part dominates the closed-loop system stability and the higher-order terms are always upper-bounded for all admissible states and control inputs. Although the technique was demonstrated for several examples, Lin's results were restricted to a class of open-loop stable systems.

The control design methods discussed so far provide constructive forms for the control variable. But in order to consider higher-order unstable systems, several approximation and numerical methods have been explored. The intuitive idea has been to indirectly stabilize the system by varying the control derivative. In order to do so the non-affine problem given in (1.4) is augmented with control input dynamics such that the resulting dynamics

$$\dot{\mathbf{x}} = \mathbf{f}(\mathbf{x}, \mathbf{u}) \tag{1.8a}$$

$$\tau \dot{\mathbf{u}} = \boldsymbol{\nu} \tag{1.8b}$$

becomes *affine* in the input vector $\boldsymbol{\nu}$. The time-constant τ is appropriately chosen such that the control input dynamics evolves faster than the dynamical system under consideration. Howakimyan [40] designed the new input vector using dynamic inversion. The technique was motivated by the observation that for a single-state single-input system the following input vector

$$\nu = -\operatorname{sgn}\left(\frac{\partial f}{\partial u}\right)(f(x,u) + ax); \quad a > 0, \quad \frac{\partial f}{\partial u} > 0 \tag{1.9}$$

globally asymptotically stabilizes the system as it replaces the original nonlinear system dynamics with a linear stable form. Extension to the multi-input case was made by minimizing the objective function $J(x, u, u^*) = \frac{1}{2}||f(x,u) - \underbrace{f(x,u^*)}_{desired}||^2$ online using gradient-descent algorithm [40],[41]

$$\boldsymbol{\nu} = \nabla_u J(x, u, u^*). \tag{1.10}$$

This technique assumes that the control influence remains non-singular and a mini-

mum always exists. But as discussed earlier this assumption is quite restrictive and not satisfied in general. Similar assumptions were also made in [42],[43]. Instead of online minimization the control was approximated through radial basis functions to enforce desired state dynamics. Furthermore, Bošković [44] assumed that the vector field is smooth and the control influence is non-singular such that

$$\boldsymbol{\nu} = \frac{1}{\frac{\partial f}{\partial u}} \left(-\frac{\partial f}{\partial x} f(x,u) + f(x,u^*) \right) \tag{1.11}$$

can be employed to achieve desired stabilization.

The non-constructive approaches discussed above have been restricted to a class of systems that are monotonic in control and have non-singular control influence for all the states. This restriction is not met in general. Consider

$$\dot{x} = x - 2xu^4 \tag{1.12}$$

as an example of such a system. Observe that $u = 1$ globally stabilizes the origin. However, this system cannot be controlled using either the general dynamic inversion [45] or modeling error compensation [46] technique since the $\frac{\partial f}{\partial u} = -8xu^3$ is zero at the origin. Motivated by Sontag's [47] universal formula for affine systems one is lead to the natural question

Open Problem 3: *Assume that a control Lyapunov function exists for the dynamic system given in (1.4). Can a constructive control law be formulated to stabilize an unstable non-affine system?*

For unstable systems, an intuitive approach for controlling systems of the form given in (1.4) is to employ feedback equivalence. But soon, one encounters a highly nonlinear algebraic equation whose solution determines the explicit control law. Ad-

ditional difficulties arise as multiple solutions to this equation exist and some of which are not feasible for a physical system. For example, one way of stabilizing $\dot{x} = x - u^2$ is through $u = \sqrt{(a+1)x}$, $a > 0$. Notice that the control takes on imaginary values and is undefined whenever $x < 0$. Some work in the direction of switching controllers has been investigated [48],[49]. A hierarchical switching strategy was designed to switch between local controllers to guide the system through a map of fixed points to finally approach origin in finite time. This map of fixed points and the corresponding stabilizing local controllers are determined offline resulting in a system specific design.

This dissertation addresses the three major open problems discussed in Section 1.2 and Section 1.3. The theoretical developments are supported by stability proofs and applications to several engineering problems are illustrated. Furthermore, it is shown that the synthesized controllers alleviate the restrictions of stable internal dynamics for various under-actuated aerospace applications. The remainder of this dissertation is organized as follows. Section 2 presents the formal statement of problems considered in this dissertation, followed by a discussion of challenging research issues surrounding these problems. Section 3 addresses the control problem for non-affine systems by extending the general feedback passivation approach. This section introduces the necessary concepts of passivity, develops a generalization of the important Kalman-Yakubovich-Popov lemma and derives sufficiency conditions for stabilizing an unstable non-affine system by static compensation. The developments are proven using Lyapunov's direct method and verified in simulation. Section 4 and Section 5 address the open problems 1 and 2 discussed in Section 1.2 for affine non-standard two time scale systems respectively. These sections are linked with Appendix A and Appendix B which review important concepts of singular perturbation theory and composite Lyapunov function approach for stability. Rigorous proofs along with

application to an F-18 high angle-of-attack aircraft model and discussion of benefits and limitations of the developed techniques is presented. Section 6 presents the main result of this dissertation and combines methods developed in Section 3 and Section 4 to stabilize non-affine non-standard multiple time scale system. Application of this novel technique to class of non-minimum phase aerospace systems is detailed in Section 7. Finally conclusions and future recommendations are discussed in Section 8.

2. RESEARCH OBJECTIVES

2.1 System Class Description

The objective of this research is to address *Open Problems 1-3* identified in Section 1 with specific emphasis on stabilization of continuous-time non-standard nonlinear singularly perturbed dynamical systems represented by the following ordinary differential equations:

$$\mathscr{S}: \begin{cases} \dot{\mathbf{x}} = \mathbf{f}(\mathbf{x}, \mathbf{z}, \boldsymbol{\delta}); \quad \mathbf{x}(0) = \mathbf{x}_0 \\ \epsilon \dot{\boldsymbol{\delta}}_{\boldsymbol{\epsilon}} = \mathbf{f}_{\delta_\epsilon}(\boldsymbol{\delta}_\epsilon, \mathbf{u}_\epsilon, \epsilon); \quad \boldsymbol{\delta}_\epsilon(0) = \boldsymbol{\delta}_{\epsilon_0} \\ \mu \dot{\mathbf{z}} = \mathbf{g}(\mathbf{x}, \mathbf{z}, \boldsymbol{\delta}, \mu); \quad \mathbf{z}(0) = \mathbf{z}_0 \\ \varrho \dot{\boldsymbol{\delta}}_\varrho = \mathbf{f}_{\delta\varrho}(\boldsymbol{\delta}_\varrho, \mathbf{u}_\varrho, \varrho); \quad \boldsymbol{\delta}_\varrho(0) = \boldsymbol{\delta}_{\varrho_0}. \end{cases} \tag{2.1}$$

In (2.1) $\mathbf{x} \in \mathbb{R}^m$ is the vector of slow variables, $\mathbf{z} \in \mathbb{R}^n$ is the vector of fast variables, $\boldsymbol{\delta} = [\boldsymbol{\delta}_\epsilon, \boldsymbol{\delta}_\varrho]^T \in \mathbb{R}^p$ is the vector of actuator commands with $\boldsymbol{\delta}_\epsilon \in \mathbb{R}^l$ and $\boldsymbol{\delta}_\varrho \in \mathbb{R}^{p-l}$, $\mathbf{u} = [\mathbf{u}_\epsilon, \mathbf{u}_\varrho]^T \in \mathbb{R}^p$ is the input vector to be computed with $\mathbf{u}_\epsilon \in \mathbb{R}^l$ and $\mathbf{u}_\varrho \in \mathbb{R}^{p-l}$. The singular perturbation parameters $\epsilon \in \mathbb{R}$, $\mu \in \mathbb{R}$ and $\varrho \in \mathbb{R}$ measure the time scale separation explicitly and are unknown. All the vector fields are assumed to be sufficiently smooth.

The dynamical model $\mathscr{S}$ given in (2.1) also characterizes the following class of systems with multiple perturbation parameters:

$$\mathscr{S}: \begin{cases} \dot{\mathbf{x}} = \mathbf{f}(\mathbf{x}, \mathbf{z}, \boldsymbol{\delta}) \\ \epsilon_i \dot{\delta}_{\epsilon_i} = f_{\delta_{\epsilon_i}}(\delta_{\epsilon_i}, u_{\epsilon_i}, \epsilon_i); & \forall i = \{1, 2 \cdots, l\} \\ \mu_j \dot{z}_j = g(\mathbf{x}, \mathbf{z}, \boldsymbol{\delta}, \mu_j); & \forall j = \{1, 2, \cdots, n\} \\ \varrho_k \dot{\delta}_{\varrho_k} = f_{\delta_{\varrho_k}}(\delta_{\varrho_k}, u_{\varrho_k}, \varrho_k); & \forall k = \{1, \cdots, p-l\}, \end{cases} \tag{2.2}$$

where all ϵ_i, μ_j and ϱ_k are of same-order, separately. In (2.1) the state variables corresponding to these parameters have been collectively represented as a vector. For example, all the slow actuator states δ_{ϵ_i} have been combined in the vector $\boldsymbol{\delta}_\epsilon$ with a common perturbation parameter ϵ. One of the several ways to define this parameter is $\epsilon = (\epsilon_1\epsilon_2, \ldots \epsilon_l)^{\frac{1}{l}}$[50]. The crucial assumption is that the singular perturbation parameters are of different order and satisfy:

Assumption 2.1. $\frac{\mu}{\epsilon} \to 0$ *and* $\frac{\varrho}{\epsilon} \to 0$ *as* $\epsilon \to 0$. *Further* $\frac{\varrho}{\mu} \to 0$ *as* $\mu \to 0$. *Thus system in (2.1) is a four time scale, multiple parameter system.*

2.1.1 System Properties

The following observations regarding the model under study are made:

1. The actuator states have been separated into vectors $\boldsymbol{\delta}_\epsilon$ and $\boldsymbol{\delta}_\varrho$ to acknowledge their difference in speeds of evolution. In (2.1) $\boldsymbol{\delta}_\epsilon$ represents the actuators with slow dynamics and $\boldsymbol{\delta}_\varrho$ represents the actuators with relatively fast actuator dynamics. The corresponding vector fields $\boldsymbol{f}_{\boldsymbol{\delta}_\epsilon}(.)$ and $\boldsymbol{f}_{\boldsymbol{\delta}_\varrho}(.)$ model their dynamics respectively. This representation explicitly models systems such as propulsion-controlled aircraft where actuation introduces an additional time scale.

2. The dynamical system under study models several aerospace structures such as reusable launch vehicles, high angle-of-attack missiles and tail-less aircraft (see [13] for details). Here the control surface deflections constitute the fast controllers, while the thrust and/or torque respond at a relatively slow rate. Singular perturbation parameters for these vehicles are not accurately known. In this work forced singular perturbation technique is employed to relatively identify the rate of evolution of the states by non-dimensionalization, follow-

ing which the singular perturbation parameter is included artificially at the modeling stage. Common examples of this approach are seen in [10],[51].

3. It is assumed that the solutions of the fast dynamics converge either forward or backward in time uniformly in the slow states. This restriction is imposed due to the underlying singular perturbation methods employed in this research. Appendix A presents a review of these methods and the reader is strongly encouraged to go through the discussed concepts. Singularly perturbed systems with oscillatory fast states exhibiting limit cycle or chaotic behaviour are not analyzed in this work. Analysis of these class of systems can be found in [30],[52].

2.2 Objectives and Scope

This dissertation addresses the stabilization problem of dynamical systems described in Section 2.1. This is carried out by posing four fundamental control problems in nonlinear control theory. Each of these problems have been posed in a way such that the solution strategies and stability properties not only support the motive of this dissertation (described in Problem 4), but also are complete in their own right. Referring to Figure 2.1, the following four research objectives are addressed:

1. ***Stabilization of Unstable, Non-affine, Nonlinear Systems***

   Consider the core problem of developing stabilizing controllers for non-affine systems of the following form:

$$\Sigma : \begin{array}{c} \dot{x}_1 = f_1(\mathbf{x}) \\ \dot{x}_2 = f_2(\mathbf{x}) \\ \vdots \\ \dot{x}_n = f_n(\mathbf{x}, u) \end{array} \qquad \text{or } \Sigma = \bar{\mathbf{f}}(\mathbf{x}, u) \tag{2.3}$$

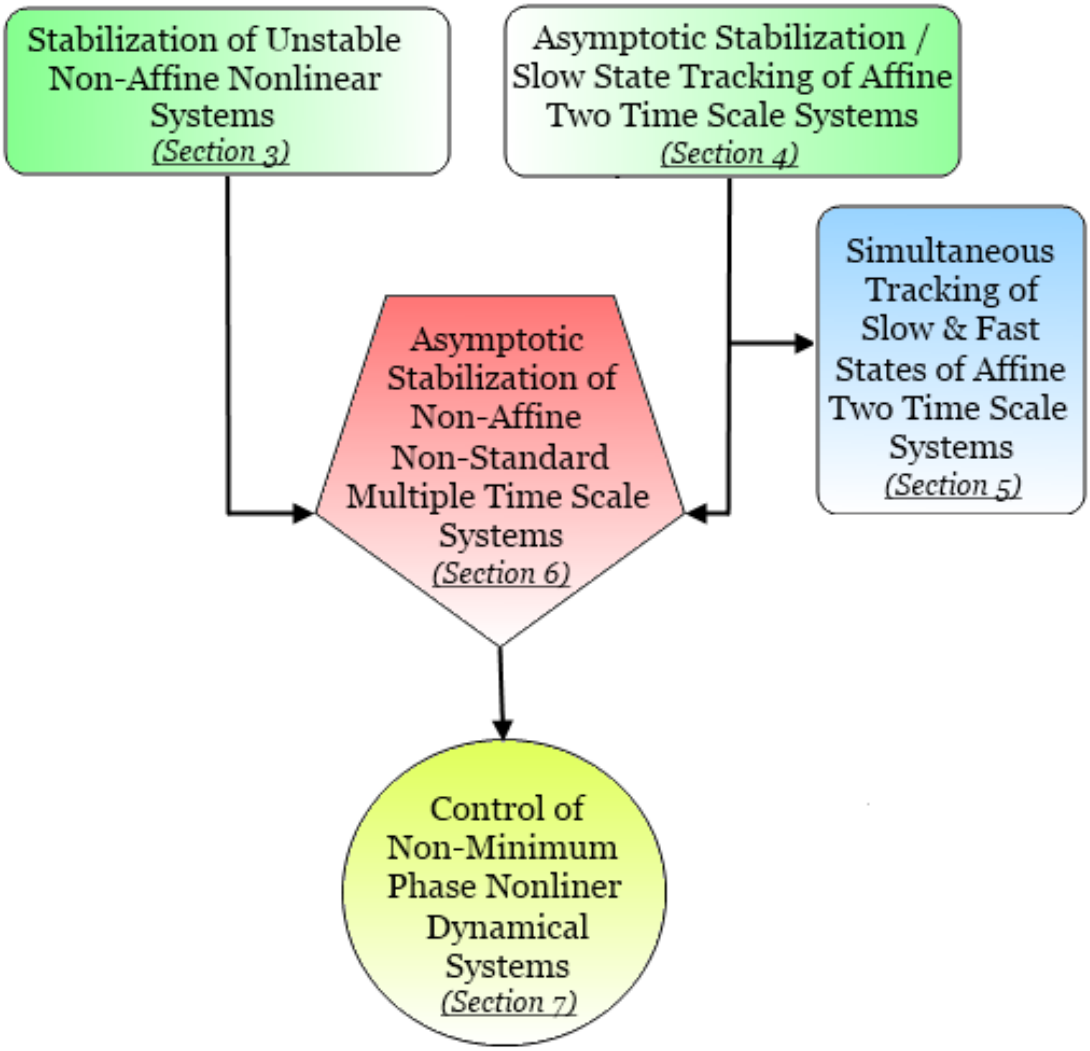

Figure 2.1: Organization and objectives of the dissertation

where $\mathbf{x} \in \mathbb{R}^n$ is the state, $u \in \mathbb{R}$ is the control input and $\overline{\mathbf{f}} : \mathbb{R}^n \times \mathbb{R} \to \mathbb{R}^n$ is sufficiently smooth. The function $\overline{\mathbf{f}}(\mathbf{x}, u)$ need not be monotonic in the control and $\frac{\partial \overline{\mathbf{f}}}{\partial u}$ can be singular at the origin. Assume that

Assumption 2.2. *The unforced dynamics of system in (2.3), namely* $\dot{\mathbf{x}} = \overline{\mathbf{f}}(\mathbf{x}, 0) \triangleq \overline{\mathbf{f}}_0(\mathbf{x})$ *is open-loop unstable.*

This first objective addresses *Open Problem 3* presented in Section 1.3 and synthesizes static compensation control laws for asymptotic stabilization of systems of the form Σ in (2.3). The goal is to use Lyapunov-based methods to prove stability and analyze requirements on smoothness of the vector fields under consideration. Toward this end, several fundamental properties such as the generalized KYP lemma for non-affine systems of the following form

$$\underline{\Sigma} : \dot{\mathbf{x}} = \mathbf{f}(\mathbf{x}, \mathbf{u}); \quad \mathbf{x}(0) = \mathbf{x}_0 \tag{2.4}$$

with state-space $X = \mathbb{R}^n$ and set of input values $U = \mathbb{R}^m$ are derived and control laws synthesized. The controller developed is tested in simulation for magnetic levitation and continuously stirred chemical reactor systems. This problem plays an integral part in the stabilization of reduced-order systems developed singularly perturbed systems of the form (2.1). The solution strategies of this problem are presented in Section 3.

2. ***Asymptotic Stabilization and Slow State Tracking of Affine in Control, Two Time Scale Systems***

Consider the following specialized form of the governing dynamics of (2.1):

$$\dot{\mathbf{x}} = \mathbf{f_1}(\mathbf{x}, \mathbf{z}) + \mathbf{f_2}(\mathbf{x}, \mathbf{z})\mathbf{u} \tag{2.5a}$$

$$\epsilon \dot{\mathbf{z}} = \mathbf{g_1}(\mathbf{x}, \mathbf{z}) + \mathbf{g_2}(\mathbf{x}, \mathbf{z})\mathbf{u} \tag{2.5b}$$

with initial conditions specified. The control objective is to enforce the slow state to asymptotically track an atleast twice continuously differentiable time-varying bounded specified trajectory, or $\mathbf{x}(t) \to \mathbf{x}_r(t)$ as $t \to \infty$. It is assumed that the control is sufficiently faster than all the system variables. The goal is to analyze the reduced-order approach introduced in Section 1.1 and Appendix A for non-standard singularly perturbed systems. Lyapunov-based methods are employed to define the explicit requirements on the form of the vector fields in terms of smoothness (e.g. continuous, continuously differentiable or infinitely smooth), dependence on affine presence of control and robustness to the singular perturbation parameter.

This second control problem addresses a special case of *Open Problem 1* identified in Section 1.2. This problem has been of interest to scientists and engineers for decades. Common applications include parallel robots, flexible link-manipulators, aircraft and enzyme models. Some of these applications are studied in Section 4 along with details of the proposed control schemes.

3. ***Simultaneous Tracking of Slow and Fast States of Affine in Control, Two Time Scale Systems***

   Consider the singularly perturbed system represented in (2.5). The control objective is to drive the states so as to track sufficiently smooth, bounded, time-varying trajectories such that $\mathbf{x}(t) \to \mathbf{x}_r(t)$ and $\mathbf{z}(t) \to \mathbf{z}_r(t)$ as $t \to \infty$. The goal is to identify actuation properties of the system (e.g completely actuated vs under-actuated) and system requirements in terms of minimum phase and well-defined relative degree.

   The third problem is inspired by aerospace applications. A motivating example is the approach flight phase to precision landing such as an arrested

landing on an aircraft carrier. In this situation an aircraft must track both fast states (angular rates and sink rate) and slow states (flight path and heading) simultaneously, accurately and reliably. Flying at higher approach speeds and therefore lower angles-of-attack can largely mitigate this two time scale dynamics effect and prevent departure due to stall. But higher approach speeds have long been known to lead to higher occurrences of landing mishaps or accidents. Another motivating example is an aircraft tracking a prescribed fast moving target, while simultaneously regulating speed and/or one or more kinematic angles. Section 5 details the control design procedure for *Open Problem 2* (see Section 1.2) and numerically simulates the response of an F-18 High Angle-of-Attack Vehicle.

4. ***Asymptotic Stabilization of Non-affine, Nonlinear, Non-Standard Singularly Perturbed Systems***

   The fundamental motive of this dissertation is to track sufficiently smooth, bounded, time-varying trajectories of the slow states or $\mathbf{x}(t) \to \mathbf{x}_r(t)$ as $t \to \infty$ for the non-standard dynamical model represented in (2.1).

   This final objective addresses *Open Problem 1* (see section 1.2) for a dynamical model with several time scales using insights determined from the two time scale counterpart addressed in the second objective. The stability proof and the details of a hierarchical control design procedure is presented in Section 6. Nonlinear control methods for control non-affine reduced-order systems is an integral part of this sequential design. As mentioned in Section 1 several non-minimum phase systems can be modeled in the form of (2.1) and some of these applications are detailed in Section 7.

2.3 Research Issues

As discussed in Section 1, the preceding four problems pose numerous difficult issues and these are detailed below.

1. ***Controllability:*** The significant issue with control of any system, whether singularly perturbed or not, is testing for controllability. Several researchers use accessibility rank test for determining these control properties. However, large computational burden is associated with these tests even for a single-input nonlinear system. This research follows the approach proposed in [3] and [35], and assumes that a control Lyapunov function for the system model exists and sufficiency conditions for controllability are met.

2. ***Limited static and dynamic feedback techniques for control non-affine systems:*** Synthesis of memoryless feedback compensation for nonlinear dynamical systems is restricted by available analytical root solving techniques. This makes the controller design process increasingly difficult and highly system dependent. Hence, recent results employ dynamic feedback compensation for stabilization. In these methods a system is indirectly controlled by changing the rate of the control variables. However, this correction depends upon the varying influence of control on the dynamical model which is unknown. Most studies assume this dependence to be constant. This assumption is violated by the simple pendulum, magnetic levitation, aerospace vehicles and most practical examples. In this research *analytical static feedback compensation is constructed by extending the control designs for passive systems without imposing this assumption.*

3. ***Restricted techniques for different speed of controllers*:** Two-stage

design schemes employ all of the control variables in stabilizing the reduced-order slow and fast subsystems. This requires all the control variables to be sufficiently faster than the system states. This assumption is met by most electrical systems but violated by aerospace applications, some of which have been discussed in Section 1. This research addresses this specific issue by designing a sequential design procedure that assigns control tasks according to speed of the actuators. Asymptotic stabilization is shown for all the system states and the actuator variables using Lyapunov-based design approach.

4. ***Complexity of constructing manifolds for non-standard singularly perturbed systems:*** Reduced-order models and in turn conclusions of geometric singular perturbation theory depend upon unique *analytical* determination of the manifold for the fast states. The nonlinear nature of the non-standard forms considered make this construction extremely difficult. Consequently, the composite control scheme fails to apply and no conclusions regarding the stability properties of the dynamical model can be made. This research issue is addressed here by *transforming the open-loop non-standard form into the closed-loop standard form* through appropriate control design. Two different control schemes are presented. The first method employs results from center manifold theory to approximate the manifold and guarantees Lyapunov stability. The second approach guarantees *asymptotic tracking* by employing the manifold as an additional control variable. Both the control formulations use singular perturbation methods and reduce the problem to control of lower-dimensional ordinary differential equations. Thus making them independent of the underlying control algorithms.

5. ***Lack of an explicit small parameter*:** The lack of knowledge of the sin-

gular perturbation parameter is an essential difficulty in the optimization of aerospace dynamic systems. Kelley [53], Mease [54], Calise [55], Ardema [56], [57] and Naidu [51] have developed systematic approaches to identify the singular perturbation parameter for both transport and fighter aircraft, but these results were limited to flight conditions under consideration due to varying aerodynamic behaviour. Hence a nonlinear control scheme that stabilizes the airframe without requiring the knowledge of the parameter is crucial. This research alleviates these problems and extends the application of multiple time scales to regulation and tracking of tail-less aircraft as well as helicopters and vertical take-off and landing aircraft.

3. A CONSTRUCTIVE STABILIZATION APPROACH FOR OPEN-LOOP UNSTABLE NON-AFFINE SYSTEMS

3.1 Introduction

This section considers the first objective discussed in Section 2 for developing stabilizing controllers for *non-affine* systems of the following form

$$\Sigma : \begin{array}{l} \dot{x}_1 = f_1(\mathbf{x}) \\ \dot{x}_2 = f_2(\mathbf{x}) \\ \vdots \\ \dot{x}_n = f_n(\mathbf{x}, u) \end{array} \qquad \text{or } \Sigma = \overline{\mathbf{f}}(\mathbf{x}, u) \tag{2.3}$$

where $\mathbf{x} \in \mathbb{R}^n$ is the state, $u \in \mathbb{R}$ is the control input and $\overline{\mathbf{f}} : \mathbb{R}^n \times \mathbb{R} \to \mathbb{R}$ is sufficiently smooth. The dynamical system under study is open-loop unstable and satisfies Assumption 2.2. Throughout the section it is assumed that a control Lyapunov function exists. This is sufficient to ensure the dynamical system Σ is asymptotically controllable [3].

In this section, the construction of an analytic state-feedback control law is pursued for systems with single input. This work is motivated by the results of Sontag [47] and explores a universal stabilization formula for an unstable non-affine system. Sufficient conditions are given for stabilization by designing the control law of the form $u(\mathbf{x}) = \alpha(\mathbf{x}) + \nu(\mathbf{x})$. The intuitive idea behind this control form is to introduce stiffness and damping into the system for stabilization through functions $\alpha(\mathbf{x})$ and $\nu(\mathbf{x})$ respectively. The major contribution comes in the design of the function $\alpha(\mathbf{x})$ that converts an open-loop unstable system into stable in the Lyapunov sense closed-loop system. This is an important task that ensures the system energy

remains bounded. The resultant closed-loop system is formally known as a *passive system*. Finally, the design proceeds with the construction of $\nu(\mathbf{x})$ to bring about the necessary energy dissipation for globally stabilizing the origin.

The design procedure presented here is based on ideas of *feedback passivation* introduced in [58] and [59] for control-affine systems. The general concept is to use state-feedback to render the system passive and then employ well-established results for stabilizing passive systems. Toward this end, several fundamental questions need to be answered for non-affine systems. Most importantly, *when is a general nonlinear system passive?* The famous Kalman-Yacubovitch-Popov lemma [60] and its nonlinear counterparts derived by Hill and Moylan [61], [62], answer this question for linear and affine-in-control systems respectively. Sufficient conditions for passivity of control non-affine systems and their relationship with the existing necessary conditions [38] are derived in Section 3.2. Passivity is a desirable property for control design. Pure output feedback render passive systems globally asymptotically stable. Section 3.3 starts by revisiting some of these properties and analyzes how these can assist in control formulation. However, not all physical systems are passive. The latter part of Section 3.3 derives conditions under which *a nonlinear system can be rendered passive through state-feedback*. This section closely follows the developments of [58], [63] and uses generalized KYP results derived in Section 3.2. The main result for stabilization of general multiple-input is presented in Section 3.4. This result is derived using properties developed in Section 3.2 and Section 3.3. This result provides sufficiency conditions under which a general nonlinear system can be stabilized by use of static compensation. Using these sufficiency conditions, Section 3.4 also presents a novel method for construction of control laws for single-input non-affine systems defined in (2.3) without making any assumptions about the nature of the control influence. The theoretical findings are verified in simulation and examples

are presented in Section 3.5. Finally, closing remarks are discussed in Section 3.6.

3.2 Passive Systems

In this section consider the following nonlinear dynamical system:

$$\Sigma_1 : \begin{array}{l} \dot{\mathbf{x}} = \mathbf{f}(\mathbf{x}, \mathbf{u}) \\ \mathbf{y} = \mathbf{h}(\mathbf{x}, \mathbf{u}) \end{array} \tag{3.1}$$

with state-space $X = \mathbb{R}^n$, set of input values $U = \mathbb{R}^m$ and set of output values $Y = \mathbb{R}^m$. The set $\mathcal{U}$ of admissible inputs consists of all U-valued piecewise continuous functions defined on $\mathbb{R}$. The functions $\mathbf{f}(.)$ and $\mathbf{h}(.)$ are continuously differentiable maps defined on the open subset $O \subset \mathbb{R}^n$. It is assumed that these vector fields are smooth mappings, with atleast one equilibrium. Without loss of generality, the origin is chosen as the equilibrium of Σ_1, that is, $\mathbf{f}(\mathbf{0}, \mathbf{0}) = \mathbf{0}$ and $\mathbf{h}(\mathbf{0}, \mathbf{0}) = \mathbf{0}$. In order to derive conditions for Σ_1 to be passive, several necessary definitions are reviewed and presented below.

Definition 3.2.1. [58] A system Σ_1 is said to be *passive* if there exists a storage function $V(\mathbf{x})$ that satisfies $V(\mathbf{0}) = 0$ and for any $\mathbf{u} \in \mathcal{U}$ and initial condition $\mathbf{x}_0 \in X$

$$V(\mathbf{x}) - V(\mathbf{x}_0) \leq \int_0^t \mathbf{y}^T(s)\mathbf{u}(s)ds. \tag{3.2}$$

If the storage function is C^r times continuously differentiable with $r \geq 1$ then differentiating both sides of (3.2)

$$\dot{V} \leq \mathbf{y}^T\mathbf{u}. \tag{3.3}$$

Definition 3.2.1 is the mathematical analog of saying that a system is passive if the amount of energy stored is less than or equal to the energy being input. This means

that either there is an effective energy dissipation from the system or the system energy is conserved for all time. Notice for a positive-definite storage function and zero input it can be concluded from (3.3) that passive system Σ_1 is stable in the Lyapunov sense. Similar behaviour is seen under the constraint $\mathbf{y} = \mathbf{0}$. Thus, it can be deduced that passive systems having a positive definite storage function have Lyapunov stable zero dynamics.

The next definition gives the necessary conditions for an input/output nonlinear system Σ_1 to be passive. For convenience, define the following vector fields

$$\mathbf{f}_0(\mathbf{x}) = \mathbf{f}(\mathbf{x}, \mathbf{0}) \in \mathbb{R}^n \tag{3.4a}$$

$$\mathbf{h}_0(\mathbf{x}) = \mathbf{h}(\mathbf{x}, \mathbf{0}) \tag{3.4b}$$

$$\mathbf{g}_i^0(\mathbf{x}) = \mathbf{g}_i(\mathbf{x}, \mathbf{0}) = \frac{\partial \mathbf{f}}{\partial u_i}(\mathbf{x}, \mathbf{0}) \in \mathbb{R}^n; \quad 1 \leq i \leq m \tag{3.4c}$$

$$\mathbf{g}_0(\mathbf{x}) = \frac{\partial \mathbf{f}}{\partial \mathbf{u}}(\mathbf{x}, \mathbf{0}) = \left[\mathbf{g}_1^0(\mathbf{x}), \ldots, \mathbf{g}_m^0(\mathbf{x})\right] \in \mathbb{R}^{n \times m}. \tag{3.4d}$$

In the above definitions, $\mathbf{f}_0(\mathbf{x})$ represents the open-loop dynamics of the dynamical system Σ_1 while $\mathbf{h}_0(\mathbf{x})$ is the output of Σ_1 at zero-input. The vector field $\mathbf{g}_i^0(\mathbf{x})$ defines the influence of input u_i on the system about the origin and is collected for all inputs under the vector $\mathbf{g}_0(\mathbf{x})$. Using these introduced notations and the fact that the vector fields in Σ_1 are smooth, the nonlinear dynamical system is equivalently represented as

$$\dot{\mathbf{x}} = \mathbf{f}_0(\mathbf{x}) + \mathbf{g}(\mathbf{x}, \mathbf{u})\mathbf{u} \tag{3.5a}$$

$$\mathbf{h}(\mathbf{x}, \mathbf{u}) = \mathbf{h}_0(\mathbf{x}) + \mathbf{j}(\mathbf{x}, \mathbf{u})\mathbf{u}, \tag{3.5b}$$

where the following identities have been used:

$$\mathbf{f}(\mathbf{x},\mathbf{u}) - \mathbf{f}_0(\mathbf{x}) = \left(\int_0^1 \frac{\partial \mathbf{f}(\mathbf{x},\gamma)}{\partial \boldsymbol{\gamma}}\bigg|_{\boldsymbol{\gamma}=\theta\mathbf{u}} d\theta \right) \mathbf{u}(\mathbf{x}) \triangleq \mathbf{g}(\mathbf{x},\mathbf{u})\mathbf{u} \tag{3.6}$$

$$\mathbf{h}(\mathbf{x},\mathbf{u}) - \mathbf{h}_0(\mathbf{x}) = \left(\int_0^1 \frac{\partial \mathbf{h}(\mathbf{x},\gamma)}{\partial \boldsymbol{\gamma}}\bigg|_{\boldsymbol{\gamma}=\theta\mathbf{u}} d\theta \right) \mathbf{u}(\mathbf{x}) \triangleq \mathbf{j}(\mathbf{x},\mathbf{u})\mathbf{u}. \tag{3.7}$$

Hence the vector fields $\mathbf{g}(\mathbf{x},\mathbf{u})$ and $\mathbf{j}(\mathbf{x},\mathbf{u})$ capture the effect of the control input on the motion of the dynamical system states and the output. Recall, for control-affine systems these vector fields are independent of the control input vector. Using smoothness of the vector $\mathbf{g}(\mathbf{x},\mathbf{u})$, (3.5a) is further decomposed as

$$\dot{\mathbf{x}} = \mathbf{f}_0(\mathbf{x}) + \mathbf{g}_0(\mathbf{x})\mathbf{u} + \sum_{i=1}^{m} u_i \left[\mathbf{R}_i(\mathbf{x},\mathbf{u})\mathbf{u}\right] \tag{3.8}$$

with $\mathbf{R}_i(\mathbf{x},\mathbf{u}) : \mathbb{R}^n \times \mathbb{R}^m \to \mathbb{R}^{n\times m}$, being a smooth map for $1 \leq i \leq m$.

For convenience, let $V : \mathbb{R}^n \to \mathbb{R}$ be a $C^r (r \geq 1)$ storage function and the expression

$$\mathcal{L}_{\mathbf{f}_0} V = \left\langle \frac{\partial V}{\partial \mathbf{x}}, \mathbf{f}_0(\mathbf{x}) \right\rangle \tag{3.9}$$

represent the Lie derivative of the functional V along the vector field $\mathbf{f}_0(\mathbf{x})$.

Definition 3.2.2. [38]. Let $\Omega_1 \triangleq \{\mathbf{x} \in \mathbb{R}^n : \mathcal{L}_{\mathbf{f}_0} V(\mathbf{x}) = 0\}$. Necessary conditions for Σ_1 to be passive with a C^2 storage function V are

(i) $\mathcal{L}_{\mathbf{f}_0} V(\mathbf{x}) \leq 0$,

(ii) $\mathcal{L}_{\mathbf{g}_0} V(\mathbf{x}) = \mathbf{h}_0^T(\mathbf{x}) \quad \forall \mathbf{x} \in \Omega_1$,

(iii) $\sum_{i=1}^{n} \frac{\partial^2 f_i}{\partial \mathbf{u}^2}(\mathbf{x},\mathbf{0}).\frac{\partial V}{\partial x_i} \leq \mathbf{j}^T(\mathbf{x},\mathbf{0}) + \mathbf{j}(\mathbf{x},\mathbf{0}) \quad \forall \mathbf{x} \in \Omega_1$,

where $f_i(\mathbf{x},\mathbf{u})$ is the ith component of the vector function $\mathbf{f}(\mathbf{x},\mathbf{u})$.

If the storage function was positive-definite, property (i) would be analogous to Lyapunov's condition $\dot{V} \leq 0$ for bounded stability. The other conditions in Definition 3.2.2 follow directly from Definition 3.2.1 by noticing that the difference $\frac{\partial V}{\partial \mathbf{x}}\mathbf{f}(\mathbf{x},\mathbf{u}) - \mathbf{h}^T(\mathbf{x},\mathbf{u})\mathbf{u}$ attains its maximum at $\mathbf{u} = \mathbf{0}$ on the set Ω_1.

The following theorem completes Definition 3.2.2 by presenting the sufficiency conditions required for a system Σ_1 to be passive.

Theorem 3.1. *Let V be a C^1 positive semidefinite function. A system Σ_1 is passive if there exist some functions $q : \mathbb{R}^n \to \mathbb{R}^k$, $W : \mathbb{R}^n \to \mathbb{R}^{k\times m}$ and $H : \mathbb{R}^n \times \mathbb{R}^m \to \mathbb{R}^{k\times m}$, for some integer k such that*

(i) $\mathcal{L}_{\mathbf{f}_0}V(\mathbf{x}) = -\frac{1}{2}q^T(\mathbf{x})q(\mathbf{x})$,

(ii) $\mathcal{L}_{\mathbf{g}_0}V(\mathbf{x}) = \mathbf{h}_0^T(\mathbf{x}) - q^T(\mathbf{x})W(\mathbf{x})$,

(iii) $\frac{1}{2}\left[W(\mathbf{x}) + H(\mathbf{x},\mathbf{u})\right]^T\left[W(\mathbf{x}) + H(\mathbf{x},\mathbf{u})\right] = \frac{1}{2}\left[\mathbf{j}(\mathbf{x},\mathbf{u})^T + \mathbf{j}(\mathbf{x},\mathbf{u})\right] - \mathcal{L}_{\mathbf{R}(\mathbf{x},\mathbf{u})}V$,

(iv) $W^T(\mathbf{x})H(\mathbf{x},\mathbf{u}) + H^T(\mathbf{x},\mathbf{u})W(\mathbf{x})$ *is positive-definite.*

In the conditions above $\mathcal{L}_{\mathbf{R}(\mathbf{x},\mathbf{u})}V = \left[\mathcal{L}_{\mathbf{R}_1(\mathbf{x},\mathbf{u})}V, \cdots, \mathcal{L}_{\mathbf{R}_m(\mathbf{x},\mathbf{u})}V\right]^T \in \mathbb{R}^{m\times m}$.

Proof. The proof follows the developments given in [63]. Assume functions $q(\mathbf{x})$, $W(\mathbf{x})$ and $H(\mathbf{x},\mathbf{u})$ exist. Then, along the solutions of Σ_1

$$\dot{V} \leq \dot{V} + \frac{1}{2}\left[W(\mathbf{x})\mathbf{u} + q(\mathbf{x})\right]^T\left[W(\mathbf{x})\mathbf{u} + q(\mathbf{x})\right] + \frac{1}{2}\mathbf{u}^T\Big[W^T(\mathbf{x})H(\mathbf{x},\mathbf{u}) + H^T(\mathbf{x},\mathbf{u})W(\mathbf{x})\Big]\mathbf{u} + \frac{1}{2}\mathbf{u}^T H^T(\mathbf{x},\mathbf{u})H(\mathbf{x},\mathbf{u})\mathbf{u} \tag{3.10}$$

Rearrange further to get

$$\dot{V} \leq \mathcal{L}_{\mathbf{f}_0}V + \mathcal{L}_{\mathbf{g}_0}V\mathbf{u} + \mathbf{u}^T\mathcal{L}_{\mathbf{R}(\mathbf{x},\mathbf{u})}V\mathbf{u} + \frac{1}{2}q^T(\mathbf{x})q(\mathbf{x}) + \frac{1}{2}\left[q^T(\mathbf{x})W(\mathbf{x})\mathbf{u} + \mathbf{u}^T W^T(\mathbf{x})q(\mathbf{x})\right] + \frac{1}{2}\left[W(\mathbf{x}) + H(\mathbf{x},\mathbf{u})\right]^T\left[W(\mathbf{x}) + H(\mathbf{x},\mathbf{u})\right] \tag{3.11}$$

Using properties (i) through (iii) given in Theorem 3.1

$$\begin{aligned}\dot{V} &\leq \mathbf{h}_0^T(\mathbf{x})\mathbf{u} + \frac{1}{2}\mathbf{u}^T\left[\mathbf{j}(\mathbf{x},\mathbf{u})^T + \mathbf{j}(\mathbf{x},\mathbf{u})\right]\mathbf{u} \\ &\leq \mathbf{y}^T\mathbf{u}. \end{aligned} \tag{3.12}$$

Thus, comparing (3.12) with (3.3) it is concluded that Σ_1 is passive and $V(\mathbf{x})$ is the storage function. This completes the proof. □

Notice on the set Ω_1 defined in Definition 3.2.2, property (i) through (iii) of Theorem 3.1 become exactly the necessary conditions for passivity. Thus, Theorem 3.1 plays the role of the generalized KYP lemma for non-affine systems on the set Ω_1. For an affine Σ_1, Theorem 3.1 has the following interesting consequence.

Corollary 3.2. *Let V be a C^1 positive semidefinite function. A system*

$$\begin{aligned}\dot{\mathbf{x}} &= \mathbf{f}_0(\mathbf{x}) + \mathbf{g}_0(\mathbf{x})\mathbf{u} \\ \mathbf{y} &= \mathbf{h}_0(\mathbf{x}) + \mathbf{j}(\mathbf{x})\mathbf{u}\end{aligned}$$

is passive if and only if

(i) $\mathcal{L}_{\mathbf{f}_0}V = -\frac{1}{2}q^T(\mathbf{x})q(\mathbf{x})$,

(ii) $\mathcal{L}_{\mathbf{g}_0}V = \mathbf{h}_0^T(\mathbf{x}) - q^T(\mathbf{x})W(\mathbf{x})$,

(iii) $\frac{1}{2}W^T(\mathbf{x})W(\mathbf{x}) = \frac{1}{2}\left[j(\mathbf{x})^T + j(\mathbf{x})\right]$.

Proof. The sufficient conditions follow directly from Theorem 3.1 by noticing in this case that $H(\mathbf{x},\mathbf{u})$ and $R(\mathbf{x},\mathbf{u})$ are identically zero. The necessity is shown by observing the function $-\dot{V} + \mathbf{y}^T\mathbf{u}$ is positive, semidefinite and quadratic in the

control for a passive system. Thus, a non-unique representation satisfying properties (i) through (iii) exist. This completes the proof. □

Corollary 3.2 is the nonlinear version of the KYP lemma derived by Hill and Moylan [61].

3.3 Feedback Equivalence to a Passive System/Feedback Passivation

In this section, the conditions under which the following system

$$\Sigma_2 : \begin{aligned} \dot{\mathbf{x}} &= \mathbf{f}(\mathbf{x}, \mathbf{u}) \\ \mathbf{y} &= \mathbf{h}(\mathbf{x}) \end{aligned} \tag{3.13}$$

is feedback equivalent to a passive system with positive definite storage function $V(\mathbf{x})$ are derived. These conditions are developed to exploit the following interesting stabilizing property of passive systems. Assume that Σ_2 is passive and zero-state observable. This means that if the output $\mathbf{h}(\mathbf{x}) = \mathbf{0}$ is zero, then the state is identically zero. With this property the following theorem states that the system is globally stabilized purely by output feedback.

Definition 3.3.1. [60][Theorem 14.4] If Σ_2 is

(i) passive with a radially unbounded positive definite storage function and

(ii) zero-state observable

then the origin $\mathbf{x} = \mathbf{0}$ can be globally stabilized by $\mathbf{u} = -\phi(\mathbf{y})$, where ϕ is any locally Lipschitz function such that $\phi(\mathbf{0}) = \mathbf{0}$ and $\mathbf{y}^T\phi(\mathbf{y}) > 0$ for all $\mathbf{y} \neq \mathbf{0}$.

The control in Definition 3.3.1 has been formulated to ensure the passivity condition in Definition 3.2.1 holds globally. Then the zero-state observable property helps conclude that the origin is the largest invariant set and hence the global equilibrium

of the closed-loop system. In order to use this powerful result for control design, conditions under which systems can be made passive need to be studied. The first result toward this end, studies the relative degree of a passive system. Relative degree of a system is number of times the output must be differentiated for the input to appear explicitly. The following definition expresses this condition using Lie derivatives.

Definition 3.3.2. The system Σ_2 is said to have a relative degree $(r_1, r_2, \ldots, r_m)$ at a point $(\mathbf{x}_0, \mathbf{u}_0)$ if:

(i) $\frac{\partial}{\partial u}\left[\mathcal{L}_{\mathbf{f}}^{k}\mathbf{h}_i(\mathbf{x})\right] = 0$ for all $1 \leq i \leq m$, $\mathbf{x}$ in the neighbourhood of $\mathbf{x}_0$ and all $\mathbf{u}$ in the neighbourhood of $\mathbf{u}_0$ and all $k < r_i$,

(ii) $\frac{\partial}{\partial \mathbf{u}}\left[\mathcal{L}_{\mathbf{f}}^{r_i} h_i(\mathbf{x})\right]\big|_{(\mathbf{x}_0, u_0)} \neq 0$.

Note the relative degree of a nonlinear system is a local concept defined about the point $(\mathbf{x}_0, \mathbf{u}_0)$ and also depends on the domain of control. This dependence is a result of the non-affinity of the system. Next a lemma is derived that will help determine the relative degree of Σ_2.

Lemma 3.3. *Origin belongs to the set Ω_1 given in Definition 3.2.2.*

Proof. Consider the open-loop system Σ_2. The necessary condition for passivity with positive definite storage function is

$$\mathcal{L}_{\mathbf{f}_0} V(\mathbf{x}) \leq 0.$$

This indicates that the system is stable in the Lyapunov sense. Further, by Laselle's theorem [64] it is known that the state of this open-loop system will enter the set $\{\mathbf{x} \in \mathbb{R}^n : \mathcal{L}_{\mathbf{f}_0} V(\mathbf{x}) = 0\}$. This is exactly the set Ω_1 in Definition 3.2.2. This result also can be shown by Barbalat's lemma [65].

Further, the set Ω_1 contains the invariant sets of the system. Since origin is the fixed-point of the system Σ_1, it is concluded that it belongs to the set Ω_1. This completes the proof. □

The next theorem analyzes the relative degree of the passive system Σ_2.

Theorem 3.4. *Suppose Σ_2 is passive with a C^2 storage function V which is positive definite. If $\mathbf{g}_0(\mathbf{0})$ and $\frac{\partial h}{\partial \mathbf{x}}(\mathbf{0})$ have full rank, then Σ_2 has relative degree $(1, 1, \ldots, 1)$ at $(\mathbf{x} = 0, \mathbf{u} = 0)$.*

Proof. The relative degree of Σ_2 is one if $\left[\frac{\partial \dot{\mathbf{y}}}{\partial \mathbf{u}}\right](\mathbf{0}, \mathbf{0})$ is non-singular, or

$$\begin{aligned}\frac{\partial \dot{\mathbf{y}}}{\partial \mathbf{u}}(\mathbf{0}, \mathbf{0}) &= \left\{ \frac{\partial \mathbf{h}}{\partial \mathbf{x}} \mathbf{g}_0(\mathbf{x}) + \frac{\partial}{\partial \mathbf{u}} \left[\frac{\partial \mathbf{h}}{\partial \mathbf{x}} \left[\sum_{i=1}^{m} u_i \mathbf{R}_i(\mathbf{x}, \mathbf{u}) \right] \mathbf{u} \right] \right\} (\mathbf{0}, \mathbf{0}) \\ &= \frac{\partial \mathbf{h}}{\partial \mathbf{x}} \mathbf{g}_0(\mathbf{0}) \\ &= \mathcal{L}_{\mathbf{g}_0} \mathbf{h}(\mathbf{0})\end{aligned} \tag{3.14}$$

are $m \times m$ and non-singular. The above relations are obtained by using the smooth property of the vector fields. Hence conditions for which (3.14) holds true need to be determined. This is carried out in the following two steps.

Firstly, since Σ_2 is passive, it satisfies the necessary conditions given in Definition 3.2.2. But property (ii) in Definition 3.2.2 is defined only for set Ω_1. Hence the first step in the proof is to show that origin belongs to this set. This has been shown in Lemma 3.3. Thus, from property (ii) of Definition 3.2.2

$$\frac{\partial}{\partial \mathbf{x}} \left[\mathbf{g}_0^T(\mathbf{x}) \frac{\partial V}{\partial \mathbf{x}} \right] \mathbf{g}_0(\mathbf{x}) = \frac{\partial \mathbf{h}}{\partial \mathbf{x}} \mathbf{g}_0(\mathbf{x}) \tag{3.15}$$

is satisfied at $\mathbf{x} = \mathbf{0}$. Differentiating and using the fact $\frac{\partial V}{\partial \mathbf{x}}(\mathbf{0}) = 0$ in (3.15)

$$\mathbf{g}_0^T(\mathbf{0})\frac{\partial^2 V}{\partial \mathbf{x}^2}(\mathbf{0})\mathbf{g}_0(\mathbf{0}) = \frac{\partial \mathbf{h}}{\partial \mathbf{x}}\mathbf{g}_0(\mathbf{0}). \tag{3.16}$$

The rest of the proof proceeds similar to Proposition 2.44 given in [63]. The Hessian $\frac{\partial^2 V}{\partial \mathbf{x}^2}(\mathbf{0})$ is symmetric positive definite by properties of the storage function and can be factored as $R^T R$ with some matrix R. Then,

$$\mathbf{g}_0^T(\mathbf{0})R^T R(\mathbf{0})\mathbf{g}_0(\mathbf{0}) = \frac{\partial \mathbf{h}}{\partial \mathbf{x}}\mathbf{g}_0(\mathbf{0}). \tag{3.17}$$

Since $\frac{\partial \mathbf{h}}{\partial \mathbf{x}}(\mathbf{0}) = \mathbf{g}_0^T(\mathbf{0})R^T R(\mathbf{0})$ is assumed to be full rank, $R\mathbf{g}_0(\mathbf{0})$ has full rank. Hence it is concluded that $\frac{\partial \mathbf{h}}{\partial \mathbf{x}}\mathbf{g}_0(\mathbf{0})$ is $m \times m$ and full rank. This completes the proof. □

Remark 3.3.1. For an affine system, the conditions of Definition 3.2.2 are satisfied for all control inputs. Since the relative degree for an affine system does not depend on input, Theorem 3.4 consequently reduces to Proposition 2.44 [63].

The next result examines the nature of the zero dynamics of Σ_2.

Theorem 3.5. *Suppose Σ_2 is passive with a C^2 storage function V which is positive definite. If $\mathbf{g}_0(\mathbf{0})$ and $\frac{\partial \mathbf{h}}{\partial \mathbf{x}}(\mathbf{0})$ have full rank, then zero dynamics of Σ_2 locally exist about $(\mathbf{x} = \mathbf{0}, \mathbf{u} = \mathbf{0})$ and is weakly minimum phase.*

Proof. From Theorem 3.4, Σ_2 has a well-defined relative degree and local zero dynamics exist. Let the set $\Omega_2 = \{\mathbf{x} \in \mathbf{R}^n : \mathbf{h}(\mathbf{x}) = \mathbf{0}\}$ define the points on the zero-output manifold. By definition of Σ_2 this set contains the origin. By Lemma 3.3 origin is also contained in the set Ω_1. Thus, in order to study the local nature of the zero dynamics about the origin, only those state trajectories that fall in the intersection set $\Omega_2 \bigcap \Omega_1$ need to be considered. On these set of points properties (i) through (ii) of Theorem 3.1 hold. Hence,

$$\begin{aligned}\dot{V} &= \mathcal{L}_{\mathbf{f}(\mathbf{x},\mathbf{u})}V \\ &= \mathcal{L}_{\mathbf{f}_0}V + \mathcal{L}_{\mathbf{g}_0}V\mathbf{u} + \mathbf{u}^T\mathcal{L}_{\mathbf{R}(\mathbf{x},\mathbf{u})}V\mathbf{u} \\ &= \mathbf{u}^T\mathcal{L}_{\mathbf{R}(\mathbf{x},\mathbf{u})}V\mathbf{u}.\end{aligned} \tag{3.18}$$

By Definition 3.2.1, for passive systems $\dot{V} \leq \mathbf{y}^T\mathbf{u}$. Furthermore, this condition becomes $\dot{V} \leq 0$ on the set $\Omega_2 \bigcap \Omega_1$. This inference along with condition (3.18) implies that the origin is Lyapunov stable and hence zero dynamics is weakly minimum phase. This completes the proof. □

Theorems 3.4 and 3.5 together give the necessary conditions for feedback equivalence to a passive system. This result is summarized by the following theorem.

Theorem 3.6. *Suppose* $\mathbf{g}_0(\mathbf{0})$ *and* $\frac{\partial \mathbf{h}}{\partial \mathbf{x}}(\mathbf{0})$ *have full rank. The necessary conditions for transforming* Σ_2 *into a passive system with* C^2 *positive definite storage function* V *using static state-feedback compensation are:*

(i) Σ_2 *has relative degree* $\{1, 1, \ldots, 1\}$ *and*

(ii) is weakly minimum phase

Proof. From Theorem 3.4 and Theorem 3.5 it is known that the resulting system will have relative degree $(1, 1, \ldots)$ with weakly minimum phase zero dynamics. Further, it is well understood that relative degree and zero dynamics are invariant under static feedback [66][Lemma 2.4]. Hence the conditions in the proof follow. □

Theorem 3.6 extends the powerful feedback equivalence approach to general nonlinear systems. It provides necessary conditions for a system to be made passive by feedback under mild restrictions. The equivalent theorem for affine systems derived in [58] shows that Theorem 3.6 is also sufficient for feedback passivity. But

the topological and nonlinear nature of non-affine systems hinders this result to be sufficient.

3.4 Control Synthesis for Stabilization

This section returns to the question of control design for general non-affine systems. The central idea for stabilization is based upon Definition 3.3.1 and Theorem 3.6. Suppose the control is decomposed as $\mathbf{u}(\mathbf{x}) = \boldsymbol{\alpha}(\mathbf{x}) + \boldsymbol{\nu}(\mathbf{x})$ and the first component $\boldsymbol{\alpha}(\mathbf{x})$ is used to ensure the non-affine system under consideration is passive through input $\boldsymbol{\nu}(\mathbf{x})$. Then through Definition 3.3.1 asymptotic stabilization is guaranteed under zero-state detectability conditions. The proof that this control choice in fact asymptotically stabilizes a non-affine system is the focus of this section.

3.4.1 Control Synthesis for Multi-Input Non-Affine Systems

The first result is given for the following non-affine system:

$$\underline{\Sigma} : \dot{\mathbf{x}} = \mathbf{f}(\mathbf{x}, \mathbf{u}); \quad \mathbf{x}(0) = \mathbf{x}_0 \tag{2.4}$$

with state-space $X = \mathbb{R}^n$ and set of input values $U = \mathbb{R}^m$. The set $\mathcal{U}$ of admissible inputs consists of all U-valued piecewise continuous functions defined on $\mathbb{R}$. The vector field $\mathbf{f}(.)$ is continuously differentiable map defined on the open subset $O \subset \mathbb{R}^n$. Without loss of generality, origin is chosen as the equilibrium of $\underline{\Sigma}$. Necessary definitions for zero-state observability for a passive system are reviewed next. Toward this end, define the following vector fields

$$\underline{f}_0(\mathbf{x}) = \mathbf{f}(\mathbf{x}, \boldsymbol{\alpha}(\mathbf{x})) \in \mathbb{R}^n \tag{3.19a}$$

$$\underline{g}(\mathbf{x}, \boldsymbol{\nu}(\mathbf{x})) = \left(\int_0^1 \frac{\partial \mathbf{f}(\mathbf{x}, \boldsymbol{\alpha}(\mathbf{x}) + \boldsymbol{\gamma})}{\partial \boldsymbol{\gamma}} \bigg|_{\boldsymbol{\gamma} = \theta \boldsymbol{\nu}} d\theta \right) \in \mathbb{R}^{n \times m} \tag{3.19b}$$

$$\underline{g}_i^0 = \underline{g}_i(\mathbf{x}, \mathbf{0}) \in \mathbb{R}^n. \tag{3.19c}$$

With these definitions $\underline{\Sigma}$ is equivalently represented as

$$\dot{\mathbf{x}} = \underline{f}_0(\mathbf{x}) + \underline{g}(\mathbf{x}, \boldsymbol{\nu}(\mathbf{x}))\boldsymbol{\nu}(\mathbf{x}) \tag{3.20}$$

where $\mathbf{u}(\mathbf{x}) = \boldsymbol{\alpha}(\mathbf{x}) + \boldsymbol{\nu}(\mathbf{x})$ has been used.

Definition 3.4.1. [38] Suppose $\underline{\Sigma}$ is passive through input $\boldsymbol{\nu}(\mathbf{x})$ and dummy output $\mathbf{h}(\mathbf{x}, \boldsymbol{\nu}(\mathbf{x}))$. It is locally *zero-state detectable* if there is a neighbourhood N of $\mathbf{x} = \mathbf{0}$ such that $\forall\ \mathbf{x}_0 = \mathbf{x} \in N$

$$\mathbf{h}(\phi(t, \mathbf{x}; \boldsymbol{\nu}), \boldsymbol{\nu})|_{\boldsymbol{\nu}=\mathbf{0}} = \mathbf{0} \quad \forall\ t \geq 0 \Rightarrow \lim_{t\to\infty} \phi(t, \mathbf{x}; \mathbf{0}) = \mathbf{0}. \tag{3.21}$$

If $N = \mathbb{R}^n$, then it is *zero-state detectable*. A system is locally (respectively globally) *zero-state observable* if there is a neighbourhood N of $\mathbf{x} = \mathbf{0}$ such that $\forall\ \mathbf{x}_0 = \mathbf{x} \in N$ (respectively $\mathbb{R}^n$)

$$\mathbf{h}(\phi(t, \mathbf{x}; \mathbf{0}), \mathbf{0}) = \mathbf{0} \quad \forall\ t \geq 0 \Rightarrow \mathbf{x} = \mathbf{0}. \tag{3.22}$$

The next two conditions test the detectability and observability properties of $\underline{\Sigma}$ with input $\boldsymbol{\nu}(\mathbf{x})$ and output $\mathbf{h}(\mathbf{x}, \boldsymbol{\nu}(\mathbf{x}))$. Let the distribution

$$D = \text{span}\left\{ad^k_{\underline{f}_0}\underline{g}^0_i : 0 \leq k \leq n-1, 1 \leq i \leq m\right\}$$

and two sets Ω and S, associated with D be defined as

$$\Omega = \left\{\mathbf{x} \in N \subseteq \mathbb{R}^n : \mathcal{L}^k_{\underline{f}_0} V(\mathbf{x}) = 0, k = 1, \ldots, r\right\}, \tag{3.23}$$

$$S = \left\{\mathbf{x} \in N \subseteq \mathbb{R}^n : \mathcal{L}^k_{\underline{f}_0} \mathcal{L}_\tau V(\mathbf{x}) = 0, \forall \tau \in D, k = 0, 1, \ldots, r-1\right\} \tag{3.24}$$

where $V(\mathbf{x}) : \mathbb{R}^n \to \mathbb{R}$ is a $C^r; r \geq 1$ function. The notation $ad^k_{\underline{f}_0} \underline{g}^0_i$ is standard for Lie bracket.

Definition 3.4.2. [38] Suppose the system $\underline{\Sigma}$ is passive with $C^r(r \geq 1)$ storage function V, which is positive definite and proper. Then, $\underline{\Sigma}$ is zero-state detectable if $\Omega \cap S = \{0\}$.

The following theorem provides sufficiency conditions for asymptotic stabilization of the system $\underline{\Sigma}$ described in (2.4) and equivalently in (3.20).

Theorem 3.7. *Suppose V is C^2 positive-definite Lyapunov function and the functions $\boldsymbol{\alpha}(\mathbf{x})$ and $\boldsymbol{\nu}(\mathbf{x})$ are designed such that $\mathcal{L}_{\underline{f}_0} V \leq 0$ and $\boldsymbol{\nu}(\mathbf{x}) + [\mathcal{L}_g V]^T = 0$ respectively. If $\Omega \cap S = \{0\}$, then the control $\mathbf{u}(\mathbf{x}) = \boldsymbol{\alpha}(\mathbf{x}) + \boldsymbol{\nu}(\mathbf{x})$ asymptotically stabilizes the system $\underline{\Sigma}$.*

Proof. Asymptotic stabilization is shown using LaSelle's invariant principle and Lyapunov's direct method. The rate of change of the Lyapunov function about the trajectories of $\underline{\Sigma}$ given in (3.20) is

$$\dot{V} = \mathcal{L}_{\underline{f}_0} V + \mathcal{L}_{\underline{g}} V \boldsymbol{\nu}(\mathbf{x}). \tag{3.25}$$

Then, through construction of $\boldsymbol{\alpha}(\mathbf{x})$

$$\dot{V} \leq \mathcal{L}_{\underline{g}} V \boldsymbol{\nu}(\mathbf{x}). \tag{3.26}$$

Through Definition 3.2.1 (3.26) is passive with the output $\mathbf{y} = \left(\mathcal{L}_{\underline{g}} V\right)^T$. Since $\Omega \bigcap S = \{0\}$, this passive system is zero-state detectable. By Definition 3.3.1 $\underline{\Sigma}$ is asymptotically stabilized by input $\boldsymbol{\nu}(\mathbf{x}) = -\mathcal{L}_{\underline{g}} V$. Hence, the result follows. This completes the proof. □

Theorem 3.7 is a powerful result that guarantees asymptotic stabilization for all non-affine nonlinear systems. The concept of control synthesis is general and relies upon separate construction of stiffness and damping functions $\boldsymbol{\alpha}(\mathbf{x})$ and $\boldsymbol{\nu}(\mathbf{x})$ respectively. The necessary conditions for existence of $\boldsymbol{\alpha}(\mathbf{x})$ for a class of systems with outputs independent of control was derived in Theorem 3.6. The construction of $\boldsymbol{\nu}(\mathbf{x})$ has received considerable attention in literature under the label 'passivity-based control'. The requirements of zero-state detectability is a consequence of employing pure output feedback for passive systems [38], [39], [67]. Hence, the conditions in Theorem 3.7 can be relaxed by use of other methods for control of open-loop stable systems. The construction of control input $\boldsymbol{\alpha}(\mathbf{x})$ is discussed next.

3.4.2 Construction of Control for Single-Input Non-Affine Systems

The second result *formulates constructive feedback control to stabilize an unstable single-input non-affine system in the Lyapunov sense.* State-feedback control is synthesized using the sufficiency conditions of Lyapunov's direct method. Consider the class of single-input non-affine system

$$\Sigma : \begin{array}{l} \dot{x}_1 = f_1(\mathbf{x}) \\ \dot{x}_2 = f_2(\mathbf{x}) \\ \vdots \\ \dot{x}_n = f_n(\mathbf{x}, u) \end{array} \qquad \text{or } \Sigma = \overline{\mathbf{f}}(\mathbf{x}, u) \tag{2.3}$$

where $\mathbf{x} \in \mathbb{R}^n$ is the state, $u \in \mathbb{R}$ is the control input and $\overline{\mathbf{f}} : \mathbb{R}^n \times \mathbb{R} \to \mathbb{R}$ is sufficiently smooth. Assume that Σ satisfies Assumption 2.2. Without loss of generality, the origin is the equilibrium of Σ. Using the smoothness properties of vector field in Σ rearrange (2.3) as

$$\Sigma : \dot{\mathbf{x}} = \overline{\mathbf{f}}(\mathbf{x}, 0) + B\bar{g}(\mathbf{x}, u) \tag{3.27}$$

where matrix B is defined as

$$B = [0, 0, \cdots, 0, 1]^T \tag{3.28}$$

and the vector fields $\bar{\mathbf{f}}(\mathbf{x}, 0)$ and $\bar{g}(\mathbf{x}, u)$ represent the internal and external forces acting on Σ respectively. The control objective is to Lyapunov-stabilize the origin of Σ. The following lemma provides sufficiency conditions the control law must satisfy for stabilization.

Lemma 3.8. *Suppose V is C^2 positive-definite Lyapunov function and Σ satisfies Assumption 2.2. Then Σ is locally stabilizable by a control law $\alpha : D \to \mathbb{R}$ that satisfies the following conditions:*

(i) $sign(\bar{g}(\mathbf{x}, \alpha(\mathbf{x}))) = -sign((\nabla V)_n)$ *and*

(ii) $|(\nabla V)_n \bar{g}(\mathbf{x}, \alpha(\mathbf{x}))| \geq |\left\langle \nabla V, \bar{\mathbf{f}}(\mathbf{x}, 0) \right\rangle|$

where $(\nabla V)_n$ is the nth row element of the gradient ∇V. Further if $\bar{g}(\mathbf{x}, 0) = 0$ the control can be turned off for stable operating regions or $\alpha = 0$, if $|\left\langle \nabla V, \bar{\mathbf{f}}(\mathbf{x}, 0) \right\rangle| <= 0$.

Proof. From Lyapunov's second method, the sufficient condition for the system Σ to be stable is

$$\dot{V} = \left\langle \nabla V, \bar{\mathbf{f}}(\mathbf{x}, 0) + B\bar{g}(\mathbf{x}, \alpha) \right\rangle \leq 0. \tag{3.29}$$

For all states satisfying Assumption 2.2,

$$\begin{aligned} \langle \nabla V, B\bar{g}(\mathbf{x}, \alpha) \rangle &< 0 \\ \langle \nabla V, B\bar{g}(\mathbf{x}, \alpha) \rangle &\leq -\left\langle \nabla V, \bar{\mathbf{f}}(\mathbf{x}, 0) \right\rangle \end{aligned}$$

imply stability and the desired result follows through definition of matrix B.

Further, for states in domain D that satisfy $|\left\langle \nabla V, \bar{\mathbf{f}}(\mathbf{x},0)\right\rangle| <= 0$, $\alpha = 0$ ensures Lyapunov stability if $\bar{g}(\mathbf{x},0) = 0$. This completes the proof. □

Remark 3.4.1. Note positive-definite control Lyapunov function defined in Lemma 3.8 is a Lyapunov function candidate for results in Theorem 3.7. Thus, asymptotic stabilization follows from Theorem 3.7 with $\alpha(\mathbf{x})$ defined using conditions of Lemma 3.8.

Next the main result for construction of $\alpha(\mathbf{x})$ using Lemma 3.8 is derived.

Theorem 3.9. *Suppose V is a C^2 Lyapunov function and Σ satisfies Assumption 2.2. Further assume $|\bar{g}(\mathbf{x},\alpha)| \geq R(\mathbf{x})|\alpha|^\rho$ for some $R(\mathbf{x}) > 0 \quad \forall\, \mathbf{x}$ and $\rho > 0$. Then origin of Σ is locally stabilizable by a control law $\alpha : D \to \mathbb{R}$ that satisfies*

(i) $sign(\bar{g}(\mathbf{x},\alpha(\mathbf{x}))) = -sign((\nabla V)_n)$ *and*

(ii) $|(\nabla V)_n|R(\mathbf{x})|\alpha|^\rho = |\left\langle \nabla V, \bar{\mathbf{f}}(\mathbf{x},0)\right\rangle|$

where $(\nabla V)_n$ is the nth row element of the gradient ∇V. Further if $\bar{g}(\mathbf{x},0) = 0$ the control can be turned off for stable operating regions or $\alpha = 0$, if $|\left\langle \nabla V, \bar{\mathbf{f}}(\mathbf{x},0)\right\rangle| <= 0$.

Proof. The proof follows directly from Lemma 3.8. The magnitude of control α is determined from condition (ii) of Lemma 3.8. For Lyapunov stability,

$$|(\nabla V)_n \bar{g}(\mathbf{x},\alpha(\mathbf{x}))| \geq |\left\langle \nabla V, \bar{\mathbf{f}}(\mathbf{x},0)\right\rangle| \tag{3.30}$$

needs to be satisfied. This condition gives the minimum control energy required to stabilize the origin in the Lyapunov sense. From properties of norm and definition of $R(\mathbf{x})$ condition (ii) of Theorem 3.9 follows. Hence condition (i) and (ii) provide an algorithm for correct direction and magnitude computation of control $\alpha(\mathbf{x})$ to maintain Lyapunov stability. This completes the proof. □

Lemma 3.8 and Theorem 3.9 give an explicit algorithm for transforming an open-loop unstable non-affine system to Lyapunov-stable. The important contribution of the control scheme is that *no assumptions regarding the control influence have been made*. These algorithms along with passivity-based control asymptotically stabilize Σ through Theorem 3.7. Application of these results is presented next.

3.5 Numerical Examples

3.5.1 Purpose and Scope

The preceding theoretical developments are demonstrated with simulation. The first example qualitatively analyses the performance and design procedure for an one-dimensional system. The second example implements the results of Theorem 3.9 for stabilization of continuously stirred chemical reactor. This example demonstrates that stabilization can be guaranteed by appropriate synthesis of $\alpha(\mathbf{x})$ alone. The third example develops control laws for a nonlinear magnetic levitation system. The purpose is to synthesize an asymptotically stabilizing controller that is consistent with the dynamics of the problem.

3.5.2 One-Dimensional Non-Affine Unstable Dynamics

The purpose of this subsection is to verify the theoretical developments through an open-loop unstable non-affine system. The example considered is a polynomial system of degree three. The control law for this example was developed through analytical root solving techniques in [37]. Here an alternate control law formulation is presented to globally stabilize the origin. Additionally, the simplicity of this example allows analytical verification of the control development proposed. Consider the following system:

$$\dot{x} = x - 2u^3. \tag{3.31}$$

It is open-loop unstable and satisfies Assumption 2.2 through quadratic Lyapunov function $V(x) = \frac{1}{2}x^2$. The objective is to globally stabilize the origin of (3.31) through static compensation.

The origin of the system given in (3.31) cannot be stabilized by a fixed gain controller. To see this behaviour, suppose the control takes the form $u = Kx$ in (3.31). The resulting closed-loop dynamics is $\dot{x} = x - 2K^3x^3$. This system has the following equilibrium solutions

$$x_* = \begin{cases} 0 \quad \text{for all } K \\ \pm\frac{1}{\sqrt{2K^3}} \quad \text{for } K > 0. \end{cases} \tag{3.32}$$

These equilibrium solutions and their local stability properties are presented in Figure 3.1 for different values of the feedback gain K. This bifurcation map illustrates that the origin always remains unstable and only an infinitely high-gain can force stability. Furthermore, the system has three equilibrium solutions for all positive values of the feedback gain. The non-zero equilibrium solutions converge to the origin at infinite gain. High-gain feedback limits capabilities of the system and is not a desirable solution. An alternative solution to regulate the system is to switch feedback gains in accordance with the current state. As an example, suppose the feedback gain for (3.31) was initialized to $K_0 = 1.5$. Figure 3.1 and (3.32) conclude that the state would stabilize to $x_{steady} = \pm 0.384$ depending on its initial condition. Thus, in order to stabilize the origin, the feedback gain needs to be switched to another value. One of the several ways of switching is shown in the phase portrait in Figure 3.2. The phase portrait shows that the state begins on the blue curve corresponding to $u = 1.5x$. The origin can be stabilized only if the state switches onto the green curve that corresponds to $K = 1/|x|^{2/3}$. This switch needs to be made exactly when the

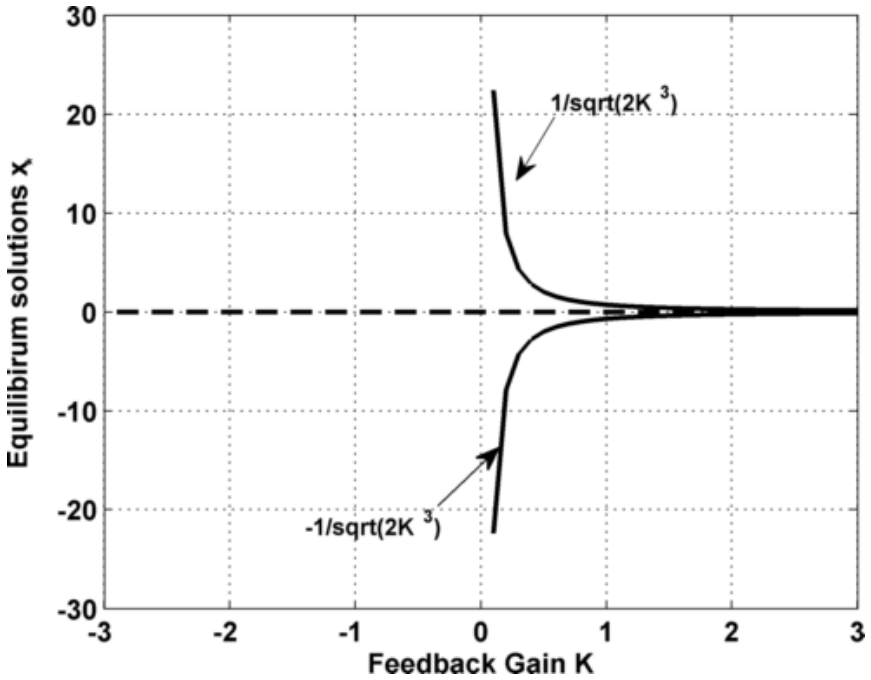

Figure 3.1: Stable (solid lines) and unstable (broken line) equilibrium solutions of (3.31) with $u = Kx$

two curves meet otherwise the state would settle at steady state of the blue curve and remain there forever. Similar trend can be seen in Figure 3.3 where phase portraits for four different feedback gains is presented. Only the green curve stabilizes the origin and all other curves must intersect with this curve to regulate the state. This observation agrees with the conclusion drawn from Figure 3.1 that only infinite gain can stabilize the origin.

System (3.31) exhibits a fundamental phenomenon observed in control of non-affine systems. These systems in general cannot be stabilized by a fixed static compensator. Switching curves for (3.31) were determined analytically through the study of the bifurcation map given in Figure 3.1. But for high dimensional systems, generation and analyses of these maps requires substantial system knowledge and offline processing. Additionally, the number of times the control must switch and conditions for which these switches must occur depends on the initial condition of the physical

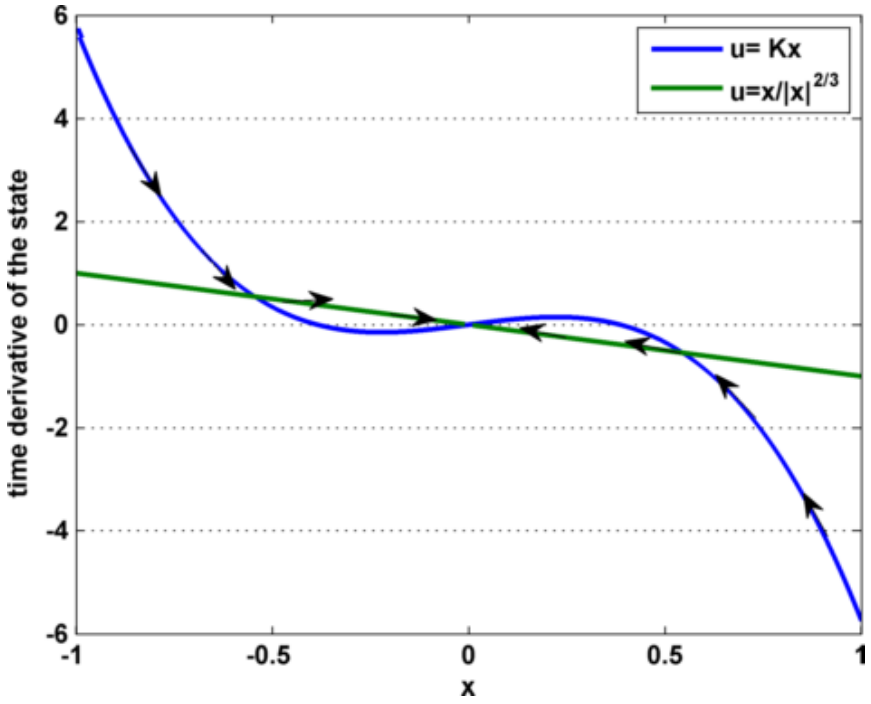

Figure 3.2: Phase portrait of (3.31) with control $u = Kx$

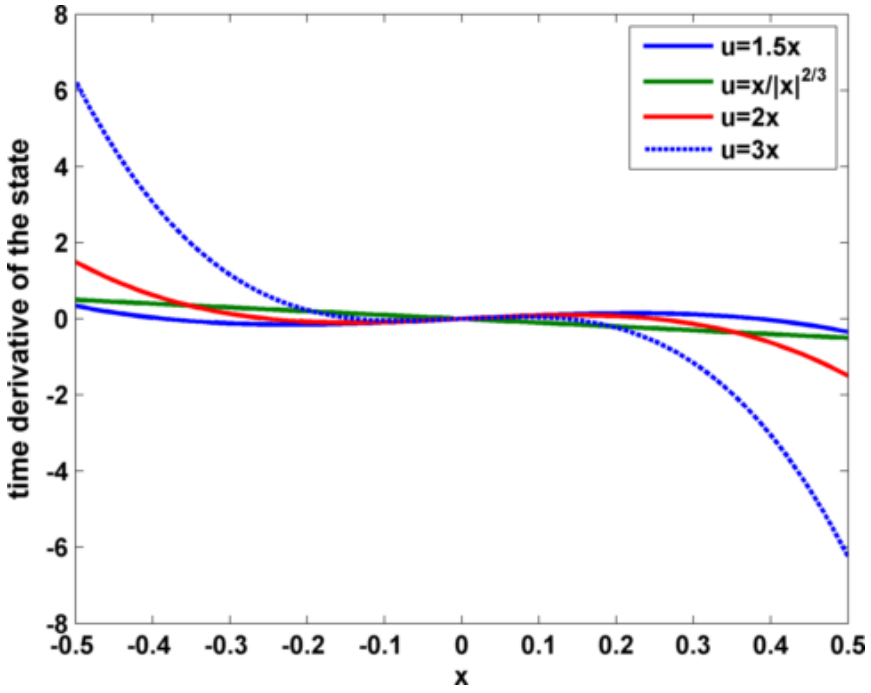

Figure 3.3: Phase portrait for (3.31) with control $u = Kx$ for four feedback gains

system. In the following, real-time implementable globally stabilizing controller is synthesized using Theorem 3.7 that is independent of the initial condition.

3.5.2.1 Controller Design

In this section, the feedback control of the following form $u = \alpha(x) + \nu(x)$ is constructed in three steps using the conditions given in Theorem 3.7.

The *first step* proceeds by substituting the control form in (3.31) and defining vector fields given in (3.19). This results in

$$\underline{f}_0(x) = x - 2\alpha^3(x) \tag{3.33}$$

$$\underline{g}(x, \nu(x)) = -6\alpha^2(x) - 6\alpha(x)\nu(x) - 2\nu^2(x) \tag{3.34}$$

$$\underline{g}^0(x) = -6\alpha^2(x). \tag{3.35}$$

In the *second step* construct $\alpha(x)$ to ensure Lyapunov stability of $\underline{f}_0(x)$. With $V(x) = \frac{1}{2}x^2$, this condition requires

$$2x\alpha^3(x) \geq x^2. \tag{3.36}$$

The following is one choice for $\alpha(x)$ that satisfies (3.36) for all $x \in \mathbb{R}$:

$$\alpha(x) = \begin{cases} \frac{1}{\sqrt[3]{2}}x & \text{if } |x| \geq 1; \\ -\frac{1}{\sqrt[3]{2}} & \text{if } -1 < x < 0; \\ 0 & \text{if } x = 0\ ; \\ \frac{1}{\sqrt[3]{2}} & \text{if } 0 < x < 1. \end{cases} \tag{3.37}$$

Using $\alpha(x)$ defined above the dynamics $\underline{f}_0(x)$ becomes

$$\underline{f}_0(x) = \begin{cases} x - x^3 & \text{if } |x| \geq 1; \\ x + 1 & \text{if } -1 < x < 0; \\ 0 & \text{if } x = 0 \ ; \\ x - 1 & \text{if } 0 < x < 1. \end{cases} \tag{3.38}$$

Note $\underline{f}_0(x)$ described in (3.38) has three stable fixed points $x = -1$, $x = 0$ and $x = 1$. Thus, the dynamics of the system (3.31) is rendered stable for all time.

The *third step* proceeds with construction of control input $\nu(x)$ that enforces stability of the origin. Toward this end, recall with design of $\alpha(x)$ the dynamics of $\underline{f}_0(x)$ is Lyapunov stable. Thus, the system in (3.20) can be seen as an open-loop stable system with respect to input $\nu(x)$. Control laws for such a class of systems has been addressed by passivity-based methods and following the formulation given in [39] to construct control input $\nu(x)$

$$\nu(x) = -\frac{\gamma(x)\mathcal{L}_{g^0}V(x)}{1 + |\mathcal{L}_{g^0}V(x)|^2} \tag{3.39}$$

where $\gamma(x) = \frac{\beta}{1+x^2(1+4+36\alpha^2(x))^2}$, $\mathcal{L}_{g_0}V(x)$ is the Lie derivative of $V(x)$ along $[0; \underline{g}^0(x)]$. The design parameter $0 < \beta < 1$ bounds the control input.

Theorem 3.7 guarantees that the control input $\alpha(x) + \nu(x)$ asymptotically stabilizes an open-loop unstable stable system if $\Omega \bigcap S = \{0\}$. A routine calculation shows that $\mathcal{L}_{\underline{f}_0}V(x) = 0$ for $\Omega = \{-1, 0, 1\}$. Additionally,

$$0 = \mathcal{L}_{\underline{g}^0}V(x) = -6x\alpha^2(x) \tag{3.40}$$

$$0 = \mathcal{L}_{[\underline{f}_0, \underline{g}^0]}V(x) \tag{3.41}$$

is satisfied for $x = 0$. Hence $\Omega \bigcap S = \{0\}$ for all $x \in \mathbb{R}$. Hence it can be con-

cluded that the control form $\alpha(x)+\nu(x)$ *globally asymptotically stabilizes* the origin. Reference [37] designed $u = \sqrt[3]{x}$ as the control law for the prescribed system using inversion which only locally regulates the system (3.31).

3.5.2.2 Results and Discussion

The proposed control law given in (3.37) and (3.39) was validated in simulation. The design parameter β was set to 0.9. The initial condition was chosen as $x(0) = 1$. The behaviour of the open-loop system and the system with control input $u = \alpha(x)$ is presented in Figure 3.4. As expected the open-loop behaviour is unstable and the system with $u = \alpha(x)$ stays at $x = 1$ for all time. The closed-loop response is shown in Figure 3.5. The initial magnitude of the control input $\nu(x)$ is small (specifically $\nu(x) = 0.00029$) but greater than zero to ensure the state of the system becomes less than 1. (Difficult to see in the figure. At time $t = 2$seconds, the state is $x(2) = 0.993$.) The control is dominated by $\alpha(x)$ since the dynamics $\underline{f}_0(x)$ inherently pushes the system toward origin. By construction in (3.39), the magnitude of $\nu(x)$ increases when the state reaches near origin to asymptotically regulate the dynamics. This is consistent with earlier conclusions that high-gain feedback is required to stabilize the origin. From then on the control is turned off and the system stays at origin for all future time. Note the discontinuous nature of the control is an artifact of the choice of $\alpha(x)$.

3.5.3 Continuously Stirred Tank Reactor

The second non-affine system is a constant volume reactor and the objective is to control the concentration of the tank through coolant flow. This example demonstrates asymptotic stabilization through design of $\alpha(x)$ using conditions of Theorem 3.9. The system is represented as

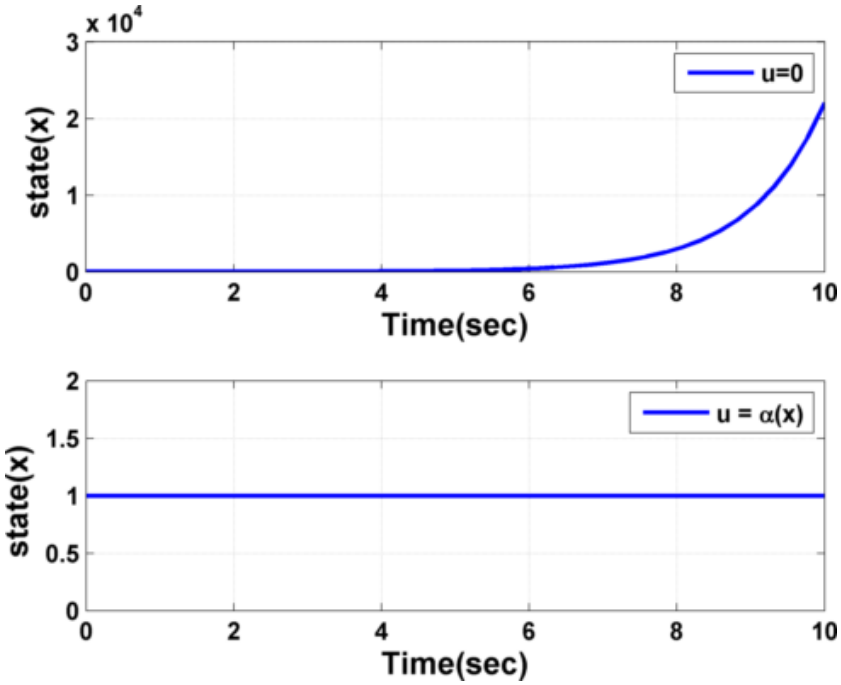

Figure 3.4: System response of (3.31) for $u = 0$ and $u = \alpha(x)$

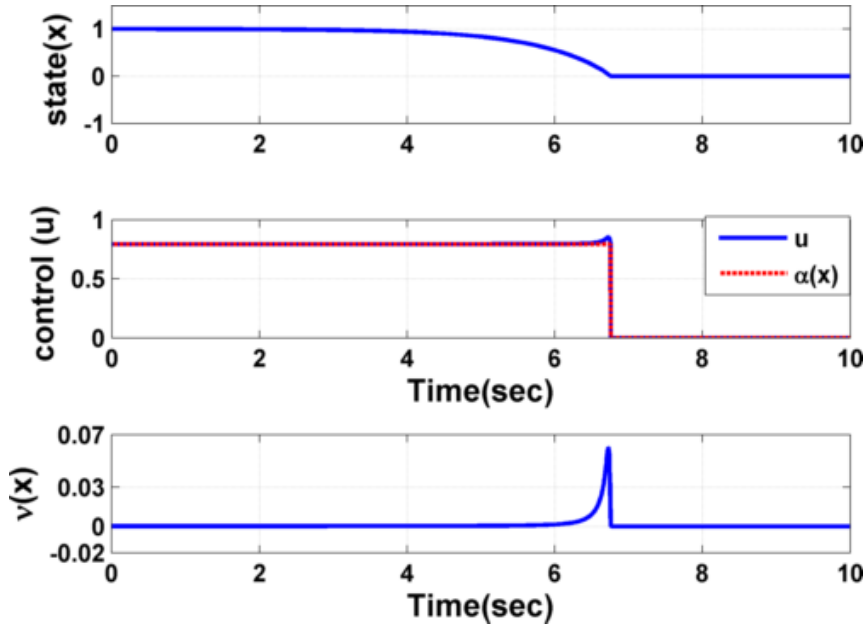

Figure 3.5: Closed-loop system response of (3.31) and control effort

$$\dot{x}_1 = 1 - x_1 - a_0 x_1 \exp^{(-10^4/x_2)} \tag{3.42a}$$

$$\dot{x}_2 = 350 - x_2 + a_1 x_1 \exp^{(-10^4/x_2)} + a_3 u(1 - \exp^{(-a_2/u)})(350 - x_2) \tag{3.42b}$$

where $0 < x_1 < 1$ is the concentration of the tank in mol/l, $x_2 > 350$ is the temperature of the tank in $^\circ K$ and $u \geq 0$ is the coolant flow rate in mol/min. The system parameters [68] are given in Table 3.1. The control influence in (3.42) is nonlinear in the control and not monotonic in any variable. This trend is presented in Figure 3.6. The two-dimensional surface plots obtained by varying temperature and coolant flow rate are shown in Figure 3.7 and Figure 3.8 respectively. Owing to this nonlinear behaviour previous studies have used neural-network based control designs to stabilize the concentration of the reactor[68], [69]. In this section an alternate constructive memoryless form of control is derived.

Table 3.1: Continuously stirred tank reactor model parameters

Parameter	Value
a_0	$7.2 \times 10^{10} min^{-1}$
a_1	1.44×10^{13}
a_2	6.987×10^2
a_3	0.01

3.5.3.1 Controller Design

The *first step* in developing a control law is to cast the system into form of Σ given in (2.3). However, the origin is not the equilibrium of the system given in (3.42). The equilibrium solutions are obtained by solving the following transcendental equations:

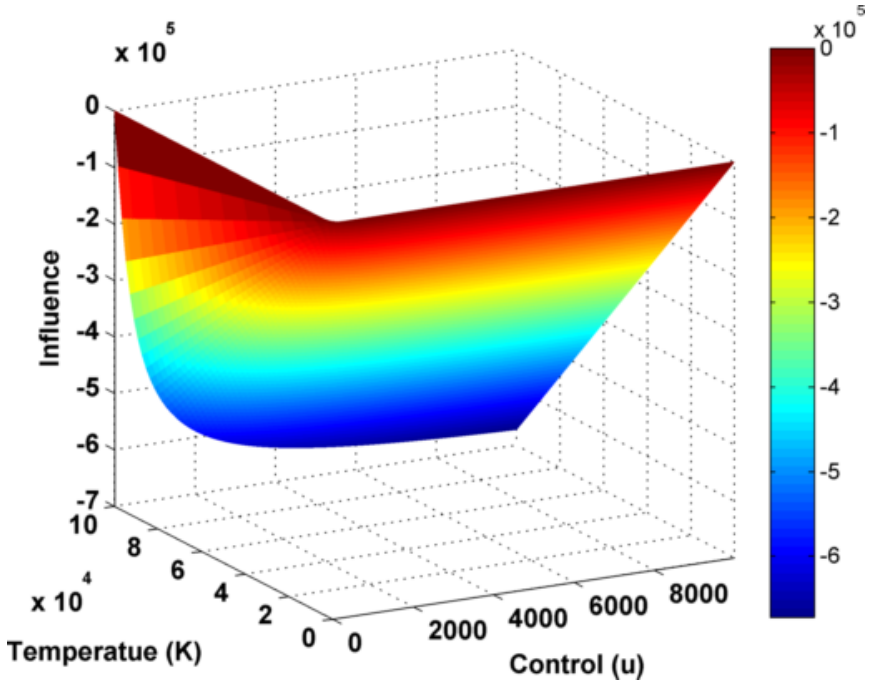

Figure 3.6: Control influence of the continuously stirred tank reactor

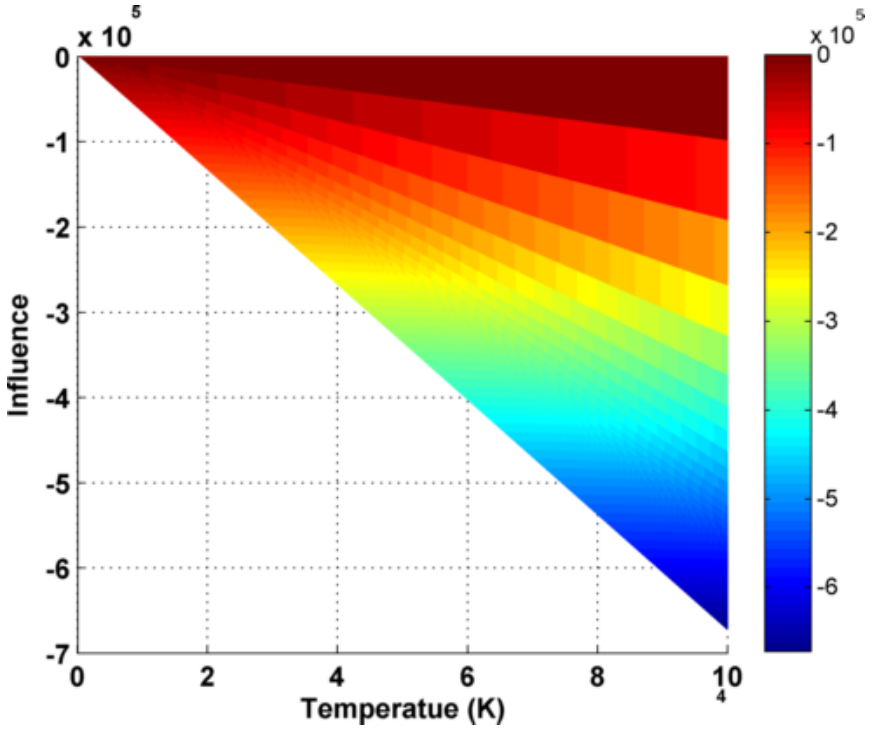

Figure 3.7: Control influence plotted with respect to temperature

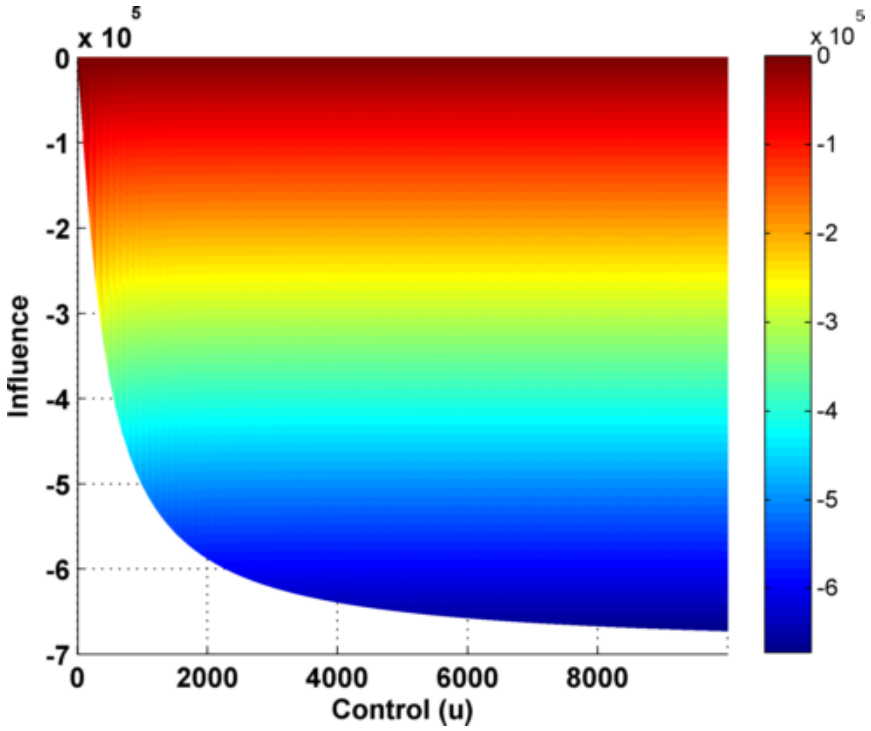

Figure 3.8: Control influence plotted with respect to coolant flow rate

$$0 = 1 - x_{1*} - a_0 x_{1*} \exp^{(-10^4/x_{2*})} \tag{3.43a}$$

$$0 = 350 - x_{2*} + a_1 x_{1*} \exp^{(-10^4/x_{2*})}. \tag{3.43b}$$

Rewrite the concentration as $x_{1*} = 1/(1 + a_0 \exp^{(-10^4/x_{2*})})$ and solve for roots of

$$0 = 350 - x_{2*} + \exp^{(-10^4/x_{2*})}[350a_0 + a_1 - a_0 x_{2*}]. \tag{3.44}$$

The algebraic equation given in (3.44) has a unique root $x_{2*} = 549.01257025°K$. Using (3.43) the unique root for concentration is $x_{1*} = 0.001128849277mol/l$. Define the states $e_1 = x_1 - x_{1*}$ and $e_2 = x_2 - x_{2*}$ to shift the equilibrium to origin. Routine calculation gives the following system:

$$\dot{e}_1 = c - e_1 - a_0(x_{1*} + e_1)\exp^{(-10^4/(x_{2*}+e_2))} \tag{3.45a}$$

$$\dot{e}_2 = d - e_2 + a_1(e_1 + x_{1*})\exp^{(-10^4/(x_{2*}+e_2))} + a_3 u(1 - \exp^{(-a_2/u)})(350 - x_2 - e_2) \tag{3.45b}$$

where $c = a_0 x_{1*}\exp^{(-10^4/x_{2*})}$ and $d = -a_1 x_{1*}\exp^{(-10^4/x_{2*})}$. In compact form

$$\bar{\mathbf{f}}(\mathbf{e}, 0) = \begin{bmatrix} c - e_1 - a_0(x_{1*} + e_1)\exp^{(-10^4/(x_{2*}+e_2))} \\ d - e_2 + a_1(e_1 + x_{1*})\exp^{(-10^4/(x_{2*}+e_2))} \end{bmatrix} \tag{3.46}$$

and

$$\bar{g}(\mathbf{e}, u) = a_3 u(1 - \exp^{(-a_2/u)})(350 - x_2 - e_2). \tag{3.47}$$

The *second step* proceeds with design of control input $\alpha(\mathbf{e})$ to stabilize (3.45). Suppose $V = \frac{1}{2}(e_1^2 + e_2^2)$ is a C^2 Lyapunov function. The correct sign of control is determined using condition (i) of Theorem 3.9, that is

$$sign(\bar{g}(\mathbf{e}, \alpha)) = -sign(e_2) \tag{3.48a}$$

$$\text{or } sign(a_3(350 - x_{2*} - e_2))sign(\alpha)sign(1 - \exp^{(-a_2/\alpha)}) = -sign(e_2) \tag{3.48b}$$

Using the facts that $sign(1 - \exp^{-(a_2/\alpha)}) = 1$ for all control values,

$$sign(\alpha) = -\frac{sign(e_2)}{sign(a_3(350 - x_{2*} - e_2))}. \tag{3.49}$$

The magnitude is computed using condition (ii) of Theorem 3.9

$$|\alpha| = \begin{cases} \beta\frac{|\langle\nabla V, \bar{\mathbf{f}}(\mathbf{e},0)\rangle|}{|a_3 e_2(350 - x_{2*} - e_2) - 1|} \text{ for } e_2 \neq 0 \\ 0 \text{ otherwise} \end{cases} \tag{3.50}$$

where the denominator is adjusted to avoid singularity and $\beta \geq 1$. The constant β

determines how negative the control influence is made. Value of $\beta = 1$ ensures that system is only Lyapunov stable where as for asymptotic stability guarantees $\beta > 1$. Hence, through Theorem 3.9 asymptotic stability in the operating region $0 < x_1 < 1$ and $x_2 > 350$ is guaranteed.

3.5.3.2 Results and Discussion

Controller performance for regulating the non-affine system (3.42) is presented in Figure 3.9 and Figure 3.10. The constant in (3.50) is set to $\beta = 1.5$ in simulation. The initial condition errors are $e_{10} = 0.001 mol/l$ and $e_{20} = 50°K$. The results show that origin is asymptotically stable equilibrium for (3.45) and consequently the trim solutions (x_{1*}, x_{2*}) are stabilized for (3.42). Notice the coolant flow rate settles down to origin once the trim solutions are obtained. Additionally, the control computed using (3.49) is positive as desired and no apriori information regarding the domain of solutions has been employed in the control design.

3.5.4 Magnetic Levitation System

Consider the control of a metallic ball with magnetic field being derived by the current passing through a coil. The current through the coil is the control input and the goal is to stabilize the vertical position of the ball to a specified reference. The dynamics of the system is described as

$$\dot{e}_1 = e_2, \tag{3.51a}$$

$$\dot{e}_2 = g - \frac{k_0}{(l_0 + x_{ref} + e_1)^2} u^2. \tag{3.51b}$$

The physical parameters of the system[70] are $g = 9.81 m/s^2$, $l_0 = 0.01m$ and $k_0 = 1 m/s^2/A^2$. The error in position of the ball is given by e_1 and error in velocity

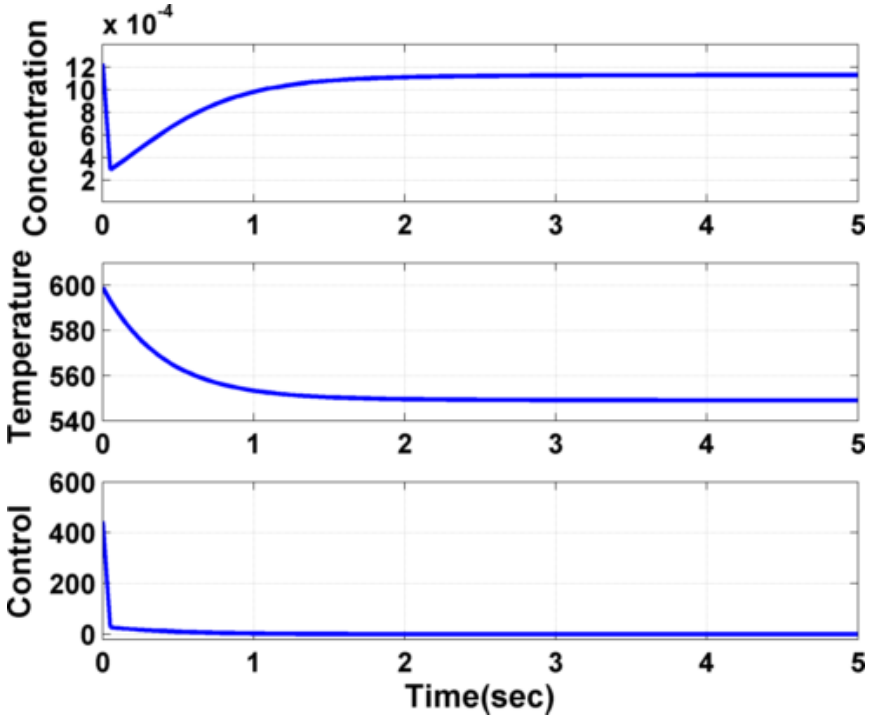

Figure 3.9: States and computed control of continuously stirred tank reactor

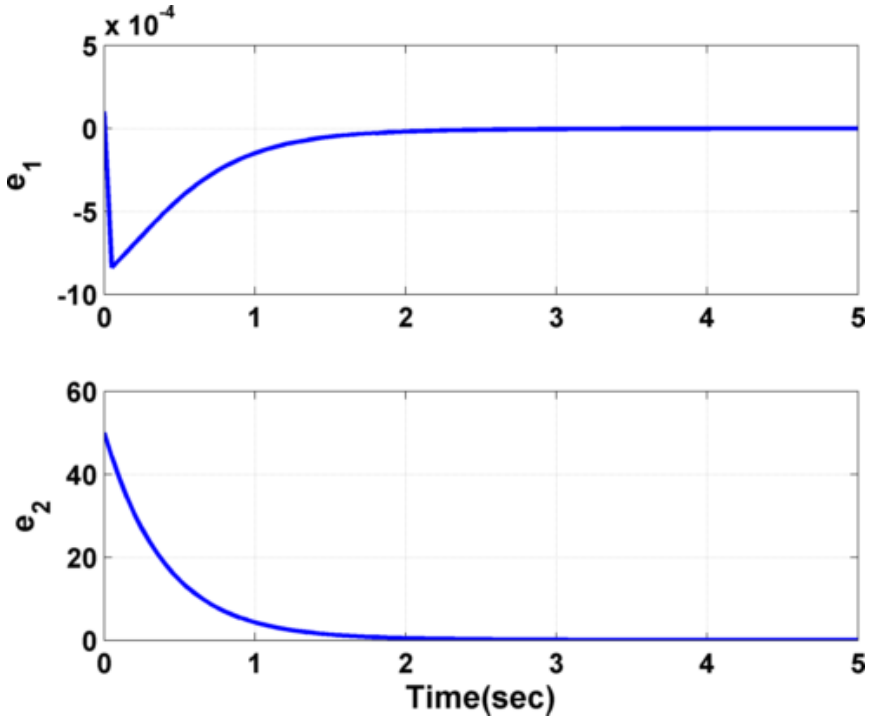

Figure 3.10: Error in system response and steady state solution for continuously stirred tank reactor

of the ball is represented as e_2. The desired position of ball is specified as $x_{ref} = 3mm$.

3.5.4.1 Controller Design

The control design proceeds by substituting the controller of the form $u(\mathbf{e}) = \alpha(\mathbf{e}) + \nu(\mathbf{e})$ into (3.51). This results in

$$\dot{e}_1 = e_2, \tag{3.52a}$$

$$\dot{e}_2 = g - \frac{k_0}{(l_0 + x_{ref} + e_1)^2}\alpha^2(\mathbf{e}) - \frac{2k_0\alpha(\mathbf{e})}{(l_0 + x_{ref} + e_1)^2}\nu(\mathbf{e}) - \frac{k_0}{(l_0 + x_{ref} + e_1)^2}\nu^2(\mathbf{e}). \tag{3.52b}$$

Compare (3.52) and (3.19) and notice

$$\underline{f}_0(\mathbf{e}) = \begin{bmatrix} e_2 \\ g - \frac{k_0}{(l_0+x_{ref}+e_1)^2}\alpha^2(\mathbf{e}) \end{bmatrix} \tag{3.53}$$

and

$$\underline{g}(\mathbf{e}, \nu) = -\frac{2k_0\alpha(\mathbf{e})}{(l_0 + x_{ref} + e_1)^2} - \frac{k_0}{(l_0 + x_{ref} + e_1)^2}\nu(\mathbf{e}). \tag{3.54}$$

Begin construction of $\alpha(\mathbf{e})$ by picking a positive-definite function $V(\mathbf{e}) = \frac{e_1^2+e_2^2}{2}$. The following choice of $\alpha(\mathbf{e})$

$$\alpha(\mathbf{e}) = \begin{cases} 0 & \text{if } e_1 + g \leq 0; \\ \sqrt{\frac{|e_1+g|}{k_0}}(l_0 + x_{ref} + e_1); & \text{otherwise} \end{cases} \tag{3.55}$$

satisfies condition given in Theorem 3.9 for the dynamics $\underline{f}_0(\mathbf{e})$ given in (3.53). The construction of $\nu(\mathbf{e})$ follows similar to the one-dimensional example and is derived[39] as

$$\nu(\mathbf{e}) = -\frac{\gamma(\mathbf{e})\mathcal{L}_{g_0}V(\mathbf{e})}{1 + ||\mathcal{L}_{g_0}V(\mathbf{e})||^2} \tag{3.56}$$

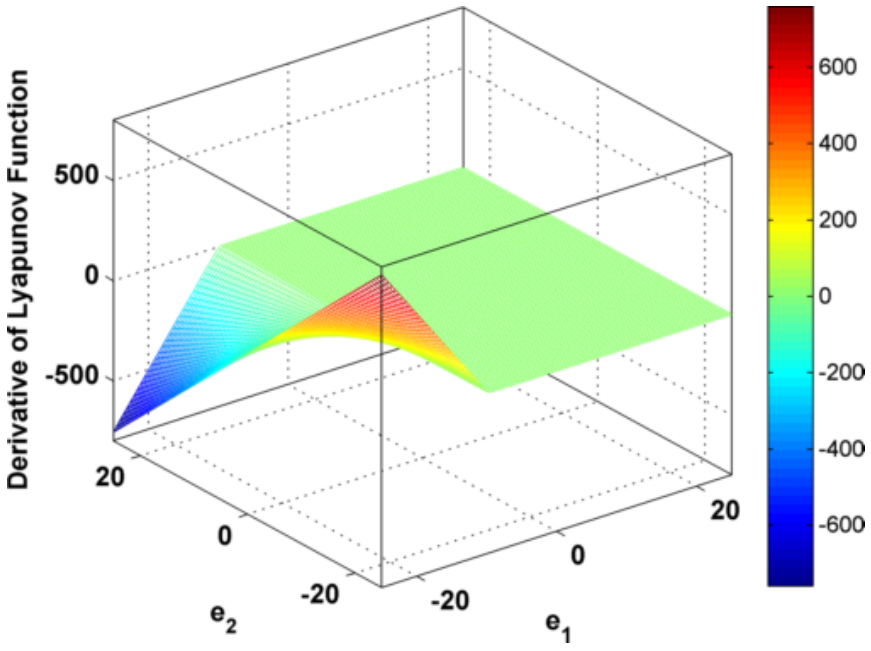

Figure 3.11: Time derivative of the Lyapunov function along trajectories of (3.51) with $u = \alpha(e)$ and $\nu(e) = 0$

where

$$\rho(\mathbf{e}) = -\frac{2k_0}{(l_0 + x_{ref} + e_1)^2},$$
$$\gamma(\mathbf{e}) = \frac{\beta}{1 + [||\frac{\partial V}{\partial \mathbf{e}}||\rho(\mathbf{e})]^2} \tag{3.57}$$

$$g_0(\mathbf{e}) = \begin{bmatrix} 0 \\ -\frac{2k_0\alpha(\mathbf{e})}{(l_0+x_{ref}+e_1)^2} \end{bmatrix} \tag{3.58}$$
$$\mathcal{L}_{g_0}V(\mathbf{e}) = -\frac{2k_0e_2\alpha(\mathbf{e})}{(l_0 + x_{ref} + e_1)^2},$$

define the appropriate functions.

Theorem 3.7 guarantees asymptotic stabilization of (3.51) by control $u(\mathbf{e}) = \alpha(\mathbf{e}) + \nu(\mathbf{e})$ only if zero-state detectability conditions are met. In order to determine

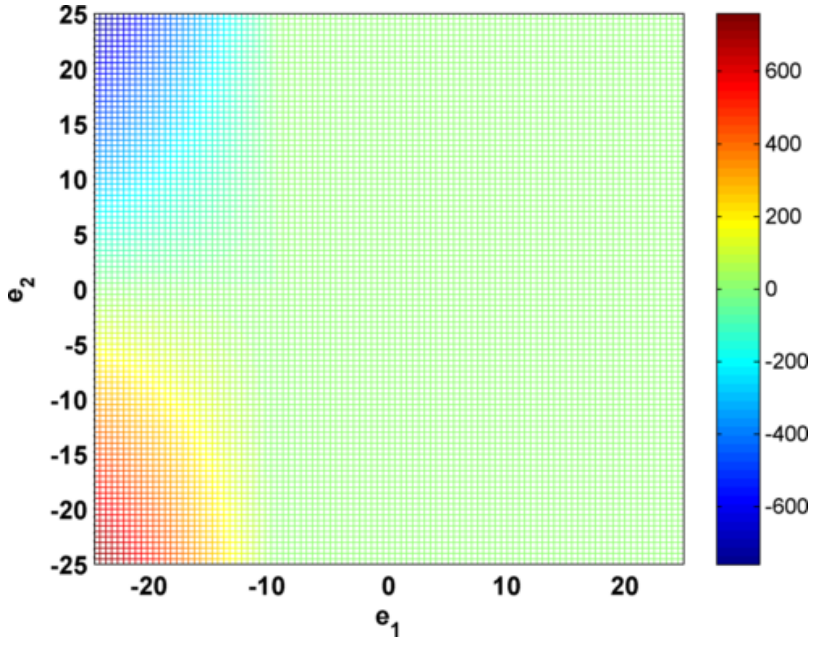

Figure 3.12: State space showing the different values of the time derivative of Lyapunov function for (3.51)

the set Ω, substitute (3.55) into $\underline{f}_0(\mathbf{e})$ given in (3.53). This results in

$$\underline{f}_0(\mathbf{e}) = \begin{bmatrix} e_2 \\ -|e_1 + g| + g \end{bmatrix}. \tag{3.59}$$

Using (3.59) and quadratic Lyapunov function $V(\mathbf{e})$ the set is obtained as $\Omega = \{e_1 \in [-g, \infty) \bigcap e_2 = 0\}$. This set is graphically represented in Figure 3.11 and Figure 3.12. Careful examination shows that the unstable maglev system cannot be stabilized in the region $(e_1 < -g, e_2 < 0)$. But physically all points $e_1 < 0$ can be discarded as the vertical position of the ball can only take positive values. Hence, it is concluded that the the choice of $\alpha(\mathbf{e})$ given in (3.55) stabilizes all physically feasible positions of the ball in the Lyapunov sense.

The set S is determined by setting $\mathcal{L}_{\mathbf{g}_0} V(\mathbf{e}) = 0$ and $\mathcal{L}_{[\underline{f}_0, \mathbf{g}_0]} V(\mathbf{e}) = 0$ where $\mathbf{g}_0 = [0; \underline{g}_0]$. This gives the solution $S = \{e_1 = -g \text{ or } e_1 = 0 \bigcap e_2 = 0\}$. Hence the

only physically feasible solution is $(e_1 = 0, e_2 = 0)$ and the set $\Omega \bigcap S = \{\mathbf{0}\}$. Thus, *asymptotic stability* is guaranteed by Theorem 3.7 in the region $(e_1 \geq 0, e_2 \in \mathbb{R})$.

3.5.4.2 Results and Discussion

The simulation results of the closed-loop magnetic levitation system is presented in Figure 3.13 and Figure 3.14. The design parameter β in this case was set to 0.5. Notice that the control $u = \alpha(\mathbf{e})$ stabilizes the unstable maglev system in Lyapunov sense. Recall, the control input is the current through the coil and varying this changes the strength of the magnetic field. The effect is clearly visible in Figure 3.13. The error in position and velocity of the ball varies with change in strength of the magnetic field. The combined control $u(\mathbf{e}) = \alpha(\mathbf{e}) + \nu(\mathbf{e})$ ensures that this Lyapunov stable system globally settles down at the origin (Seen in Figure 3.14). Notice that the control input settles down to a constant value which is consistent with the physics of the problem.

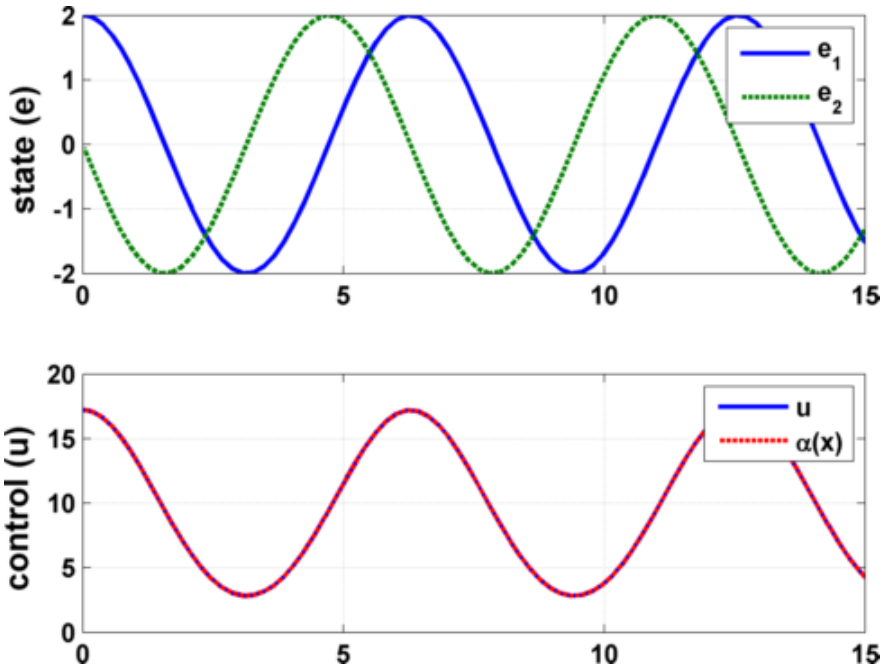

Figure 3.13: Response of the magnetic levitation system for $u = \alpha(\mathbf{e})$

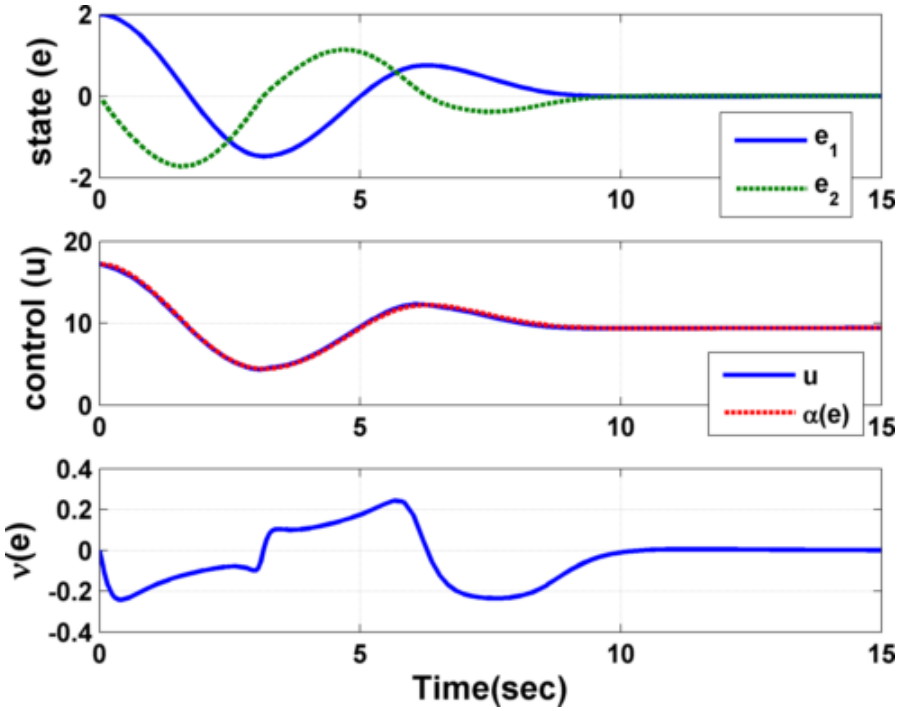

Figure 3.14: Closed-loop response of the magnetic levitation system and applied control

3.6 Closing Remarks

In this section the design procedure for analytical construction of control for unstable non-affine systems was proposed. Toward this end, several new results were derived and analyzed. This work extended the applicability of the well-established control law design procedures to unstable non-affine systems. The method presented provides a feedback stabilizer for general class of systems. The analytical developments and the simulation results indicate that $\alpha(x)$ makes the system passive, while the control $\nu(x)$ provides the required perturbation to establish stabilization (clearly seen in results of the magnetic levitation system). Furthermore, the method proposed does not require the control influence to be non-singular throughout the domain of interest. The benefits and limitations of the proposed methods are summarized below:

3.6.1 Benefits

1. Sufficient conditions for asymptotic stabilization a general non-affine system with static compensation have been derived that are independent of the operating conditions of the system.

2. The proposed control laws are real-time implementable and do not require immense offline processing unlike some of the switching schemes [48] proposed in literature.

3. No assumptions regarding the properties of the control influence have been made. Dynamic compensation techniques in [40], [46] require the control influence to be monotonic and non-zero for all values of state and control. Unlike these methods, the proposed method are general and can stabilize the system of the form $\dot{x} = x - 2xu^4$ by appropriate design of $\alpha(x)$.

4. Owing to the energy-based concept that is utilized for construction of the control, the results obtained are consistent with the physics of the problem and do not violate system constraints.

5. Numerical examples illustrates that the nature of the control function $\alpha(\mathbf{x})$ is continuous but not differentiable. This result is obtained by satisfying the nonlinear inequality of Theorem 3.9. It is interesting to note that this result has been proven in [3][Corollary 5.8.8]. It was shown that any nonlinear systems whose linear counterparts are unstable cannot be locally C^1 stabilizable. Thus, the derived control laws arrive at this well-known result without making any prior assumptions about the nature of the vector fields.

3.6.2 Limitations

1. Satisfying sufficient conditions of Theorem 3.7 sometimes requires iteration and is not constructive.

2. The theoretical developments and conclusions from simulation results are valid only for time-invariant control non-affine problems.

4. ASYMPTOTIC STABILIZATION AND SLOW STATE TRACKING OF CONTROL-AFFINE, TWO TIME SCALE SYSTEMS[1]

4.1 Introduction

This section discusses methods of solution to address the second objective detailed in Section 2, repeated below for convenience:

$$\dot{\mathbf{x}} = \mathbf{f_1}(\mathbf{x}, \mathbf{z}) + \mathbf{f_2}(\mathbf{x}, \mathbf{z})\mathbf{u} \tag{2.5a}$$

$$\epsilon\dot{\mathbf{z}} = \mathbf{g_1}(\mathbf{x}, \mathbf{z}) + \mathbf{g_2}(\mathbf{x}, \mathbf{z})\mathbf{u} \tag{2.5b}$$

where $\mathbf{x} \in \mathbb{R}^m$ is vector of slow variables, $\mathbf{z} \in \mathbb{R}^n$ is the vector of fast variables, $\mathbf{u} \in \mathbb{R}^p$ is control input to be determined and initial conditions for the state variables have been specified. The control objective is to enforce the slow state to asymptotically track an atleast twice continuously differentiable time-varying bounded specified trajectory, or $\mathbf{x}(t) \to \mathbf{x}_r(t)$ as $t \to \infty$. It is assumed that the control is sufficiently fast than all the system variables.

Although many researchers have studied the control problem for standard singularly perturbed systems, the feedback control design for non-standard singularly perturbed systems remains an open research area. The lack of an explicit small parameter and complexity of constructing the slow manifold are essential difficulties. This is because non-standard systems cannot be decomposed into reduced slow and fast systems using the asymptotic expansion technique[15]. The alternative geometric approach describes the motion of the full-order system using the concept

[1]Parts of this section reprinted with permission from "Kinetic state tracking for a class of singularly perturbed systems", Siddarth, Anshu and Valasek, John, 2011. Journal of Guidance, Control, and Dynamics, Vol. 34, No. 3, pp 734-749, Copyright ©2011 by Siddarth, Anshu and Valasek, John.

of invariant manifolds and produces the exact same reduced-order models, but with different assumptions about the system. Asymptotic methods assume that the dynamical system possesses isolated roots, while the geometric approach is more general and takes into consideration multiple non-isolated roots of nonlinear systems. The geometric approach is employed as the model-reduction in the proposed schemes. At the heart of each control scheme lies the concepts of geometric singular perturbation theory and composite Lyapunov approach, with details in Appendices A and B.

This section is organized as follows. Reduced-order systems for the dynamical model under consideration are constructed using Geometric Singular Perturbation Theory (GSPT), and are detailed in Section 4.2. Sections 4.3 and 4.4 present two different approaches developed by the author to accomplish asymptotic tracking of affine-in-control singularly perturbed systems. The benefits and limitations of both the approaches are identified and performance is demonstrated through numerical simulation. Concluding remarks and salient features of the developed approaches are discussed in Section 4.5.

4.2 Model Reduction

Following the definitions given in Appendix A, the system considered in (2.5) is the slow system. Equivalent representation in the fast time scale $\tau = \frac{t-t_0}{\epsilon}$ with t_0 being the initial time is given as

$$\mathbf{x}' = \epsilon \left[\mathbf{f_1}(\mathbf{x}, \mathbf{z}) + \mathbf{f_2}(\mathbf{x}, \mathbf{z})\mathbf{u}\right] \tag{4.1a}$$

$$\mathbf{z}' = \mathbf{g_1}(\mathbf{x}, \mathbf{z}) + \mathbf{g_2}(\mathbf{x}, \mathbf{z})\mathbf{u}. \tag{4.1b}$$

The following reduced-order models are obtained by formally substituting $\epsilon = 0$ in (2.5) and (4.1) respectively.

Reduced slow system is:

$$\dot{\mathbf{x}} = \mathbf{f_1}(\mathbf{x}, \mathbf{z}) + \mathbf{f_2}(\mathbf{x}, \mathbf{z})\mathbf{u} \tag{4.2a}$$

$$\mathbf{0} = \mathbf{g_1}(\mathbf{x}, \mathbf{z}) + \mathbf{g_2}(\mathbf{x}, \mathbf{z})\mathbf{u} \tag{4.2b}$$

and *reduced fast system* is:

$$\mathbf{x}' = \mathbf{0} \tag{4.3a}$$

$$\mathbf{z}' = \mathbf{g_1}(\mathbf{x}, \mathbf{z}) + \mathbf{g_2}(\mathbf{x}, \mathbf{z})\mathbf{u} \tag{4.3b}$$

The dynamics of the resulting reduced slow system is restricted to m dimensions and constrained to lie upon a smooth manifold defined by the set

$$\mathcal{M}_0 : \mathbf{z} = \mathbf{h}_0(\mathbf{x}, \mathbf{u}) \tag{4.4}$$

satisfying the algebraic equation (4.2b) that are identically the fixed points of (4.3b). Thus the flow on this manifold is described by the differential equation

$$\dot{\mathbf{x}} = \mathbf{f_1}(\mathbf{x}, \mathbf{h}_0(\mathbf{x}, \mathbf{u})) + \mathbf{f_2}(\mathbf{x}, \mathbf{h}_0(\mathbf{x}, \mathbf{u}))\mathbf{u} \tag{4.5}$$

if the reduced fast system is stable about the manifold $\mathcal{M}_0$. Furthermore GSPT concludes that the solutions of the full-order slow system lie on the manifold

$$\mathcal{M}_\epsilon : \mathbf{z} = \mathbf{h}(\mathbf{x}, \mathbf{u}, \epsilon) \tag{4.6}$$

and are $O(\epsilon)$ close to $\mathcal{M}_0$.

4.3 Approach I: Modified Composite Control

The thrust of asymptotic stabilization of system in (2.5) using composite control technique[20] lies on the identification of an isolated manifold $\mathcal{M}_0$ for reduced slow system and ensuring that this manifold is the unique stabilizing fixed point of the reduced fast system. However, due to the underlying nonlinearity of the system this manifold cannot always be determined analytically in terms of the slow variables and the control signals. The developed approach shows that it is possible to accomplish asymptotic stabilization and bounded tracking under certain conditions using an approximation of the manifold and modified composite control technique.

The remainder of section 4.3 is arranged as follows: Firstly, an important connection between the center manifold theory and the manifold under interest is revisited. This result is then used to formulate the control law and analyze stability of the closed-loop system. The technique is verified in simulation for a generic enzyme kinetic model and an F/A-18A Hornet model.

4.3.1 Center Manifold and Its Computation

Fenichel's theorem (Theorem A.0.1 in Appendix A) is a powerful tool to study the behaviour of stiff dynamical systems. It asserts that the solutions of the full-order singularly perturbed system can be approximated by the solution of the lower-dimensional reduced slow system, provided the fast dynamics are stable about the manifold $\mathcal{M}_0$. In other words, there exists an invariant manifold $\mathcal{M}_\epsilon$ that is $O(\epsilon)$ close to $\mathcal{M}_0$. But this result does not provide the procedure to compute the manifold $\mathcal{M}_0$. Results from center manifold theory are recalled to obtain an approximate analytical form of the manifold in terms of the system state variables.

To demonstrate these concepts, consider the following open-loop counterpart of

system given in (2.5)

$$\dot{\mathbf{x}} = \mathbf{f_1}(\mathbf{x}, \mathbf{z}) \tag{4.7a}$$

$$\epsilon\dot{\mathbf{z}} = \mathbf{g_1}(\mathbf{x}, \mathbf{z}). \tag{4.7b}$$

Assuming the fast dynamics is stabilizing, then the manifold $\mathcal{M}_\epsilon$ defined as

$$\mathcal{M}_\epsilon : \mathbf{z} = \mathbf{h}(\mathbf{x}, \epsilon) \tag{4.8}$$

is invariant for some $t \geq t^*$. Thus, differentiating this expression with respect to t,

$$\dot{\mathbf{z}} \;=\; \frac{\partial \mathbf{h}}{\partial \mathbf{x}}\dot{\mathbf{x}} \tag{4.9}$$

and using (4.7) results in the *manifold condition*

$$\epsilon\frac{\partial \mathbf{h}}{\partial \mathbf{x}}\mathbf{f_1}(\mathbf{x}, \mathbf{h}(\mathbf{x}, \epsilon)) = \mathbf{g_1}(\mathbf{x}, \mathbf{h}(\mathbf{x}, \epsilon)). \tag{4.10}$$

Note that substituting $\epsilon = 0$ in the manifold condition returns the algebraic equation satisfied by set of points on the manifold $\mathcal{M}_0$. Although implicit function theorem guarantees the existence of the manifold, the exact computation of the manifold using (4.10) is very difficult since solving this condition is equivalent to solving the complete nonlinear system. One approximate approach is to substitute a perturbation expansion for $\mathbf{h}(\mathbf{x}, \epsilon) = \mathbf{h}_0(\mathbf{x}) + \epsilon\mathbf{h}_1(\mathbf{x}) + O(\epsilon^2)$ into (4.10) and then solve for each order of $\mathbf{h}(\mathbf{x}, \epsilon)$. This perturbation expansion may be employed if the domain of interest is known. However in control formulation the inverse problem is usually encountered. The domain of interest depends on the controller form which in turn depends on the analytical manifold expressed as smooth function of its arguments.

This problem is addressed by following the approach proposed in [71] and is discussed below.

The computation procedure proposed in [71] has been laid out for dynamical systems with center manifolds. For completeness, the first step is to check whether the manifold $\mathcal{M}_\epsilon$ is the center manifold of the singularly perturbed system. In order to study this behaviour fast system is rewritten using the technique called suspension [72]

$$\begin{aligned} \mathbf{x}' &= \epsilon \mathbf{f_1}(\mathbf{x}, \mathbf{z}) && (4.11a) \\ \epsilon' &= 0 && (4.11b) \\ \mathbf{z}' &= \mathbf{g_1}(\mathbf{x}, \mathbf{z}). && (4.11c) \end{aligned}$$

Assume that the origin is the fixed point of (4.11), that is $\mathbf{f_1}(\mathbf{0}, \mathbf{0}) = \mathbf{0}$ and $\mathbf{g_1}(\mathbf{0}, \mathbf{0}) = \mathbf{0}$. Then the perturbed system obtained by linearizing these equations about the origin ($\mathbf{x} = \mathbf{0}, \epsilon = 0, \mathbf{h}(\mathbf{0}, 0) = \mathbf{0}$) is written in compact form as

$$\begin{aligned} \Delta \mathbf{w}' &= F\mathbf{w} + F_1\mathbf{z} && (4.12a) \\ \Delta \mathbf{z}' &= L\mathbf{z} + L_1\mathbf{w} && (4.12b) \end{aligned}$$

where $\mathbf{w} = [\mathbf{x}, \epsilon]^T$, $\Delta\mathbf{w}$ and $\Delta\mathbf{z}$ denote the perturbation quantities while F, F_1, L, and L_1 are constant matrices of appropriate size. Note that since the system is linearized about $\epsilon = 0$, all eigenvalues of F have zero real parts while all eigenvalues of L have negative real parts. Thus, it is concluded that the manifold $\mathcal{M}_\epsilon$ is precisely *the center manifold* and it spans the generalized eigenvectors associated with eigenvalues with zero real parts. This manifold is defined for all small values of the slow state $\mathbf{x}$ and the perturbation parameter ϵ. The requirement on eigenvalues of F supports

the existence of time scales in the system, for if the eigenvalues were nonzero then all states would be fast variables and the system is not singularly perturbed. This suggests that the eigenvalue restriction on F is always satisfied by systems with the multiple time scale property. The other requirement of negative eigenvalues of L is to ensure that the trajectories not on the manifold approach it in forward time.

From the above analysis $\mathbf{h}(\mathbf{x}, \epsilon)$ is known to be the center manifold. If the origin is the fixed point of the linearized system, then the theorem from [71] asserts that one can approximate $\mathbf{h}(\mathbf{x}, \epsilon)$ to any degree of accuracy. For functions $\phi : \mathbb{R}^m \times \mathbb{R} \to \mathbb{R}^n$ which are C^{r-1} (r defined as in Assumption A.1 of Appendix A) in the neighbourhood of the origin, the operator is defined as

$$(M\phi)(\mathbf{x}, \epsilon) = \epsilon \frac{\partial \phi}{\partial \mathbf{x}} \mathbf{f_1}(\mathbf{x}, \phi(\mathbf{x}, \epsilon)) - \mathbf{g_1}(\mathbf{x}, \phi(\mathbf{x}, \epsilon)). \tag{4.13}$$

Note that by (4.10) $(M\mathbf{h})(\mathbf{x}, \epsilon) = \mathbf{0}$.

Definition 4.3.1. [71] Let $\phi : \mathbb{R}^m \times \mathbb{R} \to \mathbb{R}^n$ satisfy $\phi(\mathbf{0}, 0) = \mathbf{0}$ and $|(M\phi)(\mathbf{x}, \epsilon)| = O(C(\mathbf{x}, \epsilon))$ for $|\mathbf{x}| \to 0$ and $\epsilon \to 0$ where $C(.)$ is a polynomial of degree greater than one, then

$$|\mathbf{h}(\mathbf{x}, \epsilon) - \phi(\mathbf{x}, \epsilon)| = O(C(\mathbf{x}, \epsilon)). \tag{4.14}$$

Definition 4.3.1 implies that an approximate function $\phi(\mathbf{x}, \epsilon)$ can be determined for small values of $\mathbf{x}$ and ϵ. The condition $\phi(\mathbf{0}, 0) = \mathbf{0}$ is to ensure that the origin remains the fixed point. To demonstrate the procedure consider the following example [71]:

$$\dot{x} = xz + ax^3 + bz^2x \tag{4.15a}$$

$$\epsilon \dot{z} = -z + cx^2 + dx^2 z \tag{4.15b}$$

The following system is obtained upon linearization about the origin:

$$\Delta x' = 0 \tag{4.16a}$$

$$\Delta \epsilon' = 0 \tag{4.16b}$$

$$\Delta z' = -1. \tag{4.16c}$$

It is seen that the system possesses a center manifold $z = h(x, \epsilon)$. To approximate h, define:

$$(M\phi)(x,\epsilon) = \epsilon \frac{\partial \phi}{\partial x}\left[x\phi(x,\epsilon) + ax^3 + b\phi^2(x,\epsilon)x\right] + \phi(x,\epsilon) - cx^2 - dx^2\phi(x,\epsilon) \tag{4.17}$$

Hence if $\phi(x, \epsilon) = cx^2$ is chosen, then $(M\phi)(x, \epsilon) = O\left(|x^4| + |\epsilon x^4|\right)$ and from the Definition 4.3.1 it is concluded $h(x, \epsilon) = cx^2 + O\left(|x^4| + |\epsilon x^4|\right)$. Since the reduced fast system is stabilizing, the stability of the complete system can be analyzed by studying the flow on the manifold

$$\dot{x} = (a + c)x^3 + bc^2x^5 + O(|x^5| + |\epsilon x^5|). \tag{4.18}$$

4.3.2 Control Law Development

The central idea in the formulation is the following. It is well understood that the complete system dynamics remains $O(\epsilon)$ close to the reduced slow system, if the reduced fast system is stabilizing about the manifold $\mathcal{M}_0$. This fact is employed to develop a stable closed-loop system. It is proposed that two separate stabilizing controllers be designed for each of the subsystems about the manifold approximation determined using center manifold theory and their composite be fed to the complete system.

The objective is to augment the two time scale system with state feedback controllers such that the system follows a specified continuous twice differentiable bounded trajectory $\mathbf{x}_r(t)$. The first step is to transform the system given in (2.5) into a non-autonomous stabilization problem. Define the error signal as $\tilde{\mathbf{x}}(t) = \mathbf{x}(t) - \mathbf{x}_r(t)$. Then

$$\dot{\tilde{\mathbf{x}}} = \mathbf{f_1}(\tilde{\mathbf{x}}, \mathbf{x}_r, \mathbf{z}) + \mathbf{f_2}(\tilde{\mathbf{x}}, \mathbf{x}_r, \mathbf{z})\mathbf{u} - \dot{\mathbf{x}}_r \tag{4.19a}$$

$$\epsilon\dot{\mathbf{z}} = \mathbf{g_1}(\tilde{\mathbf{x}}, \mathbf{x}_r, \mathbf{z}) + \mathbf{g_2}(\tilde{\mathbf{x}}, \mathbf{x}_r, \mathbf{z})\mathbf{u}. \tag{4.19b}$$

The objective is to seek the control vector of the form $\mathbf{u} = \mathbf{u}_s + \mathbf{u}_f$, where *slow controller*

$$\mathbf{u}_s = \Gamma_s\left(\tilde{\mathbf{x}}, \mathbf{x}_r, \dot{\mathbf{x}}_r\right) \tag{4.20}$$

and *fast controller*

$$\mathbf{u}_f = \Gamma_f\left(\tilde{\mathbf{x}}, \mathbf{z}, \mathbf{x}_r, \dot{\mathbf{x}}_r\right). \tag{4.21}$$

Substituting the controls into (4.19)

$$\dot{\tilde{\mathbf{x}}} = \mathbf{f_1}(\tilde{\mathbf{x}}, \mathbf{x}_r, \mathbf{z}) + \mathbf{f_2}(\tilde{\mathbf{x}}, \mathbf{x}_r, \mathbf{z})\left[\Gamma_s\left(\tilde{\mathbf{x}}, \mathbf{x}_r, \dot{\mathbf{x}}_r\right) + \Gamma_f\left(\tilde{\mathbf{x}}, \mathbf{z}, \mathbf{x}_r, \dot{\mathbf{x}}_r\right)\right] - \dot{\mathbf{x}}_r \tag{4.22a}$$

$$\epsilon\dot{\mathbf{z}} = \mathbf{g_1}(\tilde{\mathbf{x}}, \mathbf{x}_r, \mathbf{z}) + \mathbf{g_2}(\tilde{\mathbf{x}}, \mathbf{x}_r, \mathbf{z})\left[\Gamma_s\left(\tilde{\mathbf{x}}, \mathbf{x}_r, \dot{\mathbf{x}}_r\right) + \Gamma_f\left(\tilde{\mathbf{x}}, \mathbf{z}, \mathbf{x}_r, \dot{\mathbf{x}}_r\right)\right] \tag{4.22b}$$

Assume that the right-hand side of (4.22) is C^2, i.e. the vector fields satisfy Assumption A.1 with $r = 2$. From Fenichel's theorem A.0.1 it can be concluded that there exists a manifold

$$\mathcal{M}_\epsilon : \mathbf{z} = \mathbf{h}(\tilde{\mathbf{x}}, \epsilon, \mathbf{x}_r, \dot{\mathbf{x}}_r) \tag{4.23}$$

that satisfies the manifold condition

$$\begin{aligned}\epsilon\frac{\partial \mathbf{h}}{\partial t}+\epsilon\frac{\partial \mathbf{h}}{\partial \tilde{\mathbf{x}}}\dot{\tilde{\mathbf{x}}} &= \mathbf{g_1}(\tilde{\mathbf{x}},\mathbf{x}_r,\mathbf{h}(\tilde{\mathbf{x}},\epsilon,\mathbf{x}_r,\dot{\mathbf{x}}_r))+\mathbf{g_2}(\tilde{\mathbf{x}},\mathbf{x}_r,\mathbf{h}(\tilde{\mathbf{x}},\epsilon,\mathbf{x}_r,\dot{\mathbf{x}}_r))\Gamma_s\left(\tilde{\mathbf{x}},\mathbf{x}_r,\dot{\mathbf{x}}_r\right)\\ &+ \mathbf{g_2}\left(\tilde{\mathbf{x}},\mathbf{x}_r,\mathbf{h}(\tilde{\mathbf{x}},\epsilon,\mathbf{x}_r,\dot{\mathbf{x}}_r)\right)\Gamma_f\left(\tilde{\mathbf{x}},\mathbf{h}(\tilde{\mathbf{x}},\epsilon,\mathbf{x}_r,\dot{\mathbf{x}}_r),\mathbf{x}_r,\dot{\mathbf{x}}_r\right). \qquad (4.24)\end{aligned}$$

Note that the manifold is time-dependent since the system under consideration is non-autonomous due to the time-varying nature of $\mathbf{x}_r(t)$. Define the error between the fast states and the manifold $\mathcal{M}_\epsilon$ as $\tilde{\mathbf{z}} = \mathbf{z} - \mathbf{h}(\tilde{\mathbf{x}},\epsilon,\mathbf{x}_r,\dot{\mathbf{x}}_r)$. The transformed system with the origin as the equilibrium is expressed as

$$\begin{aligned}\dot{\tilde{\mathbf{x}}} &= \mathbf{f_1}\left(\tilde{\mathbf{x}},\mathbf{x}_r,\tilde{\mathbf{z}},\mathbf{h}(\tilde{\mathbf{x}},\epsilon,\mathbf{x}_r,\dot{\mathbf{x}}_r)\right)+\mathbf{f_2}\left(\tilde{\mathbf{x}},\mathbf{x}_r,\tilde{\mathbf{z}},\mathbf{h}(\tilde{\mathbf{x}},\epsilon,\mathbf{x}_r,\dot{\mathbf{x}}_r)\right)\Gamma_s\left(\tilde{\mathbf{x}},\mathbf{x}_r,\dot{\mathbf{x}}_r\right)\\ &+ \mathbf{f_2}\left(\tilde{\mathbf{x}},\mathbf{x}_r,\tilde{\mathbf{z}},\mathbf{h}(\tilde{\mathbf{x}},\epsilon,\mathbf{x}_r,\dot{\mathbf{x}}_r)\right)\Gamma_f\left(\tilde{\mathbf{x}},\tilde{\mathbf{z}},\mathbf{h}(\tilde{\mathbf{x}},\epsilon,\mathbf{x}_r,\dot{\mathbf{x}}_r),\mathbf{x}_r,\dot{\mathbf{x}}_r\right)-\dot{\mathbf{x}}_r \qquad (4.25a)\\ \epsilon\dot{\tilde{\mathbf{z}}} &= \mathbf{g_1}\left(\tilde{\mathbf{x}},\mathbf{x}_r,\tilde{\mathbf{z}},\mathbf{h}(\tilde{\mathbf{x}},\epsilon,\mathbf{x}_r,\dot{\mathbf{x}}_r)\right)+\mathbf{g_2}\left(\tilde{\mathbf{x}},\mathbf{x}_r,\tilde{\mathbf{z}},\mathbf{h}(\tilde{\mathbf{x}},\epsilon,\mathbf{x}_r,\dot{\mathbf{x}}_r)\right)\Gamma_s\left(\tilde{\mathbf{x}},\mathbf{x}_r,\dot{\mathbf{x}}_r\right)\\ &+ \mathbf{g_2}\left(\tilde{\mathbf{x}},\mathbf{x}_r,\tilde{\mathbf{z}},\mathbf{h}(\tilde{\mathbf{x}},\epsilon,\mathbf{x}_r,\dot{\mathbf{x}}_r)\right)\Gamma_f\left(\tilde{\mathbf{x}},\tilde{\mathbf{z}},\mathbf{h}(\tilde{\mathbf{x}},\epsilon,\mathbf{x}_r,\dot{\mathbf{x}}_r),\mathbf{x}_r,\dot{\mathbf{x}}_r\right) \qquad (4.25b)\\ &- \epsilon\frac{\partial \mathbf{h}}{\partial t}-\epsilon\frac{\partial \mathbf{h}}{\partial \tilde{\mathbf{x}}}\dot{\tilde{\mathbf{x}}}.\end{aligned}$$

Note that the error $\tilde{\mathbf{z}} = \mathbf{0}$ when the manifold condition is satisfied. It is known that the exact manifold $\mathbf{h}(\tilde{\mathbf{x}},\epsilon,\mathbf{x}_r,\dot{\mathbf{x}}_r)$ is impossible to compute. Let $\phi(\tilde{\mathbf{x}},\mathbf{x}_r,\dot{\mathbf{x}}_r,\Gamma_s)$ be an approximate manifold obtained using the procedure presented in subsection 4.3.1. The approximate manifold is chosen to contain terms independent of ϵ, similar to the example considered at the end of subsection 4.3.1. Define the operator

$$\begin{aligned}(M\phi)(\tilde{\mathbf{x}},\epsilon,\mathbf{x}_r,\dot{\mathbf{x}}_r,\Gamma_s,\Gamma_f) &= \epsilon\frac{\partial \phi}{\partial t}+\epsilon\frac{\partial \phi}{\partial \tilde{\mathbf{x}}}\dot{\tilde{\mathbf{x}}}-\mathbf{g_1}(\tilde{\mathbf{x}},\mathbf{x}_r,\phi(\tilde{\mathbf{x}},\mathbf{x}_r,\dot{\mathbf{x}}_r,\Gamma_s))\\ &- \mathbf{g_2}(\tilde{\mathbf{x}},\mathbf{x}_r,\phi(\tilde{\mathbf{x}},\mathbf{x}_r,\dot{\mathbf{x}}_r,\Gamma_s))\Gamma_s\left(\tilde{\mathbf{x}},\mathbf{x}_r,\dot{\mathbf{x}}_r\right) \qquad (4.26)\\ &- \mathbf{g_2}(\tilde{\mathbf{x}},\mathbf{x}_r,\phi(\tilde{\mathbf{x}},\mathbf{x}_r,\dot{\mathbf{x}}_r,\Gamma_s))\Gamma_f\left(\tilde{\mathbf{x}},\phi(\tilde{\mathbf{x}},\mathbf{x}_r,\dot{\mathbf{x}}_r,\Gamma_s),\mathbf{x}_r,\dot{\mathbf{x}}_r\right)\end{aligned}$$

and let $(M\phi)(t,\tilde{\mathbf{x}},\epsilon) = O(C(\tilde{\mathbf{x}},\epsilon,\mathbf{x}_r,\dot{\mathbf{x}}_r))$ that depends on the choice of controls Γ_s

and Γ_f. Further, assume

Assumption 4.1. *Control choice* Γ_s *and* Γ_f *lead to* $O(C(\tilde{\mathbf{x}}, \epsilon = 0, \mathbf{x}_r, \dot{\mathbf{x}}_r)) = \mathbf{0}$.

The exact manifold is given as $\mathbf{h}(\tilde{\mathbf{x}}, \epsilon, \mathbf{x}_r, \dot{\mathbf{x}}_r) = \phi(\tilde{\mathbf{x}}, \mathbf{x}_r, \dot{\mathbf{x}}_r, \Gamma_s) + O(C(\tilde{\mathbf{x}}, \epsilon, \mathbf{x}_r, \dot{\mathbf{x}}_r))$ with the above choice of $\phi(\tilde{\mathbf{x}}, \mathbf{x}_r, \dot{\mathbf{x}}_r, \Gamma_s)$. Substituting the approximate expression for the manifold into (4.25)

$$
\begin{aligned}
\dot{\tilde{\mathbf{x}}} &= \mathbf{f_1}\left(\tilde{\mathbf{x}}, \mathbf{x}_r, \tilde{\mathbf{z}} + \phi(\tilde{\mathbf{x}}, \mathbf{x}_r, \dot{\mathbf{x}}_r, \Gamma_s) + O(C(\tilde{\mathbf{x}}, \epsilon, \mathbf{x}_r, \dot{\mathbf{x}}_r))\right) \\
&+ \mathbf{f_2}\left(\tilde{\mathbf{x}}, \mathbf{x}_r, \tilde{\mathbf{z}} + \phi(\tilde{\mathbf{x}}, \mathbf{x}_r, \dot{\mathbf{x}}_r, \Gamma_s) + O(C(\tilde{\mathbf{x}}, \epsilon, \mathbf{x}_r, \dot{\mathbf{x}}_r))\right) \Gamma_s\left(\tilde{\mathbf{x}}, \mathbf{x}_r, \dot{\mathbf{x}}_r\right) \qquad (4.27a) \\
&+ \mathbf{f_2}\left(\tilde{\mathbf{x}}, \mathbf{x}_r, \tilde{\mathbf{z}} + \phi(\tilde{\mathbf{x}}, \mathbf{x}_r, \dot{\mathbf{x}}_r, \Gamma_s) + O(C(\tilde{\mathbf{x}}, \epsilon, \mathbf{x}_r, \dot{\mathbf{x}}_r))\right) \Gamma_f\left(\tilde{\mathbf{x}}, \tilde{\mathbf{z}}, \mathbf{x}_r, \dot{\mathbf{x}}_r, \Gamma_s\right) - \dot{\mathbf{x}}_r \\
\epsilon\dot{\tilde{\mathbf{z}}} &= \mathbf{g_1}\left(\tilde{\mathbf{x}}, \mathbf{x}_r, \tilde{\mathbf{z}} + \phi(\tilde{\mathbf{x}}, \mathbf{x}_r, \dot{\mathbf{x}}_r, \Gamma_s) + O(C(\tilde{\mathbf{x}}, \epsilon, \mathbf{x}_r, \dot{\mathbf{x}}_r))\right) \\
&+ \mathbf{g_2}\left(\tilde{\mathbf{x}}, \mathbf{x}_r, \tilde{\mathbf{z}} + \phi(\tilde{\mathbf{x}}, \mathbf{x}_r, \dot{\mathbf{x}}_r, \Gamma_s) + O(C(\tilde{\mathbf{x}}, \epsilon, \mathbf{x}_r, \dot{\mathbf{x}}_r))\right) \Gamma_s\left(\tilde{\mathbf{x}}, \mathbf{x}_r, \dot{\mathbf{x}}_r\right) \qquad (4.27b) \\
&+ \mathbf{g_2}\left(\tilde{\mathbf{x}}, \mathbf{x}_r, \tilde{\mathbf{z}} + \phi(\tilde{\mathbf{x}}, \mathbf{x}_r, \dot{\mathbf{x}}_r, \Gamma_s) + O(C(\tilde{\mathbf{x}}, \epsilon, \mathbf{x}_r, \dot{\mathbf{x}}_r))\right) \Gamma_f\left(\tilde{\mathbf{x}}, \tilde{\mathbf{z}}, \mathbf{x}_r, \dot{\mathbf{x}}_r, \Gamma_s\right) \\
&- \epsilon\frac{\partial(\phi + O(C(\tilde{\mathbf{x}}, \epsilon, \mathbf{x}_r, \dot{\mathbf{x}}_r)))}{\partial t} - \epsilon\frac{\partial(\phi + O(C(\tilde{\mathbf{x}}, \epsilon, \mathbf{x}_r, \dot{\mathbf{x}}_r)))}{\partial \tilde{\mathbf{x}}}\dot{\tilde{\mathbf{x}}}
\end{aligned}
$$

Note that Γ_f is a function of Γ_s due to the choice of $\phi(\tilde{\mathbf{x}}, \mathbf{x}_r, \dot{\mathbf{x}}_r, \Gamma_s)$. The reduced slow and fast systems for the system given in (4.27) are obtained by substituting $\epsilon = 0$, resulting in the *reduced slow system*:

$$
\begin{aligned}
\dot{\tilde{\mathbf{x}}} &= \mathbf{f_1}\left(\tilde{\mathbf{x}}, \mathbf{x}_r, \tilde{\mathbf{z}} + \phi(\tilde{\mathbf{x}}, \mathbf{x}_r, \dot{\mathbf{x}}_r, \Gamma_s)\right) \\
&+ \mathbf{f_2}\left(\tilde{\mathbf{x}}, \mathbf{x}_r, \tilde{\mathbf{z}} + \phi(\tilde{\mathbf{x}}, \mathbf{x}_r, \dot{\mathbf{x}}_r, \Gamma_s)\right) \Gamma_s\left(\tilde{\mathbf{x}}, \mathbf{x}_r, \dot{\mathbf{x}}_r\right) \qquad (4.28a) \\
&+ \mathbf{f_2}\left(\tilde{\mathbf{x}}, \mathbf{x}_r, \tilde{\mathbf{z}} + \phi(\tilde{\mathbf{x}}, \mathbf{x}_r, \dot{\mathbf{x}}_r, \Gamma_s)\right) \Gamma_f\left(\tilde{\mathbf{x}}, \tilde{\mathbf{z}}, \mathbf{x}_r, \dot{\mathbf{x}}_r, \Gamma_s\right) - \dot{\mathbf{x}}_r \\
\mathbf{0} &= \mathbf{g_1}\left(\tilde{\mathbf{x}}, \mathbf{x}_r, \tilde{\mathbf{z}} + \phi(\tilde{\mathbf{x}}, \mathbf{x}_r, \dot{\mathbf{x}}_r, \Gamma_s)\right) \\
&+ \mathbf{g_2}\left(\tilde{\mathbf{x}}, \mathbf{x}_r, \tilde{\mathbf{z}} + \phi(\tilde{\mathbf{x}}, \mathbf{x}_r, \dot{\mathbf{x}}_r, \Gamma_s)\right) \Gamma_s\left(\tilde{\mathbf{x}}, \mathbf{x}_r, \dot{\mathbf{x}}_r\right) \qquad (4.28b) \\
&+ \mathbf{g_2}\left(\tilde{\mathbf{x}}, \mathbf{x}_r, \tilde{\mathbf{z}} + \phi(\tilde{\mathbf{x}}, \mathbf{x}_r, \dot{\mathbf{x}}_r, \Gamma_s)\right) \Gamma_f\left(\tilde{\mathbf{x}}, \tilde{\mathbf{z}}, \mathbf{x}_r, \dot{\mathbf{x}}_r, \Gamma_s\right)
\end{aligned}
$$

and *reduced fast system*:

$$\begin{aligned}
\tilde{\mathbf{x}}' &= \mathbf{0} && (4.29a)\\
\tilde{\mathbf{z}}' &= \mathbf{g_1}\left(\tilde{\mathbf{x}}, \mathbf{x}_r, \tilde{\mathbf{z}} + \phi(\tilde{\mathbf{x}}, \mathbf{x}_r, \dot{\mathbf{x}}_r, \Gamma_s)\right) \\
&+ \mathbf{g_2}\left(\tilde{\mathbf{x}}, \mathbf{x}_r, \tilde{\mathbf{z}} + \phi(\tilde{\mathbf{x}}, \mathbf{x}_r, \dot{\mathbf{x}}_r, \Gamma_s)\right)\Gamma_s\left(\tilde{\mathbf{x}}, \mathbf{x}_r, \dot{\mathbf{x}}_r\right) && (4.29b)\\
&+ \mathbf{g_2}\left(\tilde{\mathbf{x}}, \mathbf{x}_r, \tilde{\mathbf{z}} + \phi(\tilde{\mathbf{x}}, \mathbf{x}_r, \dot{\mathbf{x}}_r, \Gamma_s)\right)\Gamma_f\left(\tilde{\mathbf{x}}, \tilde{\mathbf{z}}, \mathbf{x}_r, \dot{\mathbf{x}}_r, \Gamma_s\right)
\end{aligned}$$

In general the composite control approach first computes the slow control Γ_s required to maintain stability of the reduced slow system by assuming that the fast states lie upon the manifold and $\Gamma_f = \mathbf{0}$. In the next step the fast control Γ_f is designed to satisfy two conditions; guarantee uniform convergence of the fast states onto the manifold, and remain inactive when the fast state remains on the manifold. The second condition is implemented to avoid affecting the conclusions drawn about the reduced slow system stability. In the proposed control scheme, the second condition is avoided by designing Γ_f ahead of Γ_s. Thus, design $\Gamma_f(\tilde{\mathbf{x}}, \tilde{\mathbf{z}}, \mathbf{x}_r, \dot{\mathbf{x}}_r, \Gamma_s)$ as a function of Γ_s such that (4.29b) is transformed into the *closed-loop reduced fast system*

$$\tilde{\mathbf{z}}' = -\mathbf{L_f}(\tilde{\mathbf{x}}, \tilde{\mathbf{z}}, \mathbf{x}_r, \dot{\mathbf{x}}_r) + \mathbf{K_f}(\tilde{\mathbf{z}}) \tag{4.30}$$

such that $-\mathbf{L_f}(\tilde{\mathbf{x}}, \mathbf{0}, \mathbf{x}_r, \dot{\mathbf{x}}_r) + \mathbf{K_f}(\mathbf{0}) = \mathbf{0}$. With this choice of Γ_f and assumptions about vector fields $\mathbf{L_f}$ and $\mathbf{K_f}$, $\tilde{\mathbf{z}} = \mathbf{0}$ becomes the isolated root of (4.28b). Therefore the reduced slow system reduces to

$$\begin{aligned}
\dot{\tilde{\mathbf{x}}} &= \mathbf{f_1}\left(\tilde{\mathbf{x}}, \mathbf{x}_r, \phi(\tilde{\mathbf{x}}, \mathbf{x}_r, \dot{\mathbf{x}}_r, \Gamma_s)\right) \\
&+ \mathbf{f_2}\left(\tilde{\mathbf{x}}, \mathbf{x}_r, \phi(\tilde{\mathbf{x}}, \mathbf{x}_r, \dot{\mathbf{x}}_r, \Gamma_s)\right)\Gamma_s\left(\tilde{\mathbf{x}}, \mathbf{x}_r, \dot{\mathbf{x}}_r\right) && (4.31)
\end{aligned}$$

$$+\mathbf{f_2}\left(\tilde{\mathbf{x}}, \mathbf{x}_r, \phi(\tilde{\mathbf{x}}, \mathbf{x}_r, \dot{\mathbf{x}}_r, \Gamma_s)\right) \Gamma_f\left(\tilde{\mathbf{x}}, \mathbf{0}, \mathbf{x}_r, \dot{\mathbf{x}}_r, \Gamma_s\right) - \dot{\mathbf{x}}_r$$

The only unknown in (4.31) is Γ_s and therefore it may be designed to transform the reduced slow system into the *closed-loop reduced slow system*

$$\dot{\tilde{\mathbf{x}}} = -\mathbf{F_s}(\tilde{\mathbf{x}}, \mathbf{x}_r, \dot{\mathbf{x}}_r) + \mathbf{G_s}(\tilde{\mathbf{x}}) \tag{4.32}$$

and exact forms of $\Gamma_f(\tilde{\mathbf{x}}, \tilde{\mathbf{z}}, \mathbf{x}_r, \dot{\mathbf{x}}_r)$, $\phi(\tilde{\mathbf{x}}, \mathbf{x}_r, \dot{\mathbf{x}}_r)$.Correspondingly, $C(\tilde{\mathbf{x}}, \epsilon, \mathbf{x}_r, \dot{\mathbf{x}}_r)$ can be determined through relations given in (4.30) and (4.26) respectively.

Remark 4.3.1. In the reduced systems obtained, $\tilde{\mathbf{z}} = \mathbf{z} - \phi(\tilde{\mathbf{x}}, \mathbf{x}_r, \dot{\mathbf{x}}_r)$ by virtue of Assumption 4.1. Thus at the implementation level the control Γ_f is a function of known quantities.

The complete closed-loop system is obtained by rewriting (4.27) as

$$\begin{aligned}
\dot{\tilde{\mathbf{x}}} &= \mathbf{f_1}\left(\tilde{\mathbf{x}}, \mathbf{x}_r, \phi(.)\right) + \mathbf{f_2}\left(\tilde{\mathbf{x}}, \mathbf{x}_r, \phi(.)\right) \Gamma_s\left(\tilde{\mathbf{x}}, \mathbf{x}_r, \dot{\mathbf{x}}_r\right) \\
&+ \mathbf{f_2}\left(\tilde{\mathbf{x}}, \mathbf{x}_r, \phi(.)\right) \Gamma_f\left(\tilde{\mathbf{x}}, \mathbf{0}, \mathbf{x}_r, \dot{\mathbf{x}}_r, \Gamma_s\right) - \dot{\mathbf{x}}_r \\
&+ \mathbf{f_1}\left(\tilde{\mathbf{x}}, \mathbf{x}_r, \tilde{\mathbf{z}} + \phi(.)\right) - \mathbf{f_1}\left(\tilde{\mathbf{x}}, \mathbf{x}_r, \phi(.)\right) \\
&+ \left[\mathbf{f_2}\left(\tilde{\mathbf{x}}, \mathbf{x}_r, \tilde{\mathbf{z}} + \phi(.)\right) - \mathbf{f_2}\left(\tilde{\mathbf{x}}, \mathbf{x}_r, \phi(.)\right)\right] \Gamma_s\left(\tilde{\mathbf{x}}, \mathbf{x}_r, \dot{\mathbf{x}}_r\right) \\
&+ \mathbf{f_2}\left(\tilde{\mathbf{x}}, \mathbf{x}_r, \tilde{\mathbf{z}} + \phi(.)\right) \Gamma_f\left(\tilde{\mathbf{x}}, \tilde{\mathbf{z}}, \mathbf{x}_r, \dot{\mathbf{x}}_r, \Gamma_s\right) - \mathbf{f_2}\left(\tilde{\mathbf{x}}, \mathbf{x}_r, \phi(.)\right) \Gamma_f\left(\tilde{\mathbf{x}}, \mathbf{0}, \mathbf{x}_r, \dot{\mathbf{x}}_r, \Gamma_s\right) \\
&+ \mathbf{f_1}\left(\tilde{\mathbf{x}}, \mathbf{x}_r, \tilde{\mathbf{z}} + \phi(.) + O(C(\tilde{\mathbf{x}}, \epsilon, \mathbf{x}_r, \dot{\mathbf{x}}_r))\right) - \mathbf{f_1}\left(\tilde{\mathbf{x}}, \mathbf{x}_r, \tilde{\mathbf{z}} + \phi(.)\right) \\
&+ \left[\mathbf{f_2}\left(\tilde{\mathbf{x}}, \mathbf{x}_r, \tilde{\mathbf{z}} + \phi(.) + O(C(\tilde{\mathbf{x}}, \epsilon, \mathbf{x}_r, \dot{\mathbf{x}}_r))\right) - \mathbf{f_2}\left(\tilde{\mathbf{x}}, \mathbf{x}_r, \tilde{\mathbf{z}} + \phi(.)\right)\right] \Gamma_s\left(\tilde{\mathbf{x}}, \mathbf{x}_r, \dot{\mathbf{x}}_r\right) \\
&+ \left[\mathbf{f_2}\left(\tilde{\mathbf{x}}, \mathbf{x}_r, \tilde{\mathbf{z}} + \phi(.) + O(C(\tilde{\mathbf{x}}, \epsilon, \mathbf{x}_r, \dot{\mathbf{x}}_r))\right)\right. \\
&- \left.\mathbf{f_2}\left(\tilde{\mathbf{x}}, \mathbf{x}_r, \tilde{\mathbf{z}} + \phi(\tilde{\mathbf{x}}, \mathbf{x}_r, \dot{\mathbf{x}}_r, \Gamma_s)\right)\right] \Gamma_f\left(\tilde{\mathbf{x}}, \tilde{\mathbf{z}}, \mathbf{x}_r, \dot{\mathbf{x}}_r, \Gamma_s\right)
\end{aligned} \tag{4.33}$$

$$
\begin{aligned}
\epsilon\dot{\tilde{\mathbf{z}}} &= \mathbf{g_1}\left(\tilde{\mathbf{x}}, \mathbf{x}_r, \tilde{\mathbf{z}} + \phi(\tilde{\mathbf{x}}, \mathbf{x}_r, \dot{\mathbf{x}}_r, \Gamma_s)\right) \\
&+ \mathbf{g_2}\left(\tilde{\mathbf{x}}, \mathbf{x}_r, \tilde{\mathbf{z}} + \phi(\tilde{\mathbf{x}}, \mathbf{x}_r, \dot{\mathbf{x}}_r, \Gamma_s)\right) \Gamma_s\left(\tilde{\mathbf{x}}, \mathbf{x}_r, \dot{\mathbf{x}}_r\right) \\
&+ \mathbf{g_2}\left(\tilde{\mathbf{x}}, \mathbf{x}_r, \tilde{\mathbf{z}} + \phi(\tilde{\mathbf{x}}, \mathbf{x}_r, \dot{\mathbf{x}}_r, \Gamma_s)\right) \Gamma_f\left(\tilde{\mathbf{x}}, \tilde{\mathbf{z}}, \mathbf{x}_r, \dot{\mathbf{x}}_r, \Gamma_s\right) \\
&+ \mathbf{g_1}\left(\tilde{\mathbf{x}}, \mathbf{x}_r, \tilde{\mathbf{z}} + \phi(\tilde{\mathbf{x}}, \mathbf{x}_r, \dot{\mathbf{x}}_r, \Gamma_s) + O(C(\tilde{\mathbf{x}}, \epsilon, \mathbf{x}_r, \dot{\mathbf{x}}_r))\right) \\
&- \mathbf{g_1}\left(\tilde{\mathbf{x}}, \mathbf{x}_r, \tilde{\mathbf{z}} + \phi(\tilde{\mathbf{x}}, \mathbf{x}_r, \dot{\mathbf{x}}_r, \Gamma_s)\right) \\
&+ \left[\mathbf{g_2}\left(\tilde{\mathbf{x}}, \mathbf{x}_r, \tilde{\mathbf{z}} + \phi(\tilde{\mathbf{x}}, \mathbf{x}_r, \dot{\mathbf{x}}_r, \Gamma_s) + O(C(\tilde{\mathbf{x}}, \epsilon, \mathbf{x}_r, \dot{\mathbf{x}}_r))\right)\right. \\
&- \left.\mathbf{g_2}\left(\tilde{\mathbf{x}}, \mathbf{x}_r, \tilde{\mathbf{z}} + \phi(\tilde{\mathbf{x}}, \mathbf{x}_r, \dot{\mathbf{x}}_r, \Gamma_s)\right)\right] \Gamma_s\left(\tilde{\mathbf{x}}, \mathbf{x}_r, \dot{\mathbf{x}}_r\right) \\
&+ \left[\mathbf{g_2}\left(\tilde{\mathbf{x}}, \mathbf{x}_r, \tilde{\mathbf{z}} + \phi(\tilde{\mathbf{x}}, \mathbf{x}_r, \dot{\mathbf{x}}_r, \Gamma_s) + O(C(\tilde{\mathbf{x}}, \epsilon, \mathbf{x}_r, \dot{\mathbf{x}}_r))\right)\right. \\
&- \left.\mathbf{g_2}\left(\tilde{\mathbf{x}}, \mathbf{x}_r, \tilde{\mathbf{z}} + \phi(\tilde{\mathbf{x}}, \mathbf{x}_r, \dot{\mathbf{x}}_r, \Gamma_s)\right)\right] \Gamma_f\left(\tilde{\mathbf{x}}, \tilde{\mathbf{z}}, \mathbf{x}_r, \dot{\mathbf{x}}_r, \Gamma_s\right) \\
&- \epsilon\frac{\partial(\phi + O(C(\tilde{\mathbf{x}}, \epsilon, \mathbf{x}_r, \dot{\mathbf{x}}_r)))}{\partial t} - \epsilon\frac{\partial(\phi + O(C(\tilde{\mathbf{x}}, \epsilon, \mathbf{x}_r, \dot{\mathbf{x}}_r)))}{\partial \tilde{\mathbf{x}}}\dot{\tilde{\mathbf{x}}}
\end{aligned}
\tag{4.34}
$$

Using the closed-loop reduced systems (4.30), (4.32); (4.33), (4.34) become

$$
\begin{aligned}
\dot{\tilde{\mathbf{x}}} &= -\mathbf{F_s}(\tilde{\mathbf{x}}, \mathbf{x}_r, \dot{\mathbf{x}}_r) + \mathbf{G_s}(\tilde{\mathbf{x}}) \\
&+ \mathbf{f_1}\left(\tilde{\mathbf{x}}, \mathbf{x}_r, \tilde{\mathbf{z}} + \phi(\tilde{\mathbf{x}}, \mathbf{x}_r, \dot{\mathbf{x}}_r, \Gamma_s)\right) - \mathbf{f_1}\left(\tilde{\mathbf{x}}, \mathbf{x}_r, \phi(\tilde{\mathbf{x}}, \mathbf{x}_r, \dot{\mathbf{x}}_r, \Gamma_s)\right) \\
&+ \left[\mathbf{f_2}\left(\tilde{\mathbf{x}}, \mathbf{x}_r, \tilde{\mathbf{z}} + \phi(\tilde{\mathbf{x}}, \mathbf{x}_r, \dot{\mathbf{x}}_r, \Gamma_s)\right) - \mathbf{f_2}\left(\tilde{\mathbf{x}}, \mathbf{x}_r, \phi(\tilde{\mathbf{x}}, \mathbf{x}_r, \dot{\mathbf{x}}_r, \Gamma_s)\right)\right] \Gamma_s\left(\tilde{\mathbf{x}}, \mathbf{x}_r, \dot{\mathbf{x}}_r\right) \\
&+ \mathbf{f_2}\left(\tilde{\mathbf{x}}, \mathbf{x}_r, \tilde{\mathbf{z}} + \phi(\tilde{\mathbf{x}}, \mathbf{x}_r, \dot{\mathbf{x}}_r, \Gamma_s)\right) \Gamma_f\left(\tilde{\mathbf{x}}, \tilde{\mathbf{z}}, \mathbf{x}_r, \dot{\mathbf{x}}_r, \Gamma_s\right) \\
&- \mathbf{f_2}\left(\tilde{\mathbf{x}}, \mathbf{x}_r, \phi(\tilde{\mathbf{x}}, \mathbf{x}_r, \dot{\mathbf{x}}_r, \Gamma_s)\right) \Gamma_f\left(\tilde{\mathbf{x}}, \mathbf{0}, \mathbf{x}_r, \dot{\mathbf{x}}_r, \Gamma_s\right) \\
&+ \mathbf{f_1}\left(\tilde{\mathbf{x}}, \mathbf{x}_r, \tilde{\mathbf{z}} + \phi(\tilde{\mathbf{x}}, \mathbf{x}_r, \dot{\mathbf{x}}_r, \Gamma_s) + O(C(\tilde{\mathbf{x}}, \epsilon, \mathbf{x}_r, \dot{\mathbf{x}}_r))\right) \\
&- \mathbf{f_1}\left(\tilde{\mathbf{x}}, \mathbf{x}_r, \tilde{\mathbf{z}} + \phi(\tilde{\mathbf{x}}, \mathbf{x}_r, \dot{\mathbf{x}}_r, \Gamma_s)\right) \\
&+ \left[\mathbf{f_2}\left(\tilde{\mathbf{x}}, \mathbf{x}_r, \tilde{\mathbf{z}} + \phi(\tilde{\mathbf{x}}, \mathbf{x}_r, \dot{\mathbf{x}}_r, \Gamma_s) + O(C(\tilde{\mathbf{x}}, \epsilon, \mathbf{x}_r, \dot{\mathbf{x}}_r))\right)\right. \\
&- \left.\mathbf{f_2}\left(\tilde{\mathbf{x}}, \mathbf{x}_r, \tilde{\mathbf{z}} + \phi(\tilde{\mathbf{x}}, \mathbf{x}_r, \dot{\mathbf{x}}_r, \Gamma_s)\right)\right] \Gamma_s\left(\tilde{\mathbf{x}}, \mathbf{x}_r, \dot{\mathbf{x}}_r\right) \\
&+ \left[\mathbf{f_2}\left(\tilde{\mathbf{x}}, \mathbf{x}_r, \tilde{\mathbf{z}} + \phi(\tilde{\mathbf{x}}, \mathbf{x}_r, \dot{\mathbf{x}}_r, \Gamma_s) + O(C(\tilde{\mathbf{x}}, \epsilon, \mathbf{x}_r, \dot{\mathbf{x}}_r))\right)\right. \\
&- \left.\mathbf{f_2}\left(\tilde{\mathbf{x}}, \mathbf{x}_r, \tilde{\mathbf{z}} + \phi(\tilde{\mathbf{x}}, \mathbf{x}_r, \dot{\mathbf{x}}_r, \Gamma_s)\right)\right] \Gamma_f\left(\tilde{\mathbf{x}}, \tilde{\mathbf{z}}, \mathbf{x}_r, \dot{\mathbf{x}}_r, \Gamma_s\right)
\end{aligned}
\tag{4.35}
$$

$$
\begin{aligned}
\epsilon\dot{\tilde{\mathbf{z}}} &= -\mathbf{L_f}(\tilde{\mathbf{x}}, \tilde{\mathbf{z}}, \mathbf{x}_r, \dot{\mathbf{x}}_r) + \mathbf{K_f}(\tilde{\mathbf{z}}) \\
&+ \mathbf{g_1}\left(\tilde{\mathbf{x}}, \mathbf{x}_r, \tilde{\mathbf{z}} + \phi(\tilde{\mathbf{x}}, \mathbf{x}_r, \dot{\mathbf{x}}_r, \Gamma_s) + O(C(\tilde{\mathbf{x}}, \epsilon, \mathbf{x}_r, \dot{\mathbf{x}}_r))\right) \\
&- \mathbf{g_1}\left(\tilde{\mathbf{x}}, \mathbf{x}_r, \tilde{\mathbf{z}} + \phi(\tilde{\mathbf{x}}, \mathbf{x}_r, \dot{\mathbf{x}}_r, \Gamma_s)\right) \\
&+ \left[\mathbf{g_2}\left(\tilde{\mathbf{x}}, \mathbf{x}_r, \tilde{\mathbf{z}} + \phi(\tilde{\mathbf{x}}, \mathbf{x}_r, \dot{\mathbf{x}}_r, \Gamma_s) + O(C(\tilde{\mathbf{x}}, \epsilon, \mathbf{x}_r, \dot{\mathbf{x}}_r))\right)\right. \\
&- \left.\mathbf{g_2}\left(\tilde{\mathbf{x}}, \mathbf{x}_r, \tilde{\mathbf{z}} + \phi(\tilde{\mathbf{x}}, \mathbf{x}_r, \dot{\mathbf{x}}_r, \Gamma_s)\right)\right] \Gamma_s\left(\tilde{\mathbf{x}}, \mathbf{x}_r, \dot{\mathbf{x}}_r\right) \\
&+ \left[\mathbf{g_2}\left(\tilde{\mathbf{x}}, \mathbf{x}_r, \tilde{\mathbf{z}} + \phi(\tilde{\mathbf{x}}, \mathbf{x}_r, \dot{\mathbf{x}}_r, \Gamma_s) + O(C(\tilde{\mathbf{x}}, \epsilon, \mathbf{x}_r, \dot{\mathbf{x}}_r))\right)\right. \\
&- \left.\mathbf{g_2}\left(\tilde{\mathbf{x}}, \mathbf{x}_r, \tilde{\mathbf{z}} + \phi(\tilde{\mathbf{x}}, \mathbf{x}_r, \dot{\mathbf{x}}_r, \Gamma_s)\right)\right] \Gamma_f\left(\tilde{\mathbf{x}}, \tilde{\mathbf{z}}, \mathbf{x}_r, \dot{\mathbf{x}}_r, \Gamma_s\right) \\
&- \epsilon\frac{\partial(\phi + O(C(\tilde{\mathbf{x}}, \epsilon, \mathbf{x}_r, \dot{\mathbf{x}}_r)))}{\partial t} - \epsilon\frac{\partial(\phi + O(C(\tilde{\mathbf{x}}, \epsilon, \mathbf{x}_r, \dot{\mathbf{x}}_r)))}{\partial \tilde{\mathbf{x}}}\dot{\tilde{\mathbf{x}}}
\end{aligned}
\tag{4.36}
$$

Remark 4.3.2. If $\phi(\tilde{\mathbf{x}}, \mathbf{x}_r, \dot{\mathbf{x}}_r)$ is the unique manifold for the complete system, then the terms of $O(C(\tilde{\mathbf{x}}, \epsilon, \mathbf{x}_r, \dot{\mathbf{x}}_r))$ are identically zero and the closed-loop complete system given in (4.35) and (4.36) take the form as in [9] and [20], which have been proven to be closed-loop stable.

4.3.3 Stability Analysis

The following theorem [73] summarizes the main result of the developed approach.

Theorem 4.1. *Suppose the controls* $\mathbf{u}_s$ *and* $\mathbf{u}_f$ *are designed according to (4.30) and (4.32), and Assumption 4.1 and conditions (a)-(h) hold. Then for all initial conditions* $(\tilde{\mathbf{x}}, \tilde{\mathbf{z}}) \in D_x \times D_z$ *the composite control* $\mathbf{u} = \mathbf{u}_s + \mathbf{u}_f$ *uniformly stabilizes the nonlinear singularly perturbed system given in (2.5) for all* $\epsilon < \epsilon^*$*, where* ϵ^* *is given by the inequality (4.42) and the error signals* $\tilde{\mathbf{x}}(t)$ *and* $\tilde{\mathbf{z}}(t)$ *are uniformly bounded by (4.43) and (4.44) respectively.*

Proof. Closed-loop system stability is analyzed using the composite Lyapunov function approach[22]. It is required to prove that the closed-loop system behaviour remains close to the closed-loop reduced slow system. Suppose that there exists

quadratic Lyapunov functions $V(t,\tilde{\mathbf{x}}) = \frac{1}{2}\tilde{\mathbf{x}}^T\tilde{\mathbf{x}}$ and $W(t,\tilde{\mathbf{z}}) = \frac{1}{2}\tilde{\mathbf{z}}^T\tilde{\mathbf{z}}$ for the closed-loop reduced-order models given in (4.32) and (4.30) respectively, satisfying the following conditions:

(a) $V(t,\tilde{\mathbf{x}})$ is positive-definite and decrescent, that is

$$c_1||\tilde{\mathbf{x}}||^2 \leq V(t,\tilde{\mathbf{x}}) \leq c_2||\tilde{\mathbf{x}}||^2, \quad \tilde{\mathbf{x}} \in D_x \subset \mathbb{R}^m$$

(b)

$$\frac{\partial V}{\partial \tilde{\mathbf{x}}}\big[-\mathbf{F_s}(\tilde{\mathbf{x}},\mathbf{x}_r,\dot{\mathbf{x}}_r) + \mathbf{G_s}(\tilde{\mathbf{x}})\big] \leq -\alpha_1||\tilde{\mathbf{x}}||^2 - b_1||\tilde{\mathbf{x}}||, \quad \alpha_1 > 0, b_1 \geq 0$$

(c) There exists a constant $\beta_1 > 0$ such that

$$\begin{aligned}
&\frac{\partial V}{\partial \tilde{\mathbf{x}}}\big[\mathbf{f_1}\left(\tilde{\mathbf{x}},\mathbf{x}_r,\tilde{\mathbf{z}}+\phi(\tilde{\mathbf{x}},\mathbf{x}_r,\dot{\mathbf{x}}_r,\Gamma_s)\right) - \mathbf{f_1}\left(\tilde{\mathbf{x}},\mathbf{x}_r,\phi(\tilde{\mathbf{x}},\mathbf{x}_r,\dot{\mathbf{x}}_r,\Gamma_s)\right)\big] \\
+&\frac{\partial V}{\partial \tilde{\mathbf{x}}}\big[\mathbf{f_2}\left(\tilde{\mathbf{x}},\mathbf{x}_r,\tilde{\mathbf{z}}+\phi(\tilde{\mathbf{x}},\mathbf{x}_r,\dot{\mathbf{x}}_r,\Gamma_s)\right) \\
-&\mathbf{f_2}\left(\tilde{\mathbf{x}},\mathbf{x}_r,\phi(\tilde{\mathbf{x}},\mathbf{x}_r,\dot{\mathbf{x}}_r,\Gamma_s)\right)\big]\Gamma_s\left(\tilde{\mathbf{x}},\mathbf{x}_r,\dot{\mathbf{x}}_r\right) \\
+&\frac{\partial V}{\partial \tilde{\mathbf{x}}}\big[\mathbf{f_2}\left(\tilde{\mathbf{x}},\mathbf{x}_r,\tilde{\mathbf{z}}+\phi(\tilde{\mathbf{x}},\mathbf{x}_r,\dot{\mathbf{x}}_r,\Gamma_s)\right)\Gamma_f\left(\tilde{\mathbf{x}},\tilde{\mathbf{z}},\mathbf{x}_r,\dot{\mathbf{x}}_r,\Gamma_s\right) \\
-&\mathbf{f_2}\left(\tilde{\mathbf{x}},\mathbf{x}_r,\phi(\tilde{\mathbf{x}},\mathbf{x}_r,\dot{\mathbf{x}}_r,\Gamma_s)\right)\Gamma_f\left(\tilde{\mathbf{x}},\mathbf{0},\mathbf{x}_r,\dot{\mathbf{x}}_r,\Gamma_s\right)\big] \leq \beta_1||\tilde{\mathbf{x}}||||\tilde{\mathbf{z}}||
\end{aligned}$$

(d) There exist constants $\beta_2 > 0$, $\beta_3 > 0$ and $\beta_4 \geq 0$ such that

$$\begin{aligned}
&\frac{\partial V}{\partial \tilde{\mathbf{x}}}\big[\mathbf{f_1}\left(\tilde{\mathbf{x}},\mathbf{x}_r,\tilde{\mathbf{z}}+\phi(\tilde{\mathbf{x}},\mathbf{x}_r,\dot{\mathbf{x}}_r,\Gamma_s) + O(C(\tilde{\mathbf{x}},\epsilon,\mathbf{x}_r,\dot{\mathbf{x}}_r))\right) \\
-\quad&\mathbf{f_1}\left(\tilde{\mathbf{x}},\mathbf{x}_r,\tilde{\mathbf{z}}+\phi(\tilde{\mathbf{x}},\mathbf{x}_r,\dot{\mathbf{x}}_r,\Gamma_s)\right)\big] \\
+\quad&\frac{\partial V}{\partial \tilde{\mathbf{x}}}\big[\mathbf{f_2}\left(\tilde{\mathbf{x}},\mathbf{x}_r,\tilde{\mathbf{z}}+\phi(\tilde{\mathbf{x}},\mathbf{x}_r,\dot{\mathbf{x}}_r,\Gamma_s) + O(C(\tilde{\mathbf{x}},\epsilon,\mathbf{x}_r,\dot{\mathbf{x}}_r))\right)
\end{aligned}$$

$$
\begin{aligned}
&- \quad \mathbf{f_2}\left(\tilde{\mathbf{x}}, \mathbf{x}_r, \tilde{\mathbf{z}} + \phi(\tilde{\mathbf{x}}, \mathbf{x}_r, \dot{\mathbf{x}}_r, \Gamma_s)\right)\Big]\Gamma_s\left(\tilde{\mathbf{x}}, \mathbf{x}_r, \dot{\mathbf{x}}_r\right) \\
&+ \quad \frac{\partial V}{\partial \tilde{\mathbf{x}}}\Big[\mathbf{f_2}\left(\tilde{\mathbf{x}}, \mathbf{x}_r, \tilde{\mathbf{z}} + \phi(\tilde{\mathbf{x}}, \mathbf{x}_r, \dot{\mathbf{x}}_r, \Gamma_s) + O(C(\tilde{\mathbf{x}}, \epsilon, \mathbf{x}_r, \dot{\mathbf{x}}_r))\right) \\
&- \quad \mathbf{f_2}\left(\tilde{\mathbf{x}}, \mathbf{x}_r, \tilde{\mathbf{z}} + \phi(\tilde{\mathbf{x}}, \mathbf{x}_r, \dot{\mathbf{x}}_r, \Gamma_s)\right)\Big]\Gamma_f\left(\tilde{\mathbf{x}}, \tilde{\mathbf{z}}, \mathbf{x}_r, \dot{\mathbf{x}}_r, \Gamma_s\right) \leq \epsilon\beta_2||\tilde{\mathbf{x}}||^2 \\
&+ \quad \epsilon\beta_3||\tilde{\mathbf{x}}||||\tilde{\mathbf{z}}|| + \epsilon\beta_4||\tilde{\mathbf{x}}||
\end{aligned}
$$

(e) $W(t, \tilde{\mathbf{z}})$ is positive-definite and decrescent scalar function satisfying,

$$
c_3||\tilde{\mathbf{z}}||^2 \leq W(t, \tilde{\mathbf{z}}) \leq c_4||\tilde{\mathbf{z}}||^2, \quad \tilde{\mathbf{z}} \in D_z \subset \mathbb{R}^n
$$

(f)

$$
\frac{\partial W}{\partial \tilde{\mathbf{z}}}\left(-\mathbf{L_f}(\tilde{\mathbf{x}}, \tilde{\mathbf{z}}, \mathbf{x}_r, \dot{\mathbf{x}}_r) + \mathbf{K_f}(\tilde{\mathbf{z}})\right) \leq -\alpha_2||\tilde{\mathbf{z}}||^2, \quad \alpha_2 > 0
$$

(g) There exist scalars $\beta_5 > 0$, $\beta_6 > 0$ and $\beta_7 \geq 0$ such that

$$
\begin{aligned}
&\frac{\partial W}{\partial \tilde{\mathbf{z}}}\left[\mathbf{g_1}\left(\tilde{\mathbf{x}}, \mathbf{x}_r, \tilde{\mathbf{z}} + \phi(\tilde{\mathbf{x}}, \mathbf{x}_r, \dot{\mathbf{x}}_r, \Gamma_s) + O(C(\tilde{\mathbf{x}}, \epsilon, \mathbf{x}_r, \dot{\mathbf{x}}_r))\right)\right. \\
&- \quad \left.\mathbf{g_1}\left(\tilde{\mathbf{x}}, \mathbf{x}_r, \tilde{\mathbf{z}} + \phi(\tilde{\mathbf{x}}, \mathbf{x}_r, \dot{\mathbf{x}}_r, \Gamma_s)\right)\right] \\
&+ \quad \frac{\partial W}{\partial \tilde{\mathbf{z}}}\Big[\mathbf{g_2}\left(\tilde{\mathbf{x}}, \mathbf{x}_r, \tilde{\mathbf{z}} + \phi(\tilde{\mathbf{x}}, \mathbf{x}_r, \dot{\mathbf{x}}_r, \Gamma_s) + O(C(\tilde{\mathbf{x}}, \epsilon, \mathbf{x}_r, \dot{\mathbf{x}}_r))\right) \\
&- \quad \mathbf{g_2}\left(\tilde{\mathbf{x}}, \mathbf{x}_r, \tilde{\mathbf{z}} + \phi(\tilde{\mathbf{x}}, \mathbf{x}_r, \dot{\mathbf{x}}_r, \Gamma_s)\right)\Big]\Gamma_s\left(\tilde{\mathbf{x}}, \mathbf{x}_r, \dot{\mathbf{x}}_r\right) \\
&+ \quad \frac{\partial W}{\partial \tilde{\mathbf{z}}}\Big[\mathbf{g_2}\left(\tilde{\mathbf{x}}, \mathbf{x}_r, \tilde{\mathbf{z}} + \phi(\tilde{\mathbf{x}}, \mathbf{x}_r, \dot{\mathbf{x}}_r, \Gamma_s) + O(C(\tilde{\mathbf{x}}, \epsilon, \mathbf{x}_r, \dot{\mathbf{x}}_r))\right) \\
&- \quad \mathbf{g_2}\left(\tilde{\mathbf{x}}, \mathbf{x}_r, \tilde{\mathbf{z}} + \phi(\tilde{\mathbf{x}}, \mathbf{x}_r, \dot{\mathbf{x}}_r, \Gamma_s)\right)\Big]\Gamma_f\left(\tilde{\mathbf{x}}, \tilde{\mathbf{z}}, \mathbf{x}_r, \dot{\mathbf{x}}_r, \Gamma_s\right) \\
&\leq \quad \epsilon\beta_5||\tilde{\mathbf{z}}||^2 + \epsilon\beta_6||\tilde{\mathbf{x}}||||\tilde{\mathbf{z}}|| + \epsilon\beta_7||\tilde{\mathbf{z}}||
\end{aligned}
$$

(h) There exist constants $\beta_8 \geq 0$ and $\beta_9 > 0$ such that

$$
- \quad \frac{\partial W}{\partial \tilde{\mathbf{z}}}\left[\epsilon\frac{\partial(\phi + O(C(\tilde{\mathbf{x}}, \epsilon, \mathbf{x}_r, \dot{\mathbf{x}}_r)))}{\partial t} + \epsilon\frac{\partial(\phi + O(C(\tilde{\mathbf{x}}, \epsilon, \mathbf{x}_r, \dot{\mathbf{x}}_r)))}{\partial \tilde{\mathbf{x}}}\dot{\tilde{\mathbf{x}}}\right]
$$

$$\leq \quad \epsilon\beta_8||\tilde{\mathbf{z}}|| + \epsilon\beta_9||\tilde{\mathbf{x}}||||\tilde{\mathbf{z}}||$$

Conditions (a),(b) and (e),(f) are conditions for asymptotic stability of closed-loop reduced-order models. The constant b_1 in condition (b) depends upon the bounds of the specified trajectory $\mathbf{x}_r(t)$ and its derivative $\dot{\mathbf{x}}_r$. If the control Γ_s is designed to maintain regulation of the closed-loop slow subsystem then $b_1 = 0$. Additionally, conditions (c), (d) and (g),(h) are interconnection conditions obtained by assuming the vector fields are locally Lipschitz. The constants β_4, β_7, and β_8 appear due to the time-varying nature of the manifold and depend upon the bounds of $\mathbf{x}_r(t)$ and its derivative $\dot{\mathbf{x}}_r$. The constant β_8 also depends upon the derivative $\ddot{\mathbf{x}}_r$, which is known to be bounded by the choice of the reference trajectory.

Consider the Lyapunov function candidate

$$\nu(t, \tilde{\mathbf{x}}, \tilde{\mathbf{z}}) = (1-d)V(t, \tilde{\mathbf{x}}) + dW(\mathbf{t}, \tilde{\mathbf{z}}); \quad 0 < d < 1 \tag{4.37}$$

for the closed-loop system given in (4.35) and (4.36) with the design constant d. From the properties of V and W it follows that $\nu(t, \tilde{\mathbf{x}}, \tilde{\mathbf{z}})$ is positive-definite and decrescent. The derivative of ν along the trajectories of (4.35) and (4.36) is given by

$$\dot{\nu} = (1-d)\frac{\partial V}{\partial \tilde{\mathbf{x}}}\dot{\tilde{\mathbf{x}}} + \frac{d}{\epsilon}\frac{\partial W}{\partial \tilde{\mathbf{z}}}\tilde{\mathbf{z}}'. \tag{4.38}$$

Substituting conditions (a)-(h) into (4.38)

$$\begin{aligned} \dot{\nu} \leq \quad & - \quad (1-d)\big[\alpha_1||\tilde{\mathbf{x}}||^2 - b_1||\tilde{\mathbf{x}}|| + \beta_1||\tilde{\mathbf{x}}||||\tilde{\mathbf{z}}|| + \epsilon\beta_2||\tilde{\mathbf{x}}||^2 + \epsilon\beta_3||\tilde{\mathbf{x}}||||\tilde{\mathbf{z}}|| \\ & + \quad \epsilon\beta_4||\tilde{\mathbf{x}}||\big] - d\big[\frac{\alpha_2}{\epsilon}||\tilde{\mathbf{z}}||^2 + \beta_5||\tilde{\mathbf{z}}||^2 + \beta_6||\tilde{\mathbf{x}}||||\tilde{\mathbf{z}}|| + \beta_7||\tilde{\mathbf{z}}|| \\ & + \quad \beta_8||\tilde{\mathbf{z}}|| + \beta_9||\tilde{\mathbf{x}}||||\tilde{\mathbf{z}}||\big]. \end{aligned} \tag{4.39}$$

Collecting like terms

$$\begin{aligned}\dot{\nu} \leq \; & - \; (1-d)(\alpha_1 - \epsilon\beta_2)||\tilde{\mathbf{x}}||^2 - (1-d)(b_1 - \epsilon\beta_4)||\tilde{\mathbf{x}}|| + ((1-d)\beta_1 \\ & + \; \epsilon(1-d)\beta_3 + d\beta_6 + d\beta_9)||\tilde{\mathbf{x}}||||\tilde{\mathbf{z}}|| - d\left(\frac{\alpha_2}{\epsilon} - \beta_5\right)||\tilde{\mathbf{z}}||^2 - d(-\beta_7 - \beta_8)||\tilde{\mathbf{z}}||.\end{aligned} \tag{4.40}$$

Rearrange (4.40) to get

$$\begin{aligned}\dot{\nu} \leq & \begin{bmatrix} ||\tilde{\mathbf{x}}|| \\ ||\tilde{\mathbf{z}}|| \end{bmatrix}^T \begin{bmatrix} -(1-d)(\alpha_1 - \epsilon\beta_2) & \Xi \\ \Xi & -d\left(\frac{\alpha_2}{\epsilon} - \beta_5\right) \end{bmatrix} \begin{bmatrix} ||\tilde{\mathbf{x}}|| \\ ||\tilde{\mathbf{z}}|| \end{bmatrix} \\ & - ||\tilde{\mathbf{x}}||\left\{(\alpha_1 - \epsilon\beta_2)||\tilde{\mathbf{x}}|| - (\epsilon\beta_4 - b_1)\right\} - ||\tilde{\mathbf{z}}||\left\{\left(\frac{\alpha_2}{\epsilon} - \beta_5\right)||\tilde{\mathbf{z}}|| - (\beta_7 + \beta_8)\right\}. \end{aligned} \tag{4.41}$$

where $\Xi = \frac{1-d}{2}(\beta_1 + \epsilon\beta_3) + \frac{d}{2}(\beta_6 + d\beta_9)$. The matrix becomes negative definite when

$$d(1-d)(\alpha_1 - \epsilon\beta_2)\left(\frac{\alpha_2}{\epsilon} - \beta_5\right) < \frac{1}{4}((1-d)(\beta_1 + \epsilon\beta_3) + d(\beta_6 + \beta_9))^2 \tag{4.42}$$

Thus there exists an upper bound ϵ^* and upper bounds on the errors

$$\tilde{\mathbf{x}}_b = \frac{\epsilon\beta_4 - b_1}{(\alpha_1 - \epsilon\beta_2)} \tag{4.43}$$

$$\tilde{\mathbf{z}}_b = \frac{\beta_7 + \beta_8}{\left(\frac{\alpha_2}{\epsilon} - \beta_5\right)} \tag{4.44}$$

for which $\dot{\nu} \leq 0$. From the Lyapunov theorem it can then be concluded that the closed-loop signals $\tilde{\mathbf{x}}$ and $\tilde{\mathbf{z}}$ are uniformly bounded for all initial conditions $(\tilde{\mathbf{x}}, \tilde{\mathbf{z}}) \in D_x \times D_z$. Consequently the control vector $\mathbf{u} = \mathbf{\Gamma}_s + \mathbf{\Gamma}_f$ is bounded. Furthermore, since the trajectory $\mathbf{x}_r(t)$ is bounded the manifold $\mathbf{h}(\tilde{\mathbf{x}}, \tilde{\mathbf{z}}, \mathbf{x}_r, \dot{\mathbf{x}}_r)$ and the closed-loop signals $\mathbf{x}(t)$ and $\mathbf{z}(t)$ are bounded. This completes the proof. □

Remark 4.3.3. Notice the weight d introduced in the composite of Lyapunov functions

appears in the inequality for the upper-bound on the perturbation parameter. Thus, by varying the value of d the robustness of the controller to the singular perturbation parameter may be adjusted accordingly. Furthermore, as expected the upper-bounds on the states are only dependent on the properties of the system and not on this free parameter.

The following corollary gives an interesting result for the stabilization problem.

Corollary 4.2. *Suppose the controls $\mathbf{u}_s$ and $\mathbf{u}_f$ are designed according to (4.30) and (4.32), and Assumption 4.1 and conditions (a)-(h) hold with $\tilde{\mathbf{x}} = \mathbf{x}$ and $\tilde{\mathbf{z}} = \mathbf{z}$. Then for all initial conditions $(\mathbf{x}, \mathbf{z}) \in D_x \times D_z$, the composite control $\mathbf{u} = \mathbf{u}_s + \mathbf{u}_f$ asymptotically stabilizes the origin of the nonlinear singularly perturbed system in (2.5) for all $\epsilon < \epsilon_s^*$, where ϵ_s^* is given by the inequality (4.46).*

Proof. Note that in this case the manifold $\mathbf{h}(\mathbf{x}, \epsilon)$ is not time-varying, with $\tilde{\mathbf{x}} = \mathbf{x}$ and $\tilde{\mathbf{z}} = \mathbf{z}$. Since this problem is autonomous the decrescent conditions on the Lyapunov functions V and W can be relaxed. The constants β_4, β_7, and β_8 in conditions (d),(g),(h) are all equal to zero and the constant $b_1 = 0$, since $\mathbf{x}_r = \mathbf{0}$ and $\dot{\mathbf{x}}_r = \mathbf{0}$. With these modifications and $d = 0.5$, (4.41) is modified as

$$\dot{\nu} \leq 0.5 \begin{bmatrix} ||\mathbf{x}|| \\ ||\mathbf{z}|| \end{bmatrix}^T \begin{bmatrix} -(\alpha_1 - \epsilon\beta_2) & \frac{1}{2}(\beta_1 + \epsilon\beta_3 + \beta_6 + \beta_9) \\ \frac{1}{2}(\beta_1 + \epsilon\beta_3 + \beta_6 + \beta_9) & -\left(\frac{\alpha_2}{\epsilon} - \beta_5\right) \end{bmatrix} \begin{bmatrix} ||\mathbf{x}|| \\ ||\mathbf{z}|| \end{bmatrix} \tag{4.45}$$

Therefore, there exists an ϵ_s^* such that $\dot{\nu} < 0$ where ϵ_s^* satisfies the following inequality

$$(\alpha_1 - \epsilon\beta_2)\left(\frac{\alpha_2}{\epsilon} - \beta_5\right) < \frac{1}{4}((\beta_1 + \epsilon\beta_3) + (\beta_6 + \beta_9))^2 \tag{4.46}$$

This completes the proof. □

Remark 4.3.4. Theorem 4.1 and Corollary 4.2 depend upon the approximation of the invariant manifold leading to local results. If it were possible to obtain the expression of the exact manifold these results would be valid globally.

Remark 4.3.5. Fenichel's theorem implies that the behaviour of the complete nonlinear system remains close to the reduced slow system if the reduced fast system is stable. Theorem 4.1 and Corollary 4.2 state the same result for the closed-loop singularly perturbed system.

4.3.4 Numerical Examples

4.3.4.1 Purpose and Scope

The preceding theoretical developments are demonstrated with simulation. The first example is a generic planar nonlinear system. This planar example enables the study of the geometric constructs which are generally difficult to visualize in higher-dimension problems. A step-by-step procedure of controller development is detailed for the system to track a desired slow kinetic state. A comparison between the manifold approximation and the attained actual fast state is made. The closed-loop results are studied for a sinusoidal time-varying trajectory and the regulator problem. The second example develops control laws for a nonlinear F/A-18A Hornet model. The objective of this example is to test the performance of the controller for a highly nonlinear two time scale system. It is required to perform a turning maneuver while maintaining zero sideslip and tracking a specified angle-of-attack profile.

4.3.4.2 Generic Two Degrees-of-Freedom Nonlinear Kinetic Model

The fast dynamics of a generic kinetic model [72][Ch.3,Sec.3.6] is modified to include an arbitrarily chosen quadratic nonlinearity in the fast state and a 'pseudo'

control term with unit effectiveness

$$\dot{x} = -x + (x + 0.5)z + u \tag{4.47a}$$

$$\epsilon\dot{z} = x - (x + 1)z + z^2 + u. \tag{4.47b}$$

In this example $x \in \mathbb{R}$ and $z \in \mathbb{R}$ represent the slow and the fast states respectively. The control $u \in \mathbb{R}$ is developed to track a smooth desired slow state trajectory $x_r(t)$. Note that in the limit $\epsilon \to 0$

$$\dot{x} = -x + (x + 0.5)z + u \tag{4.48a}$$

$$0 = x - (x + 1)z + z^2 + u \tag{4.48b}$$

and the transcendental equation has two isolated solutions for the manifold. In order to stabilize the system using composite control the designer is required to choose one of these solutions. But the domain for the fast state is unknown and none of the solutions can be discarded. The following control formulation discusses how this issue is considered in the proposed approach.

Assume that the unknown exact manifold is represented by $h(x, \epsilon, x_r, \dot{x}_r)$ such that the slow state follows the desired trajectory. Define the errors $\tilde{x} = x - x_r$ and $\tilde{z} = z - h(\tilde{x}, \epsilon, x_r, \dot{x}_r)$. The objective is to seek the control vector of the form $u = u_s + u_f$, where

$$u_s = \Gamma_s\left(\tilde{x}, x_r, \dot{x}_r\right); u_f = \Gamma_f\left(\tilde{x}, \tilde{z}, x_r, \dot{x}_r\right). \tag{4.49}$$

Using the definitions given in (4.49) transform the system given in (4.47) into error coordinates

$$\dot{\tilde{x}} = -(\tilde{x} + x_r) + (\tilde{x} + x_r + 0.5)(\tilde{z} + h(\tilde{x}, \epsilon, x_r, \dot{x}_r)) - \dot{x}_r + \Gamma_s + \Gamma_f \tag{4.50a}$$

$$\begin{aligned}\epsilon\dot{\tilde{z}} &= (\tilde{x} + x_r) - (\tilde{x} + x_r + 1)(\tilde{z} + h(\tilde{x}, \epsilon, x_r, \dot{x}_r)) \\ &\quad + (\tilde{z} + h(\tilde{x}, \epsilon, x_r, \dot{x}_r))^2 + \Gamma_s + \Gamma_f - \epsilon\frac{\partial h}{\partial t} - \epsilon\frac{\partial h}{\partial \tilde{x}}\dot{\tilde{x}}\end{aligned} \tag{4.50b}$$

Let $\phi(\tilde{x}, x_r, \dot{x}_r, \Gamma_s)$ be the approximate manifold. Define the error introduced in the manifold condition, defined in (4.24) due to this approximation as

$$(M\phi)(\tilde{x}, x_r, \dot{x}_r) = \epsilon\frac{\partial \phi}{\partial t} + \epsilon\frac{\partial \phi}{\partial \tilde{x}}\dot{\tilde{x}} - \tilde{x} - x_r + (\tilde{x} + x_r)\phi(.) + \phi(.) - \phi(.)^2 - \Gamma_s - \Gamma_f \tag{4.51}$$

such that the exact manifold is

$$h(x, \epsilon, x_r., \dot{x}_r) = \phi(x, x_r, \dot{x}_r, \Gamma_s) + (M\phi)(\tilde{x}, x_r, \dot{x}_r). \tag{4.52}$$

Select $\phi(\tilde{x}, x_r, \dot{x}_r, \Gamma_s) = \tilde{x} + x_r + \Gamma_s$ so that

$$(M\phi)(\tilde{x}, x_r, \dot{x}_r) = \epsilon\frac{\partial \phi}{\partial t} + \epsilon\frac{\partial \phi}{\partial \tilde{x}}\dot{\tilde{x}} + (\tilde{x} + x_r)(\tilde{x} + x_r + \Gamma_s) - \phi(.)^2 - \Gamma_f. \tag{4.53}$$

Recall that the fast controller is designed to ensure $\tilde{z} = 0$ becomes the isolated manifold such that exact manifold in (4.52) and its approximation match upto $O(1)$. In order to do so, develop the reduced fast system for the error system given in (4.50)

$$\tilde{x}' = 0 \tag{4.54a}$$

$$\begin{aligned}\tilde{z}' &= -(\tilde{x} + x_r + 1)\tilde{z} + \tilde{z}^2 + 2\tilde{z}\phi(.) + \tilde{x} + x_r - (\tilde{x} + x_r + 1)\phi(.) \\ &+ \phi(.)^2 + \Gamma_s + \Gamma_f\end{aligned} \tag{4.54b}$$

Design

$$\Gamma_f = -A_f\tilde{z} - 2\tilde{z}\phi(.) + (\tilde{x} + x_r + 1)\phi(.) - \tilde{x} - x_r - \phi^2 - \Gamma_s \tag{4.55}$$

such that the closed-loop reduced fast system becomes

$$\tilde{z}' = -(\tilde{x} + x_r + 1 + A_f)\tilde{z} + \tilde{z}^2 \tag{4.56}$$

where A_f is the feedback gain. The next step is to determine the slow controller Γ_s. Develop the reduced slow system and substitute for Γ_f from (4.55) to get

$$\begin{aligned} \dot{\tilde{x}} &= -2\tilde{x} - 2x_r + (\tilde{x} + x_r + 0.5)\tilde{z} - \dot{x}_r \\ &- \phi(.)^2 - 2\tilde{z}\phi(.) + (2\tilde{x} + 2x_r + 1.5)\phi(.) - A_f\tilde{z} \qquad (4.57a) \\ 0 &= -(\tilde{x} + x_r + 1 + A_f)\tilde{z} + \tilde{z}^2 \qquad (4.57b) \end{aligned}$$

Since $\tilde{z} = 0$ is the unique root of the algebraic solution given in (4.57b), the resulting reduced slow system becomes

$$\dot{\tilde{x}} = -2\tilde{x} - 2x_r - \dot{x}_r - \phi(.)^2 + (2\tilde{x} + 2x_r + 1.5)\phi(.). \tag{4.58}$$

Substitute the expression for $\phi(.)$ in (4.58) to get

$$\dot{\tilde{x}} = -2\tilde{x} - 2x_r - \dot{x}_r + (2\tilde{x} + 2x_r + 1.5)(\tilde{x} + x_r + \Gamma_s) - (\tilde{x} + x_r + \Gamma_s)^2. \tag{4.59}$$

Design the slow controller Γ_s as

$$\Gamma_s = -\tilde{x} - x_r + \dot{x}_r - A\tilde{x} \tag{4.60}$$

with A as the feedback gain to result in the following closed-loop reduced slow system:

$$\begin{aligned}\dot{\tilde{x}} &= -(2 - 2\dot{x}_r + 2Ax_r + 1.5A - 2A\dot{x}_r)\tilde{x} + (-A^2 - 2A)\tilde{x}^2 \\ &+ (-2x_r + 0.5\dot{x}_r + 2x_r\dot{x}_r - \dot{x}_r^2). \end{aligned} \tag{4.61}$$

In order to implement the control laws use the slow controller Γ_s from (4.60) to develop the approximate manifold

$$\phi = \dot{x}_r - A\tilde{x} \tag{4.62}$$

and the fast controller

$$\begin{aligned}\Gamma_f &= (-A^2 - A)\tilde{x}^2 + \tilde{x}(\dot{x}_r + 2A\dot{x}_r - Ax_r) + 2A\tilde{x}\tilde{z} \\ &- \tilde{z}(2\dot{x}_r + A_f) - \dot{x}_r^2 + x_r\dot{x}_r. \end{aligned} \tag{4.63}$$

Recall that this design ensures $(M\phi)(\tilde{x}, x_r, \dot{x}_r) = 0$ in the limit $\epsilon \to 0$. Thus by definition of the exact manifold given in (4.52), the error $\tilde{z} = z - \phi(.)$, where $\phi(.)$ given in (4.62) is used for implementation of the controllers. Finally, the control laws Γ_s and Γ_f are expressed in original coordinates as

$$\Gamma_s = -x + \dot{x}_r - A(x - x_r) \tag{4.64a}$$

$$\begin{aligned}\Gamma_f &= (-A^2 - A)(x - x_r)^2 + (x - x_r)(\dot{x}_r + 2A\dot{x}_r - Ax_r) \\ &+ 2A(x - x_r)(z - \phi(.)) - (z - \phi(.))(2\dot{x}_r + A_f) - \dot{x}_r^2 + x_r\dot{x}_r. \end{aligned} \tag{4.64b}$$

The control laws developed in (4.64) are verified in simulation for time-varying reference and stabilization. The following presents the results for these two cases.

Case (a) Controller performance for tracking a continuously time-varying sine-wave of $0.2sin(0.2t)$ is presented in Figure 4.1. The feedback gains chosen are $A = 3$ and $A_f = 1$. The domain of the errors are $D_x = [-0.3 \quad 0.3]$ and $D_z = [-1.5 \quad 1.5]$. The domain of convergence of the complete system is limited due to two factors. First, the fast controller given in (4.64b) locally asymptotically stabilizes the reduced fast system about the error $\tilde{z} = 0$. This can be observed by the studying the closed-loop reduced fast dynamics given in (4.56). Second, the slow controller locally stabilizes reduced slow system about the tracking error $\tilde{x} = 0$, resulting in local convergence properties of the complete system. The approximate tracking is a result of the manifold approximation made for control design. Several constants in conditions (a)-(h) are computed as $\alpha_1 = 1$, $b_1 = 0.26$, $\beta_1 = 1.4$, $\beta_2 = 30$, $\beta_3 = 0$, $\beta_4 = 0.686$, $\alpha_2 = 1$, $\beta_5 = 1.96$, $\beta_6 = 250$, $\beta_7 = 0.5096$, $\beta_8 = 3.778$ and $\beta_9 = 250$. These values and a choice of $d = 0.3$ results in $\epsilon^* = 2000 >> 1$. From the simulation results it is seen that the system response is bounded for all time. Additionally, for simulations with $\epsilon = 0.2$ the bounds $\tilde{x}_b = 0.0818$ and $\tilde{z}_b = 4.701$, the control is bounded for all time. Note that the fast state response remains close to its approximation $\phi(t, x)$.

Case (b) This case simulates the regulator problem with $x_r = 0$ and $\dot{x}_r(t) = 0$. The control laws are the same as derived in (4.64). The constants $b_1 = 0$, $\beta_4 = 0$, $\beta_7 = 0$, and $\beta_8 = 0$ while the other constants have the same values as in Case 1(a) and $\epsilon_s^* = 1000 >> 1$. The results are presented in Figure 4.2, which shows that the system asymptotically settles down to the origin.

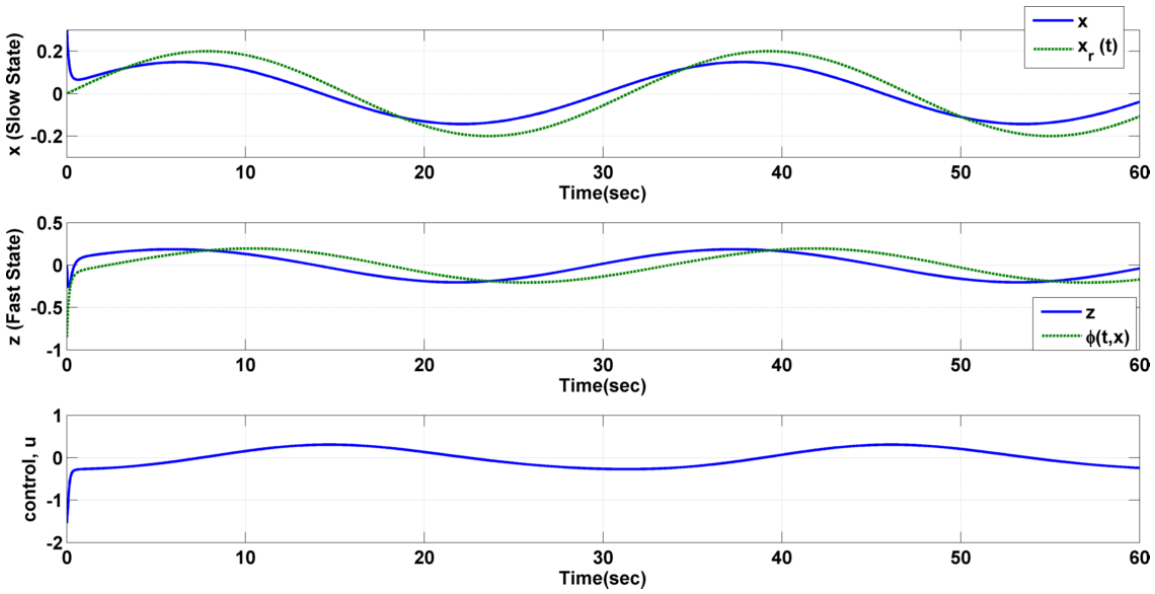

Figure 4.1: Case (a) Kinetic slow state compared to specified sine-wave reference, fast state compared to manifold approximation and computed control

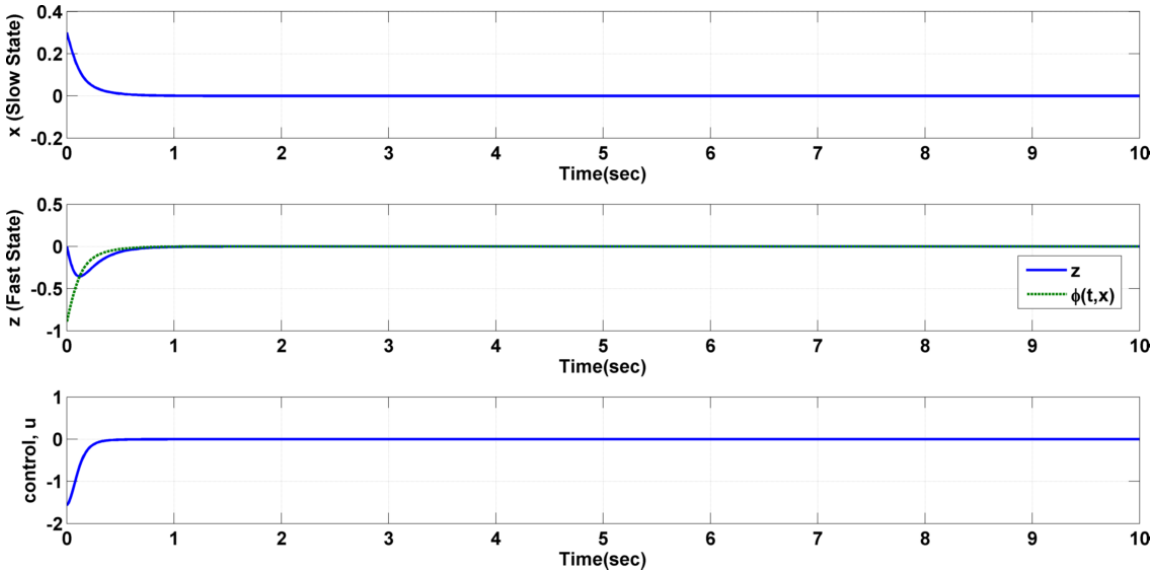

Figure 4.2: Case (b) Kinetic slow state, fast state compared to manifold approximation and computed control (regulator problem)

4.3.4.3 Lateral/Directional Maneuver for F/A-18A Hornet Aircraft

The complete nonlinear dynamic model in the stability-axes is represented by nine states $(M, \alpha, \beta, p, q, r, \phi, \theta, \psi)$ and four controls $(\eta, \delta_e, \delta_a, \delta_r)$. For this example the vector $[M, \alpha, \beta, \phi, \theta, \psi]^T$ comprise the slow states and the angular rates $[p, q, r]^T$ comprise the fast states. The aerodynamic database for the symmetric F/A-18A Hornet (seen in Figure 4.3) is used [74]. The aerodynamic coefficients are given as analytical functions of the sideslip angle, angle-of-attack, angular rates and the control surface deflections. Considering the number of controls available only three of the six slow states can be controlled. Throttle is maintained constant at $\eta = 0.523$ and is not used as a control. This is a result of using dynamic inversion [75]. The control objective is to perform a 45 degree turn at or near zero sideslip angle while tracking a specified angle-of-attack profile. Pitch attitude angle θ and bank angle ϕ are left uncontrolled.

Figure 4.3: F/A-18A Hornet external physical characteristics

The control laws are developed according to the theory developed in the previous subsections. For brevity only the equations required for incorporating the control law in the simulation are presented here. Since the aircraft equations of motion are highly coupled, the first step is to transform them into slow and fast sets. Let $\mathbf{x} = [\alpha, \beta, \psi]^T$ represent the subset of the slow states and $\mathbf{u} = [\delta_e, \delta_a, \delta_r]^T$ represent

the control variables

$$\dot{\mathbf{x}} = \underbrace{\mathbf{f_{11}}(\mathbf{x}, M, \theta, \phi) + \mathbf{f_{12}}(\mathbf{x}, \theta, \phi)\mathbf{z}}_{\mathbf{f_1}(.)} + \mathbf{f_2}(\mathbf{x}, M)\mathbf{u} \tag{4.65a}$$

$$\epsilon\dot{\mathbf{z}} = \underbrace{\mathbf{g_{11}}(\mathbf{z}) + \mathbf{g_{12}}(\mathbf{x}, M) + \mathbf{g_{13}}(\mathbf{x}, M)\mathbf{z}}_{\mathbf{g_1}(.)} + \mathbf{g_2}(\mathbf{x}, M)\mathbf{u}. \tag{4.65b}$$

The parameter ϵ is introduced on the left-hand side of the (4.65b) to indicate the time scale difference between body-axis angular rates and the other states [10]. In the translational equations of motion functions such as gravitational forces and aerodynamic forces due to angle-of-attack and sideslip angle are collectively represented as $\mathbf{f_{11}}(\mathbf{x}, M, \theta, \phi)$. Terms in the translational equations of motion due to the cross products between the angular rates and the slow states are labeled $\mathbf{f_{12}}(\mathbf{x}, \theta, \phi)\mathbf{z}$. The remaining terms in the slow state equations are the control effectiveness terms labeled $\mathbf{f_2}(\mathbf{x}, M)$. The nonlinearity in the fast dynamics due to the cross product between the angular rates is represented by $\mathbf{g_{11}}(\mathbf{z})$. The aerodynamic moment terms that depend solely upon the slow state are denoted as $\mathbf{g_{12}}(\mathbf{x}, M)$ and the aerodynamic moment terms that depend linearly on the angular rates are denoted as $\mathbf{g_{13}}(\mathbf{x}, M)$. The term $\mathbf{g_2}(\mathbf{x}, M)$ is the control effectiveness term in the angular rate dynamics. The exact form of these functions is derived in Appendix C. Define the errors $\tilde{\mathbf{x}} = \mathbf{x} - \mathbf{x}_r$ and $\tilde{\mathbf{z}} = \mathbf{z} - \mathbf{h}(\tilde{\mathbf{x}}, \epsilon, \mathbf{x}_r, \dot{\mathbf{x}}_r, M)$ and transform (4.65) into error coordinates equivalent to (4.25)

$$\begin{aligned}\dot{\tilde{x}} &= \mathbf{f_{11}}(\tilde{\mathbf{x}}, \mathbf{x}_r, M, \theta, \phi) + \mathbf{f_{12}}(\tilde{\mathbf{x}}, \mathbf{x}_r, \theta, \phi)\left[\tilde{\mathbf{z}} + \mathbf{h}(.)\right] \\ &+ \mathbf{f_2}(\tilde{\mathbf{x}}, \mathbf{x}, M)\left[\mathbf{\Gamma_s} + \mathbf{\Gamma_f}\right] - \dot{\mathbf{x}}_r \end{aligned} \tag{4.66a}$$

$$\begin{aligned}\epsilon\dot{\tilde{z}} &= \mathbf{g_{11}}(\tilde{\mathbf{z}}, \mathbf{h}(.)) + \mathbf{g_{12}}(\tilde{\mathbf{x}}, \mathbf{x}_r, M) + \mathbf{g_{13}}(\tilde{\mathbf{x}}, \mathbf{x}_r, M)\left[\tilde{\mathbf{z}} + \mathbf{h}(.)\right] \\ &+ \mathbf{g_2}(\tilde{\mathbf{x}}, \mathbf{x}_r, M)\left[\mathbf{\Gamma_s} + \mathbf{\Gamma_f}\right] - \epsilon\frac{\partial \mathbf{h}}{\partial t} - \epsilon\frac{\partial \mathbf{h}}{\partial \tilde{\mathbf{x}}}\dot{\tilde{\mathbf{x}}} - \epsilon\frac{\partial \mathbf{h}}{\partial M}\dot{M} \end{aligned} \tag{4.66b}$$

Note that for the aircraft example the manifold will also be a function of Mach number. Let

$$\mathbf{\Phi}(\tilde{\mathbf{x}}, \mathbf{x}_r, \dot{\mathbf{x}}_r, \mathbf{\Gamma_s}) = -\mathbf{g_{13}}^{-1}(\tilde{\mathbf{x}}, \mathbf{x}_r, M)\left[\mathbf{g_{12}}(\tilde{\mathbf{x}}, \mathbf{x}_r, M) + \mathbf{g_2}(\tilde{\mathbf{x}}, \mathbf{x}_r, M)\mathbf{\Gamma_s}\right] \tag{4.67}$$

be the approximate manifold such that manifold condition (4.24) becomes

$$(M\mathbf{\Phi})(\tilde{\mathbf{x}}, \mathbf{x}_r, \dot{\mathbf{x}}_r, \mathbf{\Gamma_s}) = \epsilon\frac{\partial \mathbf{\Phi}}{\partial t} + \epsilon\frac{\partial \mathbf{\Phi}}{\partial \tilde{\mathbf{x}}}\dot{\tilde{\mathbf{x}}} + \epsilon\frac{\partial \mathbf{\Phi}}{\partial M}\dot{M} - \mathbf{g_{11}}(\mathbf{\Phi}) - \mathbf{g_2}(\tilde{\mathbf{x}}, \mathbf{x}_r, M)\mathbf{\Gamma_f}. \tag{4.68}$$

To design the fast controller Γ_f, develop the reduced fast system

$$\tilde{\mathbf{x}}' = \mathbf{0} \tag{4.69a}$$

$$\begin{aligned}\tilde{\mathbf{z}}' = {} & \mathbf{g_{11}}(\tilde{\mathbf{z}}, \mathbf{\Phi}(.)) + \mathbf{g_{12}}(\tilde{\mathbf{x}}, \mathbf{x}_r, M) + \mathbf{g_{13}}(\tilde{\mathbf{x}}, \mathbf{x}_r, M)\left[\tilde{\mathbf{z}} + \mathbf{\Phi}(.)\right] \\ & + \mathbf{g_2}(\tilde{\mathbf{x}}, \mathbf{x}_r, M)\left[\mathbf{\Gamma_s} + \mathbf{\Gamma_f}\right]\end{aligned} \tag{4.69b}$$

Using dynamic inversion and (4.67) design

$$\mathbf{\Gamma_f} = \mathbf{g_2}^{-1}(\mathbf{x}, \mathbf{x}_r, M)\left[-A_f\tilde{\mathbf{z}} - \mathbf{g_{11}}(\tilde{\mathbf{z}}, \mathbf{\Phi}(.)) - \mathbf{g_{13}}(\tilde{\mathbf{x}}, \mathbf{x}_r, M)\tilde{\mathbf{z}}\right] \tag{4.70}$$

where A_f is the chosen feedback gain. Then the closed-loop reduced system becomes

$$\tilde{\mathbf{z}}' = -A_f\tilde{\mathbf{z}}. \tag{4.71}$$

Comparing with (4.30)

$$\mathbf{L_f}(.) = A_f\tilde{\mathbf{z}}; \quad \mathbf{K_f}(.) = \mathbf{0}. \tag{4.72}$$

Similarly, develop the reduced slow system

$$\begin{aligned}\dot{\tilde{\mathbf{x}}} &= \mathbf{f_{11}}(\tilde{\mathbf{x}}, \mathbf{x}_r, M, \theta, \phi) - \mathbf{f_{12}}(\tilde{\mathbf{x}}, \mathbf{x}_r, \theta, \phi)\mathbf{g_{13}}^{-1}(\tilde{\mathbf{x}}, \mathbf{x}_r, M)\mathbf{g_{12}}(\tilde{\mathbf{x}}, \mathbf{x}_r, M) \\ &- \mathbf{f_2}(\tilde{\mathbf{x}}, \mathbf{x}_r, M)\mathbf{g_2}^{-1}(\tilde{\mathbf{x}}, \mathbf{x}_r, M)\mathbf{g_{11}}(\mathbf{\Phi}) - \dot{\mathbf{x}}_r \\ &+ \left[-\mathbf{f_{12}}(\tilde{\mathbf{x}}, \mathbf{x}_r, \theta, \phi)\mathbf{g_{13}}(\tilde{\mathbf{x}}, \mathbf{x}_r, M)^{-1}\mathbf{g_2}(\tilde{\mathbf{x}}, \mathbf{x}_r, M) + \mathbf{f_2}(\tilde{\mathbf{x}}, \mathbf{x}_r, M)\right]\Gamma_s. \end{aligned} \tag{4.73}$$

Then the following choice of slow controller

$$\begin{aligned}\mathbf{\Gamma_s} &= \mathbf{B}^{-1}\left\{-A\tilde{\mathbf{x}} + \dot{\mathbf{x}}_r\right\} + \mathbf{B}^{-1}\left\{-\mathbf{f_{11}}(\tilde{\mathbf{x}}, \mathbf{x}_r, M, \theta, \phi)\right\} \\ &+ \mathbf{B}^{-1}\left\{\mathbf{f_{12}}(\tilde{\mathbf{x}}, \mathbf{x}_r, \theta, \phi)\mathbf{g_{13}}^{-1}(\tilde{\mathbf{x}}, \mathbf{x}_r, M)\mathbf{g_{12}}(\tilde{\mathbf{x}}, \mathbf{x}_r, M)\right\} \end{aligned} \tag{4.74}$$

with $\mathbf{B} = [-\mathbf{f_{12}}(\tilde{\mathbf{x}}, \mathbf{x}_r, \theta, \phi)\mathbf{g_{13}}(\tilde{\mathbf{x}}, \mathbf{x}_r, M)^{-1}\mathbf{g_2}(\tilde{\mathbf{x}}, \mathbf{x}_r, M) + \mathbf{f_2}(\tilde{\mathbf{x}}, \mathbf{x}_r, M)]$ and A is the feedback gain gives the following closed-loop reduced slow system:

$$\dot{\tilde{\mathbf{x}}} = -A\tilde{\mathbf{x}} - \mathbf{f_2}(\tilde{\mathbf{x}}, \mathbf{x}_r, M)\mathbf{g_2}^{-1}(\tilde{\mathbf{x}}, \mathbf{x}_r, M)\mathbf{g_{11}}(\mathbf{\Phi}(.)) \tag{4.75}$$

where $\mathbf{\Phi}(.)$is obtained from (4.67). Note by the choice of Γ_f, (4.68) becomes

$$(M\mathbf{\Phi})(\tilde{\mathbf{x}}, \mathbf{x}_r, \dot{\mathbf{x}}_r, \mathbf{\Gamma_s}) = \epsilon\frac{\partial \mathbf{\Phi}}{\partial t} + \epsilon\frac{\partial \mathbf{\Phi}}{\partial \tilde{\mathbf{x}}}\dot{\tilde{\mathbf{x}}} + \epsilon\frac{\partial \mathbf{\Phi}}{\partial M}\dot{M} \tag{4.76}$$

and thus $O(C(\epsilon = 0, \tilde{\mathbf{x}}, \mathbf{x}_r, \dot{\mathbf{x}}_r)) = 0$. Furthermore, since the aerodynamic moments are a function of the angular rates, matrix $\mathbf{g_{13}}(\tilde{\mathbf{x}}, \mathbf{x}_r, M)$ is full-rank. The control effectiveness terms $\mathbf{g_2}(\tilde{\mathbf{x}}+\mathbf{x}_r, M)$ represent the aerodynamic moment coefficients due to control effector deflections, which are nonzero.

The control laws are verified in simulation. The specified maneuver is a 45 degree turn near zero sideslip angle while simultaneously tracking a step input in angle-of-attack. The flight condition is Mach 0.3 at 20,000 feet altitude (0.3/20k). The

trim and initial conditions are $\alpha(0) = 2\text{deg}$, $p(0) = 4\text{deg/sec}$, $q(0) = -2\text{deg/sec}$, $r(0) = 2\text{deg/sec}$. The feedback gain matrices are

$$A = \begin{bmatrix} 1 & 0 & 0 \\ 0 & 1 & 0 \\ 0 & 0 & 1 \end{bmatrix}, A_f = \begin{bmatrix} 5 & 0 & 0 \\ 0 & 5 & 0 \\ 0 & 0 & 5 \end{bmatrix}. \tag{4.77}$$

Note that for an aircraft, the parameter ϵ is normally only introduced in the modeling stage to take advantage of the presence of different time scales in the system. In reality this parameter is a function of the flight condition and is difficult to quantify. Thus, it is advantageous to derive and implement controllers that do not require knowledge of this parameter. Theorem 4.1 guarantees the existence of the bound ϵ^*, but the nonlinearity of this example restricts its analytical computation.

Figures 4.4-4.7 evaluate control law performance for the specified maneuver. After initial transients settle out the angle-of-attack, sideslip angle and heading angle states closely track the reference. The angle-of-attack error is within $\pm 0.2\text{deg}$ and the sideslip angle tracking error is within $\pm 0.2\text{deg}$ throughout the maneuver. The heading angle is maintained within $\pm 0.25\text{deg}$. Close tracking of the slow states implies that the fast states are successfully being driven onto the approximate manifold, as in seen in Figure 4.6. The angular rates are smooth and errors are within $\pm 2\text{deg/sec}$. The control surface deflections are within bounds and generate the desired nonzero angular rates. In this example the Mach number, pitch-attitude angle and bank angle remain bounded by virtue of the reference trajectory design. Recall that bounded tracking demands that the angular rates remain bounded and consequently the Euler angles remain bounded through the exact kinematic relationships. Additionally, since angle-of-attack is being tracked and thrust remains constant, Mach number

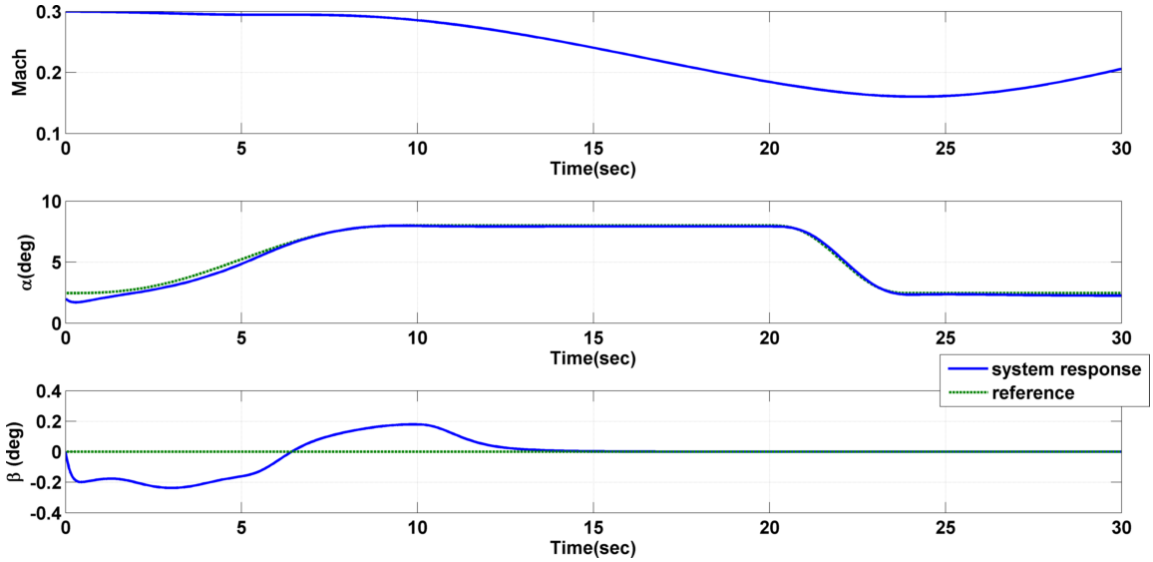

Figure 4.4: F/A-18A lateral/directional maneuver: Mach number, angle of attack and sideslip angle responses, 0.3/20k

remains bounded.

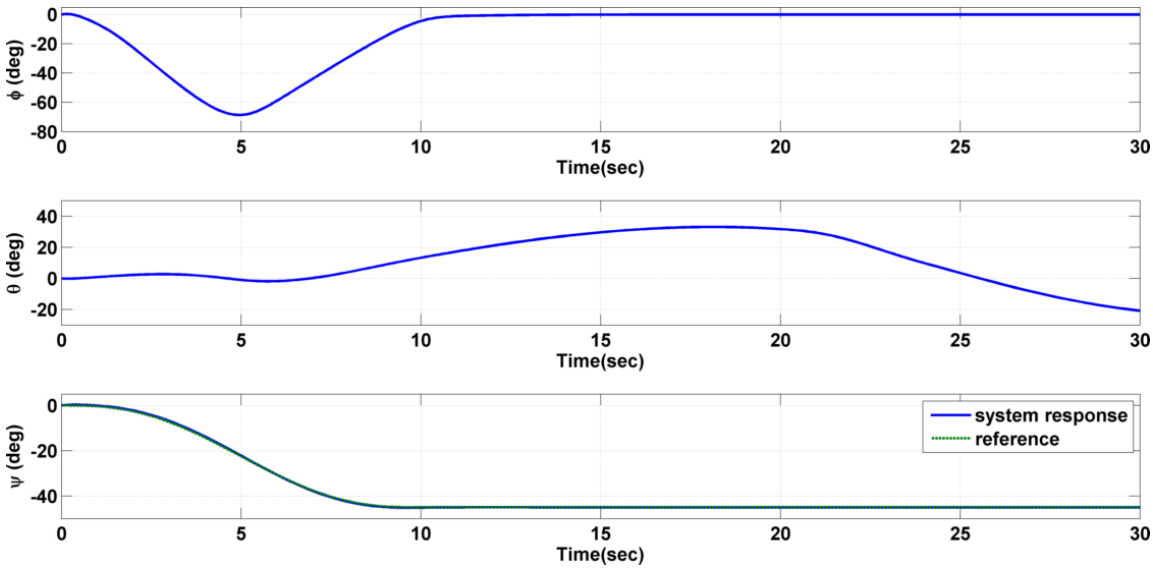

Figure 4.5: F/A-18A lateral/directional maneuver: kinematic angle responses, 0.3/20k

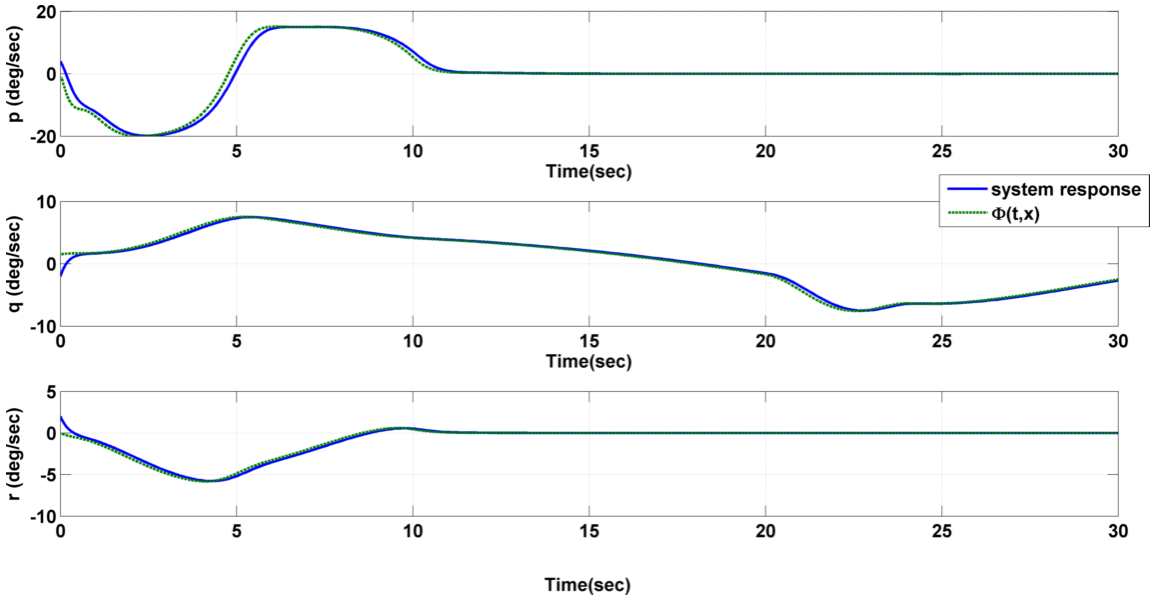

Figure 4.6: F/A-18A lateral/directional maneuver: angular rates, 0.3/20k

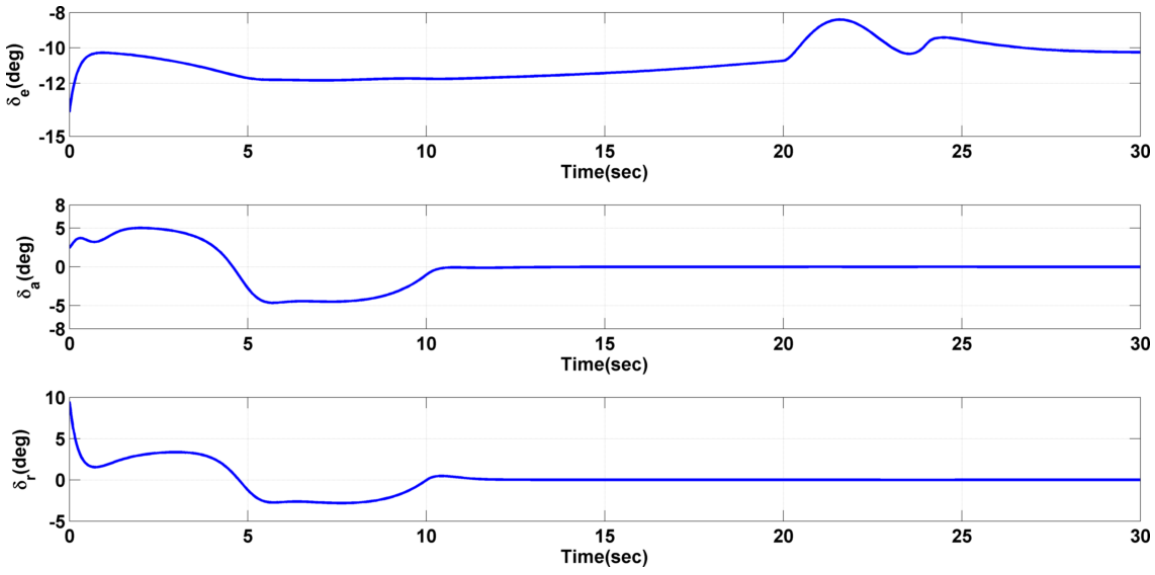

Figure 4.7: F/A-18A lateral/directional maneuver: control responses, 0.3/20k

4.3.5 Summary

Closed-loop stability and uniform boundedness of all signals demonstrated above was shown by the author in [73] using the modified composite Lyapunov approach. The stability proof detailed in the subsections above provide additional conditions that the system must satisfy such that the closed-loop system behaviour remains close to the closed-loop reduced-order systems. These conditions capture the effect of the singular perturbation parameter that was neglected in the control design. The asymptotic tracking results of standard singularly perturbed systems given by Saberi and Khalil[20] are shown to be a special case of the proposed approach. The stability proof also provides designers with a conservative upper-bound for the singular perturbation parameter such that closed-loop stability results hold. Additionally, upper bounds for all the states of the system are analytically determined. The benefits and limitations of the proposed approach are summarized below:

4.3.5.1 Benefits

1. The proposed approach extends composite control technique to a larger class of nonlinear singularly perturbed systems that are nonlinear in both the slow and the fast states.

2. Asymptotic stabilization and bounded local uniform tracking is guaranteed for non-standard singularly perturbed systems.

3. Exact knowledge of the singular perturbation parameter is not required as the controllers are designed using reduced-order models independent of the perturbation parameter.

4. The stability of the closed-loop system is robust to changes in singular perturbation parameter and is guaranteed to hold for a range of perturbation

parameter values.

5. The technique does not require the control to appear in affine form. This is because the control design is based on the reduced-order systems obtained using general nonlinear concepts of geometric singular perturbation theory and center manifolds that are represented by ordinary differential equations.

4.3.5.2 Limitations

1. The vector fields need to be at least twice continuously differentiable to ensure that the manifold and the control computed is continuous and sufficiently smooth.

2. The control variables need to have actuator dynamics faster than all the system states, since all available control variables are employed in stabilization of both the slow and fast subsystems. This stabilization is possible only when the controller responds faster than the system response.

3. The technique is limited to a class of non-standard models. It cannot be applied to systems with infinite manifolds such as $\dot{x} = \tan z + u$, $\epsilon\dot{z} = x - u$ where any real value of the fast state comprises the manifold for the system.

4. The fast control is dependent on the slow control resulting in a complicated design procedure. This is because the fast controller is designed ahead of the slow controller.

4.4 Approach II

Only local stabilization results have been shown in [73](Approach I above) for a general class of nonlinear systems as a consequence of employing approximation to

the manifold and modified composite control technique. In this approach the objective is to develop control laws that achieve desired slow state tracking while globally stabilizing the nonlinear singularly perturbed system. As before geometric singular perturbation theory is retained for model-reduction but the central difference is to consider the fast states as additional control variable. For sake of clarity consider only the stabilization problem of the nonlinear singularly perturbed system. By specifying the desired closed-loop dynamics for the reduced slow system, a smooth relation for the fast state in terms of the slow state and the control can be computed. Furthermore, if the control variable is designed such that the computed fast state becomes the stable unique manifold of the reduced fast system, then global stabilization is guaranteed. Clearly the above approach can be extended for the general tracking problem. These ideas are mathematically formulated and analyzed in this section.

4.4.1 Control Law Development

The objective is to augment the two time scale system given in (2.5) with controllers such that the slow state of the system follows smooth, bounded, time-varying trajectories $\mathbf{x}_r(t)$. The first step is to transform the problem into a non-autonomous stabilization control problem. Define the tracking error signal as

$$\tilde{\mathbf{x}}(t) = \mathbf{x}(t) - \mathbf{x}_r(t) \tag{4.78}$$

and express the two time scale system as

$$\dot{\tilde{\mathbf{x}}} = \mathbf{F}(\tilde{\mathbf{x}}, \mathbf{z}, \mathbf{x}_r, \dot{\mathbf{x}}_r, \mathbf{u}) \tag{4.79a}$$

$$\epsilon\dot{\mathbf{z}} = \mathbf{G}(\tilde{\mathbf{x}}, \mathbf{z}, \mathbf{x}_r, \mathbf{u}) \tag{4.79b}$$

where $\mathbf{F}(\tilde{\mathbf{x}}, \mathbf{z}, \mathbf{x}_r, \dot{\mathbf{x}}_r) \triangleq \mathbf{f_1}(\tilde{\mathbf{x}} + \mathbf{x}_r, \mathbf{z}) - \dot{\mathbf{x}}_r + \mathbf{f_2}(\tilde{\mathbf{x}} + \mathbf{x}_r, \mathbf{z})\mathbf{u}$, $\mathbf{G}(\tilde{\mathbf{x}}, \mathbf{z}, \mathbf{x}_r, \mathbf{u}) \triangleq \mathbf{g_1}(\tilde{\mathbf{x}} + \mathbf{x}_r, \mathbf{z}) + \mathbf{g_2}(\tilde{\mathbf{x}} + \mathbf{x}_r, \mathbf{z})\mathbf{u}$ have been defined for convenience. Using the procedure described in Section 4.2, obtain the reduced-order models for the above two time scale system.

Reduced slow system is given as:

$$\dot{\tilde{\mathbf{x}}} = \mathbf{F}(\tilde{\mathbf{x}}, \mathbf{z}, \mathbf{x}_r, \dot{\mathbf{x}}_r, \mathbf{u}) \tag{4.80a}$$

$$\mathbf{0} = \mathbf{G}(\tilde{\mathbf{x}}, \mathbf{z}, \mathbf{x}_r, \mathbf{u}) \tag{4.80b}$$

and *reduced fast system*:

$$\tilde{\mathbf{x}}' = \mathbf{0} \tag{4.81a}$$

$$\mathbf{z}' = \mathbf{G}(\tilde{\mathbf{x}}, \mathbf{z}, \mathbf{x}_r, \mathbf{u}) \tag{4.81b}$$

In order to ensure $\tilde{\mathbf{x}} = \mathbf{0}$ is an asymptotically stable equilibrium of the reduced slow system (4.80) define a positive-definite and decrescent Lyapunov function that satisfies:

Condition 1. $V(t, \tilde{\mathbf{x}}) : [0, \infty) \times D_{\mathbf{x}} \to \mathbb{R}$ is continuously differentiable and $D_{\mathbf{x}} \subset \mathbb{R}^m$ contains the origin, such that

$$0 < \psi_1(||\tilde{\mathbf{x}}||) \leq V(t, \tilde{\mathbf{x}}) \leq \psi_2(||\tilde{\mathbf{x}}||)$$

for some **class** $\mathcal{K}$ functions $\psi_1(.)$ and $\psi_2(.)$.

Design a manifold $\mathbf{z} = \mathbf{h}(\tilde{\mathbf{x}}, \mathbf{x_r}, \dot{\mathbf{x}}_\mathbf{r}, \mathbf{u})$ such that the slow state error system (4.80a) satisfies:

Condition 2. $\frac{\partial V}{\partial t} + \frac{\partial V}{\partial \tilde{\mathbf{x}}}\mathbf{F}(\tilde{\mathbf{x}}, \mathbf{h}, \mathbf{x}_r, \dot{\mathbf{x}}_r, \mathbf{u}) \leq -\alpha_1 \psi_3^2(\tilde{\mathbf{x}}), \quad \alpha_1 > 0$ where $\psi_3(.)$ is a

continuous positive-definite scalar function that satisfies $\psi_3(\mathbf{0}) = 0$.

Conditions 1 and 2 complete the design of control for the reduced slow system. Notice that the manifold $\mathbf{h}(\tilde{\mathbf{x}}, \mathbf{x_r}, \dot{\mathbf{x}}_\mathbf{r}, \mathbf{u})$ computed in the above control design is a function of the control $\mathbf{u}$ which is unknown. From the discussion detailed in Section 4.2, it is known that this manifold is a fixed point of the reduced fast system

$$\tilde{\mathbf{x}}' = \mathbf{0} \tag{4.82a}$$

$$\mathbf{z}' = \mathbf{G}(\tilde{\mathbf{x}}, \mathbf{z}, \mathbf{x}_r, \mathbf{u}). \tag{4.82b}$$

The complete system will have the properties of the reduced slow system if the fast state asymptotically stabilizes about $\mathbf{h}(.)$. This condition is enforced by designing the control signal $\mathbf{u}$. Define the error in the fast state vector $\tilde{\mathbf{z}} := \mathbf{z} - \mathbf{h}$ and rewrite (4.82b) as

$$\tilde{\mathbf{z}}' = \mathbf{G}(\tilde{\mathbf{x}}, \tilde{\mathbf{z}}, \mathbf{x}_r, \mathbf{u}) \tag{4.83}$$

while noting that $\mathbf{h}' = \epsilon\dot{\mathbf{h}} = \mathbf{0}$ for the reduced fast system. Define a positive-definite and decrescent Lyapunov function that satisfies:

Condition 3. $W(t, \tilde{\mathbf{x}}, \tilde{\mathbf{z}}) : [0, \infty) \times D_\mathbf{x} \times D_\mathbf{z} \to \mathbb{R}$ is continuously differentiable and $D_\mathbf{z} \subset \mathbb{R}^n$ contains the origin, such that

$$0 < \phi_1(||\tilde{\mathbf{z}}||) \leq W(t, \tilde{\mathbf{x}}, \tilde{\mathbf{z}}) \leq \phi_2(||\tilde{\mathbf{z}}||)$$

for some **class** $\mathcal{K}$ functions $\phi_1(.)$ and $\phi_2(.)$.

Design $\mathbf{u}$ such that the closed-loop reduced fast system (4.83) satisfies:

Condition 4. $\frac{\partial W}{\partial \tilde{\mathbf{z}}}\mathbf{G}(\tilde{\mathbf{x}}, \tilde{\mathbf{z}}, \mathbf{x}_r, \mathbf{u}) \leq -\alpha_3\phi_3^2(\tilde{\mathbf{z}}), \quad \alpha_3 > 0$ where $\phi_3(.)$ is a continuous positive-definite scalar function that satisfies $\phi_3(\mathbf{0}) = 0$.

This completes the control design.

4.4.2 Stability Analysis

The following theorem [76] summarizes the main result of this section.

Theorem 4.3. *Suppose the control* $\mathbf{u}$ *of the system (2.5) is designed according to the Conditions* $1-6$*. Then for all initial conditions,* $(\tilde{\mathbf{x}}, \tilde{\mathbf{z}}) \in D_{\mathbf{x}} \times D_{\mathbf{z}}$*, the control uniformly asymptotically stabilizes the nonlinear singularly perturbed system (2.5) and equivalently drives the slow state* $\mathbf{x}(t) \to \mathbf{x}_r(t)$ *for all* $\epsilon < \epsilon^*$ *defined (4.90).*

Proof. The closed-loop complete system in the error coordinates is given as

$$\dot{\tilde{\mathbf{x}}} = \mathbf{F}(\tilde{\mathbf{x}}, \tilde{\mathbf{z}} + \mathbf{h}, \mathbf{x}_r) \tag{4.84a}$$

$$\epsilon\dot{\tilde{\mathbf{z}}} = \mathbf{G}(\tilde{\mathbf{x}}, \tilde{\mathbf{z}} + \mathbf{h}, \mathbf{x}_r) - \epsilon\dot{\mathbf{h}} \tag{4.84b}$$

Closed-loop system stability of the system states is analyzed using the composite Lyapunov function approach[9]. Consider a Lyapunov function candidate

$$\nu(t, \tilde{\mathbf{x}}, \tilde{\mathbf{z}}) = (1-d)V(t, \tilde{\mathbf{x}}) + dW(t, \tilde{\mathbf{x}}, \tilde{\mathbf{z}}); \quad 0 < d < 1 \tag{4.85}$$

for the complete closed-loop system. From the properties of V and W it follows that $\nu(t, \tilde{\mathbf{x}}, \tilde{\mathbf{z}})$ is positive-definite and decrescent. The derivative of ν along the trajectories of (4.84) is given by

$$\dot{\nu} = (1-d)\big[\frac{\partial V}{\partial t} + \frac{\partial V}{\partial \tilde{\mathbf{x}}}\dot{\tilde{\mathbf{x}}}\big] + d\big[\frac{\partial W}{\partial t} + \frac{\partial W}{\partial \tilde{\mathbf{x}}}\dot{\tilde{\mathbf{x}}} + \frac{1}{\epsilon}\frac{\partial W}{\partial \tilde{\mathbf{z}}}\tilde{\mathbf{z}}'\big]. \tag{4.86}$$

Note that the vector fields in (4.84) can also be expressed as

$$\mathbf{F}(\tilde{\mathbf{x}}, \tilde{\mathbf{z}} + \mathbf{h}, \mathbf{x}_r, \dot{\mathbf{x}}_r) = \mathbf{F}(\tilde{\mathbf{x}}, \mathbf{h}, \mathbf{x}_r, \dot{\mathbf{x}}_r) + \mathbf{F}(\tilde{\mathbf{x}}, \tilde{\mathbf{z}} + \mathbf{h}, \mathbf{x}_r, \dot{\mathbf{x}}_r) - \mathbf{F}(\tilde{\mathbf{x}}, \mathbf{h}, \mathbf{x}_r, \dot{\mathbf{x}}_r). \tag{4.87}$$

Suppose that Lyapunov functions V and W also satisfy the following conditions with $\beta_i \geq 0$ and $\gamma_i \geq 0$.

Condition 5. $\frac{\partial V}{\partial \tilde{\mathbf{x}}}\mathbf{F}(\tilde{\mathbf{x}}, \tilde{\mathbf{z}} + \mathbf{h}, \mathbf{x}_r, \dot{\mathbf{x}}_r) - \frac{\partial V}{\partial \tilde{\mathbf{x}}}\mathbf{F}(\tilde{\mathbf{x}}, \mathbf{h}, \mathbf{x}_r, \dot{\mathbf{x}}_r) \leq \beta_1 \psi_3(\tilde{\mathbf{x}})\phi_3(\tilde{\mathbf{z}})$.

Condition 6.

$$\frac{\partial W}{\partial t} + \left[\frac{\partial W}{\partial \tilde{\mathbf{x}}} - \frac{\partial W}{\partial \tilde{\mathbf{z}}}\frac{\partial \mathbf{h}}{\partial \tilde{\mathbf{x}}}\right]\dot{\tilde{\mathbf{x}}} - \frac{\partial W}{\partial \tilde{\mathbf{z}}}\frac{\partial \mathbf{h}}{\partial \mathbf{x}_r}\dot{\mathbf{x}}_\mathbf{r} - \frac{\partial W}{\partial \tilde{\mathbf{z}}}\frac{\partial \mathbf{h}}{\partial \dot{\mathbf{x}}_\mathbf{r}}\ddot{\mathbf{x}}_\mathbf{r} \leq \gamma_1 \phi_3^2(\tilde{\mathbf{z}}) + \beta_2 \psi_3(\tilde{\mathbf{x}})\phi_3(\tilde{\mathbf{z}})$$

Conditions 5 and 6 enforce restrictions upon the difference between the complete system and the reduced systems. Use Conditions $1-6$ into (4.86) and rearrange to get:

$$\dot{\nu} \leq -\Psi^T \mathbb{K} \Psi \tag{4.88}$$

$$\mathbb{K} = \begin{bmatrix} (1-d)\alpha_1 & -\frac{1}{2}\left[(1-d)\beta_1 + d\beta_2\right] \\ -\frac{1}{2}\left[(1-d)\beta_1 + d\beta_2\right] & \frac{d\alpha_2}{\epsilon} - d\gamma_1 \end{bmatrix} \tag{4.89}$$

where $\Psi = [\psi_3, \phi_3]^T$ and matrix $\mathbb{K}$ given in (4.89) is positive-definite for $\epsilon < \epsilon^*$ defined as

$$\epsilon^* = \frac{\alpha_1 \alpha_2}{\alpha_1 \gamma_1 + \frac{1}{4d(1-d)}\left[(1-d)\beta_1 + d\beta_2\right]^2}. \tag{4.90}$$

By definition of the continuous scalar functions ψ_3 and ϕ_3 it follows that $\dot{\nu}$ is negative definite. By Lyapunov theorem it is concluded that $(\tilde{\mathbf{x}}, \mathbf{z}) = (\mathbf{0}, \mathbf{h}(\mathbf{0}, \mathbf{x}_r, \dot{\mathbf{x}}_r))$ is uniformly asymptotic stable equilibrium of the closed-loop system (4.84). Further, from definition of the tracking error it is concluded that $\mathbf{x}(t) \to \mathbf{x}_r(t)$ asymptotically. Since the desired trajectory is smooth and bounded all the other signals remain bounded for all time. This completes the proof. □

4.4.3 Numerical Examples

4.4.3.1 Purpose and Scope

The purpose of this section is to illustrate the preceding theoretical developments and demonstrate the controller performance for both standard and non-standard forms. The first example is taken from [20] and the purpose is to see how the proposed approach compares with composite control for standard singularly perturbed systems. The objective of the second example is to compare the performance of the two approaches developed in this chapter for the generic enzyme kinetic model described in Section 4.3. The third example analyzes the performance and robustness characteristics of the controller for non-standard form of singularly perturbed system with infinite manifolds.

4.4.3.2 Standard Singularly Perturbed Model

The following example is taken from [20]. The objective is to design a regulator to stabilize both the slow and the fast state in the domain $D_x \in [-1, 1]$ and $D_z = [-1/2, 1/2]$ of

$$\dot{x} = xz^3 \tag{4.91a}$$

$$\epsilon\dot{z} = z + u. \tag{4.91b}$$

The reduced-order models for the system under study are:

reduced slow system:

$$\dot{x} = xz^3 \tag{4.92a}$$

$$0 = z + u \tag{4.92b}$$

and *reduced fast system*:

$$x' = 0 \tag{4.93a}$$

$$z' = z + u. \tag{4.93b}$$

Notice that the algebraic equation in the reduced slow system has an isolated root for the fast state, thus the system given is in standard form.

The controller is designed using the same Lyapunov functions and closed-loop characteristics as in [20]. Using $V(x) = \frac{1}{6}x^6$ as Lyapunov function for the slow subsystem, the desired manifold $h = -x^{\frac{4}{3}}$ satisfies condition 2 with $\alpha_1 = 1$ and $\psi_3(x) = |x|^5$. The control is designed as $u = -3z - 2x^{\frac{4}{3}}$ to satisfy condition 4 with Lyapunov function $W = \frac{1}{2}(z-h)^2$, $\alpha_3 = 2$ and $\phi_3(x,z) = |z-h|$. The closed-loop system with $\tilde{z} = z - h$ becomes

$$\dot{x} = x(\tilde{z} + h)^3 \tag{4.94a}$$

$$\epsilon\dot{\tilde{z}} = -2\tilde{z} + \frac{4}{3}\epsilon x^{\frac{4}{3}}(\tilde{z} + h)^3. \tag{4.94b}$$

The other constants in the inequality (4.88) in the domain of interest are $\beta_1 = 7/4$, $\beta_2 = 4/3$ and $\gamma_1 = 7/3$. Thus asymptotic stabilization is guaranteed for all $\epsilon < 0.4286$ with choice of $d = 21/37$. Notice that the control law designed is exactly the same as that obtained using composite control.

4.4.3.3 Generic Two Degrees-of-Freedom Nonlinear Kinetic Model

The control design for generic two degrees-of-freedom model given in (4.47) described in Section 4.3.4.2 is presented. The following presents a discussion of how asymptotic tracking can be guaranteed using the approach developed earlier.

The objective is to seek the control vector that guarantees asymptotic slow

state tracking. Assume that the fast variables have settled onto the exact manifold $h(\tilde{x}, x_r, \dot{x}_r)$. Define errors $\tilde{x} = x - x_r$ and $z - h(.)$ and rewriting system (4.47) in error coordinates,

$$\dot{\tilde{x}} = -\tilde{x} - x_r - \dot{x}_r + (\tilde{x} + x_r + 0.5)[\tilde{z} + h] + u(\tilde{x}, \tilde{z}) \tag{4.95a}$$

$$\epsilon\dot{\tilde{z}} = \tilde{x} + x_r - (\tilde{x} + x_r + 1)[\tilde{z} + h] + [\tilde{z} + h]^2 + u(\tilde{x}, \tilde{z}). \tag{4.95b}$$

Then the resulting reduced slow system becomes

$$\dot{\tilde{x}} = -\tilde{x} - x_r + (\tilde{x} + x_r + 0.5)h + u(\tilde{x}, 0). \tag{4.96}$$

The manifold $h(\tilde{x}, x_r, \dot{x}_r)$ is designed to enforce asymptotic tracking of the desired slow state

$$h(\tilde{x}, x_r, \dot{x}_r) = \frac{-A\tilde{x} + \dot{x}_r + \tilde{x} + x_r - u(\tilde{x}, 0)}{(x_r + \tilde{x} + 0.5)} \tag{4.97}$$

where A is the feedback gain. The resulting reduced slow system becomes

$$\dot{\tilde{x}} = -A\tilde{x}. \tag{4.98}$$

The control is computed to ensure the fast variables settle onto the manifold given in (4.97). The reduced fast system is given as

$$\tilde{x}' = 0 \tag{4.99a}$$

$$\tilde{z}' = \tilde{x} + x_r - (\tilde{x} + x_r + 1)[\tilde{z} + h] + [\tilde{z} + h]^2 + u(\tilde{x}, \tilde{z}). \tag{4.99b}$$

The following feedback control design

$$u(\tilde{x},\tilde{z}) = -\tilde{x} - x_r + (\tilde{x} + x_r + 1)(\tilde{z} + h) - (\tilde{z} + h)^2 - A_f\tilde{z} \tag{4.100}$$

with A_f is the feedback gain results in closed-loop reduced fast system of the form $z' = -A_f\tilde{z}$. The resulting exact manifold $h(\tilde{x}, x_r, \dot{x}_r)$ satisfies the following relation that is determined by substituting (4.100) in (4.97):

$$h^2 - (2\tilde{x} + 2x_r + 1.5)h + [-A\tilde{x} + \dot{x}_r + 2\tilde{x}] = 0. \tag{4.101}$$

Either one of the solutions of the exact manifold given in (4.101) may be chosen for control design. The lesser of the two solutions

$$h(\tilde{x}, x_r, \dot{x}_r) = \tilde{x} + x_r + 0.75 - 0.5\sqrt{(2\tilde{x} + 2x_r + 1.5)^2 - 4[(-A + 2)\tilde{x} + 2x_r + \dot{x}_r]} \tag{4.102}$$

is chosen for implementation in this example. Note the manifold ϕ obtained in approach I is an approximation of the above equality.

The controller developed above is verified in simulation. The specified reference is a continuously time-varying sine-wave of $0.2\sin(t)$. The results are presented in Figure 4.8. The closed-loop gains for both the approaches are chosen as $A = 3$ and $A_f = 1$. The initial conditions are $x(0) = 0.3$ and $z(0) = 0.3$. From the simulation results it is seen that the system response for Modified composite/Approach I is bounded for all time. The fast state lags the exact manifold causing the error in the slow-state response. The analytic bounds on the states are determined to be $\tilde{x}_b = 0.0818$ and $\tilde{z}_b = 4.701$. The simulation results show that Approach II accomplishes asymptotic tracking since the fast state more closely follow the exact manifold

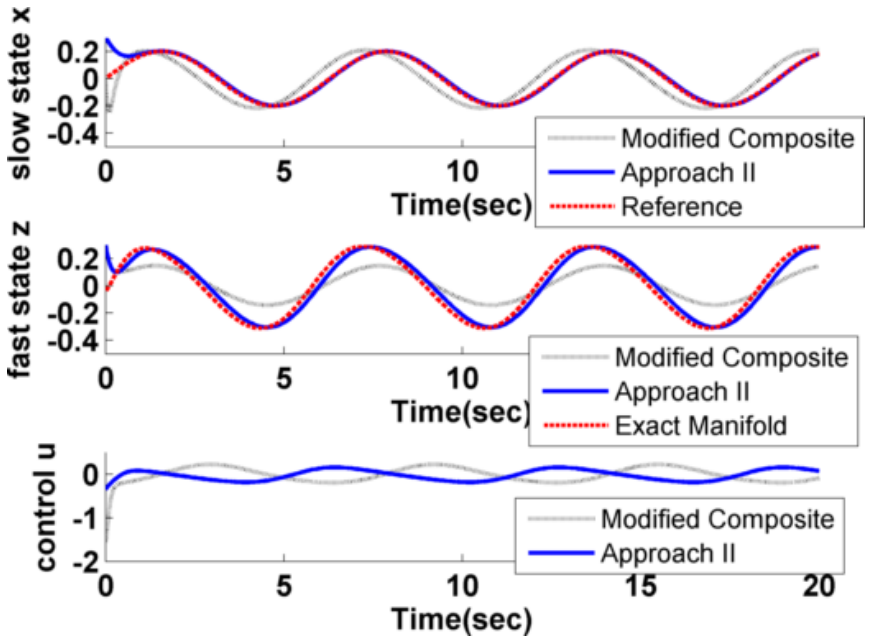

Figure 4.8: Closed-loop response and computed control of (4.47) using modified composite approach and approach II for $\epsilon = 0.2$

required for tracking. Results of approach I apply only locally in the domain of the errors are $D_x = [-0.3 \quad 0.3]$ and $D_z = [-1.5 \quad 1.5]$, whereas Approach II guarantees global asymptotic tracking. Using Lyapunov methods the upper bound for both the approaches was found to be $\epsilon^* = 2000$.

4.4.3.4 Non-Standard Singularly Perturbed Model

Consider the following unstable linear system:

$$\dot{x} = z - u \tag{4.103a}$$

$$\epsilon \dot{z} = x + u. \tag{4.103b}$$

The objective is to stabilize the system about $x = 0$ and $z = 0$ or equivalently to find the control $u(x, z)$ for regulation. Notice that the algebraic equation obtained by setting $\epsilon = 0$ has infinitely many solutions and composite control cannot be applied.

The control design procedure using the definitions $\tilde{x} := x$ and $\tilde{z} := z - h(\tilde{x})$ is summarized below.

The reduced slow system is

$$\dot{\tilde{x}} = h - u(\tilde{x}, 0) \tag{4.104a}$$

$$0 = \tilde{x} + u(\tilde{x}, 0). \tag{4.104b}$$

Recall that in designing for the manifold h it is assumed the error in fast states $\tilde{z}$ is identically zero and thus the control reduces to $u(\tilde{x}, 0)$. Choose $h = -\alpha_1\tilde{x} + u(\tilde{x}, 0)$. With $V(\tilde{x}) = \frac{1}{2}\tilde{x}^2$ condition 2 is satisfied with $\psi_3(e) = \tilde{x}$.

The reduced fast system is

$$\tilde{x}' = 0 \tag{4.105a}$$

$$\tilde{z}' = \tilde{x} + u(\tilde{x}, \tilde{z}). \tag{4.105b}$$

Choose $u(\tilde{x}, \tilde{z}) = -\tilde{x} - \alpha_2\tilde{z}$. With $W(\tilde{x}, \tilde{z}) = \frac{1}{2}\tilde{z}^2$ condition 4 is satisfied with $\phi_3(\tilde{z}) = \tilde{z}$.

The manifold h as a function of the slow state error, $\tilde{x}$ is computed using the control computed above. This gives

$$h = -\alpha_1\tilde{x} + u(\tilde{x}, 0) \equiv -(1 + \alpha_1)\tilde{x}. \tag{4.106}$$

The closed-loop slow system is

$$\dot{\tilde{x}} = -\alpha_1\tilde{x} + (1 + \alpha_2)\tilde{z} \tag{4.107a}$$

$$\epsilon\dot{\tilde{z}} = -\alpha_2\tilde{z} + (1 + \alpha_1)\epsilon\left[-\alpha_1\tilde{x} + (1 + \alpha_2)\tilde{z}\right]. \tag{4.107b}$$

Table 4.1: Maximum values of upper-bound ϵ^*

α_1	α_2	ϵ^*	d
1	1	0.25	0.5
1	0.1	0.04545	0.355
0.1	1	0.4543	0.95
0.1	0.1	0.08264	0.91

The interconnection conditions are satisfied with constants $\beta_1 = (1 + \alpha_2)$, $\beta_2 = -\alpha_1(1 + \alpha_2)$ and $\gamma_1 = (1 + \alpha_1)(1 + \alpha_2)$. The upper-bound on the perturbation parameter given in (4.90) is computed as

$$\epsilon^* = \frac{\alpha_1\alpha_2}{(1+\alpha_1)(1+\alpha_2)\alpha_1 + \frac{1}{d(1-d)}c^2} \tag{4.108}$$

with $c = \frac{1}{2}\left[(1-d)\beta_1 + d\beta_2\right]$. Equation (4.108) gives the relation between the design constants α_i and the upper-bound ϵ^*. This dependence is qualitatively analyzed by plotting the upper-bound as a function of weight d for different choice of α_i. Figure 4.9 and Table 4.1 summarize the results. The plot indicates that decreasing α_2 results in major changes in trend of the upper-bound curve. The upper-bound reduces and suggests that stability is guaranteed for a small class of systems. This can also be seen by noting that α_2 affects the fast system stability and in turn the closed-loop system stability. Change in α_1 primarily affects the reduced slow system and consequently only the performance of the system. Thus a decrease in α_1 does not cause the upper-bound to decrease. These trends suggest that a judicious choice of parameters α_1 and α_2 must be made to achieve desired performance and robustness properties of the closed-loop system.

The system given in (4.103) is the linearized model of the nonlinear, non-standard

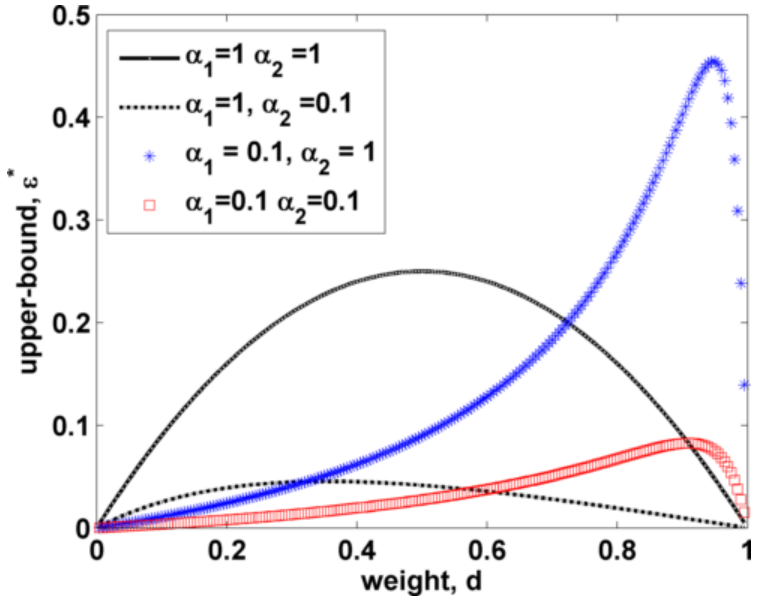

Figure 4.9: Upper-bound as a function of the weight, d for different values of α_i

form [29]

$$\dot{x} = \tan z - u \tag{4.109a}$$

$$\epsilon \dot{z} = x + u. \tag{4.109b}$$

Notice that the fast state appears nonlinearly in the slow dynamics and hence determining a manifold h to meet the control objective can be difficult. Instead, the same controller that was developed for the linear counterpart is used. The resulting closed-loop system with $\alpha_1 = \alpha_2 = 0.5$ is

$$\dot{x} = 1.75x + \tan z + 0.5z \tag{4.110a}$$

$$\epsilon \dot{z} = -0.75x - 0.5z. \tag{4.110b}$$

Notice that the controller converts the non-standard form into a standard form which uniquely restricts the system onto the desired manifold, which in this case

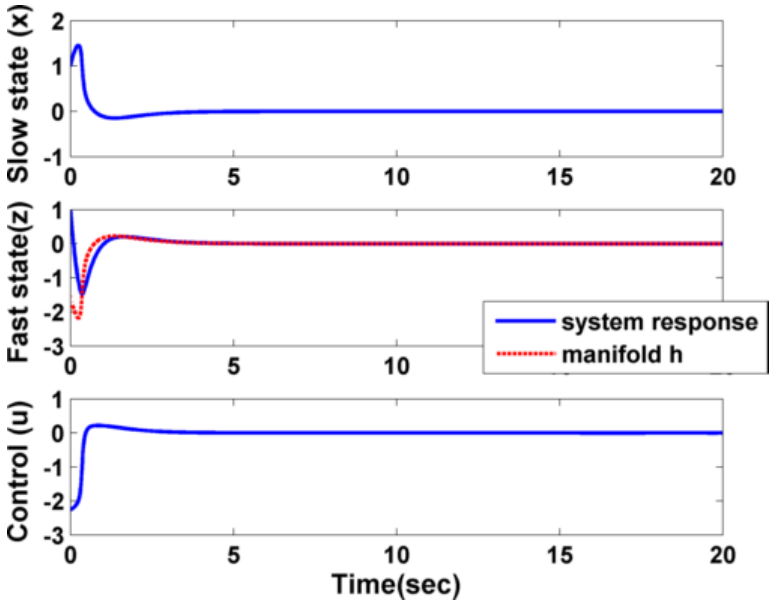

Figure 4.10: Nonlinear system (4.109) closed-loop response ($\epsilon = 0.1$)

is $h = -1.5x$. It is clear that due to the nonlinear nature of the system and local control design, the domain of attraction is now restricted to a subspace of the two-dimensional Euclidean space. The upper-bound on the singular perturbation parameter is computed as $\epsilon^* = \frac{2}{9}$ for $d = \frac{3}{5}$. Theorem 4.3 guarantees stability for the domain $D_x \in [0, -1)$ and $D_z \in [-1, 2]$. Simulation results indicate that stability is maintained for all $\epsilon < 0.4$ and the nonlinear system is asymptotically stabilized in the domain $D_x \in [-2, 2]$ and $D_z \in [-1.5, 2]$. Simulation results for the case of $\epsilon = 0.1$ are shown in Figure 4.10. Notice that the non-zero control is applied until the fast state falls onto the desired manifold.

4.4.4 Summary

The stability of the closed-loop system using Lyapunov approach [76] shows global uniform asymptotic tracking for the nonlinear system and provides an analytical upper bound for the singular perturbation parameter for the results to hold. Additional conditions on the terms neglected in the reduced-order models are also determined.

The technique requires that the dynamics of the reduced slow system depend upon the fast variables. This does not impose any additional restriction and is satisfied for singularly perturbed systems in general. Note that if the dynamics of the slow states did not depend on the fast variables then the presence of multiple scales need not be addressed. The benefits and limitations of the proposed approach are detailed below.

4.4.4.1 Benefits

1. Asymptotic stabilization and asymptotic slow-state tracking is accomplished for non-standard singularly perturbed systems, including systems with infinite manifolds.

2. Second, not all controllers are required to be fast and controllers with different speeds can be addressed in comparison to composite control and approach I[73] that requires all control variables to be sufficiently fast.

3. Third, the control laws are computed using Lyapunov-based designs that are able to capture the nonlinear behaviour that is lost in linearization of the system. Owing to this, the global or local nature of results are relaxed from the complexities of analytic construction of the manifold and are entirely a consequence of the choice of underlying controllers for the reduced-order models.

4. Additionally, the control laws developed are independent of the singular perturbation parameter. Also an upper bound for the scalar perturbation parameter is derived as a necessary condition for asymptotic stability.

5. The control is not required to be in affine form as the control design is based on reduced-order systems obtained using geometric singular perturbation theory.

4.4.4.2 Limitations

1. The vector fields need to be at least twice continuously differentiable to ensure that the manifold and the control computed is sufficiently smooth.

2. The fast variables whose manifolds are not prescribed by control design of the reduced slow system need to have stable dynamics to ensure complete system stability.

4.5 Closing Remarks

In this section, basic methodologies for asymptotic tracking of slow states of non-standard singularly perturbed systems have been developed. Two control law formulations based on geometric singular perturbation theory concepts have been presented. The salient features of the techniques developed are compared and detailed below.

1. **Systems Handled:** Geometric singular perturbation theory plays an integral part in convergence and stability properties of the developed techniques. Consequently the control problem of a two time scale system is reduced down to appropriate control design for two lower-dimensional nonlinear systems. Further, these controllers may be designed using any nonlinear technique available and suitable for system under consideration. Thus the stabilization results do not require the system to be affine in control.

   It must be noted that modified composite approach stabilizes only a class of non-standard systems due to center manifold approximation. The second approach presented has no such limitations and applies to all classes of non-standard systems.

2. **Required Actuator Characteristics:** Modified composite control technique employs all the available control signals for stabilizing both the reduced slow and the reduced fast systems. This requires that all the available actuators respond sufficiently fast relative to the inherent state response.

   This requirement is slightly weakened in the second approach. Recall that in this approach the control signals stabilize the reduced fast system and the reduced slow system is stabilized by the fast states alone. If the system under study possesses actuators that are relatively slower than the fast states, then these can be employed along with the fast states to control the reduced slow system. However, note that sufficient number of fast actuators must still be available to ensure the stability of the fast states.

3. **Convergence Characteristics:** Both the developed approaches guarantee asymptotic regulation for the two time scale system. However, the domain of convergence of each of these approaches depends on the manifold approximation and underlying controllers respectively. Furthermore, the tracking performance of each of these schemes is independent of the reference trajectory and uniform boundedness and asymptotic behaviour is demonstrated respectively.

4. **Robustness:** Both the control formulations presented in this chapter demonstrate robustness to the singular perturbation parameter. In fact, the control schemes are also robust to system parameter changes and bounded disturbances since Lyapunov methods are employed for control design. Unlike modified composite approach, the convergence of the second approach fails to white-noise disturbance exogenous input as the stability depends on identifying the manifold exactly.

5. **Design Procedure:** The design of control laws using modified composite approach becomes increasingly complex with increase in degrees-of-freedom due to dependence of the fast controller upon the slow controller. Hence the design procedure is sequential. On the other hand, the control synthesis using second approach is less complicated and sequential in nature. Both the control schemes are causal, that is depend only on current value of the states and are real-time implementable.

In summary, control formulations presented in this chapter extend the composite control scheme for non-standard forms of singularly perturbed systems. The methods are robust to parameter variations and do not require knowledge of the singular perturbation parameter. The second approach further weakens the requirement of fast actuators, thus opening doors for stabilization of multiple-time scale systems of the form (2.1), which is the subject matter of Section 6.

5. SIMULTANEOUS TRACKING OF SLOW AND FAST TRAJECTORIES FOR CONTROL-AFFINE, TWO TIME SCALE SYSTEMS[1]

5.1 Introduction

This section addresses the third objective detailed in Section 2. The following nonlinear singularly perturbed model represents the class of two time scale dynamical systems considered with

$$\dot{\mathbf{x}} = \mathbf{f_1}(\mathbf{x}, \mathbf{z}) + \mathbf{f_2}(\mathbf{x}, \mathbf{z})\mathbf{u} \tag{2.5a}$$

$$\epsilon\dot{\mathbf{z}} = \mathbf{g_1}(\mathbf{x}, \mathbf{z}) + \mathbf{g_2}(\mathbf{x}, \mathbf{z})\mathbf{u} \tag{2.5b}$$

and the output

$$\mathbf{y} = \begin{bmatrix} \mathbf{x} \\ \mathbf{z} \end{bmatrix} \tag{5.1}$$

where $\mathbf{x} \in \mathbb{R}^m$ is the vector of slow variables, $\mathbf{z} \in \mathbb{R}^n$ is the vector of fast variables, $\mathbf{u} \in \mathbb{R}^p$ is the input vector and $\mathbf{y} \in \mathbb{R}^{m+n}$ is the output vector. $\epsilon \in \mathbb{R}^+$ is the singular perturbation parameter that satisfies $0 < \epsilon << 1$. The vector fields $\mathbf{f_1}(.), \mathbf{f_2}(.), \mathbf{g_1}(.)$ and $\mathbf{g_2}(.)$ are assumed to be sufficiently smooth and $p \geq (m + n)$. The control objective is to drive the output so as to track sufficiently smooth, bounded, time-varying trajectories such that $\mathbf{x}(t) \to \mathbf{x}_r(t)$ and $\mathbf{z}(t) \to \mathbf{z}_r(t)$ as $t \to \infty$.

5.2 Control Formulation and Stability Analysis

The central idea in the development is the following. If the manifold is unique and an asymptotically stable fixed point of the reduced fast system, geometric singular

[1]Parts of this section reprinted from Advances in Aerospace Guidance, Navigation and Control, 2011, pp 235-246, "Global tracking control structures for nonlinear singularly perturbed aircraft systems", Siddarth, Anshu and Valasek, John, ©Springer-Verlag Berlin Heidelberg; with kind permission from Spinger Science and Business Media.

perturbation theory concludes that the complete system follows the dynamics of the reduced slow system globally. Therefore, for a tracking problem addressed in this section it is desired that this manifold lie exactly on the desired fast state reference for all time. *This condition can be enforced if the nonlinear algebraic set of equations is augmented with a controller that enforces the reference to be the unique manifold and simultaneously drives the slow states to their specified reference.* These ideas are mathematically formulated and analyzed in the following sections.

5.2.1 Control Law Development

The objective is to augment the two time scale system with controllers such that the system follows smooth, bounded, time-varying trajectories $[\mathbf{x}_r(t), \mathbf{z}_r(t)]^T$. The first step is to transform the problem into a non-autonomous stabilization control problem. Define the tracking error signals as

$$\mathbf{e}(t) \triangleq \mathbf{x}(t) - \mathbf{x}_r(t) \tag{5.2a}$$

$$\xi(t) \triangleq \mathbf{z}(t) - \mathbf{z}_r(t). \tag{5.2b}$$

Substituting (2.5), the tracking error dynamics are expressed as

$$\dot{\mathbf{e}} = \mathbf{f_1}(\mathbf{x}, \mathbf{z}) + \mathbf{f_2}(\mathbf{x}, \mathbf{z})\mathbf{u} - \dot{\mathbf{x}}_r \triangleq \mathbf{F}(\mathbf{e}, \xi, \mathbf{x}_r, \mathbf{z}_r, \dot{\mathbf{x}}_r) + \mathbf{G}(\mathbf{e}, \xi, \mathbf{x}_r, \mathbf{z}_r)\mathbf{u} \tag{5.3a}$$

$$\epsilon\dot{\xi} = \mathbf{g_1}(\mathbf{x}, \mathbf{z}) + \mathbf{g_2}(\mathbf{x}, \mathbf{z})\mathbf{u} - \epsilon\dot{\mathbf{z}}_r \triangleq \mathbf{L}(\mathbf{e}, \xi, \mathbf{x}_r, \mathbf{z}_r, \epsilon\dot{\mathbf{z}}_r) + \mathbf{K}(\mathbf{e}, \xi, \mathbf{x}_r, \mathbf{z}_r)\mathbf{u}. \tag{5.3b}$$

The control law is formulated using the reduced-order models for the complete stabilization problem, which are obtained using the procedure developed in Section 4.2. The *reduced slow system* is given as

$$\dot{\mathbf{e}} = \mathbf{F}(\mathbf{e}, \xi, \mathbf{x}_r, \mathbf{z}_r, \dot{\mathbf{x}}_r) + \mathbf{G}(\mathbf{e}, \xi, \mathbf{x}_r, \mathbf{z}_r)\mathbf{u}_0 \tag{5.4a}$$

$$\mathbf{0} = \mathbf{L}(\mathbf{e}, \xi, \mathbf{x}_r, \mathbf{z}_r, \mathbf{0}) + \mathbf{K}(\mathbf{e}, \xi, \mathbf{x}_r, \mathbf{z}_r)\mathbf{u}_0 \tag{5.4b}$$

where the subscript 0, for the control input signifies control for the slow subsystem and is referred to as the slow control from here on. The following *reduced fast system* is derived by assuming that the slow control $\mathbf{u}_0$ is known

$$\mathbf{e}' = \mathbf{0} \tag{5.5a}$$

$$\xi' = \mathbf{L}(\mathbf{e}, \xi, \mathbf{x}_r, \mathbf{z}_r, \mathbf{z}_r') + \mathbf{K}(\mathbf{e}, \xi, \mathbf{x}_r, \mathbf{z}_r)(\mathbf{u}_0 + \mathbf{u}_f) \tag{5.5b}$$

and $\mathbf{u}_f$ is treated as the control input which is referred as the fast control. It is known that the fast tracking error ξ will settle onto the manifold that is a function of the error $\mathbf{e}$ and control input $\mathbf{u}_0$, which may not necessarily be the origin. To steer both errors to the origin, the control input must be designed such that the origin becomes the unique manifold of the reduced slow system given in (5.4). Therefore, the slow controller $\mathbf{u}_0$ is designed to take the form

$$\begin{bmatrix} \mathbf{G}(\mathbf{e}, \xi, \mathbf{x}_r, \mathbf{z}_r) \\ \mathbf{K}(\mathbf{e}, \xi, \mathbf{x}_r, \mathbf{z}_r) \end{bmatrix} \mathbf{u}_0 = - \begin{bmatrix} \mathbf{F}(\mathbf{e}, \xi, \mathbf{x}_r, \mathbf{z}_r, \dot{\mathbf{x}}_r) \\ \mathbf{L}(\mathbf{e}, \xi, \mathbf{x}_r, \mathbf{z}_r, \mathbf{0}) \end{bmatrix} + \begin{bmatrix} A_{\mathbf{e}}\mathbf{e} \\ A_\xi \xi \end{bmatrix} \tag{5.6}$$

where $A_{\mathbf{e}}$ and A_ξ specify the desired closed-loop characteristics. With this choice of slow control, the reduced fast system becomes

$$\mathbf{e}' = \mathbf{0} \tag{5.7a}$$

$$\xi' = \mathbf{L}(\mathbf{e}, \xi, \mathbf{x}_r, \mathbf{z}_r, \mathbf{z}_r') - \mathbf{L}(\mathbf{e}, \xi, \mathbf{x}_r, \mathbf{z}_r, \mathbf{0}) + A_\xi \xi + \mathbf{K}(\mathbf{e}, \xi, \mathbf{x}_r, \mathbf{z}_r)\mathbf{u}_f. \tag{5.7b}$$

To stabilize the fast subsystem, the fast control $\mathbf{u}_f$ is designed as

$$\begin{bmatrix} \mathbf{G}(\mathbf{e}, \xi, \mathbf{x}_r, \mathbf{z}_r) \\ \mathbf{K}(\mathbf{e}, \xi, \mathbf{x}_r, \mathbf{z}_r) \end{bmatrix} \mathbf{u}_f = \begin{bmatrix} \mathbf{0} \\ \mathbf{L}(\mathbf{e}, \xi, \mathbf{x}_r, \mathbf{z}_r, \mathbf{0}) - \mathbf{L}(\mathbf{e}, \xi, \mathbf{x}_r, \mathbf{z}_r, \mathbf{z}_r') \end{bmatrix}. \tag{5.8}$$

Thus, the composite control $\mathbf{u} = \mathbf{u}_0 + \mathbf{u}_f$ satisfies

$$\begin{bmatrix} \mathbf{G}(\mathbf{e}, \xi, \mathbf{x}_r, \mathbf{z}_r) \\ \mathbf{K}(\mathbf{e}, \xi, \mathbf{x}_r, \mathbf{z}_r) \end{bmatrix} \mathbf{u} = - \begin{bmatrix} \mathbf{F}(\mathbf{e}, \xi, \mathbf{x}_r, \mathbf{z}_r, \dot{\mathbf{x}}_r) \\ \mathbf{L}(\mathbf{e}, \xi, \mathbf{x}_r, \mathbf{z}_r, \mathbf{z}'_r) \end{bmatrix} + \begin{bmatrix} A_e \mathbf{e} \\ A_\xi \xi \end{bmatrix} \tag{5.9}$$

assuming that the rank of $\begin{bmatrix} \mathbf{G}(.) \\ \mathbf{K}(.) \end{bmatrix} \geq (m+n)$. The complete closed-loop and reduced slow system for this control law are given as

$$\dot{\mathbf{e}} = A_e \mathbf{e} \tag{5.10a}$$

$$\epsilon \dot{\xi} = A_\xi \xi. \tag{5.10b}$$

and

$$\dot{\mathbf{e}} = A_e \mathbf{e} \tag{5.11a}$$

$$\mathbf{0} = A_\xi \xi. \tag{5.11b}$$

respectively. Observe that with the proposed control law the nonlinear algebraic set of equations in (5.4b) have been transformed to a linear set of equations in (5.11b). With the proper choice of A_ξ, it is guaranteed that $\xi = \mathbf{0}$ is the unique manifold for both the complete and the reduced slow systems. Furthermore, this manifold is exponentially stable as can be deduced from the reduced fast system

$$\mathbf{e}' = \mathbf{0} \tag{5.12a}$$

$$\xi' = A_\xi \xi. \tag{5.12b}$$

The control law proposed in (5.9) is independent of the perturbation parameter ϵ. Furthermore it is a function of $\mathbf{z}'_r$ that implies that the reference trajectory chosen

for the fast states must be faster when compared to the reference of the slow states. Additionally, as for all singular perturbation techniques to work; the closed-loop eigenvalues A_e and A_ξ must be chosen so as to maintain the time scale separation.

5.2.2 Stability Analysis

The following theorem [77] summarizes main result of this section.

Theorem 5.1. *Suppose the control* $\mathbf{u}$ *of the system (2.5) is designed according to (5.9) and satisfies properties* $1-4$. *Then for all initial conditions, the control uniformly exponentially stabilizes the nonlinear singularly perturbed system (2.5) and equivalently drives the output* $\mathbf{x}(t) \to \mathbf{x}_r(t)$ *and* $\mathbf{z}(t) \to \mathbf{z}_r(t)$ *for all* $\epsilon < \epsilon^*$ *defined in (5.18).*

Proof. Complete system stability is analyzed using the composite Lyapunov function approach[9]. Suppose that positive definite Lyapunov functions $V(t,\mathbf{e}) = \mathbf{e}^T\mathbf{e}$ and $W(t,\xi) = \xi^T\xi$ exist for the reduced-order models, satisfying the following properties:

1. $V(t,\mathbf{0}) = 0$ and $\gamma_1||\mathbf{e}||^2 \leq V(t,\mathbf{e}) \leq \gamma_2||\mathbf{e}||^2 \ \forall t \in \mathbb{R}^+, \mathbf{e} \in \mathbb{R}^m, \gamma_1 = \gamma_2 = 1$,
2. $(\nabla_{\mathbf{e}} V(t,\mathbf{e}))^T A_{\mathbf{e}}\mathbf{e} \leq -\alpha_1 \mathbf{e}^T\mathbf{e}, \quad \alpha_1 = 2|\lambda_{\min}(A_{\mathbf{e}})|$,
3. $W(t,\mathbf{0}) = 0$ and $\gamma_3||\xi||^2 \leq W(t,\xi) \leq \gamma_4||\xi||^2 \ \forall t \in \mathbb{R}^+, \xi \in \mathbb{R}^n, \gamma_3 = \gamma_4 = 1$,
4. $(\nabla_\xi W(t,\xi))^T A_\xi \xi \leq -\alpha_2 \xi^T\xi, \quad \alpha_2 = 2|\lambda_{\min}(A_\xi)|$.

Next, consider the composite Lyapunov function $\nu(t,\mathbf{e},\xi) : \mathbb{R}^+ \times \mathbb{R}^m \times \mathbb{R}^n \to \mathbb{R}^+$ defined by the weighted sum of $V(t,\mathbf{e})$ and $W(t,\xi)$ for the complete closed-loop system

$$\nu(t,\mathbf{e},\xi) = (1-d)V(t,\mathbf{e}) + dW(t,\xi); \quad 0 < d < 1. \tag{5.13}$$

The derivative of $\nu(t, \mathbf{e}, \xi)$ along the closed-loop trajectories (5.10) is given by

$$\dot{\nu} = (1-d)(\nabla_{\mathbf{e}} V)^T \dot{\mathbf{e}} + d(\nabla_{\xi} W)^T \dot{\xi} \tag{5.14a}$$

$$\dot{\nu} = (1-d)(\nabla_{\mathbf{e}} V)^T A_{\mathbf{e}} \mathbf{e} + \frac{d}{\epsilon}(\nabla_{\xi} W)^T A_{\xi} \xi. \tag{5.14b}$$

Using properties 1-4, (5.14) becomes

$$\dot{\nu} \leq -(1-d)\alpha_1 \mathbf{e}^T \mathbf{e} - \frac{d}{\epsilon}\alpha_2 \xi^T \xi \tag{5.15a}$$

$$\dot{\nu} \leq -\begin{bmatrix} \mathbf{e} \\ \xi \end{bmatrix}^T \begin{bmatrix} (1-d)\alpha_1 & 0 \\ 0 & \frac{d}{\epsilon}\alpha_2 \end{bmatrix} \begin{bmatrix} \mathbf{e} \\ \xi \end{bmatrix}. \tag{5.15b}$$

Following the approach proposed in [43], add and subtract $2\alpha\nu(t, \mathbf{e}, \xi)$ to (5.15) to get

$$\dot{\nu} \leq -\begin{bmatrix} \mathbf{e} \\ \xi \end{bmatrix}^T \begin{bmatrix} (1-d)\alpha_1 & 0 \\ 0 & \frac{d}{\epsilon}\alpha_2 \end{bmatrix} \begin{bmatrix} \mathbf{e} \\ \xi \end{bmatrix} + 2\alpha(1-d)V + 2\alpha d W - 2\alpha\nu \tag{5.16}$$

where $\alpha > 0$. Substitute in (5.16) for the Lyapunov functions $V(t, \mathbf{e})$ and $W(t, \xi)$ to get

$$\dot{\nu} \leq -\begin{bmatrix} \mathbf{e} \\ \xi \end{bmatrix}^T \begin{bmatrix} (1-d)\alpha_1 - 2\alpha(1-d) & 0 \\ 0 & \frac{d}{\epsilon}\alpha_2 - 2\alpha d \end{bmatrix} \begin{bmatrix} \mathbf{e} \\ \xi \end{bmatrix} - 2\alpha\nu. \tag{5.17}$$

If ϵ satisfies

$$\epsilon < \epsilon^* = \frac{\alpha_2}{2\alpha} \tag{5.18}$$

provided $\alpha_1 > 2\alpha$, then from the definitions of α_2, α and d it can be concluded that the matrix in (5.17) is positive definite. Then the derivative of the Lyapunov

function is lower-bounded by

$$\dot{\nu} \leq -2\alpha\nu. \tag{5.19}$$

Since the composite Lyapunov function lies within the following bounds

$$(1-d)\gamma_1||\mathbf{e}||^2 + d\gamma_3||\xi||^2 \leq \nu(t,\mathbf{e},\xi) \leq (1-d)\gamma_2||\mathbf{e}||^2 + d\gamma_4||\xi||^2 \tag{5.20}$$

or

$$\gamma_{11}\left|\left|\left[\begin{array}{c}\mathbf{e}\\ \xi\end{array}\right]\right|\right|^2 \leq \nu(t,\mathbf{e},\xi) \leq \gamma_{22}\left|\left|\left[\begin{array}{c}\mathbf{e}\\ \xi\end{array}\right]\right|\right|^2 \tag{5.21}$$

where $\gamma_{11} = \min\left((1-d)\gamma_1, d\gamma_3\right)$ and $\gamma_{22} = \min\left((1-d)\gamma_2, d\gamma_4\right)$, the derivative of the Lyapunov function can be expressed as

$$\dot{\nu} \leq -2\alpha\gamma_{11}\left|\left|\left[\begin{array}{c}\mathbf{e}\\ \xi\end{array}\right]\right|\right|^2. \tag{5.22}$$

From the definition of the constants γ_{11}, γ_{22}, and α, and invoking Lyapunov's Direct Method[65]; *uniform exponential stability in the large of* $(\mathbf{e} = \mathbf{0}, \xi = \mathbf{0})$ *can be concluded*. Furthermore, since the reference trajectory $\mathbf{x}_r(t)$ and $\mathbf{z}_r(t)$ is bounded, it is concluded that the states $\mathbf{x}(t) \to \mathbf{x}_r(t)$ and $\mathbf{z}(t) \to \mathbf{z}_r(t)$ as $t \to \infty$. Since the matrix $\left[\begin{array}{c}\mathbf{G}(.)\\ \mathbf{K}(.)\end{array}\right]$ is restricted to be full rank, examining the expression for $\mathbf{u}$ in (5.9) it is concluded that $\mathbf{u} \in \mathcal{L}_\infty$. This completes the proof. □

Remark 5.2.1. Recall that for the special case of state regulation the system dynamics in (5.3) become autonomous. In such a case, the result of global exponential stability

is obtained with less-restrictive conditions on the Lyapunov functions $V(\mathbf{e})$, $W(\xi)$, and consequently $\nu(\mathbf{e}, \xi)$. Similar conclusions were made in [43] for the stabilization problem of a special class of singularly perturbed systems where the control affects only the fast states. Note that for the special class of systems considered in [43], the non-diagonal elements of the matrix in (5.17) are nonzero and the bound on the parameter ϵ is slightly different.

Remark 5.2.2. From (5.17), a conservative upper bound for α is $\alpha < \frac{\alpha_1}{2}$, and consequently $\epsilon^* \approx \frac{\alpha_2}{\alpha_1}$. Therefore, qualitatively this upper bound is indirectly dependent upon the choice of the closed-loop eigenvalues.

5.3 Numerical Examples

5.3.1 Purpose and Scope

The purpose of this section is to demonstrate the methodology and controller performance for two non-standard forms of two-time scale systems. The first example is the generic enzyme kinetic model and the objective is to study the robustness properties of the controller for different values of the perturbation parameter. The second example is an under-actuated, nonlinear, singularly perturbed system. The system studied is a nonlinear, coupled, six degrees-of-freedom F/A-18A Hornet aircraft detailed in Appendix C.

5.3.2 Generic Two Degrees-of-Freedom Nonlinear Kinetic Model

Consider the generic enzyme kinetic model given in (4.47) modified to obtain a fully-actuated system

$$\dot{x} = -x + (x + 0.5)z + u_1 - 2u_2 \tag{5.23a}$$

$$\epsilon\dot{z} = x - (x + 1)z + z^2 + u_1 + 3u_2. \tag{5.23b}$$

The objective is to simultaneously track smooth trajectories $x_r(t)$ and $z_r(t)$. Define the errors $e = x - x_r$ and $\xi = z - z_r$ and rewrite (5.23) in error coordinates

$$\dot{e} = -(e + x_r) + (e + x_r + 0.5)(\xi + z_r) + u_1 - 2u_2 - \dot{x}_r \tag{5.24a}$$

$$\epsilon\dot{e}_z = e + x_r - (e + x_r + 1)(\xi + z_r) + (\xi + z_r)^2 + u_1 + 3u_2 - \epsilon\dot{z}_r \tag{5.24b}$$

similar to (5.3). The controller design and simulation results are detailed below.

Assume that the control vector is a sum of slow and fast control $\mathbf{u}_0$ and $\mathbf{u}_f$ respectively. Further assume that the fast controller remains inactive when the fast state lies ideally on the manifold z_r. Then the reduced slow system is given as

$$\begin{aligned} \dot{e} &= -(e + x_r) + (e + x_r + 0.5)(\xi + z_r) + u_{10} - 2u_{20} - \dot{x}_r & (5.25a)\\ 0 &= e + x_r - (e + x_r + 1)(\xi + z_r) + (\xi + z_r)^2 + u_{10} + 3u_{20}. & (5.25b) \end{aligned}$$

Using feedback linearization the slow control components are designed to ensure that the slow state follows desired trajectory x_r and the fast state remain on the manifold z_r with $\chi = e + x_r$ defined for convenience

$$\begin{bmatrix} u_{10} \\ u_{20} \end{bmatrix} = \frac{1}{5}\begin{bmatrix} 3 & 2 \\ -1 & 1 \end{bmatrix}\begin{bmatrix} -\alpha_1 e + \chi - (\chi + 0.5)(\xi + z_r) + \dot{x}_r \\ -\alpha_2\xi - \chi + (\chi + 1)(\xi + z_r) - (\xi + z_r)^2 \end{bmatrix} \tag{5.26}$$

where α_1 and α_2 are feedback gains. The reduced fast system is given as

$$\begin{aligned} e' &= 0 & (5.27a)\\ e'_z &= e + x_r - (e + x_r + 1)(\xi + z_r) + (\xi + z_r)^2 + u_{10} + 3u_{20} + u_{1f} \\ &+ 3u_{2f} - z'_r. & (5.27b) \end{aligned}$$

With the slow controller defined in (5.26), the purpose of the fast controller is to ensure the derivative information of the fast reference is captured. Thus,

$$\begin{bmatrix} u_{1f} \\ u_{2f} \end{bmatrix} = \frac{1}{5} \begin{bmatrix} 3 & 2 \\ -1 & 1 \end{bmatrix} \begin{bmatrix} 0 \\ z_r' \end{bmatrix}. \tag{5.28}$$

The complete control is the composite of (5.26) and (5.28)

$$\begin{bmatrix} u_{1s} \\ u_{2s} \end{bmatrix} = \frac{1}{5} \begin{bmatrix} 3 & 2 \\ -1 & 1 \end{bmatrix} \begin{bmatrix} -\alpha_1 e + \chi - (\chi + 0.5)(\xi + z_r) + \dot{x}_r \\ -\alpha_2 \xi - \chi + (\xi + 1)(\xi + z_r) - (\xi + z_r)^2 + z_r' \end{bmatrix}. \tag{5.29}$$

The specified references are $x_r = 2\sin(t)$ and $z_r = 2\cos(5t)$. Notice that the reference trajectories are chosen to maintain a time scale difference. The fast-time scale is $\tau = 5t$ and $\epsilon = \frac{1}{5} = 0.2$. The derivatives of the reference trajectories are $\dot{x}_r = 2\cos(t)$ and $\dot{z}_r = -10\sin(5t)$. The derivative of the fast state reference in the fast time scale is $z_r' = -2\sin(5t)$. Note that this time scale difference was chosen by the designer. The actual system may be perturbed differently. In simulation, the actual system was chosen to have $\epsilon = 0.01$. The feedback gains were $\alpha_1 = 1$ and $\alpha_2 = 3$. Figure 5.1 presents the closed-loop response of the system. Notice that the slow states asymptotically track the reference specified. The fast state however lags the reference slightly because the time scales for the system and the reference are different. Figure 5.2 shows simulation results on the system with $\epsilon = 0.2$. Notice that there is no phase lag in the fast state trajectory and the reference. Lyapunov methods show that this behaviour is guaranteed for $\epsilon < 0.3$. The results show that the control signals remain bounded throughout.

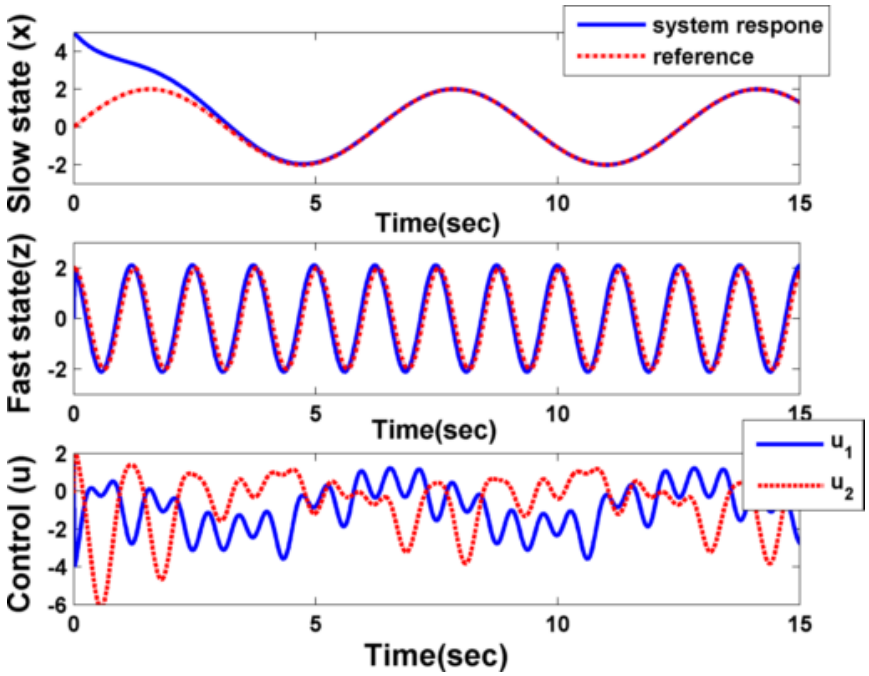

Figure 5.1: Enzyme kinetic model: simultaneous tracking of slow and fast states and computed control for $\epsilon = 0.01$

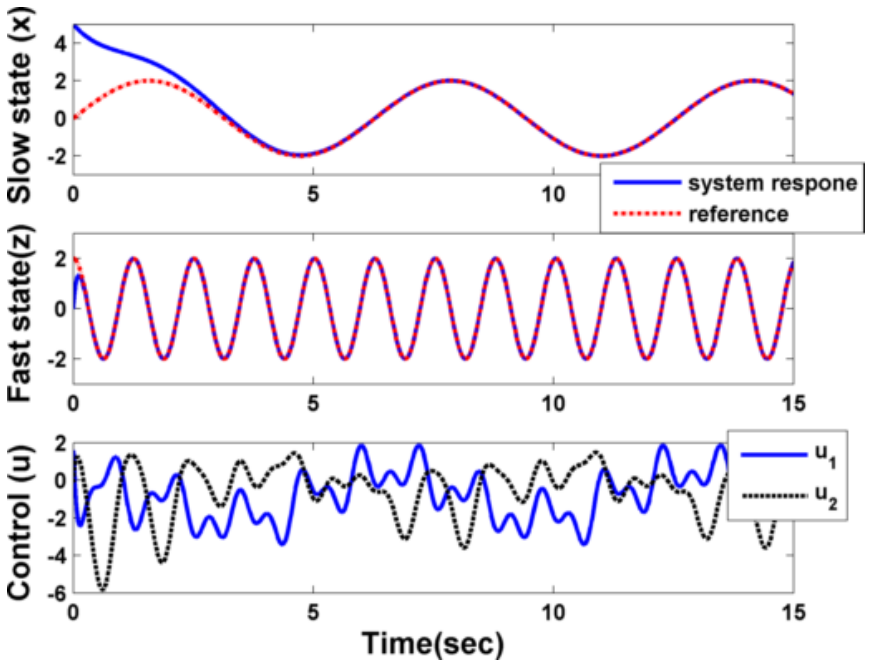

Figure 5.2: Enzyme kinetic model: simultaneous tracking of slow and fast states and computed control for $\epsilon = 0.2$

5.3.3 Combined Longitudinal and Lateral/Directional Maneuver for a F/A-18 Hornet

In this example, closed-loop characteristics such as stability, accuracy, speed of response and robustness are qualitatively analyzed for the F/A-18 model detailed in Appendix C. The F/A-18A Hornet model is expressed in stability axes. Since it is difficult to cast the nonlinear aircraft model into the singular perturbation form of (2.5), the perturbation parameter ϵ is introduced in front of those state variables that have the fastest dynamics. This is done so that the results obtained for $\epsilon = 0$ will closely approximate the complete system behaviour (with $\epsilon = 1$). This is called forced perturbation technique and is commonly used in the aircraft literature [10], [78]. Motivated by experience and previous results, the six slow states are Mach number M, angle-of-attack α, sideslip angle β and the three kinematic states: bank angle ϕ, pitch-attitude angle θ, and heading angle ψ. The three body-axis angular rates (p, q, r) constitute the fast states. The control variables for this model are elevon δ_e, aileron δ_a and rudder δ_r; which are assumed to have sufficiently fast enough actuator dynamics. The convention used is that a positive deflection generates a negative moment. The throttle η is maintained constant at 80%, because slow engine dynamics require introduction of an additional time scale in the analysis; which is the subject matter of Section 6. The aerodynamic stability and control derivatives are represented as nonlinear analytical functions of aerodynamic angles and control surface deflections. Quaternions are used to represent the kinematic relationships from which the Euler angles are extracted. The details of these relationships are discussed in [79].

The combined longitudinal-lateral/directional maneuver requires tracking of the fast variables, in this case body-axis pitch and roll rates; while maintaining zero

sideslip angle. The maneuver consists of an aggressive vertical climb with a pitch rate of 25 deg/sec followed by a roll at a rate of 50 deg/sec while maintaining zero sideslip angle. The Mach number and angle-of-attack are assumed to be input-to-state stable. The initial conditions are: Mach number of 0.4 at $15,000$ feet, an angle-of-attack of 10 deg and elevon angle of -11.85 deg. All other states are zero. The control design closely follows the developments presented in Section 5.2 and is not repeated here.

Simulation results in Figures 5.3-5.8 show that all controlled states closely track their references. At two seconds the aircraft is commanded to perform a vertical climb and after eight seconds the pitch rate command changes direction and Mach number drops. The lateral/directional states and controls are identically zero until the roll command is introduced at time equals 15 seconds. Observe that all of the states asymptotically track the reference. Figure 5.4 shows that the elevon deflection remains within specified limits [74] throughout the vertical climb, and the commanded roll produces a sideslip angle which is negated by application of the rudder. The aileron and the rudder deflections remain within bounds while the aircraft rolls and comes back to level flight. The maximum pitch-attitude angle is 81 deg, maximum bank angle is 81 deg (see Figure 5.6) and the maximum sideslip error is $\pm$4deg. The quaternions and the complete trajectory are shown in Figure 5.7 and Figure 5.8 respectively. Note that after completing the combined climb and roll maneuver, the aircraft is commanded to remain at zero sideslip angle, roll rate, and pitch rate. It then enters a steady dive as seen in Figure 5.8 with all other aircraft states bounded. The controller response is judged to be essentially independent of the reference trajectory designed. The robustness properties of the controller are quantified by the upper bound ϵ^*. For this example, the design variables are $d = 0.5$, $\alpha_1 = 10$, $\alpha = 2$, and $\alpha_2 = 15$, so the upper bound becomes $\epsilon^* = 7.5$. Therefore for

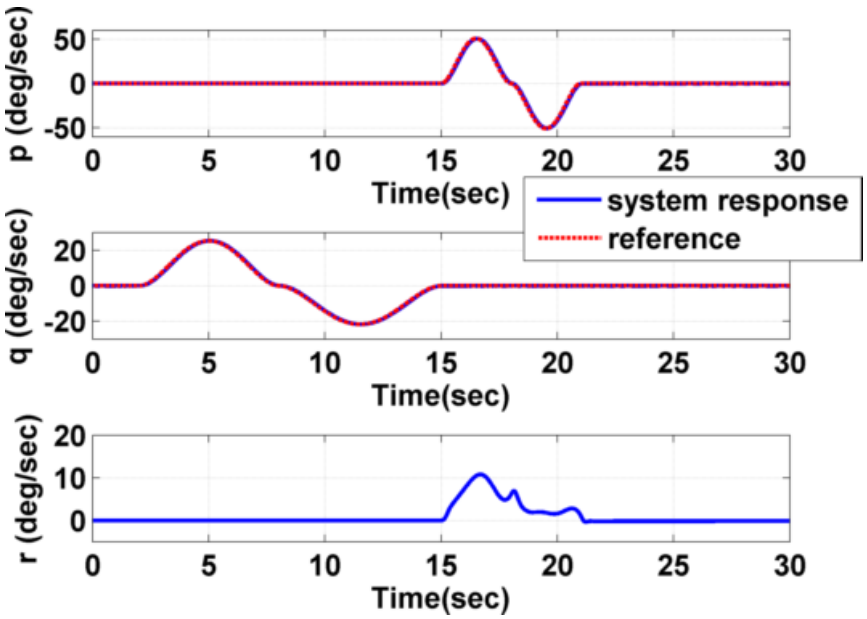

Figure 5.3: Body axis angular rate response for F/A-18A combined longitudinal and lateral/directional maneuver

all $\epsilon < \epsilon^*$ global asymptotic tracking is guaranteed and in this case $\epsilon = 1$.

5.4 Closing Remarks

In summary, a control law for global asymptotic tracking of both the slow and the fast states for a general class of nonlinear singularly perturbed systems was developed. A composite control approach was adopted to satisfy two objectives. First, it enforces the specified reference for the fast states to be 'the unique manifold' of the fast dynamics for all time. Second, it ensures that the slow states are tracked simultaneously as desired. Following [77] stability of the closed-loop signals was analyzed using the composite Lyapunov approach and controller performance was demonstrated through numerical simulation of a nonlinear kinetic model and coupled, six degrees-of-freedom model of an F/A-18A Hornet. The control laws were implemented without making any assumptions about the nonlinearity of the six degrees-of-freedom aircraft model.

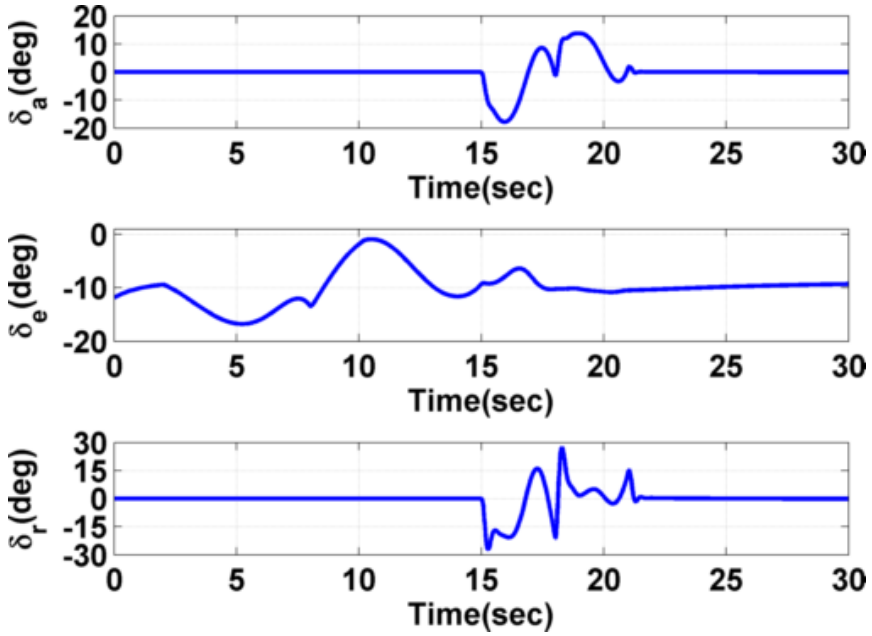

Figure 5.4: Commanded control surface deflections for F/A-18A combined longitudinal and lateral/directional maneuver

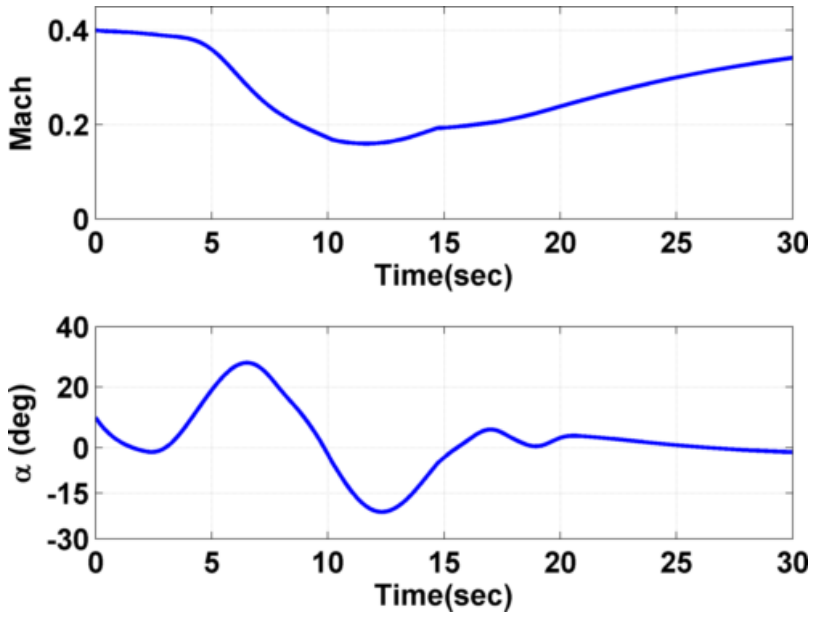

Figure 5.5: Mach number and angle of attack response for F/A-18A combined longitudinal and lateral/directional maneuver

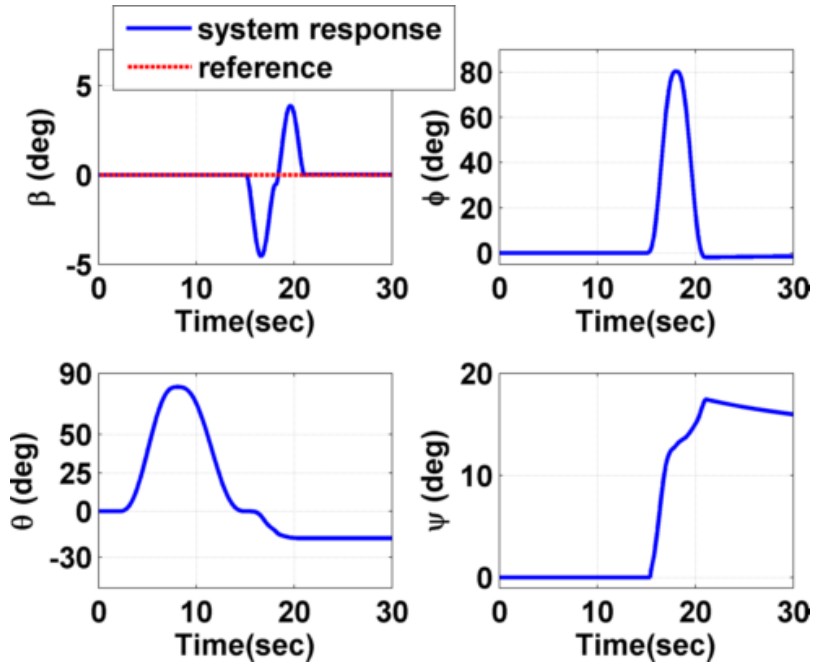

Figure 5.6: Sideslip angle and kinematic angle response for F/A-18A combined longitudinal and lateral/directional maneuver

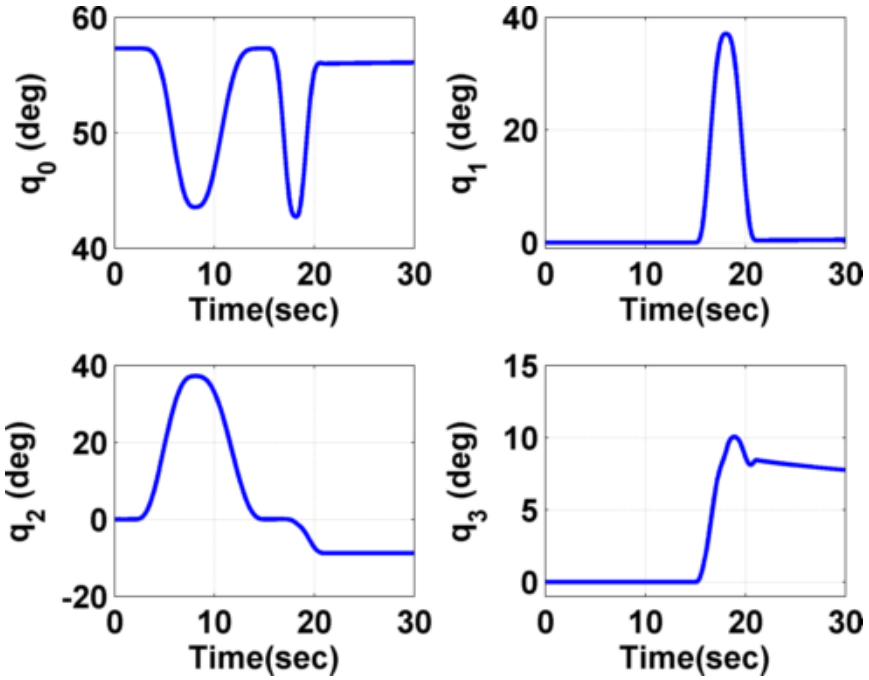

Figure 5.7: Quaternion parameters for F/A-18A combined longitudinal and lateral/directional maneuver

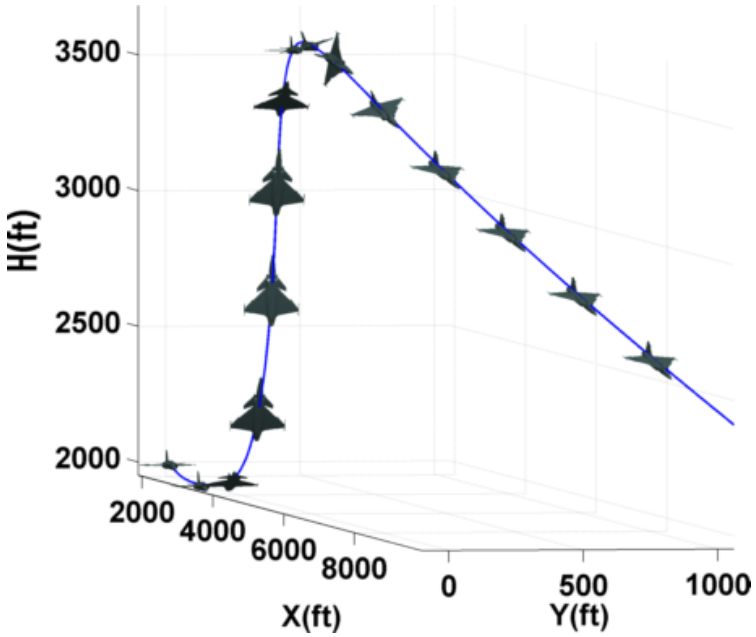

Figure 5.8: Three dimensional trajectory for F/A-18A combined longitudinal and lateral/directional maneuver

Based on the results presented in this section, the following conclusions are drawn. First, both positive and negative angular rate commands were seen to be perfectly tracked by the controller and consistent tracking was guaranteed independent of the desired reference trajectory. Second, throughout the maneuver the controller demonstrated global asymptotic tracking even though the desired reference trajectory requires the aircraft to switch between linear and nonlinear regimes. This robust performance of the controller was shown to hold for all $\epsilon < \epsilon^* = 7.5$. The benefits and the limitations of the proposed approach are detailed below:

5.4.1 Benefits

1. The reduced-order approach is shown to be applicable for simultaneous tracking of both slow and fast states of non-standard singularly perturbed systems.

2. Although feedback-linearization was employed to design slow control in (5.26) and fast control in (5.28), the control variable is not required to be in affine

form. Infact, any control technique that ensures properties $1-4$ are satisfied may be employed.

3. Asymptotic tracking results are shown to be robust for a range of singular perturbation values using composite Lyapunov approach. Furthermore, since geometric singular perturbation theory is employed for model-reduction, exact knowledge about the perturbation parameter is not required. This is an important consideration for systems such as aircraft where quantifying this parameter can be difficult. However, the reference trajectories must be chosen such that time scale properties of the original system are preserved.

5.4.2 Limitations

1. The vector fields are required to be at least twice differentiable such that the control is sufficiently smooth.

2. The system must be fully-actuated. In case the system is under-actuated, the uncontrolled degrees-of-freedom are required to be stable to ensure closed-loop asymptotic results.

3. The actuator dynamics should be sufficiently fast, since all the control channels are used in stabilizing both the reduced slow and the reduced fast systems.

6. CONTROL OF NONLINEAR, NON-AFFINE, NON-STANDARD MULTIPLE TIME SCALE SYSTEMS

6.1 Introduction

This section addresses the fourth objective detailed in Section 2. The class of nonlinear singularly perturbed dynamical systems being considered are repeated below for convenience with

$$\mathscr{S}: \begin{cases} \dot{\mathbf{x}} = \mathbf{f}(\mathbf{x}, \mathbf{z}, \delta) \\ \epsilon\dot{\delta}_\epsilon = \mathbf{f}_{\delta_\epsilon}(\delta_\epsilon, \mathbf{u}_\epsilon, \epsilon) \\ \mu\dot{\mathbf{z}} = \mathbf{g}(\mathbf{x}, \mathbf{z}, \delta, \mu); \\ \varrho\dot{\delta}_\varrho = \mathbf{f}_{\delta_\varrho}(\delta_\varrho, \mathbf{u}_\varrho, \varrho) \end{cases} \tag{2.1}$$

where $\mathbf{x} \in \mathbb{R}^m$, is the vector of slow variables, $\mathbf{z} \in \mathbb{R}^n$ is the vector of fast variables, $\delta = [\delta_\epsilon, \delta_\varrho]^T \in \mathbb{R}^p$ is the vector of actuator commands with $\delta_\epsilon \in \mathbb{R}^l$ and $\delta_\varrho \in \mathbb{R}^{p-l}$, $\mathbf{u} = [\mathbf{u}_\epsilon, \mathbf{u}_\varrho]^T \in \mathbb{R}^p$ is the input vector that is to be computed with $\mathbf{u}_\epsilon \in \mathbb{R}^l$ and $\mathbf{u}_\varrho \in \mathbb{R}^{p-l}$. The singular perturbation parameters $\epsilon \in \mathbb{R}$, $\mu \in \mathbb{R}$ and $\varrho \in \mathbb{R}$ measure the time scale separation explicitly and satisfy Assumption 2.1. All the vector fields are assumed to be sufficiently smooth. The control objective is to drive the slow state so as to track sufficiently smooth, bounded, time-varying trajectories or $\mathbf{x}(t) \to \mathbf{x}_r(t)$ as $t \to \infty$. The control laws developed here extend approach II detailed in Section 4.4. The necessary background and control formulation are detailed in the following sections.

6.2 Background: Reduced-Order Models

The system considered in (2.1) is labeled the *Slow System* and the independent variable t is called the *slow time scale*. Notice that the slow variables evolve at a

rate of $O(1)$ whereas all the other states evolve faster at rates of $O(\frac{1}{\epsilon})$, $O(\frac{1}{\mu})$ and $O(\frac{1}{\varrho})$. Hence (2.1) describes the evolution of all the other states relative to the rate of evolution of the slow variables. So it is called the slow system. In order to study the rate of evolution of the system states relative to either the slow actuators δ_ϵ, the fast variables $\mathbf{z}$, or the fast actuators δ_ϱ, the slow system (2.1) is represented in three other time scales. These representations are given by $\mathscr{S}_\epsilon$, $\mathscr{S}_\mu$ and $\mathscr{S}_\varrho$ defined below. *Slow actuator system* is

$$\mathscr{S}_\epsilon : \begin{cases} \breve{\mathbf{x}} = \epsilon \mathbf{f}(\mathbf{x}, \mathbf{z}, \delta) \\ \breve{\delta}_\epsilon = \mathbf{f}_{\delta_\epsilon}(\delta_\epsilon, \mathbf{u}_\epsilon, \epsilon) \\ \frac{\mu}{\epsilon}\breve{\mathbf{z}} = \mathbf{g}(\mathbf{x}, \mathbf{z}, \delta, \mu) \\ \frac{\varrho}{\epsilon}\breve{\delta}_\varrho = \mathbf{f}_{\delta_\varrho}(\delta_\varrho, \mathbf{u}_\varrho, \varrho) \end{cases} \tag{6.1}$$

where $\breve{}$ represents the derivative with respect to the time scale $\tau_\epsilon = \frac{t-t_0}{\epsilon}$ and t_0 is the initial time. *Fast system* is

$$\mathscr{S}_\mu : \begin{cases} \mathbf{x}' = \mu \mathbf{f}(\mathbf{x}, \mathbf{z}, \delta) \\ \delta_\epsilon{}' = \frac{\mu}{\epsilon}\mathbf{f}_{\delta_\epsilon}(\delta_\epsilon, \mathbf{u}_\epsilon, \epsilon) \\ \mathbf{z}' = \mathbf{g}(\mathbf{x}, \mathbf{z}, \delta, \mu) \\ \frac{\varrho}{\mu}\delta_\varrho{}' = \mathbf{f}_{\delta_\varrho}(\delta_\varrho, \mathbf{u}_\varrho, \varrho) \end{cases} \tag{6.2}$$

where $'$ is the derivative with respect to the time scale $\tau_\mu = \frac{t-t_0}{\mu}$. *Fast actuator system* is

$$\mathscr{S}_\varrho : \begin{cases} \check{\mathbf{x}} = \varrho \mathbf{f}(\mathbf{x}, \mathbf{z}, \delta) \\ \check{\delta}_\epsilon = \frac{\varrho}{\epsilon}\mathbf{f}_{\delta_\epsilon}(\delta_\epsilon, \mathbf{u}_\epsilon, \epsilon) \\ \check{\mathbf{z}} = \frac{\varrho}{\mu}\mathbf{g}(\mathbf{x}, \mathbf{z}, \delta, \mu) \\ \check{\delta}_\varrho = \mathbf{f}_{\delta_\varrho}(\delta_\varrho, \mathbf{u}_\varrho, \varrho) \end{cases} \tag{6.3}$$

and $\breve{}$ represents derivative with respect to the time scale $\tau_\varrho = \frac{t-t_0}{\varrho}$. Observe that the systems $\mathscr{S}$, $\mathscr{S}_\epsilon$, $\mathscr{S}_\mu$ and $\mathscr{S}_\varrho$ defined above are all equivalent. The subscripts denote the parameter used to define the respective 'stretched time scale' in which the systems have been expressed.

Geometric singular perturbation theory [5] examines the behaviour of these singularly perturbed systems by studying the geometric constructs of their discontinuous limiting behaviour as $\epsilon \to 0$, $\mu \to 0$ and $\varrho \to 0$. Using Assumption 2.1 the reduced-order models thus obtained are:

reduced slow system:

$$\mathscr{S}^0 : \begin{cases} \dot{\mathbf{x}} = \mathbf{f}(\mathbf{x}, \mathbf{z}, \delta) \\ \mathbf{0} = \mathbf{f}_{\delta_\epsilon}(\delta_\epsilon, \mathbf{u}_\epsilon, 0) \\ \mathbf{0} = \mathbf{g}(\mathbf{x}, \mathbf{z}, \delta, 0) \\ \mathbf{0} = \mathbf{f}_{\delta_\varrho}(\delta_\varrho, \mathbf{u}_\varrho, 0) \end{cases} \tag{6.4}$$

reduced slow actuator system:

$$\mathscr{S}_\epsilon{}^0 : \begin{cases} \breve{\mathbf{x}} = \mathbf{0} \\ \breve{\delta}_\epsilon = \mathbf{f}_{\delta_\epsilon}(\delta_\epsilon, \mathbf{u}_\epsilon, 0) \\ \mathbf{0} = \mathbf{g}(\mathbf{x}, \mathbf{z}, \delta, 0) \\ \mathbf{0} = \mathbf{f}_{\delta_\varrho}(\delta_\varrho, \mathbf{u}_\varrho, 0) \end{cases} \tag{6.5}$$

reduced fast system:

$$\mathscr{S}_\mu{}^0 : \begin{cases} \mathbf{x}' = \mathbf{0} \\ \delta_\epsilon{}' = \mathbf{0} \\ \mathbf{z}' = \mathbf{g}(\mathbf{x}, \mathbf{z}, \delta, 0) \\ \mathbf{0} = \mathbf{f}_{\delta_\varrho}(\delta_\varrho, \mathbf{u}_\varrho, 0) \end{cases} \tag{6.6}$$

and *reduced fast actuator system:*

$$\mathscr{S}_{\varrho}^{\,0}: \begin{cases} \check{\mathbf{x}} = \mathbf{0} \\ \check{\delta}_{\epsilon} = \mathbf{0} \\ \check{\mathbf{z}} = \mathbf{0} \\ \check{\delta}_{\varrho} = \mathbf{f}_{\delta_{\varrho}}(\delta_{\varrho}, \mathbf{u}_{\varrho}, 0). \end{cases} \tag{6.7}$$

Superscript 0 has been introduced to emphasize that these systems describe the limiting behaviour. Notice the dynamics of the reduced slow system are constrained to lie upon an m dimensional smooth manifold defined by the set of points $(\mathbf{x}) \in \mathbb{R}^m$ that satisfy the algebraic equations of $\mathscr{S}^0$:

$$\mathcal{M}_0: \begin{cases} \delta_{\epsilon}^0 = \delta_{\epsilon}(\mathbf{x}, \mathbf{u}_{\epsilon}) \\ \mathbf{z}^0 = \mathbf{z}(\mathbf{x}, \delta_{\epsilon}, \delta_{\varrho}) \\ \delta_{\varrho}^0 = \delta_{\varrho}(\mathbf{x}, \mathbf{u}_{\varrho}). \end{cases} \tag{6.8}$$

This set of points is identically the fixed points of the $\mathscr{S}_{\epsilon}^{\,0}$, $\mathscr{S}_{\mu}^{\,0}$ and $\mathscr{S}_{\varrho}^{\,0}$ reduced systems respectively. This observation assists in making two important conclusions. First, the flow on the manifold $\mathcal{M}_0$ (and respectively the flow of the reduced slow system $\mathscr{S}^0$) is described by the differential equation

$$\dot{\mathbf{x}} = \mathbf{f}(\mathbf{x}, \mathbf{z}^0, \delta_{\epsilon}^0, \delta_{\varrho}^0) \tag{6.9}$$

if the reduced systems are stable about their respective fixed points. Second, the flow on the manifold determines the asymptotic behaviour of the solutions of the slow system $\mathscr{S}$. Specifically, if the dynamics of (6.9) are locally asymptotically stable about the manifold, then it can be concluded that the slow system $\mathscr{S}$ in (2.1)

is also locally asymptotically stable [72]. Furthermore, the flow on the manifold approximates the solution of the slow system $\mathscr{S}$. Refer to [5],[80] for details.

6.3 Control Formulation and Stability Analysis

Geometric singular perturbation theory suggests that the stability properties of the slow system $\mathscr{S}$ depend upon the properties of the reduced slow system $\mathscr{S}^0$ and that in turn relies upon the identification of the manifold $\mathcal{M}_0$. If the manifold can be uniquely identified as a function of the control vector $\mathbf{u}$, then under certain conditions the control objective is met by designing controllers that ensure the reduced systems ${\mathscr{S}_\epsilon}^0$, ${\mathscr{S}_\mu}^0$ and ${\mathscr{S}_\varrho}^0$ are uniformly stable about their fixed points and $\mathscr{S}^0$ asymptotically follows the desired reference $\mathbf{x}_r(t)$. But as discussed in the Section 1, the identification of the manifold $\mathcal{M}_0$ is not feasible for non-standard forms.

Here the reduced-order models and the results of singular perturbation theory are employed by considering the manifold in (6.8) with $(\delta_\epsilon^0, \mathbf{z}^0, \delta_\varrho^0)$ as intermediate control variables. Recall, similar ideas were implemented in approach II (see Section 4.4) and shown to asymptotically guarantee slow-state tracking for a two-time scale system. Motivated by these results, the control law is formulated in the following five steps. In the first step, the manifolds $\delta_\epsilon^0(t, \mathbf{x}, \delta_\varrho^0)$ and $\mathbf{z}^0(t, \mathbf{x}, \delta_\varrho^0)$ are determined to ensure asymptotic stability of the reduced slow system $\mathscr{S}^0$ about the desired reference. In this step it is assumed that the fast actuators have settled down to their respective fixed point δ_ϱ^0, which is unknown and is determined later. The second step proceeds with the design of the control vector $\mathbf{u}_\epsilon(t, \mathbf{x}, \delta_\epsilon)$ to ensure the reduced slow actuator system $\mathscr{S}_\epsilon^0$ uniformly stabilizes about the fixed point $\delta_\epsilon^0(t, \mathbf{x}, \delta_\varrho^0)$ designed in the first step. Similarly, the manifold $\mathbf{z}^0(t, \mathbf{x}, \delta_\varrho^0)$ is made the fixed-point of the reduced fast system $\mathscr{S}_\mu^0$ through the design of the manifold $\delta_\varrho^0(t, \mathbf{x}, \delta_\epsilon, \mathbf{z})$ in the third step. The fourth step formulates the control vector $\mathbf{u}_\varrho(t, \mathbf{x}, \delta_\epsilon, \mathbf{z}, \delta_\varrho)$ to ensure δ_ϱ^0 becomes the

fixed-point of the reduced fast actuator system, $\mathscr{S}_{\varrho}^{0}$. The final step proceeds with robustness analysis through Lyapunov functions to ensure the stability properties of the reduced systems established in steps one through four carry forward to their counterparts $\mathscr{S}$, $\mathscr{S}_{\epsilon}$, $\mathscr{S}_{\mu}$ and $\mathscr{S}_{\varrho}$.

These ideas are mathematically formulated and developed in Section 6.3.

6.3.1 Control Formulation

We start by defining the tracking error signal as

$$\mathbf{e}(t) := \mathbf{x}(t) - \mathbf{x}_r(t) \tag{6.10}$$

and express the slow system $\mathscr{S}$ given in (2.1) as[1]

$$\mathscr{S} : \begin{cases} \dot{\mathbf{e}} = \mathbf{F}(t, \mathbf{e}, \mathbf{z}, \delta) := \mathbf{f}(\mathbf{e} + \mathbf{x}_r, \mathbf{z}, \delta) - \dot{\mathbf{x}}_r \\ \epsilon\dot{\delta}_{\epsilon} = \mathbf{f}_{\delta_{\epsilon}}(\delta_{\epsilon}, \mathbf{u}_{\epsilon}, \epsilon) \\ \mu\dot{\mathbf{z}} = \mathbf{G}(t, \mathbf{e}, \mathbf{z}, \delta, \mu) := \mathbf{g}(\mathbf{e} + \mathbf{x}_r, \mathbf{z}, \delta, \mu) \\ \varrho\dot{\delta}_{\varrho} = \mathbf{f}_{\delta_{\varrho}}(\delta_{\varrho}, \mathbf{u}_{\varrho}, \varrho). \end{cases} \tag{6.11}$$

Step 1: Design slow manifolds $\delta_{\epsilon}^{0}(t, \mathbf{e}, \delta_{\varrho}^{0})$ and $\mathbf{z}^{0}(t, \mathbf{e}, \delta_{\varrho}^{0})$ for the reduced slow system $\mathscr{S}^{0}$ such that the slow states asymptotically track the desired reference $\mathbf{x}_r(t)$, or $\mathbf{e} = \mathbf{0}$ becomes the uniformly asymptotically stable equilibrium of $\mathscr{S}^{0}$. Toward this end, define a positive-definite and decrescent Lyapunov function that satisfies

(i) $V(t, \mathbf{e}) : [0, \infty) \times D_{\mathbf{e}} \to \mathbb{R}$ is continuously differentiable and $D_{\mathbf{e}} \subset \mathbb{R}^{m}$ contains the origin such that

$$0 < \psi_1(\|\mathbf{e}\|) \leq V(t, \mathbf{e}) \leq \psi_2(\|\mathbf{e}\|)$$

[1]Note, for convenience, the notation $\mathscr{S}$, $\mathscr{S}_{\epsilon}$ and so on is retained in this subsection for the system written in error coordinates.

for some **class** $\mathcal{K}$ functions $\psi_1(.)$ and $\psi_2(.)$, and

(ii) design the manifolds $\delta_\epsilon^0(t, \mathbf{e}, \delta_\varrho^0)$ and $\mathbf{z}^0(t, \mathbf{e}, \delta_\varrho^0)$ such that closed-loop reduced slow system $\mathscr{S}^0$ satisfies

$$\frac{\partial V}{\partial t} + \frac{\partial V}{\partial \mathbf{e}}\mathbf{F}(t, \mathbf{e}, \mathbf{z}^0, \delta_\epsilon^0, \delta_\varrho^0) \leq -\alpha_1 \psi_3^2(\mathbf{e}), \quad \alpha_1 > 0$$

where $\psi_3(.)$ is a continuous scalar function that satisfies $\psi_3(\mathbf{0}) = 0$.

Note the manifolds are time-varying due to the varying nature of the desired reference $\mathbf{x}_r(t)$.

Step 2: Design the control $\mathbf{u}_\epsilon$ to ensure the slow actuator states asymptotically approach the manifold $\delta_\epsilon^0(t, \mathbf{e}, \delta_\varrho^0)$. Define the error in the actuator state as $\mathbf{e}_{\delta_\epsilon} := \delta_\epsilon - \delta_\epsilon^0(t, \mathbf{e}, \delta_\varrho^0)$ and rewrite the reduced slow actuator system $\mathscr{S}_\epsilon^0$ as

$$\mathscr{S}_\epsilon^{\,0} : \begin{cases} \breve{\mathbf{e}} = \mathbf{0} \\ \breve{\mathbf{e}}_{\delta_\epsilon} = \mathbf{f}_{\delta_\epsilon}(\mathbf{e}_{\delta_\epsilon} + \delta_\epsilon^0, \mathbf{u}_\epsilon, 0) - \breve{\delta}_\epsilon^0 \\ \mathbf{0} = \mathbf{G}(t, \mathbf{e}, \mathbf{z}, \delta, 0); \mathbf{0} = \mathbf{f}_{\delta_\varrho}(\delta_\varrho, \mathbf{u}_\varrho, 0). \end{cases} \tag{6.12}$$

$\breve{\delta}_\epsilon^0$ is the derivative of the manifold in the limit $\epsilon \to 0$ determined as:

$$\begin{aligned} \breve{\delta}_\epsilon^0 &= \lim_{\epsilon \to 0} \left[\frac{\partial \delta_\epsilon^0}{\partial t}\frac{dt}{d\tau_\epsilon} + \frac{\partial \delta_\epsilon^0}{\partial \mathbf{e}}\breve{\mathbf{e}} + \frac{\partial \delta_\epsilon^0}{\partial \delta_\varrho^0}\breve{\delta}_\varrho^0 \right] \\ &= \mathbf{0} \end{aligned} \tag{6.13}$$

using the definition of time scale τ_ϵ, reduced slow actuator system $\mathscr{S}_\epsilon^0$ in (6.12) and the fact that δ_ϱ^0 is a fixed point of the reduced slow actuator system.

In order to design the control vector $\mathbf{u}_\epsilon(t, \mathbf{e}, \mathbf{e}_{\delta_\epsilon})$, define a positive-definite and decrescent Lyapunov function $W(t, \mathbf{e}, \mathbf{e}_{\delta_\epsilon})$ that satisfies

(iii) $W(t, \mathbf{e}, \mathbf{e}_{\delta_\epsilon}) : [0, \infty) \times D_{\mathbf{e}} \times D_{\mathbf{e}_{\delta_\epsilon}} \to \mathbb{R}$ is continuously differentiable and $D_{\mathbf{e}_{\delta_\epsilon}} \subset \mathbb{R}^l$ contains the origin such that

$$0 < \Phi_1(\|\mathbf{e}_{\delta_\epsilon}\|) \leq W(t, \mathbf{e}, \mathbf{e}_{\delta_\epsilon}) \leq \Phi_2(\|\mathbf{e}_{\delta_\epsilon}\|)$$

for some **class** $\mathcal{K}$ functions $\Phi_1(.)$ and $\Phi_2(.)$.

(iv) Using the Lyapunov function candidate $W(t, \mathbf{e}, \mathbf{e}_{\delta_\epsilon})$, design for the control $\mathbf{u}_\epsilon(t, \mathbf{e}, \mathbf{e}_{\delta_\epsilon})$ such that closed-loop reduced slow actuator system satisfies

$$\frac{\partial W}{\partial \mathbf{e}_{\delta_\epsilon}} \mathbf{f}_{\delta_\epsilon}(\mathbf{e}_{\delta_\epsilon} + \delta_\epsilon^0, \mathbf{u}_\epsilon, 0) \leq -\alpha_2 \Phi_3^2(\mathbf{e}_{\delta_\epsilon}), \quad \alpha_2 > 0$$

where $\Phi_3(.)$ is a continuous scalar function and $\Phi_3(\mathbf{0}) = 0$.

Step 3: Define the error in the fast variables as $\mathbf{e}_z := \mathbf{z} - \mathbf{z}^0$ and design the manifold $\delta_\varrho^0(t, \mathbf{e}, \mathbf{e}_{\delta\epsilon}, \mathbf{e_z})$ such that the fast variables asymptotically stabilize about the manifold $\mathbf{z}^0(t, \mathbf{e}, \delta_\varrho^0)$. Note the manifold for the fast variables in this design step $\mathbf{z}^0(t, \mathbf{e}, \delta_\varrho^0) = \mathbf{z}^0\left(t, \mathbf{e}, \delta_\varrho^0(t, \mathbf{e}, \mathbf{e}_{\delta_\epsilon}, \mathbf{0})\right)$ is a function of the error in slow actuator state $\mathbf{e}_{\delta_\epsilon}$ and not of the fixed point $\delta_\epsilon^0(t, \mathbf{e}, \delta_\varrho^0)$. This is because the slow actuator state evolves at a relatively slow rate and the assumption that the slow actuator has settled down to its fixed point cannot be made. The reduced fast system $\mathscr{S}_\mu^0$ rewritten in error coordinates is

$$\mathscr{S}_\mu{}^0 : \begin{cases} \mathbf{e}' = \mathbf{0} \\ \mathbf{e}_{\delta_\epsilon}{}' = \mathbf{0} \\ \mathbf{e}_z{}' = \mathbf{G}(\tau_\mu, \mathbf{e}, \mathbf{e}_z + \mathbf{z}^0, \mathbf{e}_{\delta_\epsilon}, \delta_\varrho^0, 0) \\ \mathbf{0} = \mathbf{f}_{\delta_\varrho}(\delta_\varrho, \mathbf{u}_\varrho, 0) \end{cases} \tag{6.14}$$

using the fact

$$\begin{aligned}\mathbf{z}^{0\prime} &= \lim_{\mu\to 0}\left[\frac{\partial \mathbf{z}^0}{\partial t}\frac{dt}{d\tau_\mu} + \frac{\partial \mathbf{z}^0}{\partial \mathbf{e}}\mathbf{e}' + \frac{\partial \mathbf{z}^0}{\partial \mathbf{e}_{\delta_\epsilon}}\mathbf{e}_{\delta_\epsilon}{}' + \frac{\partial \mathbf{z}^0}{\partial \delta^0_\varrho}\delta^{0\prime}_\varrho\right] \\ &= \mathbf{0}.\end{aligned} \tag{6.15}$$

For the design of the manifold $\delta^0_\varrho(t, \mathbf{e}, \mathbf{e}_{\delta\epsilon}, \mathbf{e}_\mathbf{z})$, define a positive-definite and decrescent Lyapunov function that satisfies

(v) $\mathcal{Z}(t, \mathbf{e}, \mathbf{e}_{\delta_\epsilon}, \mathbf{e}_\mathbf{z}) : [0, \infty) \times D_\mathbf{e} \times D_{\mathbf{e}_{\delta_\epsilon}} \times D_{\mathbf{e}_\mathbf{z}} \to \mathbb{R}$ is continuously differentiable and $D_{\mathbf{e}_\mathbf{z}} \subset \mathbb{R}^n$ contains the origin such that

$$0 < \varpi_1(\|\mathbf{e}_\mathbf{z}\|) \leq \mathcal{Z}(t, \mathbf{e}, \mathbf{e}_{\delta_\epsilon}, \mathbf{e}_\mathbf{z}) \leq \varpi_2(\|\mathbf{e}_\mathbf{z}\|)$$

for some **class** $\mathcal{K}$ functions $\varpi_1(.)$ and $\varpi_2(.)$.

(vi) Design $\delta^0_\varrho(t, \mathbf{e}, \mathbf{e}_{\delta\epsilon}, \mathbf{e}_\mathbf{z})$ such that the closed-loop reduced fast system, $\mathscr{S}^0_\mu$ satisfies

$$\frac{\partial \mathcal{Z}}{\partial \mathbf{e}_\mathbf{z}}\mathbf{G}(\tau_\mu, \mathbf{e}, \mathbf{e}_\mathbf{z}, \mathbf{e}_{\delta_\epsilon}, \delta^0_\varrho, 0) \leq -\alpha_3 \varpi^2_3(\mathbf{e}_\mathbf{z}), \quad \alpha_3 > 0$$

where $\varpi_3(.)$ is a continuous scalar function that satisfies $\varpi_3(\mathbf{0}) = 0$.

With the knowledge of manifold $\delta^\mathbf{0}_\varrho(t, \mathbf{e}, \mathbf{e}_{\delta\epsilon}, \mathbf{e}_\mathbf{z})$, the manifolds for the slow actuator variables and the fast states can be determined by using $\delta^0_\epsilon(t, \mathbf{e}, \delta^0_\varrho) = \delta^0_\epsilon(t, \mathbf{e}, \delta^0_\varrho(t, \mathbf{e}, \mathbf{0}, \mathbf{0}))$ and $\mathbf{z}^0(t, \mathbf{e}, \delta^0_\varrho) = \mathbf{z}^0\left(t, \mathbf{e}, \delta^0_\varrho(t, \mathbf{e}, \mathbf{0}, \mathbf{0})\right)$ in condition (ii) and $\mathbf{z}^0(t, \mathbf{e}, \delta^0_\varrho) = \mathbf{z}^0\left(t, \mathbf{e}, \delta^0_\varrho(t, \mathbf{e}, \mathbf{e}_{\delta_\epsilon}, \mathbf{0})\right)$ in condition (vi) respectively.

Step 4: Design the control vector $\mathbf{u}_\varrho$ to enforce uniform asymptotic stabilization of the fast actuators about the manifold $\delta^\mathbf{0}_\varrho(t, \mathbf{e}, \mathbf{e}_{\delta_\epsilon}, \mathbf{e}_z)$. Similar to the previous design steps, define the error in the fast actuator states $\mathbf{e}_{\delta_\varrho} := \delta_\varrho - \delta^0_\varrho$ and rewrite

the reduced fast actuator system $\mathscr{S}_{\varrho}^{0}$ in the error coordinates

$$\mathscr{S}_{\varrho}^{\,0}: \begin{cases} \check{\mathbf{e}} = \mathbf{0}; \quad \check{\mathbf{e}}_{\delta_\epsilon} = \mathbf{0} \\ \check{\mathbf{e}}_z = \mathbf{0} \\ \check{\mathbf{e}}_{\delta_\varrho} = \mathbf{f}_{\delta_\varrho}(\mathbf{e}_{\delta_\varrho} + \delta_{\varrho}^{0}, \mathbf{u}_{\varrho}, 0) \end{cases} \tag{6.16}$$

where

$$\begin{aligned} \check{\delta}_{\varrho}^{0} &= \lim_{\varrho \to 0} \left[\frac{\delta_{\varrho}^{0}}{dt} \frac{dt}{d\tau_{\varrho}} + \frac{\partial \delta_{\varrho}^{\mathbf{0}}}{\partial \mathbf{e}} \check{\mathbf{e}} + \frac{\partial \delta_{\varrho}^{0}}{\partial \mathbf{e}_{\delta_\epsilon}} \check{\mathbf{e}}_{\delta_\epsilon} + \frac{\partial \delta_{\varrho}^{0}}{\partial \mathbf{e}_{\mathbf{z}}} \check{\mathbf{e}}_z \right] \\ &= \mathbf{0}. \end{aligned} \tag{6.17}$$

Define a positive-definite and decrescent Lyapunov function that satisfies

(vii) $\mathcal{Y}(t, \mathbf{e}, \mathbf{e}_{\delta_\epsilon}, \mathbf{e}_{\mathbf{z}}, \mathbf{e}_{\delta_\varrho}) : [0, \infty) \times D_{\mathbf{e}} \times D_{\mathbf{e}_{\delta_\epsilon}} \times D_{\mathbf{e}_{\mathbf{z}}} \times D_{\mathbf{e}_{\delta_\varrho}} \to \mathbb{R}$ for the reduced fast actuator system $\mathscr{S}_{\varrho}^{0}$ that is continuously differentiable and $D_{\mathbf{e}_{\delta_\varrho}} \subset \mathbb{R}^{p-l}$ contains the origin such that

$$0 < \upsilon_1(\|\mathbf{e}_{\delta_\varrho}\|) \leq \mathcal{Y}(t, \mathbf{e}, \mathbf{e}_{\delta_\epsilon}, \mathbf{e}_{\mathbf{z}}, \mathbf{e}_{\delta_\varrho}) \leq \upsilon_2(\|\mathbf{e}_{\delta_\varrho}\|)$$

for some **class** $\mathcal{K}$ functions $\upsilon_1(.)$ and $\upsilon_2(.)$.

(viii) Design $\mathbf{u}_{\varrho}(t, \mathbf{e}, \mathbf{e}_{\delta_\epsilon}, \mathbf{e}_{\mathbf{z}}, \mathbf{e}_{\delta_\varrho})$ such that the closed-loop reduced fast actuator system $\mathscr{S}_{\varrho}^{0}$ satisfies

$$\frac{\partial \mathcal{Y}}{\partial \mathbf{e}_{\delta_\varrho}} \mathbf{f}_{\delta_\varrho}(\mathbf{e}_{\delta_\varrho} + \delta_{\varrho}^{0}, \mathbf{u}_{\varrho}, 0) \leq -\alpha_4 \upsilon_3^2(\mathbf{e}_{\delta_\varrho}), \quad \alpha_4 > 0$$

where $\upsilon_3(\mathbf{e}_{\delta_\varrho})$ is a continuous scalar function and $\upsilon_3(\mathbf{0}) = 0$.

Step 5: Verify the following interaction conditions are satisfied:

(ix) $$\frac{\partial V}{\partial \mathbf{e}}\Big[\mathbf{F}(t,\mathbf{e},\mathbf{e_z}+\mathbf{z}^0,\mathbf{e}_{\delta_\epsilon}+\delta^0_\epsilon,\mathbf{e}_{\delta_\varrho}+\delta^0_\varrho)-\mathbf{F}(t,\mathbf{e},\mathbf{z}^0,\delta^0_\epsilon,\delta^0_\varrho)\Big]\leq \beta_1\psi_3(\mathbf{e})\Phi_3(\mathbf{e}_{\delta_\epsilon}) + \beta_2\psi_3(\mathbf{e})\varpi_3(\mathbf{e}_z)+\beta_3\psi_3(\mathbf{e})\upsilon_3(\mathbf{e}_{\delta_\varrho})$$

(x) $$\frac{\partial W}{\partial \mathbf{e}_{\delta_\epsilon}}\Big[\mathbf{f}_{\delta_\epsilon}(\mathbf{e}_{\delta_\epsilon}+\delta^0_\epsilon,\mathbf{u}_\epsilon,\epsilon)-\mathbf{f}_{\delta_\epsilon}(\mathbf{e}_{\delta_\epsilon}+\delta^0_\epsilon,\mathbf{u}_\epsilon,0)\Big]\leq \epsilon\gamma_1\Phi^2_3(\mathbf{e}_{\delta_\epsilon})+\epsilon\beta_4\psi_3(\mathbf{e})\Phi_3(\mathbf{e}_{\delta_\epsilon})$$

(xi) $$\frac{\partial W}{\partial t}+\frac{\partial W}{\partial \mathbf{e}}\dot{\mathbf{e}}-\frac{\partial W}{\partial \mathbf{e}_{\delta_\epsilon}}\dot{\delta}^0_\epsilon\leq \gamma_2\Phi^2_3(\mathbf{e}_{\delta_\epsilon})+\beta_5\psi_3(\mathbf{e})\Phi_3(\mathbf{e}_{\delta_\epsilon}) + \beta_6\Phi_3(\mathbf{e}_{\delta_\epsilon})\varpi_3(\mathbf{e}_z)+\beta_7\Phi_3(\mathbf{e}_{\delta_\epsilon})\upsilon_3(\mathbf{e}_{\delta_\varrho})$$

(xii) $$\frac{\partial \mathcal{Z}}{\partial \mathbf{e_z}}\Big[\mathbf{G}(t,\mathbf{e},\mathbf{e_z},\mathbf{e}_{\delta_\epsilon},\mathbf{e}_{\delta_\varrho}+\delta^0_\varrho,\mu)-\mathbf{G}(t,\mathbf{e},\mathbf{e_z},\mathbf{e}_{\delta_\epsilon},\mathbf{e}_{\delta_\varrho}+\delta^0_\varrho,0)\Big]\leq \mu\beta_8\psi_3(\mathbf{e})\varpi_3(\mathbf{e}_z)+\mu\gamma_3\varpi^2_3(\mathbf{e}_z)+\mu\beta_9\Phi_3(\mathbf{e}_{\delta_\epsilon})\varpi_3(\mathbf{e}_z)+\mu\beta_{10}\varpi_3(\mathbf{e}_z)\upsilon_3(\mathbf{e}_{\delta_\varrho})$$

(xiii) $$\frac{\partial \mathcal{Z}}{\partial \mathbf{e_z}}\Big[\mathbf{G}(t,\mathbf{e},\mathbf{e_z},\mathbf{e}_{\delta_\epsilon},\mathbf{e}_{\delta_\varrho}+\delta^0_\varrho,0)-\mathbf{G}(t,\mathbf{e},\mathbf{e_z},\mathbf{e}_{\delta_\epsilon},\delta^0_\varrho,0)\Big]\leq \beta_{11}\varpi_3(\mathbf{e}_z)\upsilon_3(\mathbf{e}_{\delta_\varrho})$$

(xiv) $$\frac{\partial \mathcal{Z}}{\partial t}+\frac{\partial \mathcal{Z}}{\partial \mathbf{e}}\dot{\mathbf{e}}+\frac{\partial \mathcal{Z}}{\partial \mathbf{e}_{\delta_\epsilon}}\dot{\mathbf{e}}_{\delta_\epsilon}-\frac{\partial \mathcal{Z}}{\partial \mathbf{e_z}}\dot{\mathbf{z}}^0\leq \gamma_4\varpi^2_3(\mathbf{e_z}) + \beta_{12}\psi_3(\mathbf{e})\varpi_3(\mathbf{e_z})+\beta_{13}\Phi_3(\mathbf{e}_{\delta_\epsilon})\varpi_3(\mathbf{e_z})+\beta_{14}\varpi_3(\mathbf{e_z})\upsilon_3(\mathbf{e}_{\delta_\varrho})+\frac{\beta_{15}}{\epsilon}\psi_3(\mathbf{e})\varpi_3(\mathbf{e_z}) + \frac{\beta_{16}}{\epsilon}\Phi_3(\mathbf{e}_{\delta_\epsilon})\varpi_3(\mathbf{e_z})$$

(xv) $$\frac{\partial \mathcal{Y}}{\partial t}+\frac{\partial \mathcal{Y}}{\partial \mathbf{e}}\dot{\mathbf{e}}+\frac{\partial \mathcal{Y}}{\partial \mathbf{e}_{\delta_\epsilon}}\dot{\mathbf{e}}_{\delta_\epsilon}+\frac{\partial \mathcal{Y}}{\partial \mathbf{e_z}}\dot{\mathbf{e}}_z-\frac{\partial \mathcal{Y}}{\partial \mathbf{e}_{\delta_\varrho}}\dot{\delta}^0_\varrho\leq +\gamma_5\upsilon^2_3(\mathbf{e}_{\delta_\varrho})+\beta_{17}\psi_3(\mathbf{e})\upsilon_3(\mathbf{e}_{\delta_\varrho}) + \beta_{18}\Phi_3(\mathbf{e}_{\delta_\epsilon})\upsilon_3(\mathbf{e}_{\delta_\varrho})+\beta_{19}\varpi_3(\mathbf{e_z})\upsilon_3(\mathbf{e}_{\delta_\varrho})+\frac{\beta_{20}}{\epsilon}\psi_3(\mathbf{e})\upsilon_3(\mathbf{e}_{\delta_\varrho})+\frac{\beta_{21}}{\epsilon}\Phi_3(\mathbf{e}_{\delta_\epsilon})\upsilon_3(\mathbf{e}_{\delta_\varrho}) + \frac{\beta_{22}}{\mu}\psi_3(\mathbf{e})\upsilon_3(\mathbf{e}_{\delta_\varrho})+\frac{\beta_{23}}{\mu}\varpi_3(\mathbf{e}_z)\upsilon_3(\mathbf{e}_{\delta_\varrho})+\frac{\beta_{24}}{\mu}\Phi_3(\mathbf{e}_{\delta_\epsilon})\upsilon_3(\mathbf{e}_{\delta_\varrho})+\frac{\gamma_6}{\mu}\upsilon^2_3(\mathbf{e}_{\delta_\varrho})$$

(xvi) $$\frac{\partial \mathcal{Y}}{\partial \mathbf{e}_{\delta_\varrho}}\left[\mathbf{f}_{\delta_\varrho}(\mathbf{e}_{\delta_\varrho}+\delta^0_\varrho,\mathbf{u}_\varrho,\varrho)-\mathbf{f}_{\delta_\varrho}(\mathbf{e}_{\delta_\varrho}+\delta^0_\varrho,\mathbf{u}_\varrho,0)\right]\leq+\varrho\beta_{25}\psi_3(\mathbf{e})\upsilon_3(\mathbf{e}_{\delta_\varrho})$$
$$+\varrho\beta_{26}\varpi_3(\mathbf{e}_z)\upsilon_3(\mathbf{e}_{\delta_\varrho})+\varrho\beta_{27}\Phi_3(\mathbf{e}_{\delta_\epsilon})\upsilon_3(\mathbf{e}_{\delta_\varrho})+\varrho\gamma_7\upsilon_3^2(\mathbf{e}_{\delta_\varrho})$$

where β_i and γ_i are constants and the inequalities hold for all $\mathbf{e}\in D_{\mathbf{e}}$, $\mathbf{e}_{\delta_\epsilon}\in D_{\mathbf{e}_{\delta_\epsilon}}$, $\mathbf{e}_{\mathbf{z}}\in D_{\mathbf{e}_{\mathbf{z}}}$ and $\mathbf{e}_{\delta_\varrho}\in D_{\mathbf{e}_{\delta_\varrho}}$. Conditions (ix) - (xvi) capture the deviation between the reduced-order models and the complete systems. This completes the control design procedure.

6.3.2 Stability Analysis

The following theorem summarizes the main result of the section.

Theorem 6.1. *Suppose the control* $\mathbf{u}(t,\mathbf{e},\mathbf{e}_{\delta_\epsilon},\mathbf{e}_{\mathbf{z}},\mathbf{e}_{\delta_\varrho})$ *of the system,* $\mathscr{S}$*, (2.1) is designed according to Steps 1-5, then for all initial conditions* $(\mathbf{e},\mathbf{e}_{\delta_\epsilon},\mathbf{e}_{\mathbf{z}},\mathbf{e}_{\delta_\varrho})\in D_{\mathbf{e}}\times D_{\mathbf{e}_{\delta_\epsilon}}\times D_{\mathbf{e}_{\mathbf{z}}}\times D_{\mathbf{e}_{\delta_\varrho}}$*, the control uniformly asymptotically stabilizes the nonlinear singularly perturbed system (2.1) and equivalently drives the slow state* $\mathbf{x}(t)\to\mathbf{x}_r(t)$ *for all* $\epsilon<\epsilon^*$, $\mu<\mu^*$ *and* $\varrho<\varrho^*$ *with respective upper-bounds defined as*

$$\epsilon^* := \frac{\alpha_1\alpha_2}{\alpha_1(\gamma_1+\gamma_2)+\frac{1}{4w_vw_w}[w_v\beta_1+w_w(\beta_4+\beta_5)]^2} \tag{6.18}$$

$$\mu^* := \frac{N_\mu}{D_\mu} \tag{6.19}$$

$$\varrho^* := \frac{N_\varrho}{D_\varrho}. \tag{6.20}$$

where

$$\begin{aligned} N_\mu &= (w_v\alpha_1 b-a^2)\alpha_3 w_z \\ D_\mu &= w_v\alpha_1 d^2-2acd+bc^2+w_z(w_v\alpha_1 b-a^2)(\gamma_3+\gamma_4) \\ N_\varrho &= w_y\alpha_4 \\ D_\varrho &= \tfrac{\eta}{\sigma}+w_y(\gamma_5+\gamma_7+\tfrac{\gamma_6}{\mu}) \end{aligned} \tag{6.21}$$

Various other constants in (6.18) and (6.21) are

$$
\begin{aligned}
&\sigma = w_v\alpha_1(bg-d^2) - a^2g + 2adc - bc^2\\
&\eta = \lambda + w_v\alpha_1(bh^2 - dfh - f(dh-gf))\\
&+a^2h^2 + adhe + af(hc-ge) + cfah\\
&-cf(fc-de) - cbhe\\
&\lambda = e[a(dh-gf) - b(ch-eg) + d(cf-de)]\\
&a = -\tfrac{[w_v\beta_1 + w_w(\beta_4+\beta_5)]}{2}\\
&b = \tfrac{w_w\alpha_2}{\epsilon} - w_w\gamma_1 - w_w\gamma_2\\
&c = -\tfrac{\left[w_v\beta_2 + w_z(\beta_8+\beta_{12}+\frac{\beta_{15}}{\epsilon})\right]}{2}\\
&d = -\tfrac{\left[w_w\beta_6 + w_z(\beta_9+\beta_{13}+\frac{\beta_{16}}{\epsilon})\right]}{2}\\
&e = -\tfrac{\left[w_v\beta_3 + w_y(\beta_{17}+\beta_{25}+\frac{\beta_{20}}{\epsilon}+\frac{\beta_{22}}{\mu})\right]}{2}\\
&f = -\tfrac{\left[w_w\beta_7 + w_y(\beta_{18}+\beta_{27}+\frac{\beta_{21}}{\epsilon}+\frac{\beta_{24}}{\mu})\right]}{2}\\
&g = \tfrac{w_z\alpha_3}{\mu} - w_z\gamma_3 - w_z\gamma_4\\
&h = -\tfrac{\left[w_z(\beta_{10}+\beta_{14}+\frac{\beta_{11}}{\mu}) + w_y(\beta_{19}+\beta_{26}+\frac{\beta_{23}}{\mu})\right]}{2}\\
&j = \tfrac{w_y\alpha_4}{\varrho} - w_y\gamma_5 - w_y\gamma_7 - \tfrac{w_y\gamma_6}{\mu}
\end{aligned}
\tag{6.22}
$$

and w_i are positive design constants $0 < w_i < 1$.

Proof. The closed-loop slow system $\mathscr{S}$ in the error coordinates is given as

$$
\begin{aligned}
&\dot{\mathbf{e}} = \mathbf{F}(t, \mathbf{e}, \mathbf{e}_{\mathbf{z}} + \mathbf{z}^0, \mathbf{e}_{\delta_\epsilon} + \delta_\epsilon^0, \mathbf{e}_{\delta_\varrho} + \delta_\varrho^0)\\
&\epsilon\dot{\mathbf{e}}_{\delta_\epsilon} = \mathbf{f}_{\delta_\epsilon}(\mathbf{e}_{\delta_\epsilon} + \delta_\epsilon^0, \mathbf{u}_\epsilon, \epsilon) - \epsilon\dot{\delta}_\epsilon^0(t, \mathbf{e})\\
&\mu\dot{\mathbf{e}}_z = \mathbf{G}(t, \mathbf{e}, \mathbf{e}_{\mathbf{z}}, \mathbf{e}_{\delta_\epsilon}, \mathbf{e}_{\delta_\varrho} + \delta_\varrho^0, \mu) - \mu\dot{\mathbf{z}}^0(t, \mathbf{e}, \mathbf{e}_{\delta_\epsilon})\\
&\varrho\dot{\mathbf{e}}_{\delta_\varrho} = \mathbf{f}_{\delta_\varrho}(\mathbf{e}_{\delta_\varrho} + \delta_\varrho^0, \mathbf{u}_\varrho, \varrho) - \varrho\dot{\delta}_\varrho^0(t, \mathbf{e}, \mathbf{e}_{\delta_\epsilon}, \mathbf{e}_{\mathbf{z}}).
\end{aligned}
\tag{6.23}
$$

Closed-loop system stability of the system states is analyzed using the composite

Lyapunov function approach[9]. Consider a Lyapunov function candidate

$$\begin{aligned}\vartheta(t,\mathbf{e},\mathbf{e}_{\delta_\epsilon},\mathbf{e}_{\mathbf{z}},\mathbf{e}_{\delta_\varrho}) &= (1-w_w-w_z-w_y)V(t,\mathbf{e})+w_wW(t,\mathbf{e},\mathbf{e}_{\delta_\epsilon})\\ &+ w_z\mathcal{Z}(t,\mathbf{e},\mathbf{e}_{\delta_\epsilon},\mathbf{e}_{\mathbf{z}})+w_y\mathcal{Y}(t,\mathbf{e},\mathbf{e}_{\delta_\epsilon},\mathbf{e}_{\mathbf{z}},\mathbf{e}_{\delta_\varrho}).\end{aligned} \tag{6.24}$$

where w_i are positive weights. Let $w_v=(1-w_w-w_z-w_y)$. From the properties of V, W, $\mathcal{Z}$ and $\mathcal{Y}$ it follows that $\vartheta(t,\mathbf{e},\mathbf{e}_{\delta_\epsilon},\mathbf{e}_{\mathbf{z}},\mathbf{e}_{\delta_\varrho})$ is positive-definite and decrescent. The derivative of ϑ along the trajectories of (6.23) is:

$$\begin{aligned}\dot\vartheta = {}& w_v\left\{\frac{\partial V}{\partial t}+\frac{\partial V}{\partial \mathbf{e}}\dot{\mathbf{e}}\right\}+w_w\left\{\frac{\partial W}{\partial t}+\frac{\partial W}{\partial \mathbf{e}}\dot{\mathbf{e}}+\frac{\partial W}{\partial \mathbf{e}_{\delta_\epsilon}}\dot{\mathbf{e}}_{\delta_\epsilon}\right\}\\ &+w_z\left\{\frac{\partial \mathcal{Z}}{\partial t}+\frac{\partial \mathcal{Z}}{\partial \mathbf{e}}\dot{\mathbf{e}}+\frac{\partial \mathcal{Z}}{\partial \mathbf{e}_{\delta_\epsilon}}\dot{\mathbf{e}}_{\delta_\epsilon}+\frac{\partial \mathcal{Z}}{\partial \mathbf{e}_{\mathbf{z}}}\dot{\mathbf{e}}_{\mathbf{z}}\right\}\\ &+w_y\left\{\frac{\partial \mathcal{Y}}{\partial t}+\frac{\partial \mathcal{Y}}{\partial \mathbf{e}}\dot{\mathbf{e}}+\frac{\partial \mathcal{Y}}{\partial \mathbf{e}_{\delta_\epsilon}}\dot{\mathbf{e}}_{\delta_\epsilon}+\frac{\partial \mathcal{Y}}{\partial \mathbf{e}_{\mathbf{z}}}\dot{\mathbf{e}}_{\mathbf{z}}+\frac{\partial \mathcal{Y}}{\partial \mathbf{e}_{\delta_\varrho}}\dot{\mathbf{e}}_{\delta_\varrho}\right\}.\end{aligned} \tag{6.25}$$

Substitute (6.23) and rearrange (6.25) to get

$$\begin{aligned}\dot\vartheta =& w_v\frac{\partial V}{\partial t}+w_v\frac{\partial V}{\partial \mathbf{e}}\Big[\mathbf{F}(t,\mathbf{e},\mathbf{z}^0,\delta^0_\epsilon,\delta^0_\varrho)-\mathbf{F}(t,\mathbf{e},\mathbf{z}^0,\delta^0_\epsilon,\delta^0_\varrho)\\ &+\mathbf{F}(t,\mathbf{e},\mathbf{e}_{\mathbf{z}}+\mathbf{z}^0,\mathbf{e}_{\delta_\epsilon}+\delta^0_\epsilon,\mathbf{e}_{\delta_\varrho}+\delta^0_\varrho)\Big]+w_w\frac{\partial W}{\partial t}\\ &+w_w\frac{\partial W}{\partial \mathbf{e}}\dot{\mathbf{e}}-w_w\frac{\partial W}{\partial \mathbf{e}_{\delta_\epsilon}}\dot\delta^0_\epsilon+\frac{w_w}{\epsilon}\frac{\partial W}{\partial \mathbf{e}_{\delta_\epsilon}}\mathbf{f}_{\delta_\epsilon}(\mathbf{e}_{\delta_\epsilon}+\delta^0_\epsilon,\mathbf{u}_\epsilon,0)\\ &+\frac{w_w}{\epsilon}\frac{\partial W}{\partial \mathbf{e}_{\delta_\epsilon}}\Big[\mathbf{f}_{\delta_\epsilon}(\mathbf{e}_{\delta_\epsilon}+\delta^0_\epsilon,\mathbf{u}_\epsilon,\epsilon)-\mathbf{f}_{\delta_\epsilon}(\mathbf{e}_{\delta_\epsilon}+\delta^0_\epsilon,\mathbf{u}_\epsilon,0)\Big]\\ &+w_z\left\{\frac{\partial \mathcal{Z}}{\partial t}+\frac{\partial \mathcal{Z}}{\partial \mathbf{e}}\dot{\mathbf{e}}+\frac{\partial \mathcal{Z}}{\partial \mathbf{e}_{\delta_\epsilon}}\dot{\mathbf{e}}_{\delta_\epsilon}-\frac{\partial \mathcal{Z}}{\partial \mathbf{e}_{\mathbf{z}}}\dot{\mathbf{z}}^0\right\}\\ &+\frac{w_z}{\mu}\frac{\partial \mathcal{Z}}{\partial \mathbf{e}_{\mathbf{z}}}\Big[\mathbf{G}(t,\mathbf{e},\mathbf{e}_{\mathbf{z}},\mathbf{e}_{\delta_\epsilon},\delta^0_\varrho,0)\\ &+\mathbf{G}(t,\mathbf{e},\mathbf{e}_{\mathbf{z}},\mathbf{e}_{\delta_\epsilon},\mathbf{e}_{\delta_\varrho}+\delta^0_\varrho,0)-\mathbf{G}(t,\mathbf{e},\mathbf{e}_{\mathbf{z}},\mathbf{e}_{\delta_\epsilon},\delta^0_\varrho,0)\Big]\\ &+\frac{w_z}{\mu}\frac{\partial \mathcal{Z}}{\partial \mathbf{e}_{\mathbf{z}}}\Big[\mathbf{G}(t,\mathbf{e},\mathbf{e}_{\mathbf{z}},\mathbf{e}_{\delta_\epsilon},\mathbf{e}_{\delta_\varrho}+\delta^0_\varrho,\mu)\end{aligned}$$

$$
\begin{aligned}
&- \mathbf{G}(t, \mathbf{e}, \mathbf{e}_{\mathbf{z}}, \mathbf{e}_{\delta_\epsilon}, \mathbf{e}_{\delta_\varrho} + \delta^0_\varrho, 0)\Big] \\
&+ w_y \left\{ \frac{\partial \mathcal{Y}}{\partial t} + \frac{\partial \mathcal{Y}}{\partial \mathbf{e}} \dot{\mathbf{e}} + \frac{\partial \mathcal{Y}}{\partial \mathbf{e}_{\delta_\epsilon}} \dot{\mathbf{e}}_{\delta_\epsilon} + \frac{\partial \mathcal{Y}}{\partial \mathbf{e}_{\mathbf{z}}} \dot{\mathbf{e}}_{\mathbf{z}} - \frac{\partial \mathcal{Y}}{\partial \mathbf{e}_{\delta_\varrho}} \dot{\delta}^0_\varrho \right\} \\
&+ \frac{w_y}{\varrho} \frac{\partial \mathcal{Y}}{\partial \mathbf{e}_{\delta_\varrho}} \Big[\mathbf{f}_{\delta_\varrho}(\mathbf{e}_{\delta_\varrho} + \delta^0_\varrho, \mathbf{u}_\varrho, 0) \\
&+ \mathbf{f}_{\delta_\varrho}(\mathbf{e}_{\delta_\varrho} + \delta^0_\varrho, \mathbf{u}_\varrho, \varrho) - \mathbf{f}_{\delta_\varrho}(\mathbf{e}_{\delta_\varrho} + \delta^0_\varrho, \mathbf{u}_\varrho, 0) \Big]
\end{aligned}
\tag{6.26}
$$

Using the properties given in (ii),(iv),(vi),(viii) and (ix)-(xvi), (6.26) results in

$$
\dot{\vartheta} \leq -\Psi^T \mathbb{K} \Psi \tag{6.27}
$$

$$
\mathbb{K} = \begin{bmatrix}
w_v \alpha_1 & a & c & e \\
a & b & d & f \\
c & d & g & h \\
e & f & h & j
\end{bmatrix} \tag{6.28}
$$

where $\Psi = \begin{bmatrix} \psi_3(\mathbf{e}) & \Phi_3(\mathbf{e}_{\delta_\epsilon}) & \varpi_3(\mathbf{e}_{\mathbf{z}}) & \upsilon_3(\mathbf{e}_{\delta_\varrho}) \end{bmatrix}^T$ and elements of matrix $\mathbb{K}$ are defined in (6.22). The matrix $\mathbb{K}$ in (6.28) is positive-definite for all $\epsilon < \epsilon^*$, $\mu < \mu^*$ and $\varrho < \varrho^*$ defined in (6.18), (6.19) and (6.20). By definition of the continuous scalar functions ψ_3,Φ_3, ϖ_3 and υ_3, it follows that $\dot{\vartheta}$ is negative definite. By the Lyapunov theorem [60] it is concluded that $(\mathbf{e}, \delta_\epsilon, \mathbf{z}, \delta_\varrho) = (\mathbf{0}, \delta^0_\epsilon, \mathbf{z}^0, \delta^0_\varrho)$ is uniformly asymptotic stable equilibrium of the closed-loop system (4.84). Further, from the definition of the tracking error (6.10) it is concluded that $\mathbf{x}(t) \to \mathbf{x}_r(t)$ asymptotically. Since the desired trajectory is assumed to be smooth and bounded with bounded first-order derivatives, all the other signals remain bounded for all time.

The weights w_i have been introduced to form a convex combination of the Lyapunov functions. The freedom to choose these parameters can be employed to obtain

less conservative estimates of the upper bounds of the perturbation parameters and domain of convergence as shown in numerical examples of Section 4.4.3.4. Similar weights were used in composite control approach and their effect is discussed in [9]. This completes the proof. □

6.4 Numerical Examples

6.4.1 Purpose and Scope

This section illustrates the preceding theoretical developments and demonstrates the controller performance for both standard and non-standard forms of singularly perturbed systems. Two examples are presented. The first example implements the proposed approach for a two time scale standard system. The second example demonstrates the control design for a multiple time scale system of the form (2.1) with deadzone actuator characteristics.

6.4.2 Standard Two Time Scale Model

Consider (Exercise problem 11.9 [60]):

$$\dot{x} = z \tag{6.29a}$$

$$\mu\dot{z} = -x - \exp z - \mu z + 1 + u \tag{6.29b}$$

The objective is to design a regulator to stabilize the slow state, thus $e := x$. Let $e_z = z - z^0$, where $z^0(e)$ is the manifold. The system given in (6.29) has two time scales with no slow actuators and one fast control, therefore Step. 2 and Step. 4 do not apply. The control design proceeds as follows:

Step 1: The reduced slow system $\mathscr{S}^0$ is given as

$$\dot{e} = z^0 \tag{6.30a}$$

$$0 = -e - \exp z^0 + 1 + u. \tag{6.30b}$$

Choose $z^0 = -2e$. With Lyapunov function $V(e) = \frac{1}{2}e^2$, properties (i) and (ii) are satisfied with $\psi_3(e) = e$ and $\alpha_1 = 2$.

Step 3: The reduced fast system $\mathscr{S}_\mu^0$ is

$$e' = 0 \tag{6.31a}$$

$$e_z' = -e - \exp(e_z + z^0) + u + 1. \tag{6.31b}$$

Choose $u = e - 1 - 4e_z + \exp(e_z + z_0)$. With Lyapunov function $\mathscr{Z}(e_z) = \frac{1}{2}e_z^2$, properties (iii) and (iv) are satisfied with $\varpi_3(e_z) = e_z$ and $\alpha_3 = 4$.

Step 5: The interaction conditions are satisfied with constants, $\beta_1 = 0; \beta_2 = 1; \beta_3 = 0$, $\beta_8 = \alpha_1; \gamma_3 = -1; \beta_9 = \beta_{10} = 0$, $\beta_{11} = 0$, $\gamma_4 = \alpha_1; \beta_{12} = -\alpha_1^2$. All other constants being zeros.

The closed-loop system becomes

$$\dot{e} = -2e + e_z \tag{6.32a}$$

$$\mu\dot{e}_z = -4e_z + \mu[-2e + e_z] \tag{6.32b}$$

The various constants of matrix $\mathbb{K}$ in (4.89) are $c = \frac{-w_v - 2w_z}{2}$, $g = \frac{4w_z}{\mu} - w_z$ and $a = b = d = e = f = h = j = 0$. For this example, the matrix $\mathbb{K}$ degenerates to 2×2 and the upper-bound is determined by requiring the determinant of the degenerate matrix to be positive. This gives the following equality:

$$\mu^* = \frac{8w_z(1 - w_z)}{2w_z(1 - w_z) + c^2} \tag{6.33}$$

where $w_v = 1 - w_z$ has been used. With the optimum choice of $w_z = \frac{1}{3}$ and $\mu^* = 2$ it is concluded that the system (6.29) is globally asymptotically stable about the origin

for $\mu < 2$.

Note that in this example, stability can be studied through the eigenvalues of the closed-loop system given in (6.32). This analysis suggests that the system is stable for all values of $\mu < 10000$. Thus, the upper-bounds determined in Theorem 6.1 are conservative and provides only sufficient conditions for stability.

6.4.3 Non-Standard Multiple Time Scale System

To demonstrate asymptotic tracking for multiple time scale systems, consider the following open-loop unstable system:

$$\dot{x}_1 = x_2 + z + \delta_\epsilon + \delta_\varrho \tag{6.34a}$$

$$\dot{x}_2 = x_1 + z + 2\delta_\epsilon + 4\delta_\varrho \tag{6.34b}$$

$$\epsilon\dot{\delta}_\epsilon = -\delta_\epsilon + u_\epsilon \tag{6.34c}$$

$$\epsilon^2\dot{z} = x_1 + 2\delta_\epsilon + 3\delta_\varrho \tag{6.34d}$$

with a fast actuator that satisfies

$$\delta_\varrho = \begin{cases} u_\varrho + 0.4; & u_\varrho \leq -0.4 \\ 0; & -0.4 \leq u_\varrho \leq 0.4 \\ u_\varrho - 0.4; & u_\varrho \geq 0.4. \end{cases} \tag{6.35}$$

In this example, the perturbation parameter $\mu := \epsilon^2$. The fast actuator δ_ϱ is infinitely many times fast and parameter ϱ is identically zero. The control is designed following the procedure outlined in Section 6.3.

Step 1: The reduced slow system $\mathscr{S}^0$ in error coordinates $e_1 := x_1 - x_{1r}(t)$ and

$e_2 := x_2 - x_{2r}(t)$ is

$$\begin{aligned}\dot{e}_1 &= e_2 + z^0(t, \mathbf{e}, \delta^0_\varrho) + \delta^0_\epsilon(t, \mathbf{e}) + \delta^0_\varrho(t, \mathbf{e}, \delta^0_\epsilon, z^0) \\ &\quad + (x_{2r} - \dot{x}_{1r}) \qquad (6.36a) \\ \dot{e}_2 &= e_1 + z^0(t, \mathbf{e}, \delta^0_\varrho) + 2\delta^0_\epsilon(t, \mathbf{e}) + 4\delta^0_\varrho(t, \mathbf{e}, \delta^0_\epsilon, z^0) \\ &\quad + (x_{1r} - \dot{x}_{2r}) \qquad (6.36b)\end{aligned}$$

assuming the actuator states and the fast variable have settled down onto their respective manifolds. Choose

$$\begin{aligned}\delta^0_\epsilon(t, \mathbf{e}) &= -3\delta^0_\varrho(t, \mathbf{e}, \delta^0_\epsilon, z^0) - [\dot{x}_{1r} + x_{1r} - x_{2r} - \dot{x}_{2r}] \qquad (6.37a) \\ z^0(t, \mathbf{e}, \delta^0_\varrho) &= -e_1 - e_2 + 2\delta^0_\varrho(t, \mathbf{e}, \delta^0_\epsilon, z^0) \\ &\quad + [x_{1r} - 2x_{2r} + 2\dot{x}_{1r} - \dot{x}_{2r}] \qquad (6.37b)\end{aligned}$$

as the manifolds to asymptotically stabilize the errors. With the Lyapunov function candidate $V(\mathbf{e}) = \frac{1}{2}e_1^2 + \frac{1}{2}e_2^2$, property (ii) is satisfied with $\alpha_1 = 1$ and $\psi_3(\mathbf{e}) = \sqrt{e_1^2 + e_2^2}$.

Step 2: The commanded slow control is designed as

$$u_\epsilon = \delta_\epsilon - 2e_{\delta_\epsilon} \qquad (6.38)$$

to ensure that the slow actuator state achieves the desired manifold and correspondingly $e_{\delta_\epsilon} := \delta_\epsilon - \delta^0_\epsilon(t, \mathbf{e})$ stabilizes about zero. Property (iv) is satisfied with quadratic Lyapunov function $W(e_{\delta_\epsilon}) = \frac{1}{2}e^2_{\delta_\epsilon}$ with $\alpha_2 = 2$ and $\Phi(e_{\delta_\epsilon}) = e_{\delta_\epsilon}$.

Step 3: The reduced fast system $\mathscr{S}_{\mu}^{0}$ is written as

$$e_z' = e_1 + 2e_{\delta_\epsilon} + 2\delta_\epsilon^0(t, \mathbf{e}) + 3\delta_\varrho^0(t, \mathbf{e}, \delta_\epsilon, z) + x_{1r} \tag{6.39}$$

and the manifold

$$\delta_\varrho^0(t, \mathbf{e}, \delta_\epsilon, z) = \frac{-e_1 - 2e_{\delta_\epsilon} - 2\delta_\epsilon^0(t, \mathbf{e}) - 4e_z - x_{1r}}{3} \tag{6.40}$$

ensures error $e_z := z - z^0(t, \mathbf{e}, \delta_\epsilon)$ is uniformly asymptotically stable about the origin. The manifolds can be written in system states by carrying out the following three steps. First, substitute for the manifolds given in (6.37) into (6.40) to get

$$\begin{aligned}\delta_\varrho^0(t, \mathbf{e}, \delta_\epsilon, z) = \frac{-e_1 - 2e_{\delta_\epsilon} + 6\delta_\varrho^0(t, \mathbf{e}, \delta_\epsilon^0, z^0) - 4e_z}{3} \\ \frac{2[\dot{x}_{1r} + x_{1r} - x_{2r} - \dot{x}_{2r}] - x_{1r}}{3}.\end{aligned} \tag{6.41}$$

Thus,

$$\delta_\varrho^0(t, \mathbf{e}, \delta_\epsilon^0, z^0) = \frac{e_1}{3} + \frac{[-x_{1r} - 2\dot{x}_{1r} + 2x_{2r} + 2\dot{x}_{2r}]}{3}. \tag{6.42}$$

As expected, $\delta_\varrho^0(t, \mathbf{e}, \delta_\epsilon^0, z^0)$ is only a function of the slow state error and time. Second, use (6.42) in (6.37) and determine $\delta_\epsilon^0(t, \mathbf{e})$ and consequently $\delta_\varrho^0(t, \mathbf{e}, \delta_\epsilon, z)$. This results in the following expressions:

$$\delta_\epsilon^0(t, \mathbf{e}) = - e_1 - [-\dot{x}_{1r} + x_{2r} + \dot{x}_{2r}] \tag{6.43a}$$

$$\begin{aligned}\delta_\varrho^0(t, \mathbf{e}, \delta_\epsilon, z) = &+ \frac{1}{3}\Big[e_1 - 2(\delta_\epsilon - \delta_\epsilon^0(t, \mathbf{e})) - 4(z - z^0(t, \mathbf{e}, \delta_\epsilon)) \\ &+ [-x_{1r} - 2\dot{x}_{1r} + 2x_{2r} + 2\dot{x}_{2r}]\Big].\end{aligned} \tag{6.43b}$$

Finally,

$$z^0(t,\mathbf{e},\delta_\epsilon) = \frac{1}{3}\Big[-e_1 - 3e_2 - 4(\delta_\epsilon - \delta^0_\epsilon(t,\mathbf{e})) \\ +[x_{1r} + 2\dot{x}_{1r} - 2x_{2r} + \dot{x}_{2r}]\Big] \tag{6.44}$$

is obtained using $\delta^0_\varrho(t,\mathbf{e},\delta_\epsilon,z^0)$ from (6.43b) in (6.37). Property (vi) is satisfied with Lyapunov function as $Z(e_z) = \frac{1}{2}e_z^2$ with $\alpha_3 = 4$ and $\varpi(e_z) = e_z$.

Step 4: The control u_2 is determined using the algebraic relations given in (6.35).

Step 5: The various constants can be easily determined as $\beta_1 = -4$, $\beta_2 = -\frac{17}{3}$, $\gamma_2 = -2$, $\beta_5 = -1$, $\beta_6 = -\frac{4}{3}$, $\beta_{12} = -\frac{5}{3}$, $\beta_13 = -\frac{16}{3}$, $\gamma_4 = -\frac{59}{3}$, $\beta_16 = -\frac{8}{3}$ and the rest are all zeros.

The above control design is verified in simulation. For convenience, the weights w_i are set to unity and using (6.18) the upper-bound is computed as $\epsilon^* = 0.4705$. The upper-bound $\mu^* = 0.1107$ is determined by assuming $\epsilon = 0.1$. Thus, Theorem 6.1 guarantees global asymptotic stability of (6.34). The controller (specified by (6.43b),(6.44), (6.38) and (6.35)) was tested in simulation by specifying $x_{1r}(t) = \sin(t)$ and $x_{2r}(t) = -2\cos(2t)$. The transient response in Figure 6.1 and Figure 6.2 show that within two seconds the slow state transients die out and the fast state follows the desired manifold. This behaviour is the result of close tracking of the commanded inputs. The control profile for the fast actuator in Figure 6.3 presents the deadband characteristics of the controller.

6.5 Closing Remarks

An exact slow tracking controller was developed that utilizes the dependence of the slow state dynamics upon the fast states and applies to both standard and non-standard singularly perturbed systems. The sequential design procedure was proven

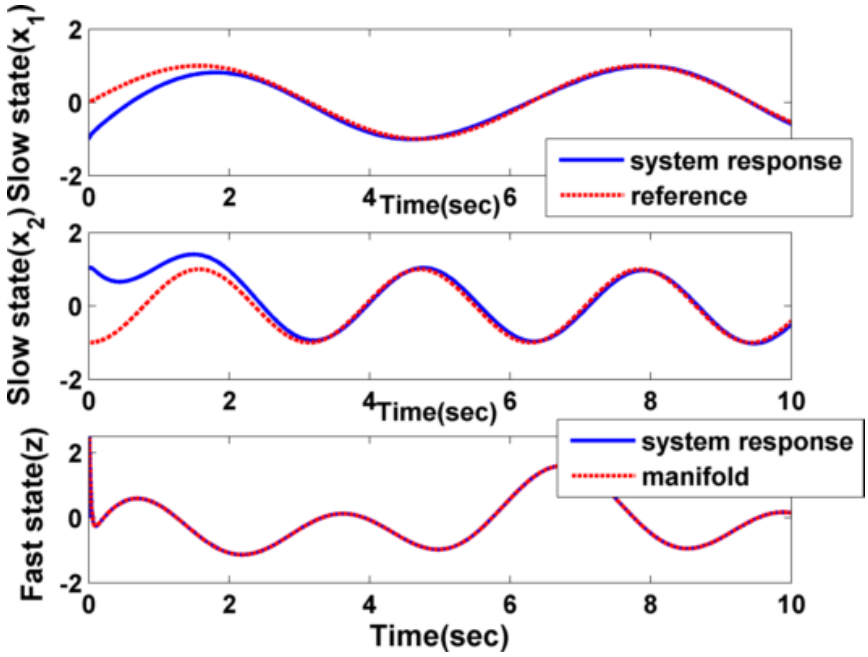

Figure 6.1: Multiple time scale non-standard system: closed-loop response for $\epsilon = 0.05$

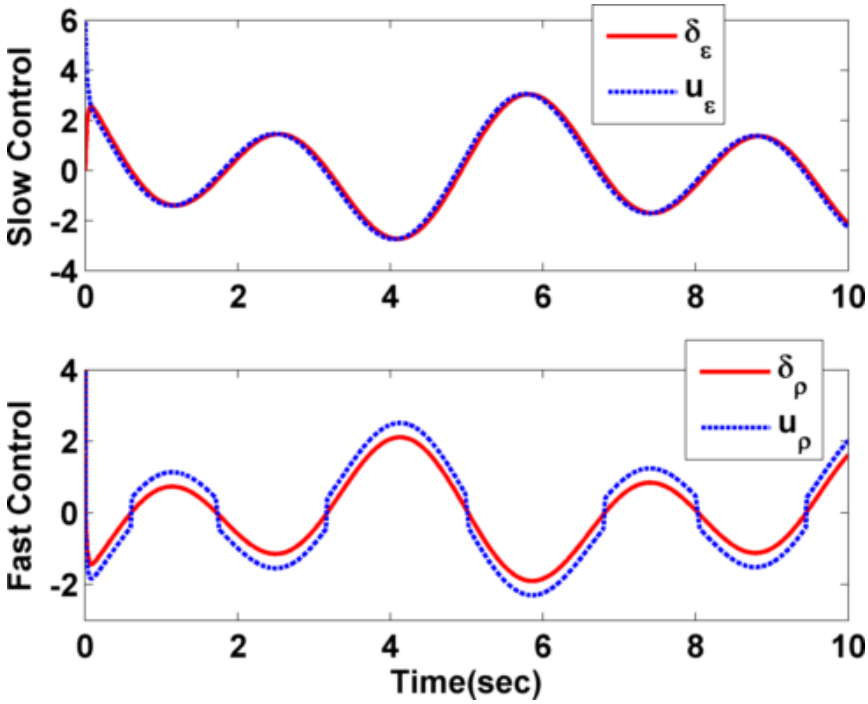

Figure 6.2: Multiple time scale non-standard system: computed control time history for $\epsilon = 0.05$

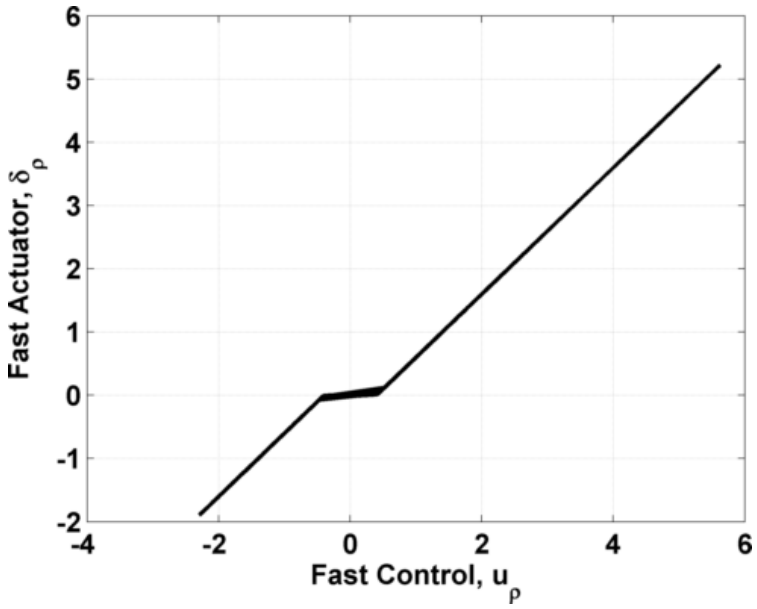

Figure 6.3: Multiple time scale non-standard system: fast control deadband characteristics $\epsilon = 0.05$

to stabilize a four time scale singularly perturbed system and can also be extended to systems with greater than four time scales.

Based on the stability proof and simulation results presented in the section the following conclusions are drawn. First, the estimate of the upper-bound is conservative and the theorem provides sufficiency conditions for stability. Second, the domain of convergence is dependent upon the underlying controllers developed for the reduced-order systems. Two of the examples showed that global results can be guaranteed by identifying controllers that satisfy the specified conditions for the complete space spanned by the system states. Third, the control design process is independent of the perturbation parameter. An estimate is required only in a final design step to determine the upper-bounds on the perturbation parameters and guarantee robustness properties of the controller. This estimate can be computed using non-dimensionalization. The benefits and limitations of the exact approach presented in Section 2 apply here.

7. SOME APPLICATIONS TO CONTROL OF WEAKLY MINIMUM AND NON-MINIMUM PHASE, NONLINEAR DYNAMICAL SYSTEMS[1]

7.1 Introduction

This section considers applications to benchmark non-minimum phase dynamical systems. It will be shown that the methods detailed in Section 6 will guarantee asymptotic tracking while providing real-time implementable control solutions. This work is motivated by the fact that most of these applications exhibit multiple time scales but are not represented in the form (2.1) studied earlier in this dissertation. There has been some work in literature that outline sequential procedures to obtain the desired form [9] but these methods require identifying a global transformation which is not always feasible. In this section, forced singular perturbation technique [81] will be employed to identify the fast variables and the perturbation parameters will be introduced only at the modeling stage. For each of the different applications studied, a description of the system is followed by time scale analysis and control synthesis. Finally, results are presented and closing remarks are discussed.

7.2 The Beam and Ball Experiment

The first dynamical model under study is the beam and ball experiment shown in Figure 7.1. The setup consists of a beam that can only rotate in the vertical plane by applying torque at the center of the beam, and a ball that is free to roll along the beam. It is desired that the ball always remains in contact with the beam and that

[1]Parts of this section reprinted with permission from "Output tracking of non-minimum phase dynamics", Siddarth, Anshu and Valasek, John, 2011. AIAA Guidance, Navigation, and Control, Conference, (Portland, Oregon), AIAA 2011-6487 Copyright ©2011 by Siddarth, Anshu and Valasek, John and "Tracking control for a non-minimum phase autonomous helicopter", Siddarth, Anshu and Valasek, John, 2012. AIAA Guidance, Navigation, and Control, Conference, (Minneapolis, Minnesota), AIAA 2012-4453 Copyright ©2012 by Siddarth, Anshu and Valasek, John.

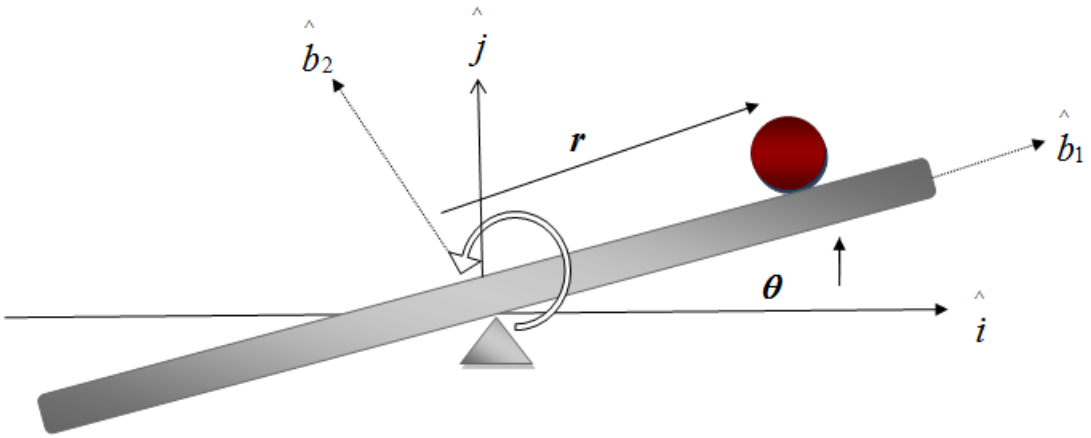

Figure 7.1: The beam and ball experiment setup

the rolling occurs without slipping. The goal is to track any trajectory from a class of admissible trajectories. The position of the ball from the center is labeled r and the angle θ is the inclination the beam makes with the horizontal.

The beam and ball system is one of the most popular laboratory models used to teach control engineering. It is open-loop unstable and exhibits the peaking phenomenon. This property is best understood by studying the forces acting on the ball. Figure 7.2 indicates that at any instant two forces influence the ball's motion. Notice, the gravitational force due to weight (represented as mg) of the ball always tries to pull the ball toward the center of the beam. The centrifugal force on the ball exerted due to rotation of the beam opposes gravitational force and tries to push the ball off the beam. This force is a function of the angular rate at which the beam rotates. It is clear that the ball can be kept on the beam only through the gravitational force. As the weight of the ball is constant only $\sin\theta$ can be used for stabilization.

However, if the ratio of the centrifugal force to the weight of the ball $\left|\frac{mr\dot{\theta}^2}{mg}\right| > 1$ the ball cannot be controlled. Even worse, this ratio acts as positive feedback on the system causing the angular rate of the beam to continually increase. This "peaking"

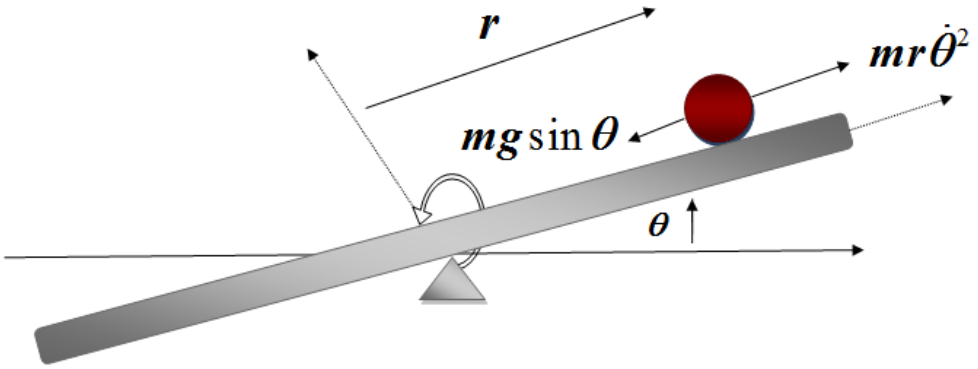

Figure 7.2: Forces acting on the beam and ball experiment

of the angular rate leads to instability and eventually the ball flies off the beam. This simple experiment captures a phenomenon seen in most modern aircraft. In an interesting article Kokotović [82] cites supersonic pilot John Hauser's following words "I can feel nonlinear aircraft dynamics on this toy system".

7.2.1 Dynamical Model

The dynamics of the beam and the ball setup is described by the translational motion of the ball and rotational motion of the beam. Consider the axes system shown in Figure 7.1. The position vector of the ball from the center of the beam in the body axes is $\vec{p} = r\hat{b}_1$. The angular velocity of the body frame with respect to the inertial frame is $\vec{\omega} = \dot{\theta}\hat{b}_3$, with $\hat{b}_3$ pointing out of the paper. Using this notation the velocity and the acceleration of the ball expressed in the body frame are

$$\vec{v} = \dot{r}\hat{b}_1 + r\dot{\theta}\hat{b}_2 \tag{7.1a}$$

$$\vec{a} = (\ddot{r} - r\dot{\theta}^2)\hat{b}_1 + (2\dot{r}\dot{\theta} + r\ddot{\theta})\hat{b}_2. \tag{7.1b}$$

The angular acceleration of the beam is

$$\vec{\alpha} = \ddot{\theta}\hat{b}_3. \tag{7.2}$$

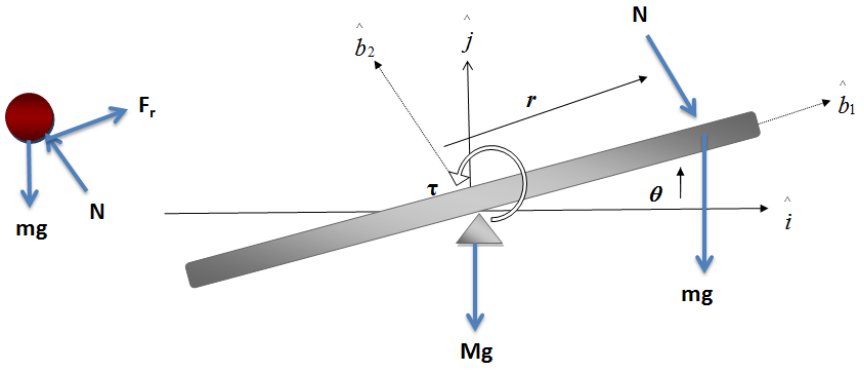

Figure 7.3: The beam and ball experiment: free body diagram

The equations of motion are derived using Newton's and Euler's second law of motion [79], [83]. Toward this end, the free-body diagram for the forces acting on the setup are determined. In Figure 7.3 the reaction force N is exerted by the beam on the ball. The force due to pure rolling is denoted as F_r. The torque acting on the system is represented by τ. Using the orthonormal transformation

$$\begin{bmatrix} \hat{b}_1 \\ \hat{b}_2 \\ \hat{b}_3 \end{bmatrix} = \begin{bmatrix} \cos\theta & \sin\theta & 0 \\ -\sin\theta & \cos\theta & 0 \\ 0 & 0 & 1 \end{bmatrix} \begin{bmatrix} \hat{i} \\ \hat{j} \\ \hat{k} \end{bmatrix} \tag{7.3}$$

the force and moment vector in the body frame is

$$\vec{F} = (F_r - mg\sin\theta)\hat{b}_1 + (N - mg\cos\theta)\hat{b}_2 \tag{7.4a}$$

$$\vec{L} = (\tau - Nr)\hat{b}_3. \tag{7.4b}$$

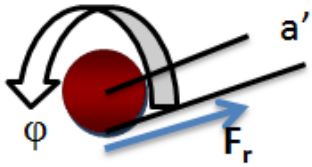

Figure 7.4: Rotation motion of the ball

Using the kinematic relations given in (7.1) and (7.2) and the above force relations the following equations are obtained

$$m(\ddot{r} - r\dot{\theta}^2) = F_r - mg\sin\theta \tag{7.5a}$$

$$m(2\dot{r}\dot{\theta} + r\ddot{\theta}) = N - mg\cos\theta \tag{7.5b}$$

$$(J + J_b)\ddot{\theta} = \tau - Nr \tag{7.5c}$$

where J and J_b represent the moment of inertia of the beam and the ball about the pivot respectively. The reaction force N is given by the relation (7.5b). The other reaction force F_r is determined by studying the rotation of the ball. Figure 7.4 indicates that the ball rotates about its own center making an angle ϕ. The torque about the center is $J_b\ddot{\phi}$. Thus, the reaction force becomes

$$F_r = \frac{J_b\ddot{\phi}}{a'} \tag{7.6}$$

where a' is the distance from the center of the ball to the point of contact with the beam. From geometry the distance the ball covers by rotating is $L = R\phi$ where R is the radius of the ball. Hence the acceleration is $\ddot{L} = R\ddot{\phi}$. But distance L is the change in the position of the ball from center since the ball experiences pure roll. Hence $\ddot{L} = -\ddot{r}$. The minus sign has been added for consistency. Finally using (7.6),

$$F_r = -\frac{J_b\ddot{r}}{a'R}. \tag{7.7}$$

Combining relations (7.5a) through (7.5c) with (7.7) results in

$$\left(m + \frac{J_b}{a'R}\right)\ddot{r} - mr\dot{\theta}^2 = -mg\sin\theta \tag{7.8a}$$

$$(mr^2 + J + J_b)\ddot{\theta} = \tau - 2mr\dot{r}\dot{\theta} - mgr\cos\theta. \tag{7.8b}$$

Rearrange (7.8) to obtain the following state-space form

$$\dot{r} = v \tag{7.9a}$$

$$\dot{v} = -Bg\sin\theta + Brq^2 \tag{7.9b}$$

$$\dot{\theta} = q \tag{7.9c}$$

$$\dot{q} = u \tag{7.9d}$$

with u as the control variable and

$$B = \frac{m}{m + \frac{J_b}{a'R}} \tag{7.10a}$$

$$\tau = 2mr\dot{r}\dot{\theta} + mgr\cos\theta + (mr^2 + J + J_b)u. \tag{7.10b}$$

The beam and ball experiment is a benchmark control problem for systems with no relative degree. Recall relative degree is the number of times output must be differentiated in order to have the input appear explicitly. The output in this case is the distance of the ball from the center of the beam. Differentiating

$$y = r \tag{7.11a}$$

$$\dot{y} = v \tag{7.11b}$$

$$\ddot{y} = -Bg\sin\theta + Brq^2 \tag{7.11c}$$

$$\dddot{y} = -Bg\cos\theta q + Bvq^2 + 2Brqu \tag{7.11d}$$

the control appears in the third derivative. But the coefficient $2Brq$ becomes zero whenever the angular velocity of the beam or the ball position are zero. Therefore, the relative degree is not well defined and feedback linearization cannot be used

for control. Approximate input-output linearization has been shown to demonstrate bounded output tracking [84, 85]. In this section, asymptotic tracking is demonstrated using approach detailed in Section 6.

7.2.2 Time Scale Separation Analysis

In order to use the theoretical developments of this dissertation, the time scale properties of the beam and ball experiment are analyzed. The system is non-dimensionalized to determine whether or not it exhibits multiple time scale behaviour. Assume a set of reference quantities $(t_0, r_0, v_0, \theta_0, q_0, u_0, B_0, g_0)$ that are all positive. Using these reference quantities several non-dimensional variables are defined as follows:

$$\hat{t} = t/t_0, \quad \hat{r} = r/r_0, \quad \hat{v} = v/v_0, \quad \hat{\theta} = \theta/\theta_0 \tag{7.12a}$$

$$\hat{q} = q/q_0, \quad \hat{B} = B/B_0, \quad \hat{g} = g/g_0. \tag{7.12b}$$

Using the definitions above, the equations of motion given in (7.9) are transformed to the following non-dimensional form:

$$\dot{\hat{r}} = \left[\frac{v_0 t_0}{r_0}\right] \hat{v} \tag{7.13a}$$

$$\dot{\hat{v}} = -\left[\frac{t_0 B_0 g_0}{v_0}\right] \hat{B}\hat{g}\sin(\theta_0\hat{\theta}) + \left[\frac{t_0 B_0 r_0 q_0^2}{v_0}\right] \hat{B}\hat{r}\hat{q}^2 \tag{7.13b}$$

$$\dot{\hat{\theta}} = \left[\frac{t_0 q_0}{\theta_0}\right] \hat{q} \tag{7.13c}$$

$$\dot{\hat{q}} = \left[\frac{t_0 u_0}{q_0}\right] \hat{u}. \tag{7.13d}$$

Based on the fact that the angular rate evolves faster than translational motion,

set $\epsilon = \frac{\theta_0}{t_0 q_0}$ and $\mu = \frac{q_0}{t_0 u_0}$. Further use the conditions

$$B_0 = B, \quad g_0 = g, \quad \frac{v_0 t_0}{r_0} = 1, \quad \theta_0 = \theta \tag{7.14a}$$

$$\frac{t_0 B_0 g_0}{v_0} = \frac{t_0 B_0 r_0 q_0^2}{v_0}, \text{ or } r_0 q_0^2 = g_0. \tag{7.14b}$$

This gives five conditions for eight free reference quantity variables. The sixth condition is found by ensuring the translational kinematics are of $O(1)$. Thus,

$$\frac{v_0}{r_0} = \frac{B_0 g_0}{v_0} \text{ or } B_0 g_0 r_0 = v_0^2. \tag{7.15}$$

For the final conditions take

$$q_0 = q, \quad u_0 = u. \tag{7.16}$$

The next step is to verify that ϵ and μ are in fact small quantities. This is done by substituting physical parameters given in Table 7.1 in the above equations. Let the control limit be $u_0 = 1$ and maximum angular deflection be $\theta_0 = 1$ and angular rate be $q_0 = \pi/6$rad/sec. With these values

$$r_0 = \frac{g_0}{q_0^2} = 35.782m \tag{7.17a}$$

$$v_0 = \sqrt{B_0 g_0 r_0} = 18.73m/sec \tag{7.17b}$$

$$t_0 = \frac{v_0}{B_0 g_0} = 1.91sec \tag{7.17c}$$

$$\mu = \frac{q_0}{t_0 u_0} = 0.27426 \tag{7.17d}$$

$$\epsilon = \frac{\theta_0}{t_0 q_0} = 0.1047. \tag{7.17e}$$

Thus, it is concluded that μ and ϵ are both of same order and the system exhibits

Table 7.1: Beam and ball setup parameters

Parameter	Value
m	$0.50kg$
g	$9.81m/sec^2$
R	$0.05m$
J_b	$\frac{2}{5}mR^2kgm^2$
a'	Rm
J	$0.02kgm^2$
B	0.999

two time scales. The system given in (7.9) is equivalently represented as

$$\dot{r} = v \tag{7.18a}$$

$$\dot{v} = -Bg\sin\theta + Brq^2 \tag{7.18b}$$

$$\mu\dot{\theta} = q \tag{7.18c}$$

$$\mu\dot{q} = u \tag{7.18d}$$

where μ is included entirely for modeling purposes and is set to one in simulation.

7.2.3 Control Formulation

The control development follows closely the steps detailed in Section 6. For brevity, only the equations required for implementation are detailed.

Step 1: The reduced slow system $\mathscr{S}^0$ in error coordinates $e_r := r - r_r(t)$ and $e_v := v - v_r(t)$ with $v_r = \dot{r}_r$ is

$$\dot{e}_r = e_v \tag{7.19a}$$

$$\dot{e}_v = -Bg\sin\theta^0 + B{q^0}^2(e_r + r_r) - \dot{v}_r \tag{7.19b}$$

$$q^0(t, e_r, e_v, \theta^0) = 0 \tag{7.19c}$$

$$u(t, e_r, e_v, \theta^0, q^0) = 0 \tag{7.19d}$$

where $\theta^0(t, e_r, e_v)$ and $q^0(t, e_r, e_v, \theta^0)$ represent the fast manifolds. Rearrange (7.19) to get

$$\dot{e}_r = e_v \tag{7.20a}$$

$$\dot{e}_v = -Bg \sin\theta^0 - \dot{v}_r. \tag{7.20b}$$

With Lyapunov function $V(e_r, e_v) = \frac{K}{2}e_r^2 + \frac{1}{2}e_v^2$; with $K > 0$ and manifold

$$\theta^0 = \arcsin \frac{[-\dot{v}_r + Ce_v + De_r]}{Bg} \tag{7.21}$$

property (ii) of Theorem 6.1 is satisfied with $\alpha_1 = \frac{D-K}{2}$ and $\psi_3 = \sqrt{e_r^2 + e_v^2}$. The feedback gains C and D are design constants that determine the closed-loop poles of the reduced slow system.

Step 2: The reduced fast system $\mathscr{S}_\mu^0$ is

$$e'_\theta = e_q + q^0(t, e_r, e_v, e_\theta) \tag{7.22a}$$

$$e'_q = u(t, e_r, e_v, e_\theta, e_q) - q'^0 \tag{7.22b}$$

with the errors $e_\theta := \theta - \theta^0(t, e_r, e_v)$ and $e_q = q - q^0(t, e_r, e_v, e_\theta)$. In order to stabilize the errors (e_θ, e_q) backstepping is employed. Let $W = \frac{1}{2}e_\theta^2$. Then the manifold $q^0(t, e_r, e_v, e_\theta) = -\rho e_\theta$ stabilizes the error e_θ. Further let $\nu = u - q'^0$. Using the Lyapunov function $\mathscr{Z} = \frac{1}{2}e_\theta^2 + \frac{1}{2}e_q^2$ condition (vi) of Theorem 6.1 is satisfied with $\alpha_3 = \rho$ and $\varpi = \sqrt{e_\theta^2 + e_q^2}$ with the control law $\nu = -e_\theta - \rho_2 e_q; \rho_2 > \rho$. The derivative of the manifold $q'^0 = -\rho(e_q + q^0)$ and results in the following control law

$$u(t, e_r, e_v, e_\theta, e_q) = -e_\theta - \rho_2 e_q - \rho(e_q + q^0). \tag{7.23}$$

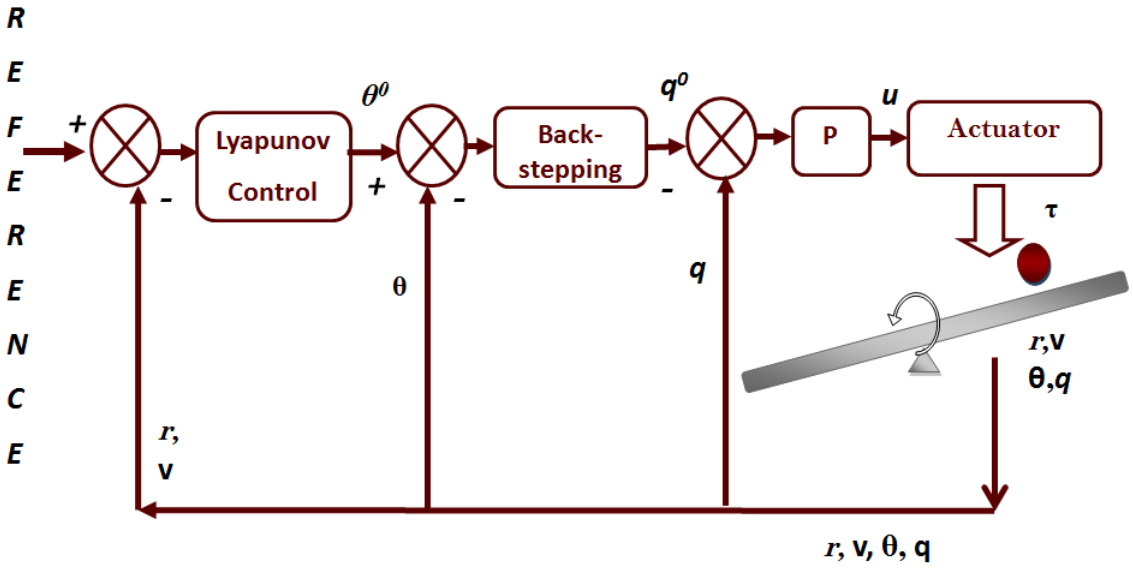

Figure 7.5: Control implementation block diagram for the beam and ball experiment

Step 3: Finally the interconnection conditions are satisfied with constants $\beta_2 = B\|r_r + 1\| - Bg$, $\gamma = C(1+\rho)$, $\beta_3 = -\frac{CD}{Bg}(1+\rho)\|r_r + 1\| + \frac{C^2}{Bg}(1+\rho)$, rest all being zeros.

The above control synthesis procedure is summarized in a block diagram shown in Figure 7.5.

7.2.4 Results and Discussion

The physical parameters for the experiment are as described in Table 7.1. The beam is two meters in length, that is one meter on each side from the pivot. It is desired that the ball moves 0.75meters on each side of the beam. The desired trajectory is $r_r(t) = A\cos(\frac{\pi t}{5})$ with $A = 0.750$m. The linear open-loop model about chosen reference is non-minimum phase with a zero in the right-half plane. Figure 7.6 indicates that the poles lie exactly on the imaginary axis close to the origin while the zero is in the right half plane.

This non-minimum phase system is controlled by theoretical developments pre-

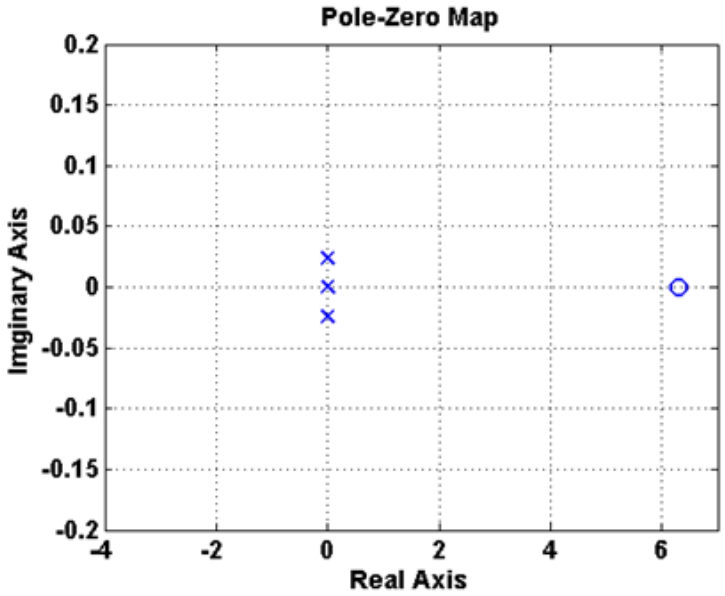

Figure 7.6: Open-loop poles ('x' marker) and zero ('o' marker) of the beam and ball experiment

sented above. The constants are chosen as $C = 4$, $D = 4$, $\rho = 4, \rho_2 = 8$. Note that these constants are chosen such that the time scale behaviour is preserved in the closed-loop system. With these constants, Theorem 6.1 guarantees asymptotic stability for all $\epsilon < 0.2$ with $d = 0.637$. Figures 7.7 through 7.12 present the simulation results. The position output and the tracking error is shown in Figure 7.7 and Figure 7.8 respectively. Notice that after the transient settles out perfect position tracking is achieved. The error remains within $\pm|1.56|$cm.

This perfect output tracking indicates that the internal states are bounded and follow their desired values closely (See figures 7.9 through 7.10). The error between the desired computed manifold and the actual system response is within 0.3598deg and $\pm$0.503deg/sec. The control input required to accomplish the exact output tracking is shown in Figure 7.11 and Figure 7.12. The peaks around the first few seconds are due to the arbitrarily chosen initial conditions that are not the equilibrium solution for the system.

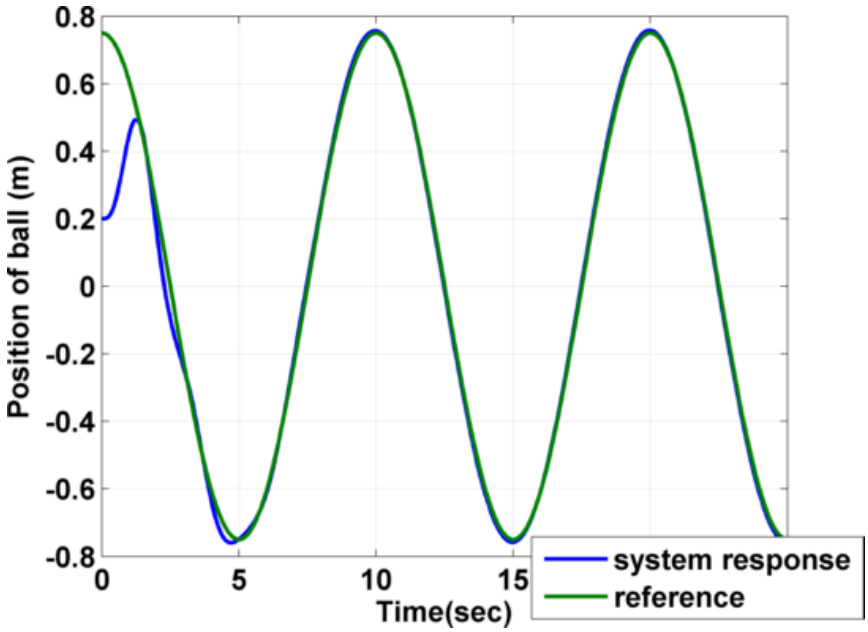

Figure 7.7: The beam and ball experiment: position of the ball

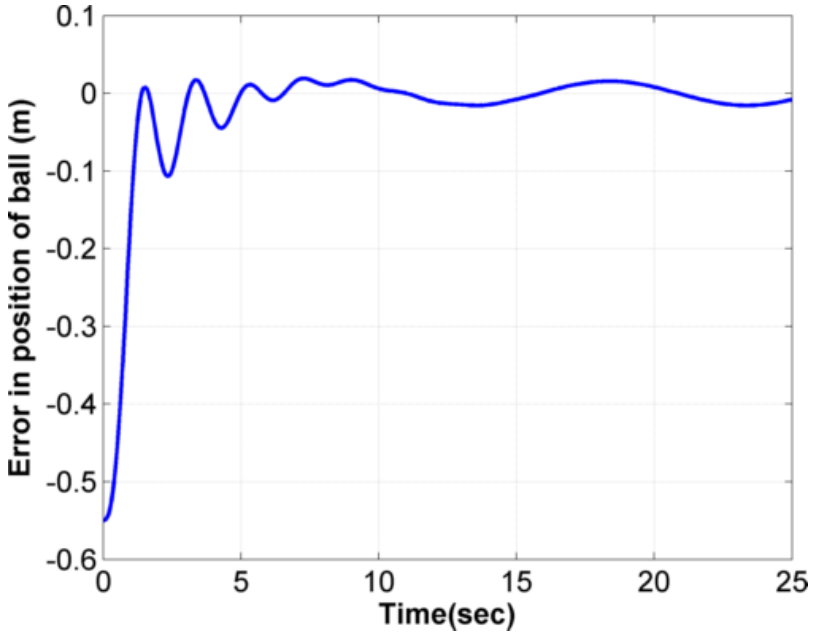

Figure 7.8: The beam and ball experiment: error in tracking

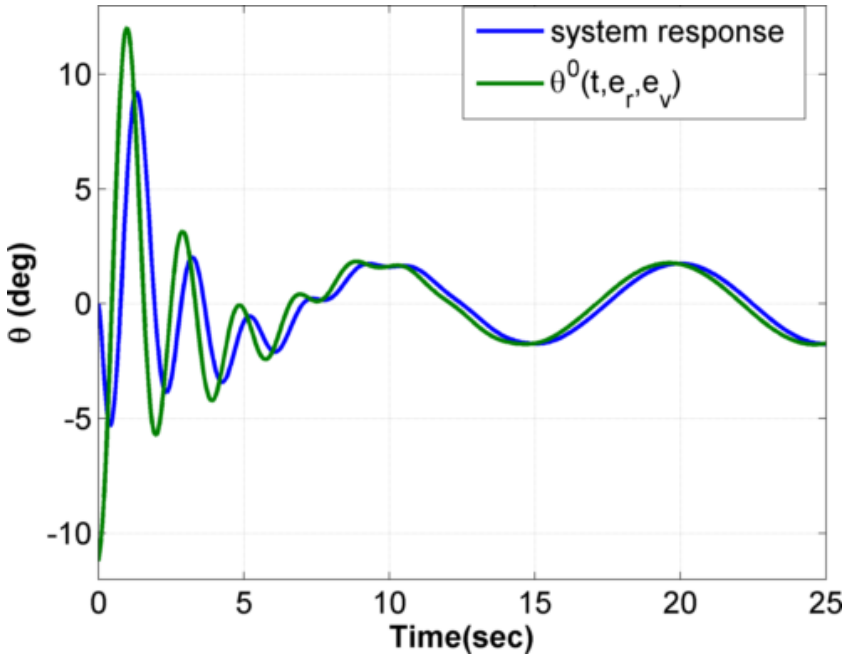

Figure 7.9: The beam and ball experiment: inclination of the beam

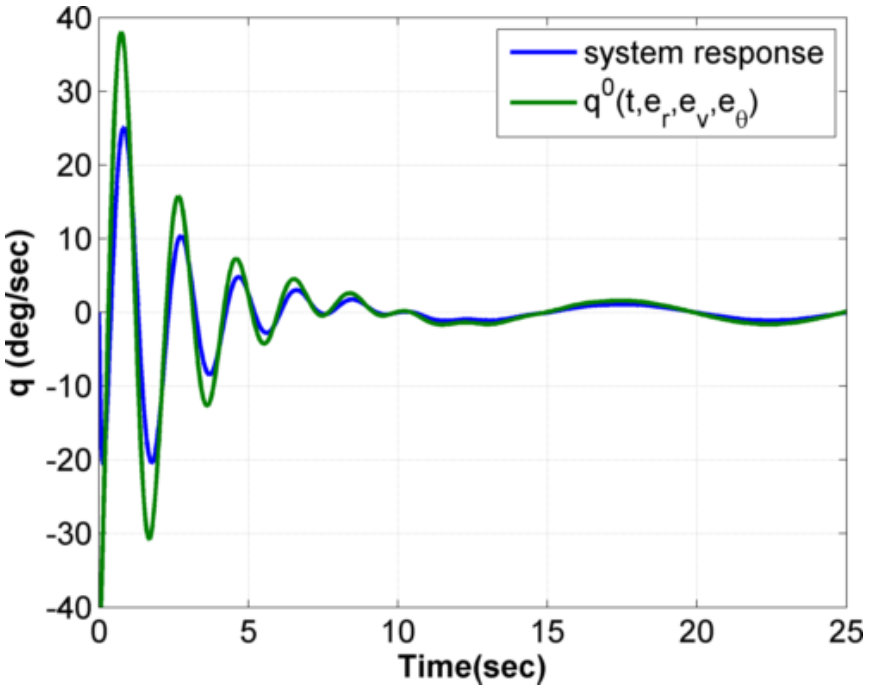

Figure 7.10: The beam and ball experiment: angular rate of the beam

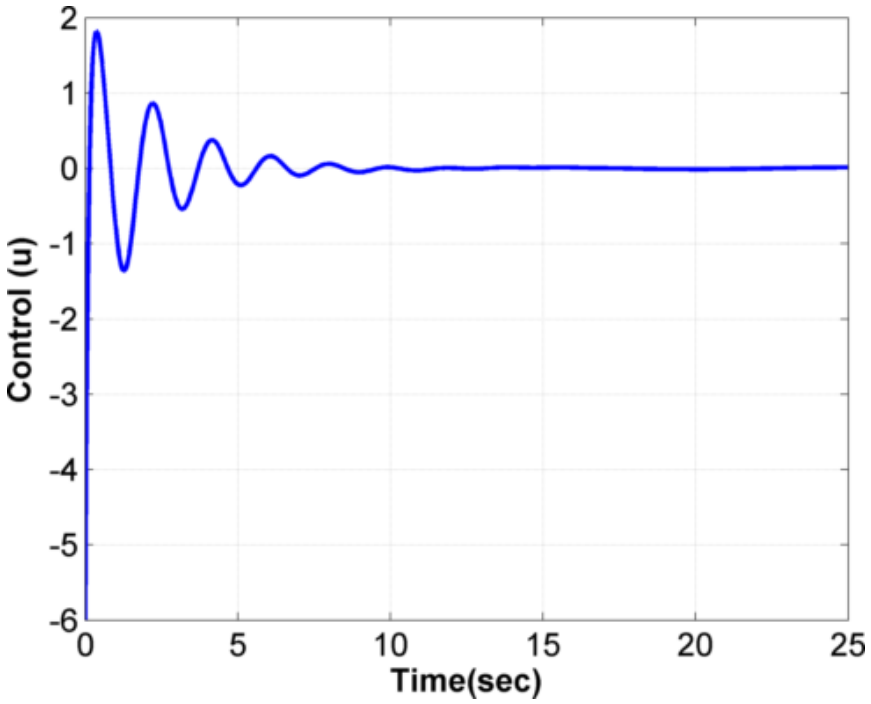

Figure 7.11: The beam and ball experiment: computed control

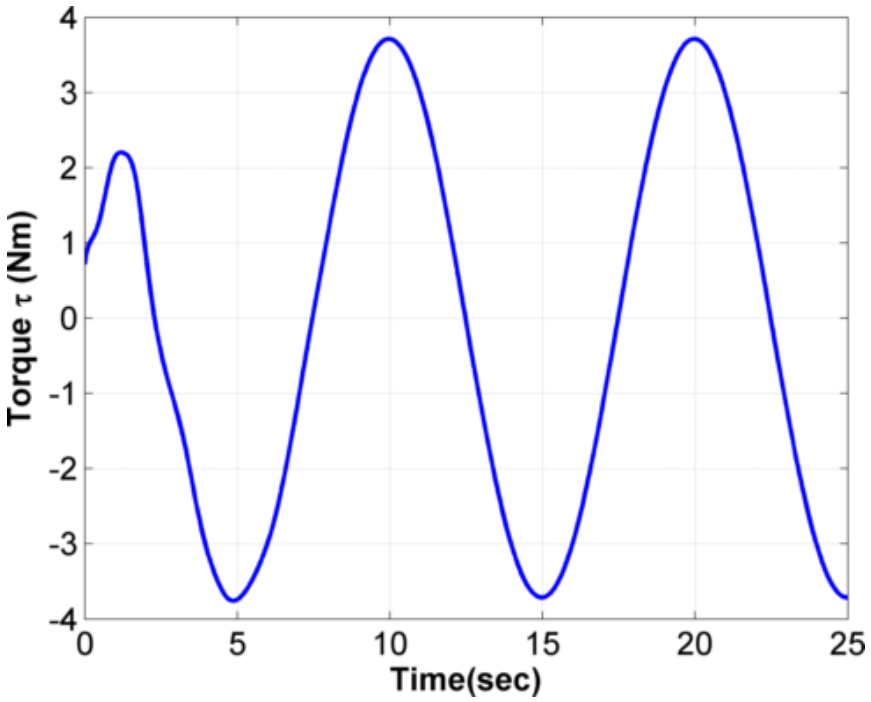

Figure 7.12: The beam and ball experiment: torque required

7.2.5 Summary

A state-feedback control law synthesis procedure for output tracking of weakly minimum phase beam and ball experiment was developed. The desired pitch-rate internal state trajectory was determined online to stabilize the unstable open-loop system. This controller exploits the presence of inherent two time scales of the system. Based on the results presented, the following conclusions are drawn. The final output remains close to the desired reference trajectory for all times. This perfect output tracking is a result of close internal state trajectory following. Additionally, Figure 7.5 shows that the controller is causal and independent of the reference trajectory. Finally, Theorem 6.1 guarantees global asymptotic tracking.

7.3 Hover Control for an Unmanned Three Degrees-of-Freedom Helicopter Model

The second study develops a general control law for precision position tracking of a nonlinear non-minimum phase dynamics of an autonomous helicopter shown in Figure 7.13. The single-rotor helicopter is constrained to fly in the longitudinal plane. The axis along the body of the helicopter is represented by (X, Y, Z). The helicopter model is allowed to pitch about the Y axis. T_M and T_T are the thrusts produced by the main and the tail rotor respectively. The angle a_{1s} is the longitudinal tilt the tip path plane makes with respect to the shaft of the main rotor. The goal is develop and verify real-time implementable control laws that follow desired output trajectories while stabilizing the unstable internal dynamics using main rotor thrust T_M and angle a_{1s} as controls.

Hover control of a helicopter is one of the most challenging non-minimum phase control problems. To qualitatively analyze this behaviour consider the helicopter shown in Figure 7.13. The motion of the helicopter is described in North-East-

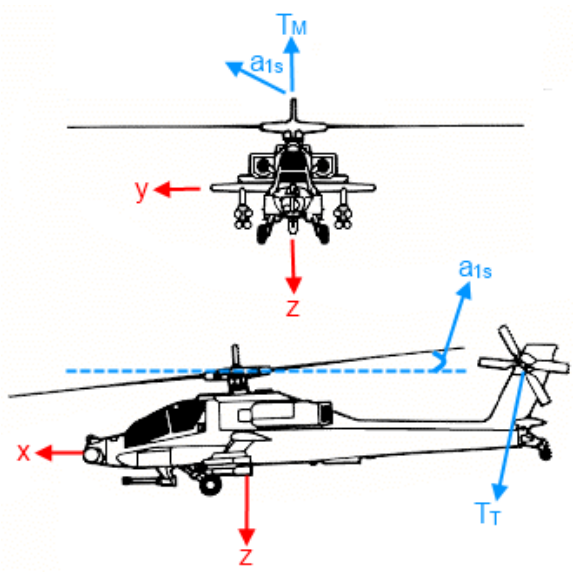

Figure 7.13: Unmanned autonomous helicopter model

Down frame shown as (X, Y, Z) in the figure. Assume that the helicopter model is allowed to pitch only about the Y axis. T_M and T_T are the thrusts generated by the main and the tail rotor respectively that keep the vehicle aloft. The angle a_{1s} is the longitudinal tilt the tip path plane makes with respect to the shaft of the main rotor. Side view of Figure 7.13 shows that non-zero tilt induces a component of the main rotor thrust along the horizontal X axis and consequently the helicopter propels forward. Hence, in order to remain in hover the main rotor thrust and the angle a_{1s} need to be controlled. However, changing this angle has another consequence. The forward component of the thrust that it creates induces a clockwise pitching moment about the center of gravity of the vehicle causing the nose to drop. In order to remain level, the angle a_{1s} needs to be corrected. But doing so alters the forces acting on the helicopter and the vehicle departs from hover. For the helicopter under study, it will be shown in Section 7.3.1 that desired T_M and a_{1s} required to maintain hover lead to unstable oscillatory pitching motion.

Previous studies for hover control assume that the dynamical behaviour of a heli-

copter is similar to that of a VTOL aircraft as both these vehicles have direct control over the aerodynamic lift. Hence several studies employ the control developments proposed for VTOL aircraft [84]. The formulation in [84] assumes that the force contribution from the longitudinal tilt angle a_{1s} is negligible. Such a simplification removes the coupling between the forces and the pitching moment and makes the resultant dynamical model, approximately input-output linearizable. Reference [86] used feedback linearization for stabilizing the resulting approximate model in order to guarantee bounded transient errors. More recently back-stepping has been used for control of small autonomous helicopters[87], [88], [89]. Other control techniques based upon the approximate model include dynamic-inversion[90] and neural-network based adaptation[91]. In order to mitigate the limitations due to under-actuation some techniques take advantage of the inherent multiple time scale behaviour of helicopters. Reference [92] compared linear and nonlinear control designs for the approximate model using the fast rotational dynamics as virtual control variables. A similar approach was proposed in [93] wherein Lyapunov based methods were used to guarantee stability of a radio/control helicopter model using the approximate dynamics.

As a consequence of neglecting the coupling between the forces and the moments, application of aforementioned methods is limited in operating regime and to reference commands that do not require to be precisely followed. Exact output tracking was demonstrated by retaining the coupling terms in [94] through stable-inversion of a linear helicopter model. This inversion computed the desired input-state trajectory that along with feedforward and feedback control led to asymptotic output tracking. Approach in [94] emphasized that internal-state feedback is necessary to stabilize a non-minimum phase system. However, the method required an infinite time preview and knowledge of the complete output trajectory beforehand.

From the above discussion it is understood that helicopter control design poses three major challenges. First, the coupling between forces and moments generated due to rotor is significant and must not be ignored during control design [28]. But retaining this coupling makes the system non-minimum phase and difficult to stabilize. Second, a non-minimum phase system cannot be asymptotically stabilized in real-time with available control techniques and control design requires substantial offline processing. Third, current real-time implementable approaches that are independent of the reference trajectory are limited in performance and operating regime.

The following sections presents a control design procedure that addresses the above technical challenges and validates the general nonlinear control procedure developed in Section 6 for a three-dimensional longitudinal model of an autonomous helicopter. Section 7.3.1 describes the helicopter model under study and examines analytically the non-minimum phase properties of the vehicle and Section 7.3.2 analyses its inherent time scale properties. The nonlinear control design and stability of the closed-loop system is analyzed in Section 7.3.3. Simulation validation for hover control is discussed in Section 7.3.4. Finally, remarks are presented in Section 7.3.5.

7.3.1 Model Description and Open-Loop Analysis

In this section the governing equations of the helicopter model are presented. Then, the exact input-output linearization of the model is carried out and it is shown that the system has oscillatory internal dynamics. The effect of neglecting the coupling between the forces and moments is also discussed.

7.3.1.1 Vehicle Description

The helicopter model is written with respect to earth-fixed inertial coordinates. The forces and moments act in the body frame shown in Figure 7.13. The origin of the body fixed frame is the center of gravity of the platform and it is assumed that

this moves with the motion of the fuselage. The three degrees-of-freedom equations of motion of a symmetric helicopter model in hover (assuming the lateral/directional components are in equilibrium) are as follows:

$$\begin{bmatrix} \dot{x} \\ \dot{z} \end{bmatrix} = \begin{bmatrix} \cos\theta & \sin\theta \\ -\sin\theta & \cos\theta \end{bmatrix} \begin{bmatrix} u \\ w \end{bmatrix} \tag{7.24a}$$

$$\begin{bmatrix} m\dot{u} \\ m\dot{w} \end{bmatrix} = \begin{bmatrix} -qw + F_x \\ qu + F_z \end{bmatrix} + \begin{bmatrix} \cos\theta & -\sin\theta \\ \sin\theta & \cos\theta \end{bmatrix} \begin{bmatrix} 0 \\ mg \end{bmatrix} \tag{7.24b}$$

$$\dot{\theta} = q \tag{7.24c}$$

$$I_y\dot{q} = M \tag{7.24d}$$

where x is the inertial position, positive pointing north, z is the inertial position, positive down, u and w are body forward and vertical velocities respectively, θ is the pitch-attitude angle, positive counter-clockwise and q is the body pitch-rate. I_y represents the moment of inertia about the Y-axis, m mass of the helicopter and g is acceleration due to gravity. F_x and F_y are body forces in the forward and vertical direction. S.I unit system is followed and all angles are in *rad*. In general the above set is augmented with dynamic equations of longitudinal flapping. However, it is assumed that the time-constant for the flapping of conventional rotor blades corresponds to one-quarter of a rotor revolution [95][pp 558-559] and this justifies the use of rigid-body equations for describing the motion.

The body forces (F_x, F_z) and pitching moment M are generated by the main rotor and controlled by T_M, main rotor thrust and a_{1s} longitudinal tilt of the tip path plane of the main rotor with respect to the shaft. The parameter h_M denotes the distance between c.g and main rotor positive in the downward direction, l_M is

Table 7.2: Helicopter model parameters

Parameter	Value
m	$4.9kg$
I_y	$0.271256kgm^2$
h_M	$0.2943m$
l_M	$-0.015m$
Q_T	$0.0110Nm$
M_a	$25.23Nm/rad$

the distance between the c.g and main rotor along forward direction and Q_T is the tail rotor torque. The aerodynamic model given below is taken from [86].

$$F_x = -T_M \sin a_{1s} \tag{7.25a}$$

$$F_z = -T_M \cos a_{1s} \tag{7.25b}$$

$$M = M_a a_{1s} - F_x h_M + F_z l_M - Q_T \tag{7.25c}$$

with the system parameters given in Table 7.2.

7.3.1.2 Exact and Approximate Input-Output Linearization

The non-minimum phase properties of the model under consideration are analyzed by studying the input-output relationship. The desired outputs for the control design are the inertial coordinates of the vehicle, namely (x, z) pointing north and down respectively. Control inputs available are the main rotor thrust T_M and longitudinal tilt a_{1s}. Taking second derivative of each output,

$$\begin{bmatrix} \ddot{x} \\ \ddot{z} \end{bmatrix} = \frac{1}{m} \begin{bmatrix} \cos\theta & \sin\theta \\ -\sin\theta & \cos\theta \end{bmatrix} \begin{bmatrix} F_x \\ F_z \end{bmatrix} + \begin{bmatrix} 0 \\ g \end{bmatrix} \tag{7.26}$$

it is found that the relative degree of each output is two. This implies that the rotational dynamics given in (7.24c), (7.24d) constitute the internal dynamics of the

system.

In order to analyze the internal stability of the system, the zero dynamics of the system needs to be examined. Toward this end, the control vector (T_M, a_{1s}) that constraints the outputs and its derivatives on the origin is computed. From (7.26) and relations given in (7.25) the following solution is determined.

$$\begin{bmatrix} T_M \\ a_{1s} \end{bmatrix} = \begin{bmatrix} mg \\ -\theta \end{bmatrix} \tag{7.27}$$

Using the moment relation given in (7.25c) and the constrained control solution (7.27) the zero dynamics are characterized by the following equations

$$\dot{\theta} = q \tag{7.28a}$$

$$\dot{q} = \frac{1}{I_y}\left[-M_a\theta - mg(h_M \sin\theta - l_M \cos\theta) - Q_T\right] \tag{7.28b}$$

The stability of the above system is analyzed by linearizing about the trim values $\theta_* = 0.018 rad$ and $q_* = 0 rad/sec$.

$$\begin{bmatrix} \Delta\dot{\theta} \\ \Delta\dot{q} \end{bmatrix} = \begin{bmatrix} 0 & 1 \\ \frac{1}{I_y}(-M_a - mgh_M \cos\theta_* + mgl_M \sin\theta_*) & 0 \end{bmatrix} \begin{bmatrix} \Delta\theta \\ \Delta q \end{bmatrix} \tag{7.29}$$

The linearized eigenvalues are $\pm 12.0439j$ and no conclusions about the stability of the system can be drawn. Rewrite the internal dynamics (7.28a) and (7.28b) as

$$\ddot{\theta} = \frac{1}{I_y}\left(-M_a\theta - mg(h_M \sin\theta - l_M \cos\theta) - Q_T\right) \tag{7.30}$$

to notice that the pitch-attitude dynamics does not contain any damping terms. In order to analyze its stability consider the quadratic positive-definite Lyapunov

function $V_\theta = \frac{1}{2}\frac{M_a}{I_y}\theta^2 + \frac{1}{2}q^2$. The rate of change of the Lyapunov function along the trajectories of (7.28) is

$$\dot{V}_\theta = \frac{M_a}{I_y}\theta\dot{\theta} + q\dot{q} \tag{7.31a}$$

$$= -\frac{mg}{I_y}h_M q\sin\theta + \frac{mg}{I_y}l_M q\cos\theta - \frac{1}{I_y}Q_T q \tag{7.31b}$$

$$= -\left[\frac{Q_T}{I_y} + \frac{mg}{I_y}h(\theta)\right]q. \tag{7.31c}$$

Note the function $h(\theta) = h_M\sin\theta - l_M\cos\theta$ is monotonically increasing on the set $\theta \in [-\pi/2, \pi/2]$. This observation along with the parameters given in table 7.2 conclude that $\dot{V}_\theta < 0$ on the set $\{\theta \in [-0.0509, \pi/2]\bigcap q \in [0,\infty)\}\bigcup\{\theta \in [-pi/2, -0.0509]\bigcap q \in (-\infty, 0]\}$. On this set (θ_*, q_*) is the only equilibrium point and hence from the Poincaré-Bendixson [60] criterion it is concluded that a family of periodic orbits exist.

This conclusion is confirmed in simulation and the results are presented in Figure 7.14 and Figure 7.15. In fact the conclusions drawn from the Poincaré-Bendixson criterion are conservative since the simulation shows that a continuum of periodic orbits exist for the complete state-space. Thus the control inputs that stabilize the inertial position of the helicopter excite the periodic behaviour in pitch and exact input-output linearization is not a desirable control solution for the longitudinal model under study.

Notice the non-minimum phase behaviour is due to the nonlinear coupling between forces and pitching moment denoted by $h(\theta)$ in (7.31). This coupling comes through longitudinal tilt solution determined in (7.27) to produce the required translational forces. This dependence is explicitly seen by expanding the force terms given in the right-hand side of (7.26) and are obtained as follows

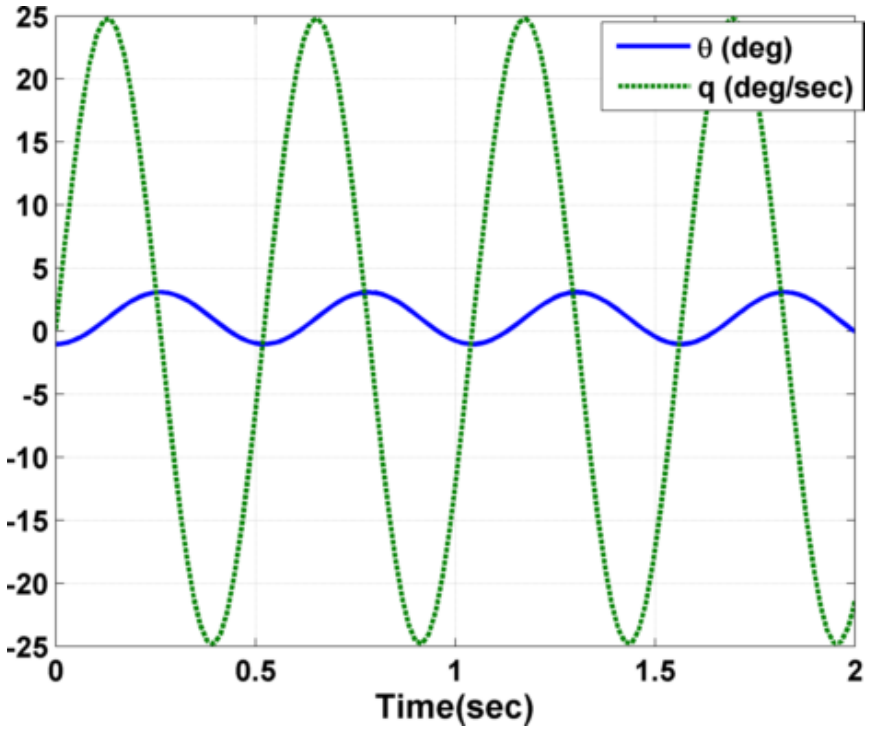

Figure 7.14: Time response of the pitching motion of helicopter model in (7.24)

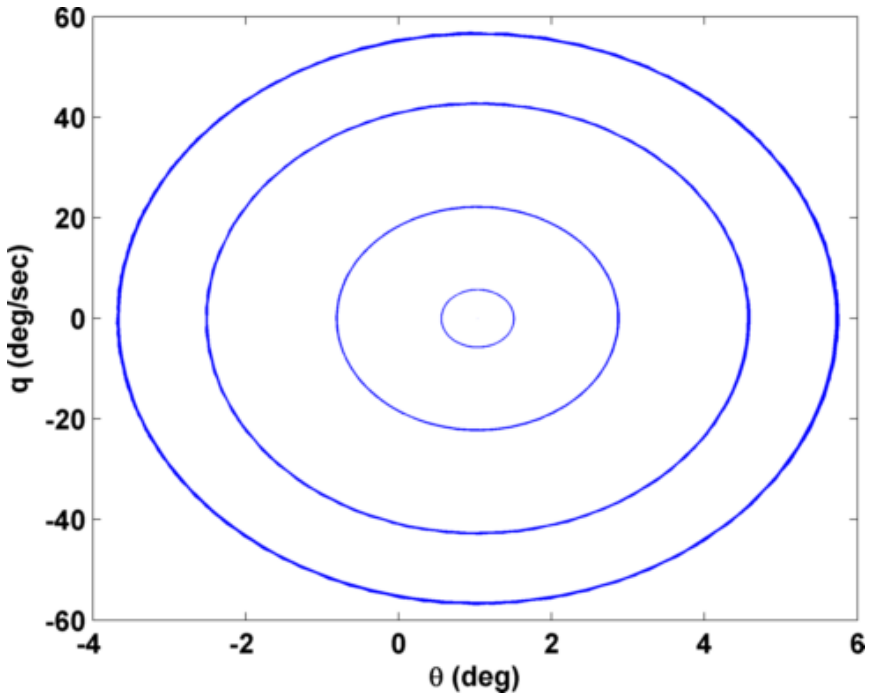

Figure 7.15: Phase portrait illustrating the oscillatory response of the pitching motion of helicopter model in (7.24)

$$X_f = -T_M \sin(\theta + a_{1s}) \tag{7.32a}$$

$$Z_f = -T_M \cos(\theta + a_{1s}) + mg \tag{7.32b}$$

In the above equations X_f and Z_f represent the forces in the inertial plane acting along the north and down directions respectively. Approximate input-output linearization of the output dynamics is possible by neglecting the dependence of the longitudinal tilt on the forces. The approximate forces thus obtained are

$$X_{app} = -T_M \sin\theta \tag{7.33a}$$

$$Z_{app} = -T_M \cos\theta + mg. \tag{7.33b}$$

The exact and approximate forces acting on the helicopter under study are shown in Figure 7.16 and Figure 7.17 for hover simulated in Section 7.3.4. Initially the helicopter is flying at an arbitrary flight condition and the forces are non-zero.

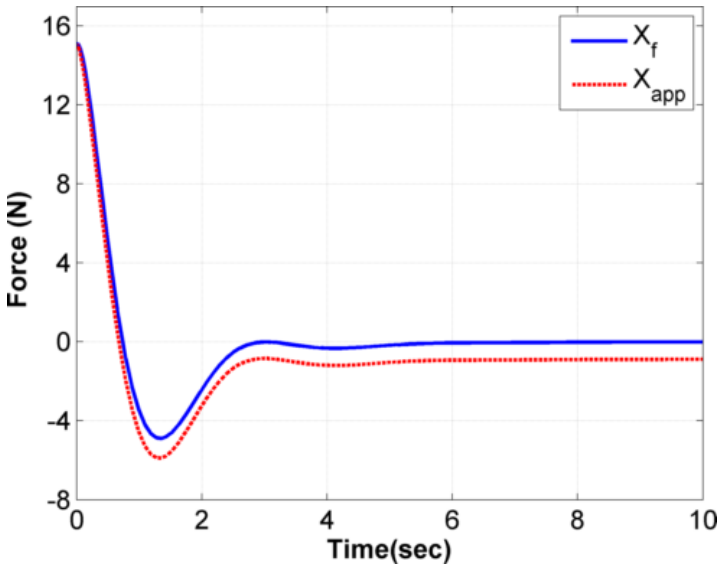

Figure 7.16: Exact and approximate forces in the horizontal direction in hover

Notice after two seconds the vehicle enters steady state and the exact horizontal

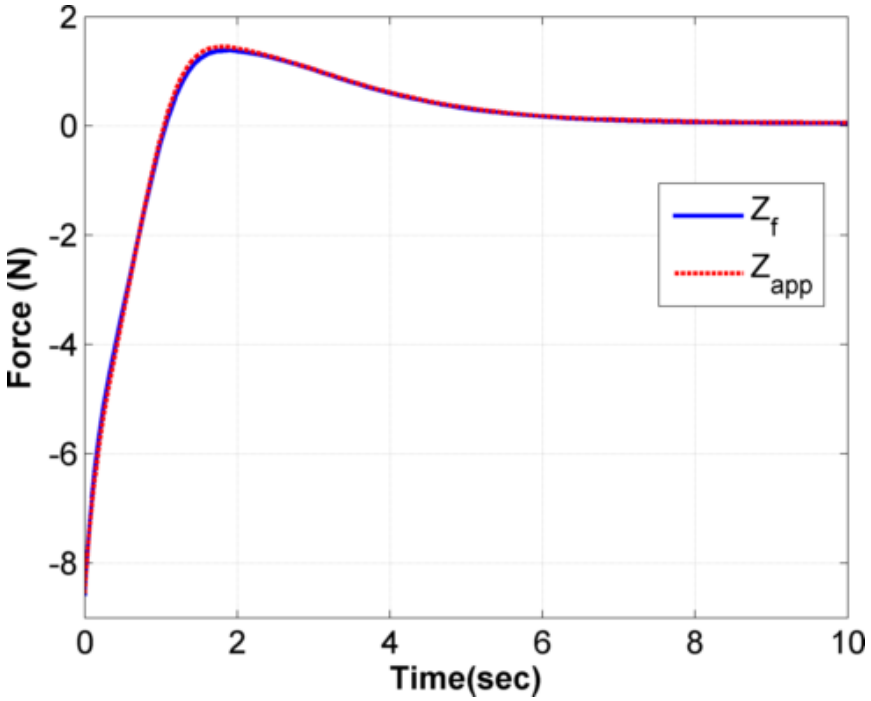

Figure 7.17: Exact and approximate forces in the vertical direction in hover

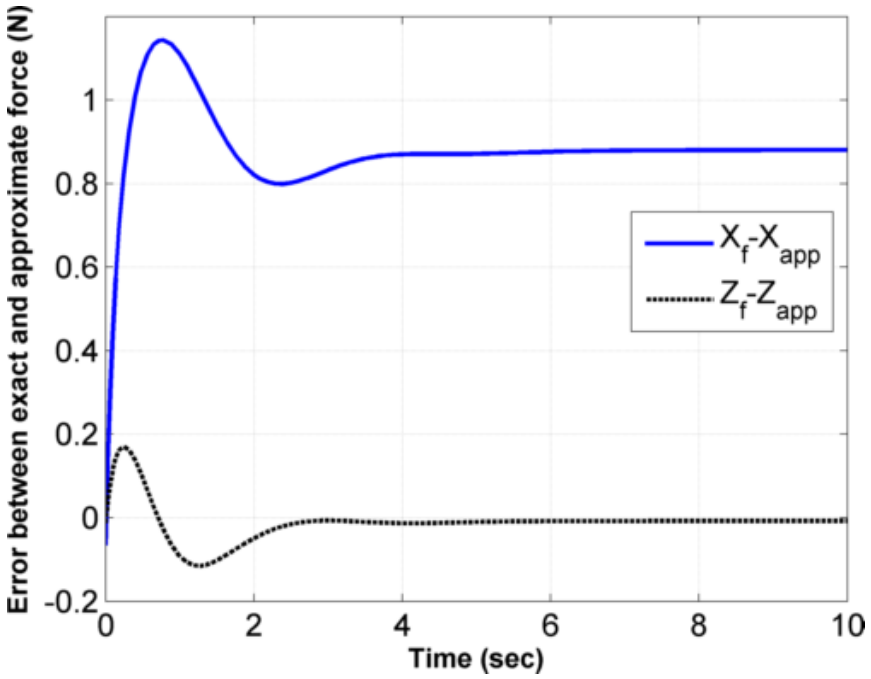

Figure 7.18: Error in exact and approximate forces in hover

and vertical forces become identically zero. However, the approximate horizontal forces remains non-zero. The error in the exact and approximate forces is shown in Figure 7.18. The error is over 100% in the horizontal forces while negligible in the vertical forces. This conclusion is consistent with the fact that rotor blade tilt induces a horizontal component of force in the helicopter and is not negligible. As mentioned earlier some studies use the approximate form given in (7.33) for control design. However, due this large error limits these methods to guarantee only local bounded tracking. In this work, the coupling terms are retained and asymptotic tracking is guaranteed.

7.3.2 Time Scale Analysis of the Helicopter Model

In this section, an important observation regarding inherent time scale characteristics of the model under consideration is made. This is done by studying the rate of change of the non-dimensional system equations. Toward this end, define a set of reference parameters $(t_0, x_0, z_0, u_0 = w_0 = V_0, \theta_0, q_0, m_0, F_{x0}, F_{z0}, M_0, g_0, I_{y0})$ and denote the respective dimension-less quantities as

$$\hat{t} = t/t_0 \quad \hat{x} = x/x_0 \quad \hat{z} = z/z_0 \quad \hat{u} = u/u_0 \tag{7.34a}$$

$$\hat{w} = w/w_0 \quad \hat{\theta} = \theta/\theta_0 \quad \hat{q} = q/q_0. \tag{7.34b}$$

The original dimensional equations given in (7.24) are transformed into following non-dimensional form using definitions given in (7.34).

$$\frac{d\hat{x}}{d\hat{t}} = \left[\frac{t_0 V_0}{x_0}\right] \{\hat{u}\cos\theta + \hat{w}\sin\theta\} \tag{7.35a}$$

$$\frac{d\hat{z}}{d\hat{t}} = \left[\frac{t_0 V_0}{z_0}\right] \{-\hat{u}\sin\theta + \hat{w}\cos\theta\} \tag{7.35b}$$

$$\frac{d\hat{u}}{d\hat{t}} = -\left[\frac{t_0 q_0}{m_0}\right]\frac{\hat{q}\hat{w}}{\hat{m}} + \left[\frac{t_0 F_{x0}}{m_0 V_0}\right]\frac{\hat{F}_x}{\hat{m}} - \left[\frac{t_0 g_0}{V_0}\right]\hat{g}\sin\theta \tag{7.36a}$$

$$\frac{d\hat{w}}{d\hat{t}} = \left[\frac{t_0 q_0}{m_0}\right]\frac{\hat{q}\hat{u}}{\hat{m}} + \left[\frac{t_0 F_{z0}}{m_0 V_0}\right]\frac{\hat{F}_z}{\hat{m}} + \left[\frac{t_0 g_0}{V_0}\right]\hat{g}\cos\theta \tag{7.36b}$$

$$\frac{d\hat{\theta}}{d\hat{t}} = \left[\frac{t_0 q_0}{\theta_0}\right]\hat{q} \tag{7.36c}$$

$$\frac{d\hat{q}}{d\hat{t}} = \left[\frac{t_0 M_0}{q_0 I_{y0}}\right]\frac{\hat{M}}{\hat{I}_y} \tag{7.36d}$$

Without loss of generality assign

$$\left[\frac{t_0 V_0}{x_0}\right] = \left[\frac{t_0 V_0}{z_0}\right] = 1 \tag{7.37}$$

and $\left[\frac{q_0 I_{y0}}{t_0 M_0}\right] = \mu$ where $\mu << 1$. This leads to

$$\frac{d\hat{x}}{d\hat{t}} = \{\hat{u}\cos\theta + \hat{w}\sin\theta\} \tag{7.38a}$$

$$\frac{d\hat{z}}{d\hat{t}} = \{-\hat{u}\sin\theta + \hat{w}\cos\theta\} \tag{7.38b}$$

$$\frac{d\hat{u}}{d\hat{t}} = -\left[\frac{\mu t_0^2 M_0}{m_0 I_{y0}}\right]\frac{\hat{q}\hat{w}}{\hat{m}} + \left[\frac{t_0 g_0}{V_0}\right]\left\{\frac{\hat{F}_x}{\hat{m}} - \hat{g}\sin\theta\right\} \tag{7.38c}$$

$$\frac{d\hat{w}}{d\hat{t}} = \left[\frac{\mu t_0^2 M_0}{m_0 I_{y0}}\right]\frac{\hat{q}\hat{u}}{\hat{m}} + \left[\frac{t_0 g_0}{V_0}\right]\left\{\frac{\hat{F}_z}{\hat{m}} + \hat{g}\cos\theta\right\} \tag{7.38d}$$

$$\frac{d\hat{\theta}}{d\hat{t}} = \left[\frac{\mu t_0^2 M_0}{I_{y0}\theta_0}\right]\hat{q} \tag{7.38e}$$

$$\mu\frac{d\hat{q}}{d\hat{t}} = \frac{\hat{M}}{\hat{I}_y} \tag{7.38f}$$

where $F_{x0} = F_{z0} = m_0 g_0$ has been used. Notice that for any reasonable value of the mass of the vehicle $\left[\frac{\mu t_0^2 M_0}{m_0 I_{y0}}\right] = \mu$. Then $m_0 = \left[\frac{t_0^2 M_0}{I_{y0}}\right]$ and $\left[\frac{\mu t_0^2 M_0}{I_{y0}\theta_0}\right] = \left[\frac{\mu m_0}{\theta_0}\right]$ is an $O(1/\epsilon)$ quantity as the ratio of pitch-angle and mass of the vehicle is very small and $\epsilon > \mu$. Finally, assuming that the vehicle is in hover $\left[\frac{t_0 g_0}{V_0}\right] = 1$ the non-dimensional form is obtained

$$\frac{d\hat{x}}{d\hat{t}} = \{\hat{u}\cos\theta + \hat{w}\sin\theta\} \tag{7.39a}$$

$$\frac{d\hat{z}}{d\hat{t}} = \{-\hat{u}\sin\theta + \hat{w}\cos\theta\} \tag{7.39b}$$

$$\frac{d\hat{u}}{d\hat{t}} = -\mu\frac{\hat{q}\hat{w}}{\hat{m}} + \left\{\frac{\hat{F}_x}{\hat{m}} - \hat{g}\sin\theta\right\} \tag{7.39c}$$

$$\frac{d\hat{w}}{d\hat{t}} = \mu\frac{\hat{q}\hat{u}}{\hat{m}} + \left\{\frac{\hat{F}_z}{\hat{m}} + \hat{g}\cos\theta\right\} \tag{7.39d}$$

$$\epsilon\frac{d\hat{\theta}}{d\hat{t}} = \hat{q} \tag{7.39e}$$

$$\mu\frac{d\hat{q}}{d\hat{t}} = \frac{\hat{M}}{\hat{I}_y} \tag{7.39f}$$

Notice the above equations indicate that the rotational dynamics evolves faster than the translational counterpart. The above equations can be cast in the following compact form

$$\dot{\mathbf{x}} = \mathbf{f}(\mathbf{x}, \mathbf{s}, \mathbf{z}, \mathbf{u}, \epsilon, \mu) \tag{7.40a}$$

$$\epsilon\dot{\mathbf{s}} = \mathbf{h}(\mathbf{x}, \mathbf{s}, \mathbf{z}, \mathbf{u}, \epsilon, \mu) \tag{7.40b}$$

$$\mu\dot{\mathbf{z}} = \mathbf{g}(\mathbf{x}, \mathbf{s}, \mathbf{z}, \mathbf{u}, \epsilon, \mu). \tag{7.40c}$$

where $\mathbf{x} = [x, z, u, w]^T$ are the slow variables, $\mathbf{s} = [\theta]^T$ is the intermediate variable, $\mathbf{z} = [q]^T$ is the fast variable and $\mathbf{u} = [T_M, a_{1s}]^T$ is the control input to the system. The singular perturbation parameters ϵ and μ characterize the different time scales in the system and satisfy $0 < \mu < \epsilon << 1$.

7.3.3 Control Formulation and Stability Analysis

The control development follows the procedure detailed in Section 6. The inherent time scale behaviour is exploited and manifold for the pitch-attitude angle θ_d and rotor thrust T_M are determined first to ensure asymptotic position tracking. The

next step computes the desired pitch-rate manifold q_d to ensure the pitch-attitude angle follows θ_d. The final step determines the angle a_{1s} required to maintain desired pitch rate q_d. This procedure allows computation of an unique reference for the internal states and stability follows from Theorem 6.1. Recall, proof for results given in Theorem 6.1 start with a singularly perturbed model and show stability for a range of singular perturbation parameter bounds. These results can also be concluded through use of Lyapunov's direct method for the helicopter model given in (7.24) which is not in singularly perturbed form. This alternate method is analyzed in this section. It will be shown that following this alternate procedure also requires some form of "interconnection" conditions to be satisfied.

7.3.3.1 Control Synthesis

Using the procedure described in Section 7.3.2, the reduced slow system for (7.24) is obtained as

$$\begin{bmatrix} \dot{x} \\ \dot{z} \end{bmatrix} = \begin{bmatrix} \cos\theta_d & \sin\theta_d \\ -\sin\theta_d & \cos\theta_d \end{bmatrix} \begin{bmatrix} u \\ w \end{bmatrix} \tag{7.41a}$$

$$\begin{bmatrix} m\dot{u} \\ m\dot{w} \end{bmatrix} = \begin{bmatrix} -q_d w + F_x \\ q_d u + F_z \end{bmatrix} + \begin{bmatrix} \cos\theta_d & -\sin\theta_d \\ \sin\theta_d & \cos\theta_d \end{bmatrix} \begin{bmatrix} 0 \\ mg \end{bmatrix} \tag{7.41b}$$

where θ_d and q_d are manifolds to be determined. Take additional derivatives of the position coordinates to rewrite (7.41) as

$$\begin{bmatrix} \ddot{x} \\ \ddot{z} \end{bmatrix} = \frac{1}{m} \begin{bmatrix} \cos\theta_d & \sin\theta_d \\ -\sin\theta_d & \cos\theta_d \end{bmatrix} \begin{bmatrix} F_x \\ F_z \end{bmatrix} + \begin{bmatrix} 0 \\ g \end{bmatrix}. \tag{7.42}$$

Equation (7.42) shows that the pitch-attitude angle along with the control variables effect the position dynamics. Thus, employ the pitch-attitude angle and the main

rotor thrust T_M to accomplish the control objective. Toward this end, rewrite (7.42) as

$$m\ddot{x} = -T_M \sin(a_{1s}(\theta_d, q_d) + \theta_d) \tag{7.43a}$$

$$m\ddot{z} = -T_M \cos(a_{1s}(\theta_d, q_d) + \theta_d) + mg. \tag{7.43b}$$

Note in forming the reduced slow system the fast variables have been assumed to be on the desired manifolds (θ_d, q_d). Hence, the longitudinal tilt used in the design of slow control variables is a function of these desired manifolds. Further, define the tracking errors $\tilde{x} := x - x_r$ and $\tilde{z} := z - z_r$. Let the desired dynamics be specified as

$$m\ddot{x} = m(\ddot{x}_r - \alpha\dot{\tilde{x}} - \beta\tilde{x}) \tag{7.44a}$$

$$m\ddot{z} = m(\ddot{z}_r - \alpha_1\dot{\tilde{z}} - \beta_1\tilde{z}). \tag{7.44b}$$

Combining (7.43) and (7.44), the following relations are obtained

$$T_M = m\sqrt{(\ddot{x}_r - \alpha\dot{\tilde{x}} - \beta\tilde{x})^2 + (\ddot{z}_r - \alpha_1\dot{\tilde{z}} - \beta_1\tilde{z} - g)^2} \tag{7.45}$$

$$\theta_d = \arctan\frac{(\ddot{x}_r - \alpha\dot{\tilde{x}} - \beta\tilde{x})}{(\ddot{z}_r - \alpha_1\dot{\tilde{z}} - \beta_1\tilde{z} - g)} - a_{1s}(\theta_d, q_d). \tag{7.46}$$

Remark 7.3.1. The choice of using main rotor thrust, T_M over the longitudinal tilt for stabilization of the reduced slow system was made considering their actuation time constants. It is well understood that thrust generation takes longer than rotation of an actuator surface or in this case the rotor blade.

Equations (7.45) and (7.46) complete the design for the slow variables of the system. Notice however that the manifold q_d is unknown at this point. Toward this end, formulate the intermediate subsystem as *reduced intermediate system:*

$$\breve{\mathbf{x}} = 0 \tag{7.47a}$$

$$\breve{\theta} = q_d \tag{7.47b}$$

$$M = 0 \tag{7.47c}$$

where $\breve{}$ is derivative with respect to $\frac{t-t_0}{\epsilon_1}$. The manifold q_d must be designed to ensure the pitch-attitude follows θ_d. This can be satisfied by the following relation obtained using dynamic inversion

$$q_d = -K_\theta(\theta - \theta_d) \tag{7.48}$$

where K_θ is the feedback gain.

The desired manifolds given in (7.46) and (7.48) depend on the longitudinal tilt a_{1s} which is unknown. From the discussion detailed in Section 7.3.2, it is known (7.48) is a fixed point of the

reduced fast system:

$$\mathbf{x}' = 0 \tag{7.49a}$$

$$\theta' = 0 \tag{7.49b}$$

$$q' = \frac{M}{I_y} \tag{7.49c}$$

Thus, it is required that the following relation holds for all time

$$M = -I_y K_q(q - q_d) \tag{7.50}$$

where K_q is the feedback gain. Rearrange (7.50) using the definitions in (7.25c),

(7.46) and(7.48) to get

$$T_M h_M \sin(a_{1s}) - T_M l_M \cos(a_{1s}) + M_a a_{1s} = Q_T - I_y K_q (q - q_d) \tag{7.51}$$

The nonlinear equation in (7.51) is solved for the control a_{1s} using the small-angle assumption

$$a_{1s} = \left[\frac{Q_T + T_M l_M}{T_M h_M + M_a}\right] - \left[\frac{I_y K_q}{T_M h_M + M_a}\right] \tilde{q} \tag{7.52}$$

where $\tilde{q} := q - q_d$. Note (7.51) can also be solved using the non-affine techniques proposed in Section 3. For completeness substitute (7.52) back in (7.46) and (7.48) to compute the desired internal states

$$\theta_d = \arctan \frac{(\ddot{x}_r - \alpha\dot{\tilde{x}} - \beta\tilde{x})}{(\ddot{z}_r - \alpha\dot{\tilde{z}} - \beta_1\tilde{z} - g)} - \left[\frac{Q_T + T_M l_M}{T_M h_M + M_a}\right] \tag{7.53a}$$

$$q_d = -K_\theta\theta + K_\theta \arctan \frac{(\ddot{x}_r - \alpha\dot{\tilde{x}} - \beta\tilde{x})}{(\ddot{z}_r - \alpha\dot{\tilde{z}} - \beta_1\tilde{z} - g)} - K_\theta \left[\frac{Q_T + T_M l_M}{T_M h_M + M_a}\right] \tag{7.53b}$$

This completes the control design procedure. The above control synthesis procedure is summarized in a block diagram shown in Figure 7.19.

7.3.3.2 Stability Analysis

The following theorem summarizes the main result of this section.

Theorem 7.1. *Suppose the controls T_M and a_{1s} of the system (7.24) are designed according to the feedback relations given in (7.45) and (7.52). Then for initial conditions in the operating region $|\tilde{\theta}| < 15deg$, $|a_{1s}| \leq 25deg$ and $0 < T_M \leq 69.48$ the control uniformly asymptotically stabilizes the non-minimum phase helicopter model (7.24) and equivalently drives the states $x(t) \to x_r(t)$ and $z(t) \to z_r(t)$ keeping all other states and control inputs bounded.*

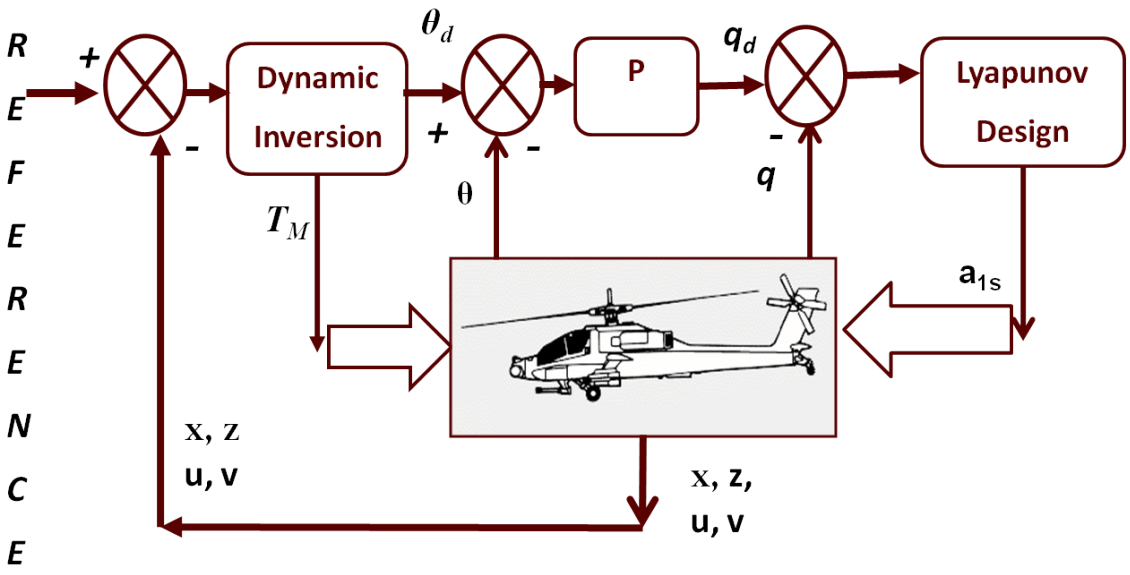

Figure 7.19: Control implementation for control of autonomous helicopter model

Proof. The closed-loop system system in error coordinates is given as

$$\dot{\tilde{x}} = \tilde{x}_1 \tag{7.54a}$$

$$\dot{\tilde{x}}_1 = \frac{1}{m}F_x \cos(\tilde{\theta} + \theta_d) + \frac{1}{m}F_z \sin(\tilde{\theta} + \theta_d) - \dot{x}_{1r} \tag{7.54b}$$

$$\dot{\tilde{z}} = \tilde{z}_1 \tag{7.54c}$$

$$\dot{\tilde{z}}_1 = -\frac{1}{m}F_x \sin(\tilde{\theta} + \theta_d) + \frac{1}{m}F_z \cos(\tilde{\theta} + \theta_d) + g - \dot{z}_{1r} \tag{7.54d}$$

$$\dot{\tilde{\theta}} = q_d + \tilde{q} - \dot{\theta}_d \tag{7.54e}$$

$$\dot{\tilde{q}} = \frac{M_d + (M - M_d)}{I_y} - \dot{q}_d \tag{7.54f}$$

where $\tilde{\theta} := \theta - \theta_d$, $\tilde{q} := q - q_d$ and

$$M_d = M_a a_{1s} + T_M h_M a_{1s} - T_M l_M - Q_T \tag{7.55}$$

is the moment obtained after making the small-angle approximation in arriving at

(7.52). The closed-loop system is equivalently written as

$$\dot{\tilde{x}} = \tilde{x}_1 \tag{7.56a}$$

$$\dot{\tilde{x}}_1 = \frac{1}{m}F_x \cos\theta_d + \frac{1}{m}F_z \sin\theta_d - \dot{x}_{1r} \tag{7.56b}$$
$$+ \frac{1}{m}F_x \Big[\cos(\tilde{\theta}+\theta_d) - \cos\theta_d\Big] + \frac{1}{m}F_z \Big[\sin(\tilde{\theta}+\theta_d) - \cos\theta_d\Big]$$

$$\dot{\tilde{z}} = \tilde{z}_1 \tag{7.56c}$$

$$\dot{\tilde{z}}_1 = -\frac{1}{m}F_x \sin\theta_d + \frac{1}{m}F_z \cos\theta_d + g - \dot{z}_{1r} \tag{7.56d}$$
$$- \frac{1}{m}F_x \Big[\sin(\tilde{\theta}+\theta_d) - \sin\theta_d\Big] + \frac{1}{m}F_z \Big[\cos(\tilde{\theta}+\theta_d) - \cos\theta_d\Big]$$

$$\dot{\tilde{\theta}} = q_d + \tilde{q} - \dot{\theta}_d \tag{7.56e}$$

$$\dot{\tilde{q}} = \frac{M_d + (M - M_d)}{I_y} - \dot{q}_d. \tag{7.56f}$$

Using the relations in (7.44), (7.48) and (7.50) rearrange (7.56) to get

$$\dot{\tilde{x}} = \tilde{x}_1 \tag{7.57a}$$

$$\dot{\tilde{x}}_1 = -\alpha\tilde{x}_1 - \beta\tilde{x} + \frac{1}{m}\cos\theta_d[F_x - F_x(a_{1s}(\theta_d, q_d))] + \frac{1}{m}\sin\theta_d[F_z - F_z(a_{1s}(\theta_d, q_d))]$$
$$+ \frac{1}{m}F_x \Big[\cos(\tilde{\theta}+\theta_d) - \cos\theta_d\Big] + \frac{1}{m}F_z \Big[\sin(\tilde{\theta}+\theta_d) - \cos\theta_d\Big] \tag{7.57b}$$

$$\dot{\tilde{z}} = \tilde{z}_1 \tag{7.57c}$$

$$\dot{\tilde{z}}_1 = -\alpha_1\tilde{z}_1 - \beta_1\tilde{z} - \frac{1}{m}\sin\theta_d[F_x - F_x(a_{1s}(\theta_d, q_d))] + \frac{1}{m}\cos\theta_d[F_z - F_z(a_{1s}(\theta_d, q_d))]$$
$$- \frac{1}{m}F_x \Big[\sin(\tilde{\theta}+\theta_d) - \sin\theta_d\Big] + \frac{1}{m}F_z \Big[\cos(\tilde{\theta}+\theta_d) - \cos\theta_d\Big] \tag{7.57d}$$

$$\dot{\tilde{\theta}} = -K_\theta\tilde{\theta} + \tilde{q} - \dot{\theta}_d \tag{7.57e}$$

$$\dot{\tilde{q}} = -K_q\tilde{q} + \frac{M - M_d}{I_y} - \dot{q}_d. \tag{7.57f}$$

Closed-loop system stability of the system states is analyzed using the Lyapunov

function approach. Consider a positive-definite and decrescent Lyapunov function candidate

$$V(\tilde{x}, \tilde{x}_1, \tilde{z}, \tilde{z}_1, \tilde{\theta}, \tilde{q}) = \frac{1}{2}\left[\beta\tilde{x}^2 + \tilde{x}_1^2 + \beta_1\tilde{z}^2 + \tilde{z}_1^2 + \tilde{\theta}^2 + \tilde{q}^2\right] \tag{7.58}$$

for the complete closed-loop system. The derivative of V along the trajectories of (7.57) is given by

$$\begin{aligned}
\dot{V} = &- \alpha\tilde{x}_1^2 + \frac{1}{m}\cos\theta_d[F_x - F_x(a_{1s}(\theta_d, q_d))]\tilde{x}_1 + \frac{1}{m}\sin\theta_d[F_z - F_z(a_{1s}(\theta_d, q_d))]\tilde{x}_1 \\
&+ \frac{1}{m}F_x\left[\cos(\tilde{\theta} + \theta_d) - \cos\theta_d\right]\tilde{x}_1 + \frac{1}{m}F_z\left[\sin(\tilde{\theta} + \theta_d) - \cos\theta_d\right]\tilde{x}_1 \\
&- \alpha_1\tilde{z}_1^2 - \frac{1}{m}\sin\theta_d[F_x - F_x(a_{1s}(\theta_d, q_d))]\tilde{z}_1 + \frac{1}{m}\cos\theta_d[F_z - F_z(a_{1s}(\theta_d, q_d))]\tilde{z}_1 \\
&- \frac{1}{m}F_x\left[\sin(\tilde{\theta} + \theta_d) - \sin\theta_d\right]\tilde{z}_1 + \frac{1}{m}F_z\left[\cos(\tilde{\theta} + \theta_d) - \cos\theta_d\right]\tilde{z}_1 \\
&- K_\theta\tilde{\theta}^2 + \tilde{\theta}\tilde{q} - \tilde{\theta}\dot{\theta}_d - K_q\tilde{q}^2 + \frac{M - M_d}{I_y}\tilde{q} - \tilde{q}\dot{q}_d.
\end{aligned} \tag{7.59}$$

Using the Lipschitz behaviour of the vector fields on the domain defined in Theorem 7.1 the following conditions hold

$$|\sin(\tilde{\theta} + \theta_d) - \sin\theta_d| \leq 0.35|\tilde{\theta}| \tag{7.60}$$

$$|F_x - F_x(a_{1s}(\theta_d, q_d))| \leq |T_M|\left|\frac{I_y K_q}{T_M h_M + M_a}\right||\tilde{q}| \tag{7.61}$$

$$|\cos(\tilde{\theta} + \theta_d) - \cos\theta_d| \approx 0 \tag{7.62}$$

$$|F_z - F_z(a_{1s}(\theta_d, q_d))| \approx 0. \tag{7.63}$$

Note conditions given in (7.62) and (7.63) give bounds on the magnitude of the error between the exact and approximate vertical force. This bound remains close to zero for large changes in $\tilde{\theta}$ and this condition was numerically verified for the model under

study in Section 7.3.1. Resulting derivative of the Lyapunov function given in (7.59) using conditions (7.60) through (7.63) becomes

$$\begin{aligned}\dot{V} \leq & -\alpha\tilde{x}_1^2 + \frac{1}{m}|T_M|\left|\frac{I_y K_q}{T_M h_M + M_a}\right||\tilde{x}_1||\tilde{q}| + 0.35\frac{1}{m}|T_M||\tilde{x}_1||\tilde{\theta}| \\ & -\alpha_1\tilde{z}_1^2 + 0.35|T_M|\left|\frac{I_y K_q}{T_M h_M + M_a}\right||\tilde{z}_1||\tilde{q}| \\ & + 0.35\frac{1}{m}|T_M||a_{1s}||\tilde{z}_1||\tilde{\theta}| - K_\theta\tilde{\theta}^2 + \tilde{\theta}\tilde{q} - \tilde{\theta}\dot{\theta}_d \\ & - K_q\tilde{q}^2 + \frac{M - M_d}{I_y}\tilde{q} - \tilde{q}\dot{q}_d.\end{aligned} \tag{7.64}$$

The time derivative of the manifolds θ_d and q_d is determined next. Toward this end, rearrange (7.46) as

$$\tan\gamma = \frac{X_{des}(t)}{Z_{des}(t)} \tag{7.65}$$

where $\gamma = \theta_d + a_{1s}(\theta_d, q_d)$, $X_{des} = \ddot{x}_r - \alpha\tilde{x}_1 - \beta\tilde{x}$ and $Z_{des} = \ddot{z}_r - \alpha_1\tilde{z}_1 - \beta\tilde{z} - g$ have been defined for convenience. Differentiate (7.65) to get

$$\dot{\gamma} = \frac{\cos\gamma}{T_M/m}\dot{X}_{des} - \frac{\sin\gamma}{T_M/m}\dot{Z}_{des} \tag{7.66}$$

using the fact $T_M/m = \sqrt{(X_{des}^2 + Z_{des}^2)}$ and definition of the angle γ. The time rate of change of the longitudinal tilt $a_{1s}(\theta_d, q_d)$ is determined by differentiating (7.52) along the inertial position trajectories.

$$\begin{aligned}\dot{a_{1s}} &= \frac{d}{dt}\left[\frac{T_M l_M + Q_T}{T_M h_M + M_a}\right] \\ &= \left[\frac{l_M M_a - h_M Q_T}{(T_M h_M + M_a)^2}\right]\dot{T}_M\end{aligned} \tag{7.67}$$

where $\dot{T}_M = m\sin\gamma\dot{X}_{des} + m\cos\gamma\dot{Z}_{des}$. Combine (7.66) and (7.67), to determine the

derivative of the manifolds

$$\dot{\theta}_d = m\left[\frac{\cos\gamma}{T_M} - a_T\sin\gamma\right]\dot{X}_{des} + m\left[\frac{-\sin\gamma}{T_M} - a_T\cos\gamma\right]\dot{Z}_{des} \tag{7.68}$$

$$\dot{q}_d = -K_\theta\dot{\tilde{\theta}} \tag{7.69}$$

where

$$a_T = \frac{L_M M_a - h_M Q_T}{(T_M h_M + M_a)^2} \tag{7.70}$$

and the various derivatives are a function of closed-loop system dynamics. Using properties (7.60) through (7.63) and (7.57)

$$\begin{aligned}|\dot{X}_{des}| \leq\ & \alpha\beta|\tilde{x}| + (\alpha^2-\beta)|\tilde{x}_1| \\ & + \frac{1}{m}|T_M|\left|\frac{\alpha I_y K_q}{T_M h_M + M_a}\right||\tilde{q}| + 0.35\frac{\alpha}{m}|T_M||\tilde{\theta}|\end{aligned} \tag{7.71a}$$

$$\begin{aligned}|\dot{Z}_{des}| \leq\ & \alpha_1\beta_1|\tilde{z}| + (\alpha_1^2-\beta_1)|\tilde{z}_1| \\ & + \frac{0.35}{m}|T_M|\left|\frac{\alpha_1 I_y K_q}{T_M h_M + M_a}\right||\tilde{q}| + 0.35\frac{\alpha_1}{m}|T_M||\tilde{\theta}|.\end{aligned} \tag{7.71b}$$

Combine (7.68), (7.71) and (7.64) to get

$$\begin{aligned}\dot{V} \leq & -\alpha\tilde{x}_1^2 + \frac{1}{m}|T_M|\left|\frac{I_y K_q}{T_M h_M + M_a}\right||\tilde{x}_1||\tilde{q}| + 0.35\frac{1}{m}|T_M||\tilde{x}_1||\tilde{\theta}| \\ & -\alpha_1\tilde{z}_1^2 + 0.35|T_M|\left|\frac{I_y K_q}{T_M h_M + M_a}\right||\tilde{z}_1||\tilde{q}| + 0.35\frac{1}{m}|T_M||a_{1s}||\tilde{z}_1||\tilde{\theta}| \\ & -K_\theta\tilde{\theta}^2 + |\tilde{\theta}||\tilde{q}| + (|\tilde{\theta}| + K_\theta|\tilde{q}|)|\dot{\theta}_d| - K_q\tilde{q}^2 + (K_\theta - K_\theta^2)|\tilde{\theta}||\tilde{q}|.\end{aligned} \tag{7.72}$$

By definition a_T is a small quantity and $|cos\gamma| = |\sin\gamma| \leq 1$, define $\kappa = \frac{m}{|T_M|}$ which is again a small quantity. Substitute for time rate of change of the manifold θ_d into

(7.72) to get

$$\begin{aligned}\dot{V} \leq & -\alpha\tilde{x}_1^2 + \frac{1}{m}|T_M|\left|\frac{I_y K_q}{T_M h_M + M_a}\right||\tilde{x}_1||\tilde{q}| + 0.35\frac{1}{m}|T_M||\tilde{x}_1||\tilde{\theta}| \\ & -\alpha_1\tilde{z}_1^2 + 0.35|T_M|\left|\frac{I_y K_q}{T_M h_M + M_a}\right||\tilde{z}_1||\tilde{q}| + 0.35\frac{1}{m}|T_M||a_{1s}||\tilde{z}_1||\tilde{\theta}| \\ & -K_\theta\tilde{\theta}^2 + |\tilde{\theta}||\tilde{q}| - K_q\tilde{q}^2 + (K_\theta - K_\theta^2)|\tilde{\theta}||\tilde{q}| \\ & +\kappa(|\tilde{\theta}| + K_\theta|\tilde{q}|)\Bigg[\alpha\beta|\tilde{x}| + (\alpha^2 - \beta)|\tilde{x}_1| + \alpha_1\beta_1|\tilde{z}| + (\alpha_1^2 - \beta_1)|\tilde{z}_1| \\ & -\frac{1}{m}|T_M|\left|\frac{I_y K_q}{T_M h_M + M_a}\right|(\alpha + 0.35\alpha_1)|\tilde{q}| - 0.35(\alpha + \alpha_1)\frac{1}{m}|T_M||\tilde{\theta}|\Bigg]\end{aligned} \tag{7.73}$$

Rearrange (7.73) to get

$$\dot{V} \leq -\Psi^T \mathbb{K} \Psi \tag{7.74}$$

where $\Psi = [\tilde{x}, \tilde{x}_1, \tilde{z}, \tilde{z}_1, \tilde{\theta}, \tilde{q}]^T$ and matrix $\mathbb{K}$ is given below

$$\mathbb{K} = \begin{bmatrix} 0 & 0 & 0 & 0 & \mu_1 & \mu_2 \\ 0 & -\alpha & 0 & 0 & \mu_3 & \mu_4 \\ 0 & 0 & 0 & 0 & \mu_5 & \mu_6 \\ 0 & 0 & 0 & -\alpha_1 & \mu_7 & \mu_8 \\ \mu_1 & \mu_3 & \mu_5 & \mu_7 & \alpha_\theta & \mu_9 \\ \mu_2 & \mu_4 & \mu_6 & \mu_8 & \mu_9 & \alpha_q \end{bmatrix} \tag{7.75}$$

where

$$\alpha_\theta = -K_\theta - 0.35(\alpha + \alpha_1)\frac{|T_M|}{m} \tag{7.76a}$$

$$\alpha_q = -K_q - \tfrac{|T_M|}{m}\kappa K_\theta(\alpha + 0.35\alpha_1)\left|\tfrac{I_y K_q}{T_M h_M + M_a}\right| \tag{7.76b}$$

and

$$\mu_1 = \frac{\kappa\alpha\beta}{2} \tag{7.77a}$$

$$\mu_2 = K_\theta \mu_1 \tag{7.77b}$$

$$\mu_3 = \tfrac{0.35|T_M|}{2m} + 0.5\kappa(\alpha^2 - \beta) \tag{7.77c}$$

$$\mu_4 = \tfrac{1}{2m}|T_M| \left|\tfrac{I_y K_q}{T_M h_M + M_a}\right| + 0.5\kappa K_\theta(\alpha^2 - \beta) \tag{7.77d}$$

$$\mu_5 = \frac{\kappa\alpha_1\beta_1}{2} \tag{7.77e}$$

$$\mu_6 = K_\theta \mu_5 \tag{7.77f}$$

$$\mu_7 = \tfrac{0.1527|T_M|}{2m} + 0.5\kappa(\alpha_1^2 - \beta_1) \tag{7.77g}$$

$$\mu_8 = \tfrac{0.35}{2m}|T_M| \left|\tfrac{I_y K_q}{T_M h_M + M_a}\right| + 0.5\kappa K_\theta(\alpha_1^2 - \beta_1) \tag{7.77h}$$

$$\begin{aligned}\mu_9 = {} & 0.5(K_\theta - K_\theta^2 + 1) - \kappa\frac{|T_M|}{2m}\left|\frac{I_y K_q}{T_M h_M + M_a}\right|(\alpha + 0.35\alpha_1) \\ & - 0.35\kappa K_\theta(\alpha + \alpha_1)\frac{1}{2m}|T_M|\end{aligned} \tag{7.77i}$$

are constants, function of the feedback gains. Hence, the matrix $\mathbb{K}$ is negative semi-definite by appropriate choice of the feedback gains. Note the semi-definiteness property is due to the small values of constants μ_1, μ_2, μ_5 and μ_6. Since $\dot{V} \leq 0$ and $V > 0$, all terms in $V \in \mathcal{L}_\infty$ that is $\{\tilde{x}, \tilde{x}_1, \tilde{z}, \tilde{z}_1, \tilde{\theta}, \tilde{q}\} in \mathcal{L}_\infty$. Furthermore, since the reference trajectory states are bounded, all terms in expressions for T_M and a_{1s} in (7.45) and (7.52) respectively are bounded. Hence the right hand side of the closed-loop system in (7.57) is bounded and thus $\dot{\Psi} \in \mathcal{L}_\infty$. Thus using Barbalat's lemma it is concluded that signals of vector $\Psi \to 0$ as $t \to \infty$ and the result in Theorem 1.4 follows. This completes the stability analysis. □

Remark 7.3.2. Conditions (7.60) through (7.63) and (7.71) are Lipschitz conditions on the terms that were neglected in the reduced-order model construction. Similar

conditions are also required in proof of Theorem 6.1.

7.3.4 Results and Discussion

The purpose of this section is to illustrate the preceding theoretical developments and demonstrate the controller performance for an autonomous helicopter model. The reference trajectory and all its derivatives are set to zero to illustrate the stabilizing performance of the controller for the open-loop non-minimum phase system (discussed in Section 7.3.1.2). The feedback gains were chosen to preserve the time scale nature of the helicopter model $\alpha = \alpha_1 = 2$,$\beta = \beta_1 = 1$, $K_\theta = 3$ and $K_q = 10$. The various constants for matrix $\mathbb{K}$ are $\mu_1 = \mu_5 = 0.082$, $\mu_2 = \mu_6 = 0.245$, $\mu_3 = 2.26$, $\mu_4 = 0.755$, $\mu_7 = 1.06$, $\mu_8 = 0.5$ and $\mu_9 = -4.68$. The corresponding eigenvalues of the matrix $\mathbb{K}$ are $\lambda_{1,2} = 0.00$, $\lambda_3 = -1.65$, $\lambda_4 = -1.99$, $\lambda_5 = -8.62$ and $\lambda_6 = -22.39$ and Theorem 7.1 guarantees asymptotic stability. The initial conditions chosen were $x(0) = -2m$, $z(0) = 2m$, $u(0) = w(0) = 0m/sec$, $\theta(0) = 15deg$ and $q(0) = 30deg/sec$.

Figure 7.20 through Figure 7.25 present the closed-loop response of the helicopter. The controller demonstrated asymptotic tracking irrespective of the desired reference trajectory in the domain $(x, z, u, w, \theta, q) \in [-50, 50]m \times [-15, 50]m \times [-30, 20]m/sec \times [-5, 20]m/sec \times (-\pi/2, \pi/2)rad \times [-\pi, \pi]rad/sec$. Notice that the large initial condition errors die out within the first 6seconds. The forward velocity is increased in order to correct the error in forward position. Close output tracking is a result of precision desired manifold following by the internal states. The pitch-attitude angle settles down to the trim value of $0.018rad(1.03deg)$ that is automatically computed by the manifold (7.53a).

The time scale behaviour of the system states is apparent in the time histories. Notice that the pitch-rate starts to follow the desired manifold within 2seconds

followed by the response of the pitch-attitude angle closely tracking the desired manifold within 4seconds. The transient errors of the slowest and also the outputs of the problem under study die out in 6seconds.

The control inputs are shown in Figure 7.24 and Figure 7.25. The control inputs settle down to the trim values $T_M = 48.02N$ and $a_{1s} = -0.018rad(-1.03deg)$ once the system errors have stabilized about the origin. The two-dimensional trajectory of the helicopter is shown in Figure 7.26. Initially the helicopter corrects the large error in the pitch-attitude angle. This is done by reducing the requirements on pitch-rate and in turn the longitudinal tilt. After this correction, the vehicle starts climbing to the desired hover position. From then on, the helicopter remains in hover.

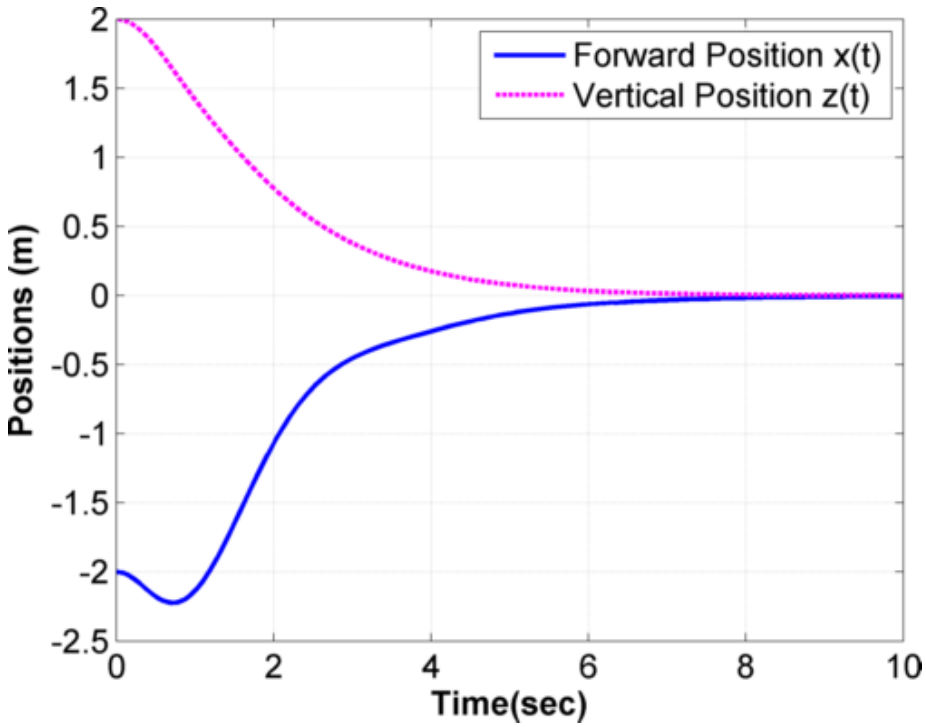

Figure 7.20: Closed-loop output response of the helicopter: position histories

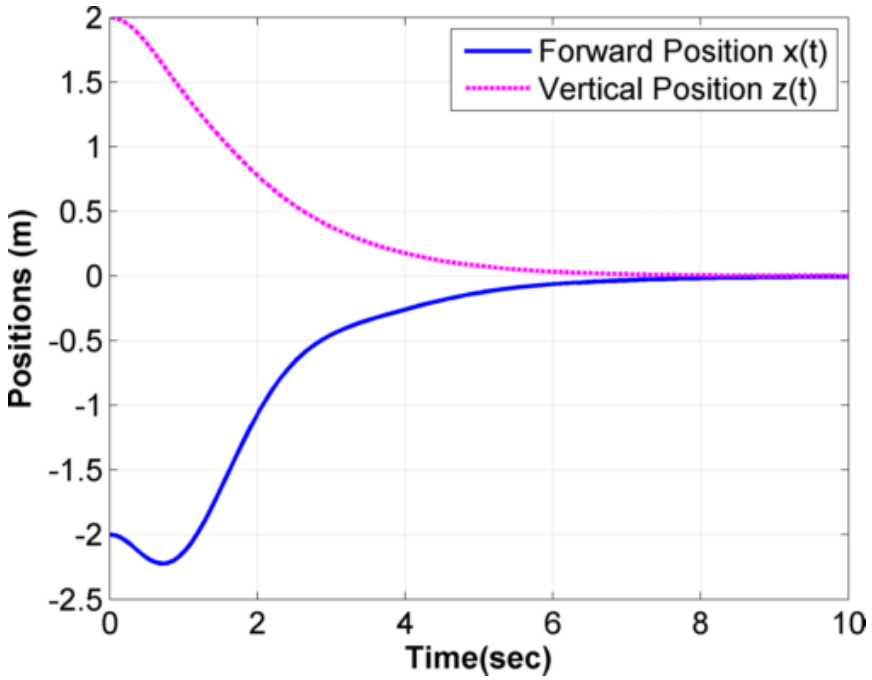

Figure 7.21: Closed-loop output response of the helicopter: velocity histories

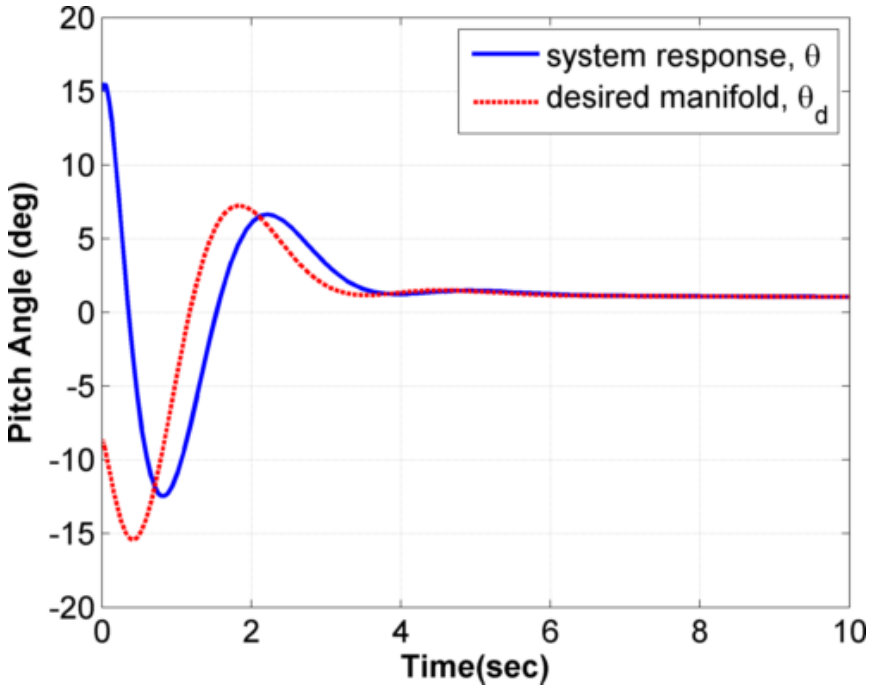

Figure 7.22: Closed-loop pitch-attitude dynamics of the helicopter

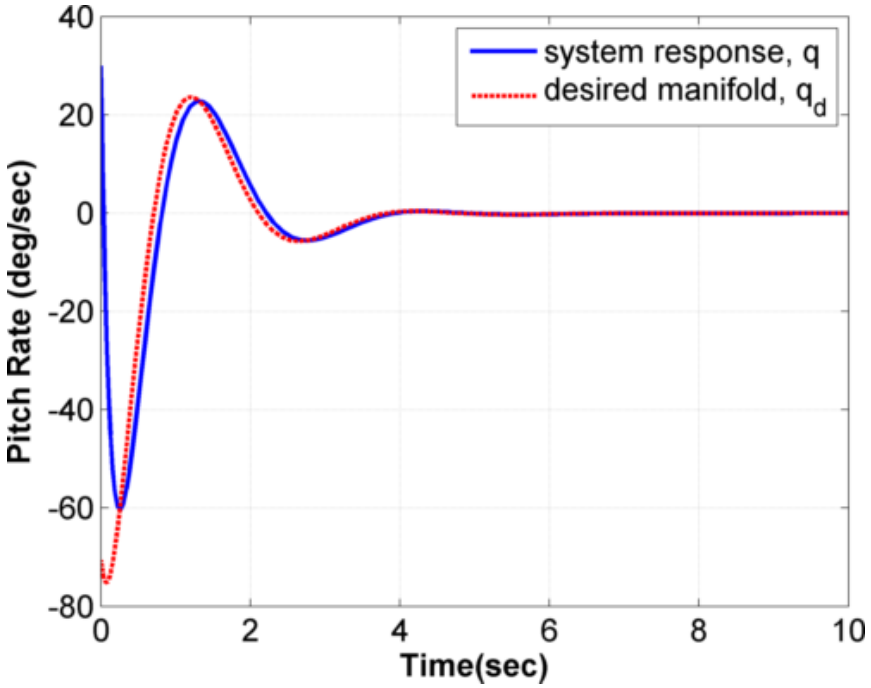

Figure 7.23: Closed-loop pitch rate dynamics of the helicopter

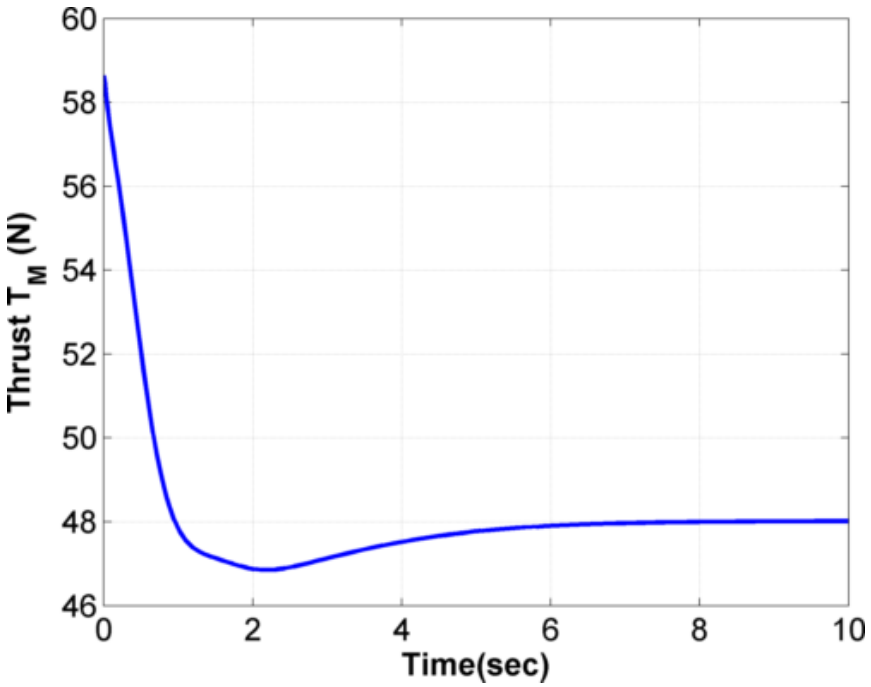

Figure 7.24: Main rotor thrust for hover control of helicopter

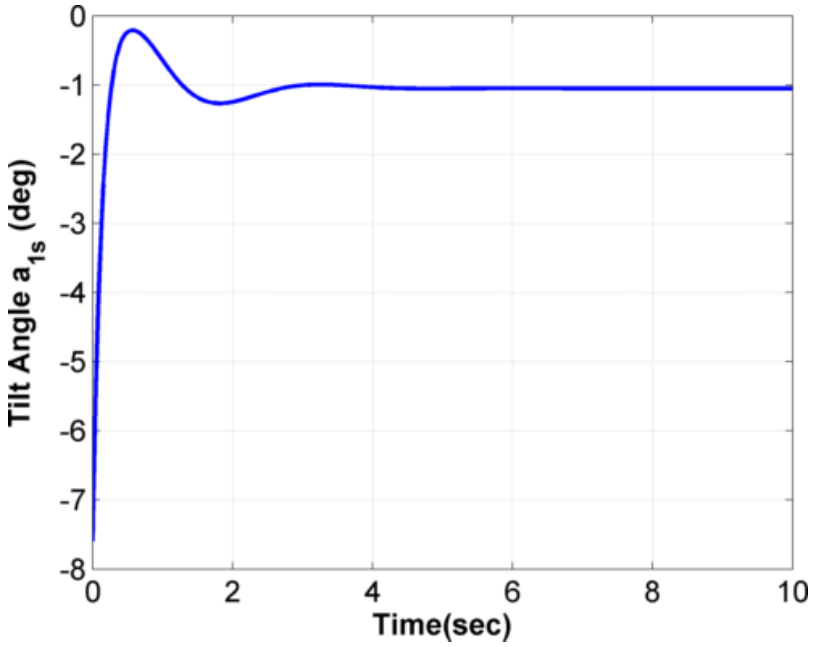

Figure 7.25: Longitudinal tilt for hover control of helicopter

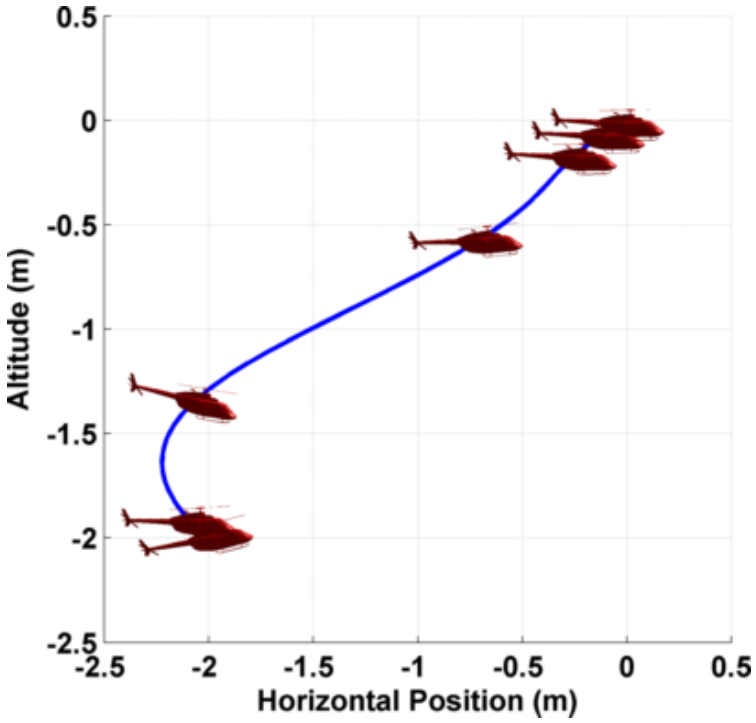

Figure 7.26: Closed-loop trajectory of the helicopter

7.3.5 Summary

A control formulation for output tracking of an autonomous nonlinear non-minimum phase helicopter was developed. The desired internal-state reference and feedback control to stabilize the unstable internal dynamics were computed using the inherent time scales of the system. Controller performance was demonstrated through numerical simulation for the helicopter in hover.

Based on the results presented, the following conclusions are drawn. The final output tracking error for the positions remained within $|0.0010|$. This perfect output tracking was a result of perfect internal state tracking that was achieved by the nonlinear feedback law. The results of Theorem 7.1 are restricted in operating regime due to the small angle approximation made in (7.52). Unlike previous approaches this limitation is not due to simplifications made to the dynamical model and can be improved by use of non-affine control methods. In fact the conclusions regarding operating region of the controller from Theorem 7.1 are conservative. As shown in the simulation section, the controller demonstrates stable performance for a large operating region. Additionally, the controller is causal and does not require any prior information or preview of the desired reference.

7.4 Nap-of-the-Earth Maneuver Control for Conventional Take-off and Landing Aircraft

The final example under study is the non-minimum phase dynamical model of a three degrees-of-freedom conventional aircraft shown in Figure 7.27. The axes along the body of the aircraft is represented as $(\hat{x}_b, \hat{z}_b)$. The inertial and the stability axes are shown by $(\hat{i}, \hat{k})$ and $(\hat{x}_s, \hat{z}_s)$ respectively. The goal is to track forward and vertical inertial velocity commands that correspond to nap-of-the-earth (NOE) maneuver using the control variables, thrust u_1 and pitching moment u_2. NOE is a low altitude

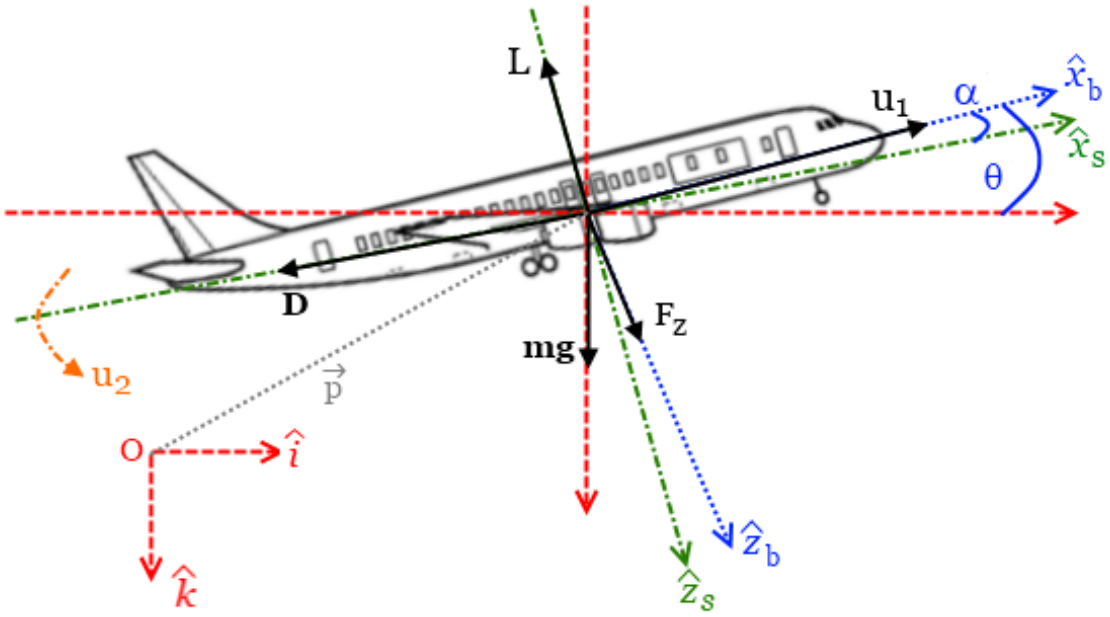

Figure 7.27: Reference frames and forces acting on the aircraft

maneuver usually flown to avoid detection. The aircraft follows the terrain closely at high airspeeds and low angle-of-attack throughout the maneuver. In this section, control laws to autonomously fly the NOE maneuver are developed.

Output tracking control for conventional take-off and landing (CTOL) aircraft is a well known non-minimum phase problem. The non-minimum phase characteristics of the dynamical model under study are due to the downward force induced by the pitching moment. Consider Figure 7.27 to qualitatively analyze this phenomenon. Note thrust u_1 opposes the aerodynamic drag D and causes forward motion of the aircraft. The vertical motion of the aircraft is due to the aerodynamic lift L induced at non-zero angle-of-attack, α. Hence, the thrust u_1 along with the pitching moment u_2 are required to accomplish the desired velocity responses. However, the pitch-up moment u_2 required to change angle-of-attack induces a downward force F_z that tends to reduce the altitude of the vehicle. This means that small corrections to the

pitching moment are required to maintain desired aerodynamic lift. But changing the pitching moment to bring about desired translational motion leaves the rotational dynamics uncontrolled. Most often in CTOL aircraft (also verified for the model under study) thrust and pitching moment desired for translational motion excites the unstable oscillatory behaviour of the rotational dynamics.

Previous studies for control of CTOL aircraft neglect the downward force being induced and modify the output to obtain approximate input-output linearization. The technique presented in [96] modified the output to remove right half-plane zeros. A similar technique was employed in [97] to track pilot g commands while satisfying flying quality specifications. These approaches were able to guarantee 'local' tracking that is specific to the desired flight condition and reference trajectory. Another approximate approach proposed in [98] took a sufficient number of derivatives of the output such that the control and its higher-order derivatives appear in the equation. The paper proposed to modify the sign of some of the control derivatives in order to render the modified output dynamics minimum phase. In contrast to the former, Shklnikov and Shtessel [99] modified the sliding surface to ensure that the right half-plane zeros are canceled out. The system was required to be in normal form with bounded nonlinearities and the technique was demonstrated for an F-16 aircraft[100]. Considering the local nature of these works [101] proposed a controller which separates the internal dynamics into linear and nonlinear parts. The linear part was stabilized by linear state feedback, whereas the nonlinear part was stabilized only when the system strayed away from the trajectory. In an effort to control the V/STOL slightly non-minimum phase aircraft, [84] neglected terms that are the cause of this unstable behaviour and proved that a stable controller can be designed using the approximate model.

Another class of the literature takes advantage of the multiple time scale be-

haviour of air vehicles. Lee and Ha [102] designed an autopilot for a Skid-To-Turn (STT) missile by splitting the dynamics into slow and fast components. The slow subsystem was composed of the zero dynamics and was indirectly controlled by the controllable fast subsystem. A similar approach was proposed by Lee and Ha[103] wherein the normal form of a nonlinear I/O feedback linearizable system was transformed to a two time scale system by a change of coordinates. But in this case the fast subsystem constituted the zero dynamics and a modified composite control scheme was employed to stabilize the complete system.

In addition to the approximate schemes described above, low gain feedback approaches have been proposed in the literature for nonlinear systems with the upper triangular form [104], [105], [106]. The exact output tracking approach proposed in [107], [108] employed a combination of feed-forward and feedback control. The feed-forward control was found using inversion, given a desired output trajectory and its higher-order derivatives. The stable inversion was non-causal and required the infinite time preview of the complete output trajectory.

It is well-understood from literature and previous examples that internal-state feedback is necessary to stabilize a non-minimum phase system. Moreover, exact output tracking is achieved only when the desired internal state trajectory is tracked. Motivated by this fact, this section develops an exact output tracking control technique for non-minimum aircraft system using control developed in Section 6. This section makes three major contributions. First, the output dynamics are not required to have a well-defined relative degree with respect to the input. The idea is to take a sufficient number of derivatives of the output and cast the system in a singularly perturbed form. This procedure forces the internal states of the system to behave as the fast variables. It also allows the internal states to be used as 'pseudo-control variables' for output tracking. A sequential procedure is devel-

oped to compute the internal states that ensure asymptotic output tracking and the controller is designed to force the internal states to follow the computed trajectory. Second, full-state feedback controller designed is independent of any particular operating condition and desired output trajectory. Third, for the first time the controller explicitly considers the slow thrust response during design of the control and show asymptotic output tracking. Previous studies assume that all controllers respond sufficiently fast. However, it will be shown that these designs when implemented to slow throttle systems perform poorly.

7.4.1 Dynamical Model and Open-Loop Analysis

In this section governing equations are derived for the aircraft model and the exact input-output linearization of the model is carried out. It is shown that system has unstable internal dynamics.

7.4.1.1 Vehicle Description

The aircraft model is written with respect to earth-fixed inertial coordinates. The forces and moment act in the body $(\hat{x}_b, \hat{z}_b)$ and stability axes $(\hat{x}_s, \hat{z}_s)$. The aircraft model has three degrees-of-freedom: horizontal and vertical position (x, z), and pitch attitude angle θ. The two available controls are thrust u_1 and pitching moment u_2. Using this notation, the position, velocity and acceleration vector in the inertial frame measured from origin O are

$$\vec{p} = x\hat{i} - z\hat{k} \tag{7.78a}$$

$$\vec{v} = \dot{x}\hat{i} - \dot{z}\hat{k} \tag{7.78b}$$

$$\vec{a} = \ddot{x}\hat{i} - \ddot{z}\hat{k} \tag{7.78c}$$

where negative sign is consistent with positive altitude. Similarly the angular acceleration about the body $\hat{y}_b$ axis is

$$\vec{\alpha} = \ddot{\theta}\hat{y}_b \tag{7.79}$$

The equations of motion are derived using Newton's and Euler's second law of motion. Toward this end, the force and moment vector acting on the body are collected as

$$\vec{F} = mg\hat{k} + u_1\hat{x}_b - D\hat{x}_s + F_z\hat{z}_b - L\hat{z}_s \tag{7.80a}$$

$$\vec{M} = u_2\hat{y}_b \tag{7.80b}$$

The orthogonal transformations

$$R_{sb} = \begin{bmatrix} \cos\alpha & -\sin\alpha \\ \sin\alpha & \cos\alpha \end{bmatrix} \tag{7.81a}$$

$$R_{ib} = \begin{bmatrix} \cos\theta & -\sin\theta \\ \sin\theta & \cos\theta \end{bmatrix} \tag{7.81b}$$

denote the rotation matrices between stability to body and inertial to body frames respectively. Using the relations given in (7.81) the resultant forces in the inertial axes are

$$\begin{aligned} \vec{F} = &\left[u_1\cos\theta - D\cos(\theta-\alpha) - L\sin(\theta-\alpha) + F_z\sin\theta\right]\hat{i} \\ &+ \left[-u_1\sin\theta + F_z\cos\theta + D\sin(\theta-\alpha) - L\cos(\theta-\alpha) + mg\right]\hat{k}. \end{aligned} \tag{7.82}$$

Hence, using the kinematic relations given in (7.78), (7.79) and the above relations the following equations of motion are obtained:

$$m\ddot{x} = u_1 \cos\theta - D\cos(\theta - \alpha) - L\sin(\theta - \alpha) + F_z \sin\theta \tag{7.83a}$$

$$m\ddot{z} = u_1 \sin\theta - F_z \cos\theta - D\sin(\theta - \alpha) + L\cos(\theta - \alpha) - mg \tag{7.83b}$$

$$I_y\ddot{\theta} = u_2 \tag{7.83c}$$

where $F_z = \varepsilon u_2$ and I_y is moment of inertia of the aircraft about the $\hat{y}_b$ axis. The aerodynamic forces are $L = a_L(u^2 + w^2)(1 + c\alpha)$, $D = a_D(u^2 + w^2)(1 + b(1 + c\alpha)^2)$ and other physical constants for the Douglas DC-8 are given in Table 7.3 [109].

Table 7.3: Aircraft model parameters

Parameter	Value
m	$85000kg$
I_y	$4 \times 10^6 kgm^2$
g	$9.81ms^{-2}$
a_L	$\frac{30m}{g}$
a_D	$\frac{2m}{g}$
b	0.01
c	6
ε	$0.3mg/I_y$

7.4.1.2 Exact Input-Output Linearization

The non-minimum phase properties of the aircraft are analyzed by studying the input-output relationship. The desired outputs for the control design are the velocities $(\dot{x}, -\dot{z})$ of the aircraft. From the equations of motion given in (7.83) it is found that the relative degree is one and the rotational dynamics constitute the internal dynamics. The stability of the internal dynamics is analyzed by studying the zero

dynamics of the aircraft. Toward this end, the control vector (u_1, u_2) that constraint the output and its derivative to zero are determined as

$$u_1 = -mg\frac{\sin\theta}{\cos 2\theta} \tag{7.84a}$$

$$u_2 = -\frac{mg}{\varepsilon}\frac{\cos\theta}{\cos 2\theta}. \tag{7.84b}$$

Using the above constrained control solution the rotational dynamics becomes

$$I_y\ddot{\theta} = -\frac{mg}{\varepsilon}\frac{\cos\theta}{\cos 2\theta}. \tag{7.85}$$

The equilibrium solutions of (7.85) are $\theta_* = \pm\pi/2$. About these trim solutions the gradient of function $h(\theta) = \frac{\cos\theta}{\cos 2\theta}$ is

$$\frac{\partial h}{\partial\theta} = \frac{-\sin\theta}{\cos 2\theta} + \frac{2\cos\theta\tan 2\theta}{cos2\theta} \tag{7.86}$$

which upon substitution yields $\frac{\partial h}{\partial\theta}|_{\theta_*=\pi/2} = 3.33$ and $\frac{\partial h}{\partial\theta}|_{\theta_*=-\pi/2} = -3.33$. This gives the following linear models

$$\Delta\ddot{\theta} = -3.33\Delta\theta \text{ about } \theta_* = \pi/2 \tag{7.87a}$$

$$\Delta\ddot{\theta} = 3.33\Delta\theta \text{ about } \theta_* = -\pi/2. \tag{7.87b}$$

From the eigenvalues of (7.87) it is concluded that $\theta_* = \pi/2$ is a center and $\theta_* = -\pi/2$ is a saddle point. This conclusion was verified in simulation and Figure 7.28 and Figure 7.29 present the results. The phase portrait shows that a continuum of closed orbits exist about $\theta_* = \pi/2$. The outer curves marks the boundary of these orbits and any further perturbation is unstable. Clearly response about either of the trim solutions is undesirable and exact input-output linearization is not possible.

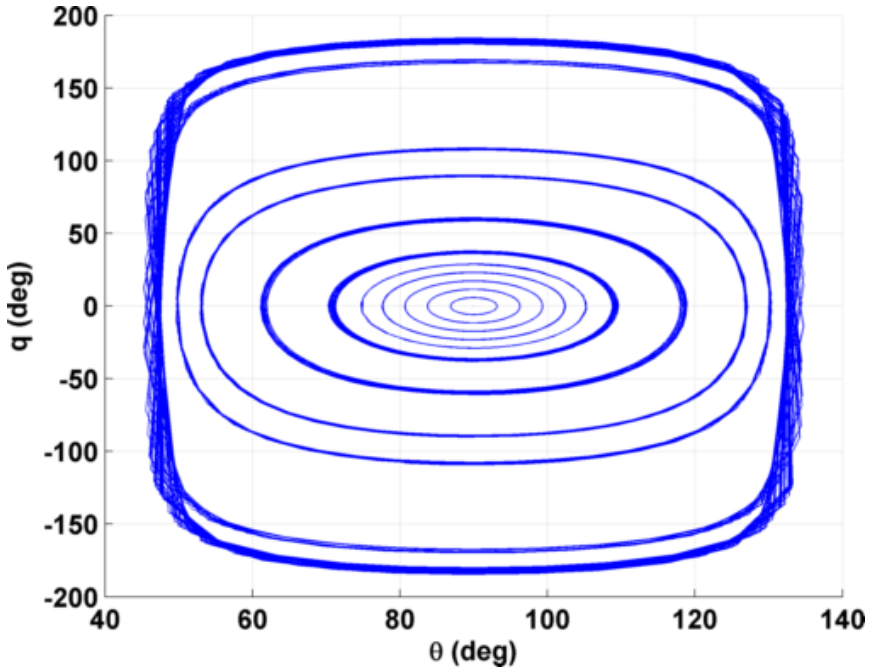

Figure 7.28: Phase portrait illustrating the oscillatory response of pitching motion of the aircraft model given in (7.83)

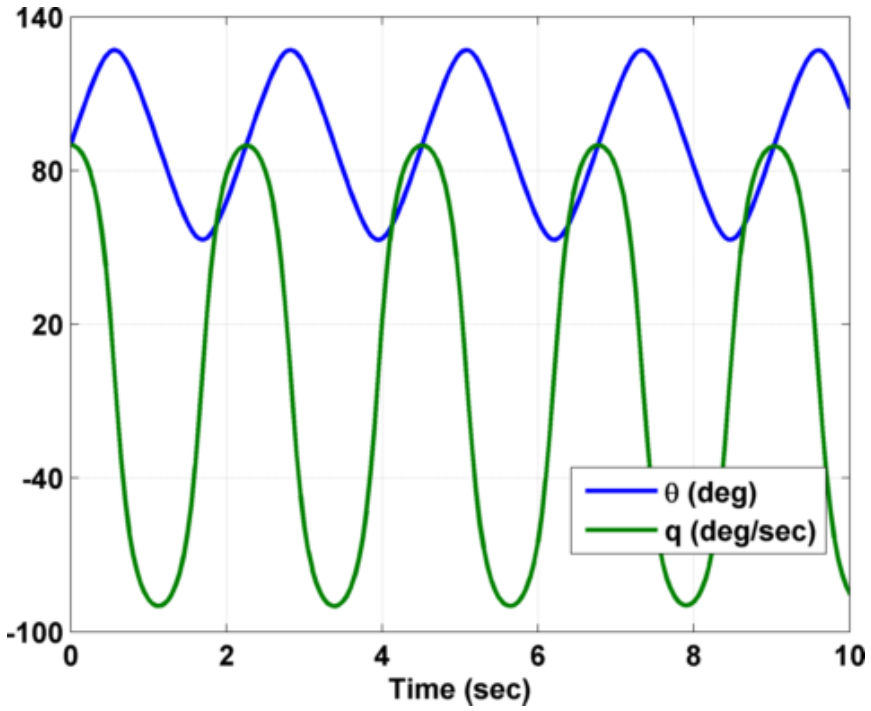

Figure 7.29: Time response of the pitching motion of the aircraft model given in (7.83)

Note this oscillatory behaviour is due to the nonlinear function $h(\theta)$. This term appears due to the constraint moment solution required to produce the desired force. As mentioned in the introduction neglecting this force/moment coupling leads to approximate input-output linearization. However, this leads to local and approximate tracking performance. In this work the coupling is retained and asymptotic tracking is guaranteed.

7.4.2 Time Scale Analysis of the Aircraft Model

In this section, an important observation regarding the inherent time scale characteristics of the DC-8 model under study is made. Toward this end, rewrite the equations of motion given in (7.83) as first order differential equations

$$\dot{x} = u \tag{7.88a}$$

$$\dot{z} = w \tag{7.88b}$$

$$\dot{u} = \frac{1}{m}\Big[u_1 \cos\theta + F_z \cos\theta - D\cos(\theta - \alpha) - L\sin(\theta - \alpha)\Big] \tag{7.88c}$$

$$\dot{w} = \frac{1}{m}\Big[u_1 \sin\theta - F_z \cos\theta - D\sin(\theta - \alpha) + L\cos(\theta - \alpha)\Big] - g \tag{7.88d}$$

$$\dot{\theta} = q \tag{7.88e}$$

$$\dot{q} = \frac{u_2}{I_y} \tag{7.88f}$$

where u and w are the forward and vertical velocities in the inertial frame and q is the body pitch rate. The angle-of-attack is defined as

$$\alpha = \theta - \tan^{-1}\frac{w}{u}. \tag{7.89}$$

Let the reference quantities be denoted as $(t_0, x_0, z_0, u_0, w_0, \theta_0, q_0)$, (u_{10}, u_{20}), and $(D_0 = L_0 = u_{10} = F_{z0})$. With these definitions the dimensional equations given in

(7.88) are transformed into the following non-dimensional form

$$\frac{d\hat{x}}{d\hat{t}} = \left[\frac{t_0 u_0}{x_0}\right]\hat{u} \tag{7.90a}$$

$$\frac{d\hat{z}}{d\hat{t}} = \left[\frac{t_0 w_0}{z_0}\right]\hat{w} \tag{7.90b}$$

$$\begin{aligned}\frac{d\hat{u}}{d\hat{t}} = &\left[\frac{t_0 u_{10}}{m_0 u_0}\right]\hat{u}_1\cos\theta - \left[\frac{t_0 F_{z0}}{m_0 u_0}\right]\hat{F}_z\sin\theta \\ &- \left[\frac{t_0 D_0}{m_0 u_0}\right]\hat{D}\cos(\theta-\alpha) - \left[\frac{t_0 L_0}{m_0 u_0}\right]\hat{L}\sin(\theta-\alpha)\end{aligned} \tag{7.90c}$$

$$\begin{aligned}\frac{d\hat{w}}{d\hat{t}} = &\left[\frac{t_0 u_{10}}{m_0 w_0}\right]\hat{u}_1\sin\theta - \left[\frac{t_0 F_{z0}}{m_0 w_0}\right]\hat{F}_z\cos\theta \\ &- \left[\frac{t_0 D_0}{m_0 w_0}\right]\hat{D}\sin(\theta-\alpha) + \left[\frac{t_0 L_0}{m_0 w_0}\right]\hat{L}\cos(\theta-\alpha) - \left[\frac{t_0 g}{w_0}\right]\end{aligned} \tag{7.90d}$$

$$\frac{d\hat{\theta}}{d\hat{t}} = \left[\frac{t_0}{q_0}\theta_0\right]\hat{q} \tag{7.90e}$$

$$\frac{d\hat{q}}{d\hat{t}} = \left[\frac{t_0 u_{20}}{I_y q_0}\right]\hat{u}_2. \tag{7.90f}$$

Assume the aircraft is straight and level $mg = L_0 = D_0 = u_{10} = F_{z0} = \varepsilon u_{20}$ and $t_0 u_0 = x_0 = z_0 = t_0 w_0$. Additionally let $t_0 u_{10} = m w_0$. With these simplifications the non-dimensional form in (7.90) reduces to

$$\frac{d\hat{x}}{d\hat{t}} = \hat{u} \tag{7.91a}$$

$$\frac{d\hat{z}}{d\hat{t}} = \hat{w} \tag{7.91b}$$

$$\frac{d\hat{u}}{d\hat{t}} = \hat{u}_1\cos\theta - \hat{F}_z\sin\theta - \hat{D}\cos(\theta-\alpha) - \hat{L}\sin(\theta-\alpha) \tag{7.91c}$$

$$\frac{d\hat{w}}{d\hat{t}} = \hat{u}_1\sin\theta - \hat{F}_z\cos\theta - \hat{D}\sin(\theta-\alpha) + \hat{L}\cos(\theta-\alpha) - 1 \tag{7.91d}$$

$$\frac{d\hat{\theta}}{d\hat{t}} = \left[\frac{t_0}{q_0}\theta_0\right]\hat{q} \tag{7.91e}$$

$$\frac{d\hat{q}}{d\hat{t}} = \left[\frac{t_0 mg}{\varepsilon I_y q_0}\right]\hat{u}_2. \tag{7.91f}$$

Given physical quantities in Table 7.3 the constant $\left[\frac{t_0 mg}{\varepsilon I_y q_0}\right] = 400$ with $t_0 = 120sec$ and $q_0 = 1rad/sec$. This is a very large quantity and thus it can be concluded that the rotational dynamics evolve faster. With above conclusion note $\left[\frac{t_0\theta_0}{q_0}\right] = 120$ is a large quantity for $\theta_0 = 1rad$. Thus the pitch rate and the pitch-attitude angle evolves faster than the translational velocities, where (x, y, u, w) evolve at a rate of $O(1)$. Finally including the first-order actuator dynamics for throttle and pitching moment (7.91) is cast in the following desired singularly perturbed form

$$\dot{x} = u \tag{7.92a}$$

$$\dot{z} = w \tag{7.92b}$$

$$\dot{u} = \frac{1}{m}\Big[\delta_\epsilon \cos\theta + \varepsilon\delta_\varrho \cos\theta - D\cos(\theta - \alpha) - L\sin(\theta - \alpha)\Big] \tag{7.92c}$$

$$\dot{w} = \frac{1}{m}\Big[\delta_\epsilon \sin\theta - \varepsilon\delta_\varrho \cos\theta - D\sin(\theta - \alpha) + L\cos(\theta - \alpha)\Big] - g \tag{7.92d}$$

$$\epsilon\dot{\delta}_\epsilon = -0.2(\delta_\epsilon - u_1) \tag{7.92e}$$

$$\epsilon\dot{\theta} = q \tag{7.92f}$$

$$\mu\dot{q} = \frac{u_2}{I_y} \tag{7.92g}$$

$$\varrho\dot{\delta}_\varrho = -20(\delta_\varrho - u_2) \tag{7.92h}$$

with singular perturbation parameters $0 < \epsilon < \mu < \varrho << 1$. As before the singular perturbation parameters have been introduced entirely for modeling purposes and are set to one in the simulation.

7.4.3 Control Formulation

The control development follows closely the steps detailed in Section 6. As the control objective is to track desired velocity commands, the translational kinematic equations need not be considered in the design and are not repeated below. For

brevity, only those equations required for implementation are detailed.

Step 1: The reduced slow system $\mathscr{S}^0$ in error coordinates $\mathbf{e_u} := u - u_r$ and $e_w := w - w_r$ is

$$\dot{e}_u = \frac{1}{m}\Big[\delta_\epsilon^0 \cos\theta^0 - D^0 \cos(\theta^0 - \alpha) - L^0 \sin(\theta^0 - \alpha)\Big] - \dot{u}_r \tag{7.93a}$$

$$\dot{e}_w = \frac{1}{m}\Big[\delta_\epsilon^0 \sin\theta - D^0 \sin(\theta^0 - \alpha) + L^0 \cos(\theta^0 - \alpha)\Big] - g - \dot{w}_r \tag{7.93b}$$

$$q^0(t, e_u, e_w, \theta^0) = 0 \tag{7.93c}$$

$$\delta_\varrho^0(t, e_u, e_w, \theta^0, q^0) = 0 \tag{7.93d}$$

where $\theta^0(t, e_u, e_w)$ and $\delta_\epsilon^0(t, e_u, e_w)$ represent the manifolds to be computed and L^0 and D^0 are lift and drag determined using these manifold definitions. With Lyapunnov function $V(e_u, e_w) = \frac{1}{2}e_u^2 + \frac{1}{2}e_w^2$ and relations

$$-\alpha_1 m e_u = \delta_\epsilon^0 \cos\theta^0 - D^0 \cos(\theta^0 - \alpha) - L^0 \sin(\theta^0 - \alpha) - m\dot{u}_r \tag{7.94a}$$

$$-\alpha_1 m e_w = \delta_\epsilon^0 \sin\theta^0 - D^0 \sin(\theta^0 - \alpha) + L^0 \cos(\theta^0 - \alpha) - mg - m\dot{w}_r \tag{7.94b}$$

property (ii) of Theorem 6.1 is satisfied with $\alpha_1 > 0$ and $\psi_3 = \sqrt{e_u^2 + e_w^2}$. Simplifying (7.94) the manifold $\theta^0(t, e_u, e_w)$ is solved using the nonlinear relation

$$\begin{aligned} -\alpha_1 m(e_u \sin\theta^0 - e_w \cos\theta^0) = {} & -D^0 \sin\alpha - L^0 \cos\alpha + mg\cos\theta^0 \\ & - m\dot{u}_r \sin\theta^0 + m\dot{w}_r \cos\theta^0. \end{aligned} \tag{7.95}$$

The manifold for thrust $\delta_\epsilon^0(t, e_u, e_w)$ is determined using (7.95) as

$$\begin{aligned} \delta_\epsilon^0(t, e_u, e_w) = {} & -\alpha_1 m(e_u \cos\theta^0 + e_w \sin\theta^0) + D^0 \cos\alpha - L\sin\alpha + m\dot{u}_r \cos\theta^0 \\ & + mg\sin\theta^0 + m\dot{w}_r \sin\theta^0. \end{aligned} \tag{7.96}$$

Step 2: The reduced intermediate system $\mathcal{S}_\epsilon^0$ is represented as

$$\breve{e}_{\delta_\epsilon} = -0.2e_{\delta_\epsilon} - 0.2\delta_\epsilon^0 + 0.2u_1 \tag{7.97a}$$

$$\breve{e}_\theta = q^0(t, e_u, e_w, e_\theta) \tag{7.97b}$$

with the errors

$$e_\theta := \theta - \theta^0(t, e_u, e_w) \tag{7.98a}$$

$$e_{\delta_\epsilon} := \delta_\epsilon - \delta_\epsilon^0(t, e_u, e_w). \tag{7.98b}$$

With Lyapunov function $W = \frac{1}{2}e_\theta^2 + \frac{1}{2}e_{\delta_\epsilon}^2$ and the manifold

$$u_1 = \delta_\epsilon^0 + e_{\delta_\epsilon} - \frac{\alpha_2}{0.2}e_{\delta_\epsilon} \tag{7.99a}$$

$$q^0(t, e_u, e_w, e_\theta) = -\alpha_2 e_\theta \tag{7.99b}$$

property (iv) of Theorem 6.1 is satisfied with $\alpha_2 > 0$ and $\Phi_3 = 4\sqrt{e_\theta^2 + e_{\delta_\epsilon}^2}$.

Step 3: The reduced fast system $\mathscr{S}_\mu^0$ is given as

$$e_q' = \delta_\varrho^0(t, e_u, e_w, e_\theta, e_q)/I_y \tag{7.100}$$

where $e_q = q - q^0(t, e_u, e_w, e_\theta)$. With Lyapunov function $\mathcal{Z} = \frac{1}{2}e_q^2$ the pitching moment manifold

$$\delta_\varrho^0(t, e_u, e_w, e_\theta, e_q) = -\alpha_3 I_y e_q \tag{7.101}$$

using proportional controller satisfies property (vi) of Theorem 6.1 with $\alpha_3 > 0$ and $\varpi = |e_q|$.

Step 4: The reduced fast actuator system $\mathscr{S}_{\varrho}^{0}$ is developed as

$$\check{e}_{\delta_{\varrho}} = -20e_{\delta_{\varrho}} - 20\delta_{\varrho}^{0} + 20u_2 \tag{7.102}$$

with $e_{\delta_{\varrho}} := \delta_{\varrho} - \delta_{\varrho}^{0}(t, e_u, e_w, e_\theta, e_q)$. The pitching moment

$$u_2 = \delta_{\varrho}^{0}(t, e_u, e_w, e_\theta, e_q) + e_{\delta_{\varrho}} - \frac{\alpha_4}{20}e_{\delta_{\varrho}} \tag{7.103}$$

stabilizes $\mathscr{S}_{\varrho}^{0}$ with Lyapunov function $\mathcal{Y} = \frac{1}{2}e_{\delta_{\varrho}}^{2}$. Property (viii) of Theorem 6.1 is satisfies with $\upsilon_3 = |e_{\delta_{\varrho}}|$ and $\alpha_4 > 0$.

Step 5: Finally, with feedback gains $\alpha_1 = \alpha_2 = 4$, $\alpha_3 = 4$ and $\alpha_4 = 6$ the various constants in Theorem 6.1 can be easily determined as $\beta_5 = 16$, $\beta_7 = 0.5$, $\beta_{13} = -16$, $\beta_{15} = 4$, $\beta_{18} = -256$, $\beta_{19} = -16$, $\gamma_6 = 0$ and rest all zeros. For convenience, the weights are set to unity and the upper-bound is computed as $\epsilon^* = 0.25$. The upper-bound $\mu^* = 0.02$ is determined by assuming $\epsilon = 0.1$ and $\rho^* = 1.06$ with $\mu = 0.01$. Thus, Theorem 6.1 guarantees asymptotic stability for all signals of (7.88).

The above control synthesis procedure is summarized in a block diagram shown in Figure 7.30.

7.4.4 Results and Discussion

The control objective is to perform a nap-of-the-earth maneuver that tracks a constant velocity at low altitude [109]. The forward velocity is commanded to be constant at $145ms^{-1}$ and the vertical velocity is chosen as $w_d = \frac{125\pi}{60}\sin(\frac{\pi t}{60})$. The nonlinear equation (7.95) was solved using the constrained optimizer `fsolve` in MATLAB with arbitrarily chosen initial conditions. The small angle assumption was made for angle-of-attack to ease the computational burden. The goal of this simulation was to test the performance of the control developed in Section 7.4.3 in comparison with a controller that does not consider explicitly the speed of controllers during

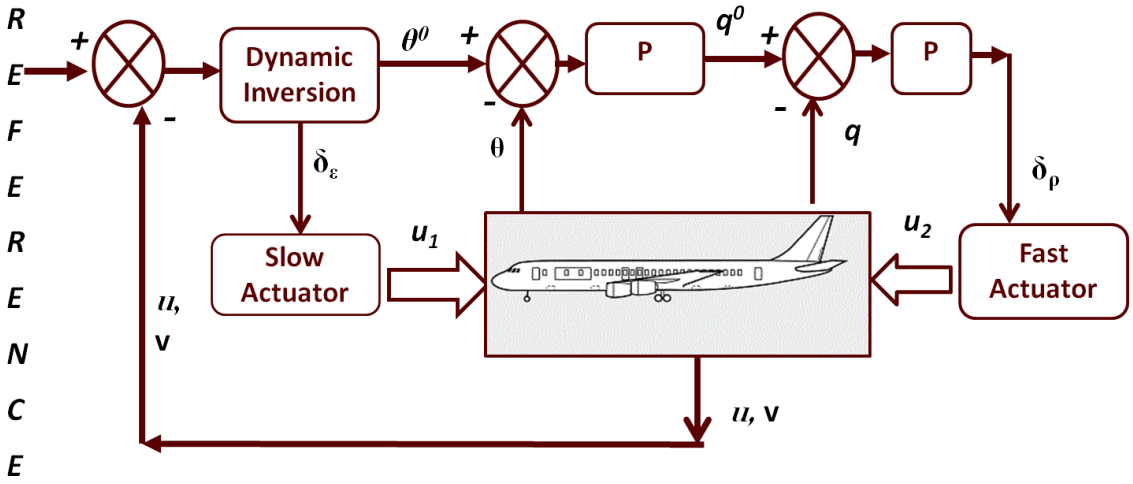

Figure 7.30: Control implementation for conventional take-off and landing aircraft

design. This was done by following steps of Section 6 with the assumption that all controllers are fast. In simulation the formulated control laws were implemented with slow throttle dynamics. The feedback gains for both the controllers were kept same for a fair comparison.

The results are presented in Figures 7.31 through Figure 7.42. Figure 7.31 through Figure 7.33 compare the forward and the vertical velocities to their respective desired references. Notice close tracking is demonstrated with an error of $0.002ms^{-1}$ in forward velocity and $\pm 0.049ms^{-1}$ in vertical velocity in the case with actuator feedback corresponding to development given in Section 7.4.3. However, huge errors in the forward velocity are seen when slow thrust response is not included in the control design. The corresponding control commands are presented in Figure 7.34 and Figure 7.35. Thrust is seen to settle down to its equilibrium value of $3.694 \times 10^8 N$ while the moment varies accordingly to provide sufficient upward force. The initial transient in applied moment is shown in Figure 7.36. As expected the directions of the vertical velocity and the applied moment are opposite: positive moment induces a negative downward force and reduces the vertical velocity to its desired value.

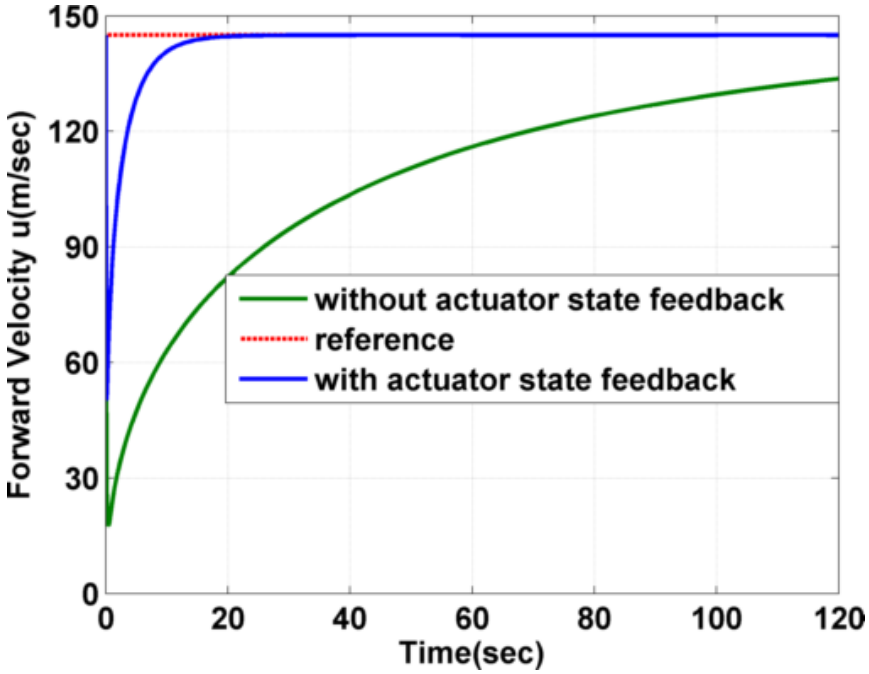

Figure 7.31: Closed-loop response of aircraft: forward velocity

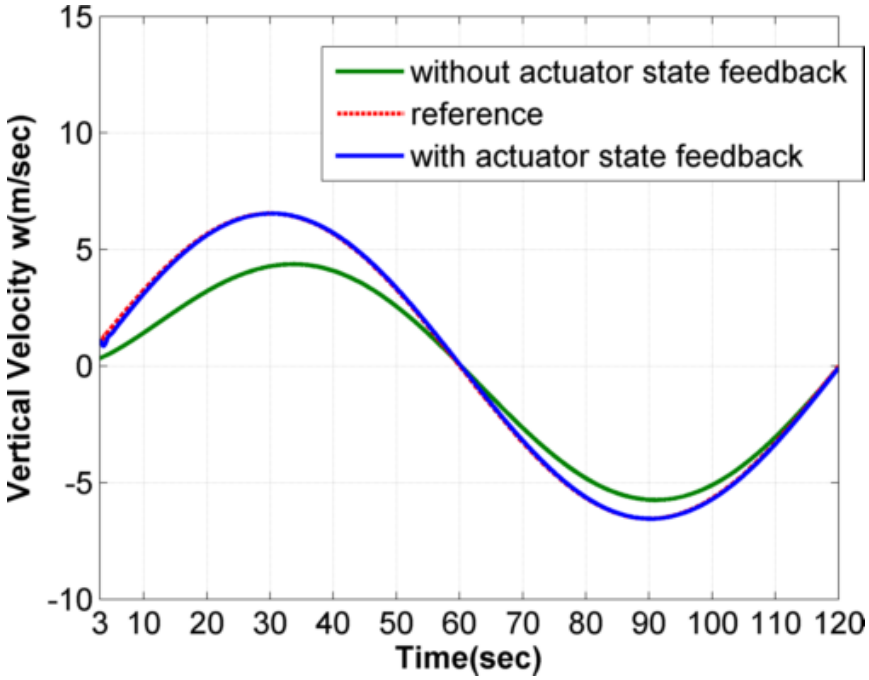

Figure 7.32: Closed-loop response of aircraft (after three seconds): vertical velocity

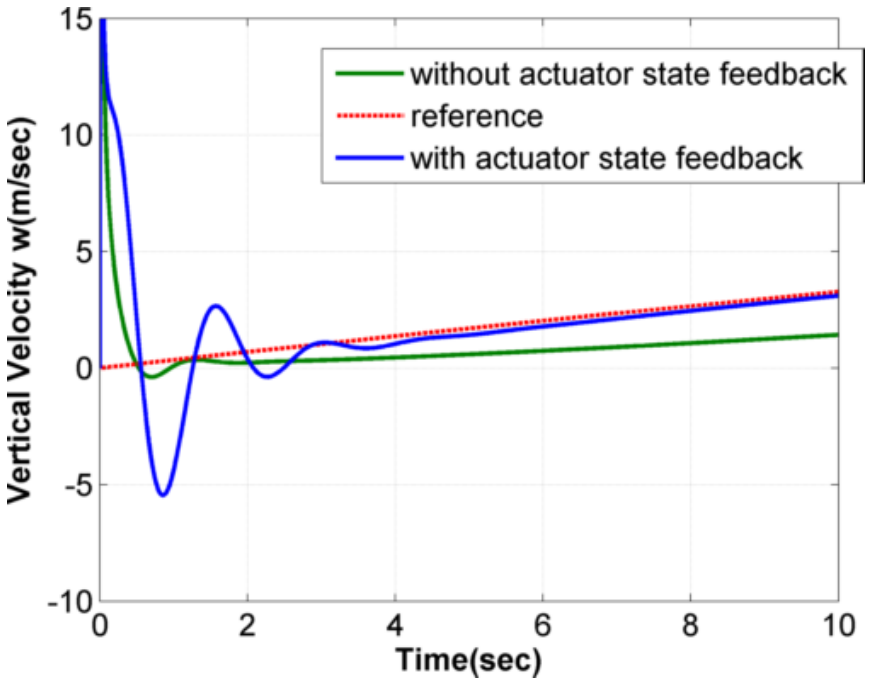

Figure 7.33: Closed-loop response of aircraft (initial transient): vertical velocity

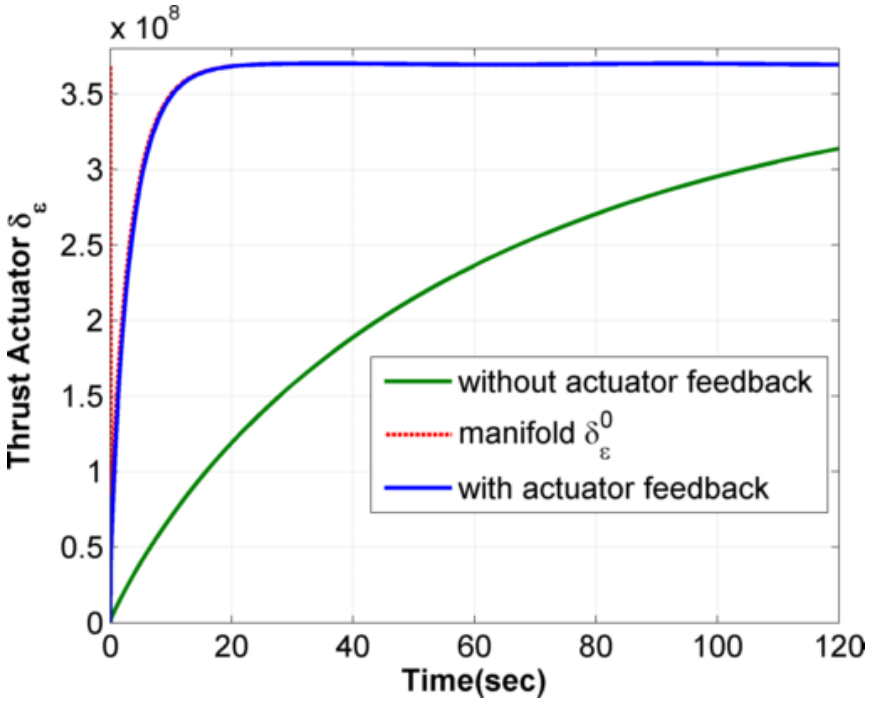

Figure 7.34: Closed-loop response of aircraft: applied thrust

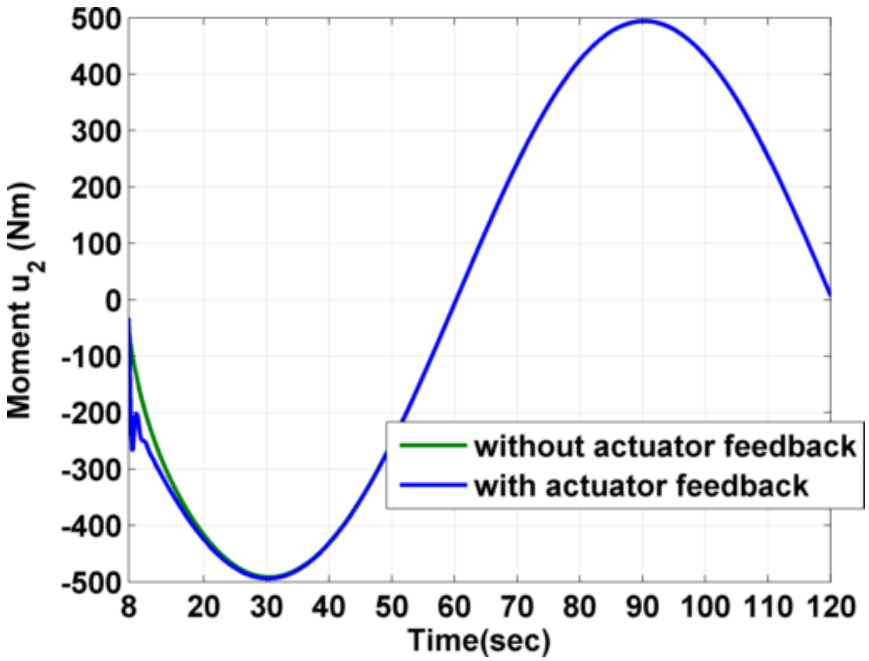

Figure 7.35: Closed-loop response of aircraft (after eight seconds): applied moment

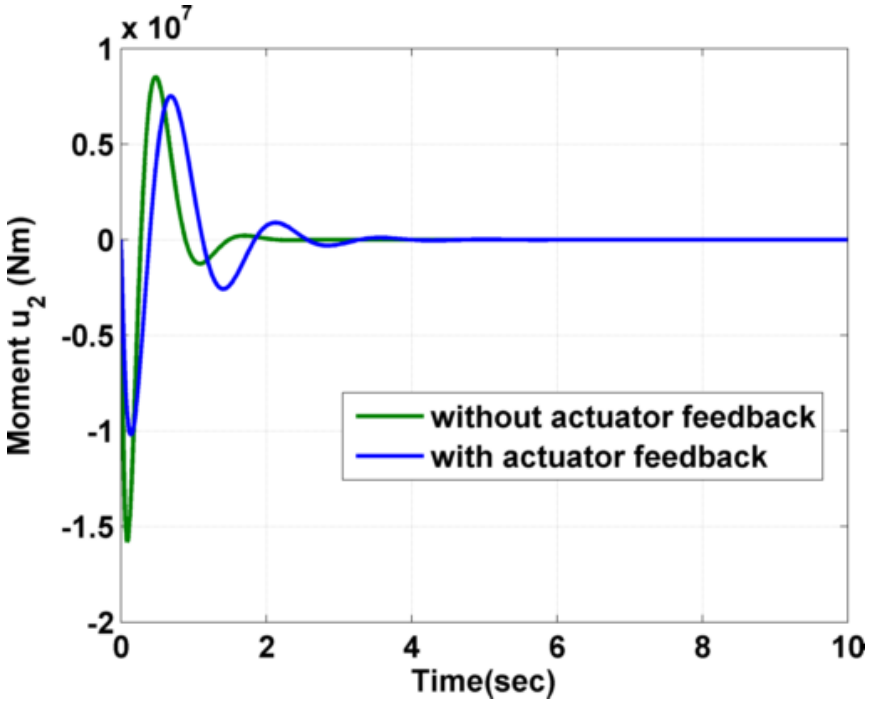

Figure 7.36: Closed-loop response of aircraft (initial transient): applied moment

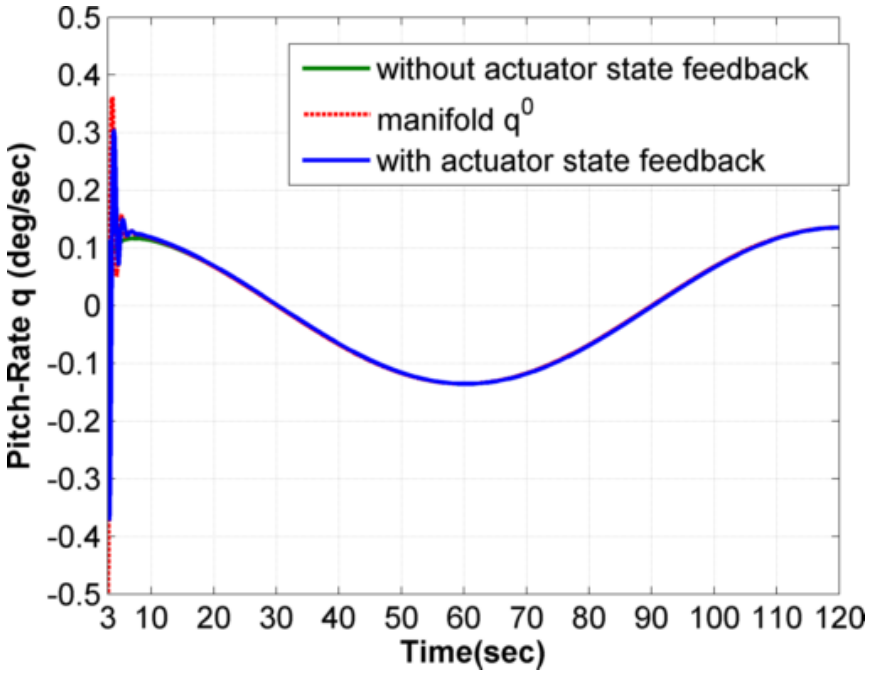

Figure 7.37: Closed-loop response of aircraft (after three seconds): pitch rate

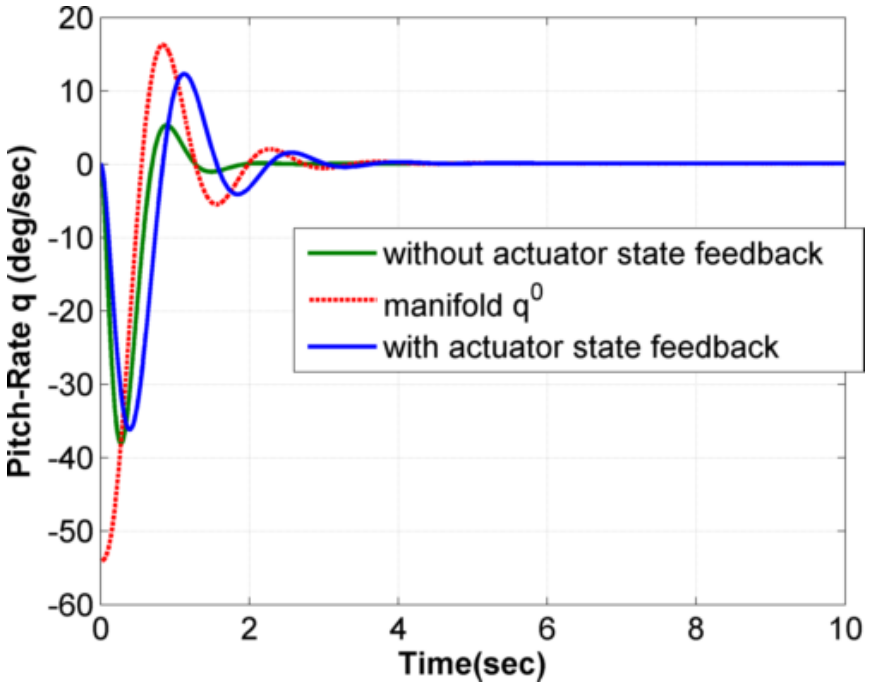

Figure 7.38: Closed-loop response of aircraft (initial transient): pitch rate

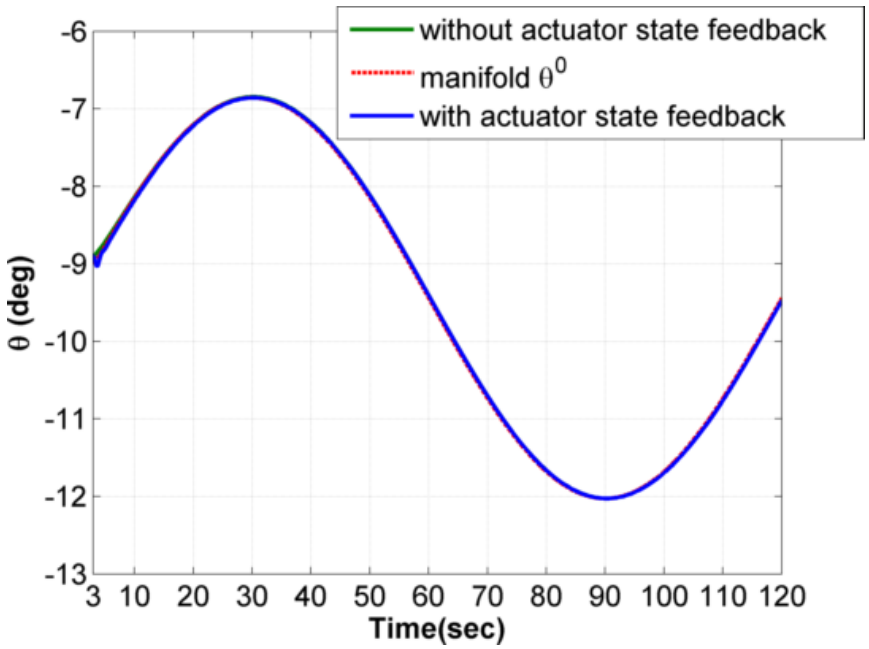

Figure 7.39: Closed-loop response of aircraft (after three seconds): pitch-attitude angle

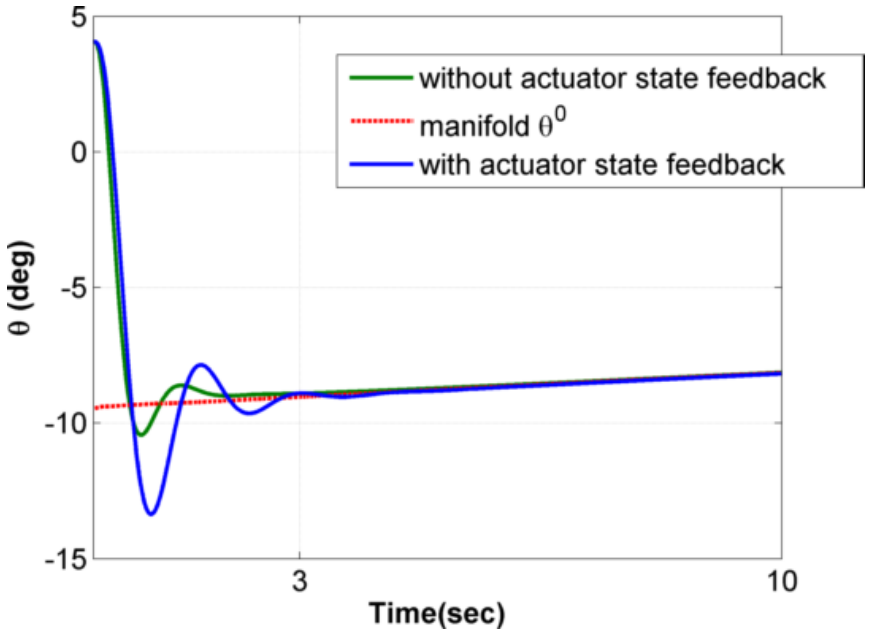

Figure 7.40: Closed-loop response of aircraft (initial transient): pitch-attitude angle

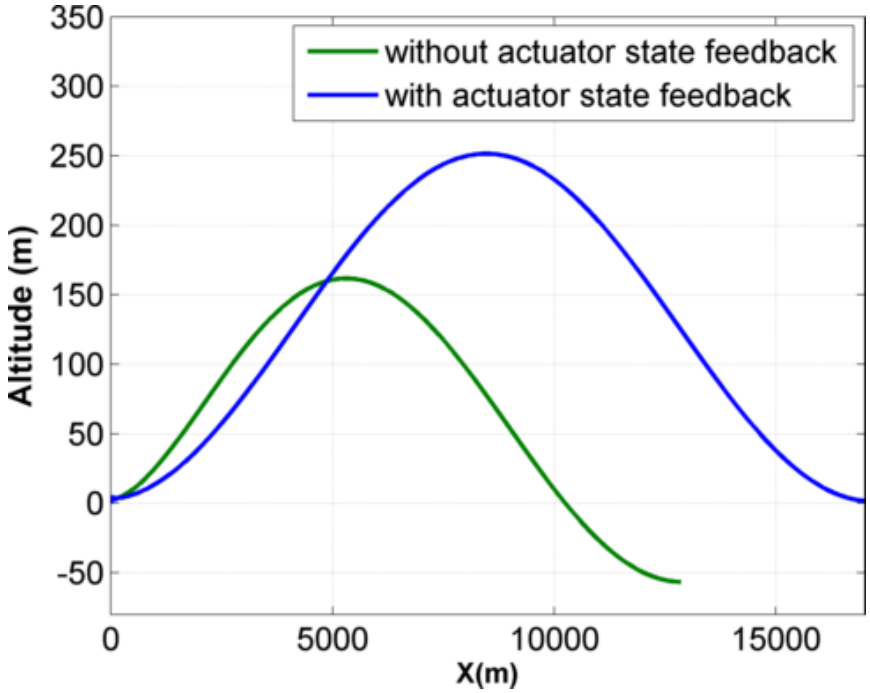

Figure 7.41: Closed-loop response of aircraft: two dimensional trajectory

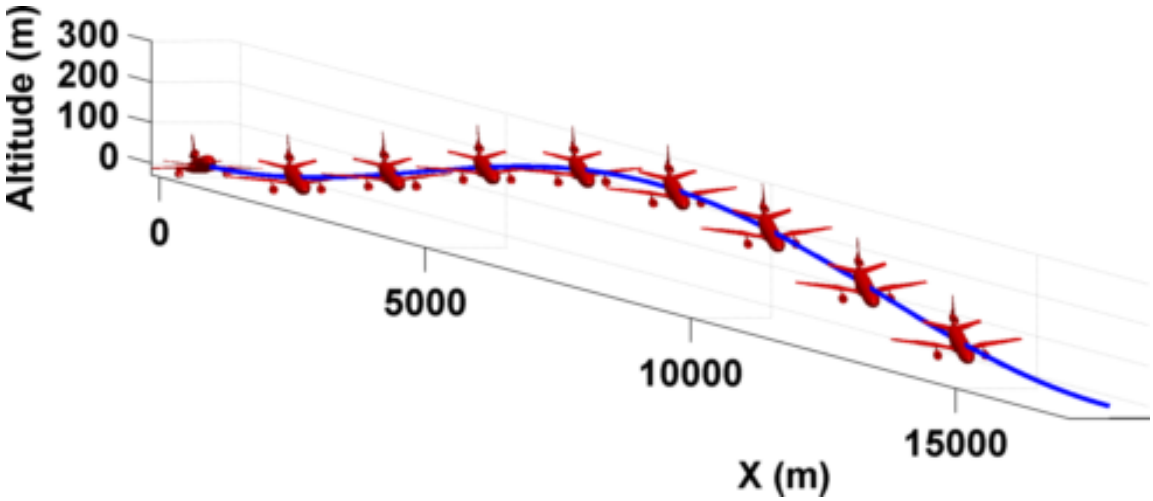

Figure 7.42: Closed-loop trajectory of the aircraft with actuator state feedback

Therefore, for the first 60 seconds the moment is negative, after which it changes sign. The case without actuator state feedback does not provide enough thrust and hence the forward velocity command is not tracked. In the other case perfect output tracking indicates that the internal aircraft states are stable. This behaviour is seen in Figure 7.37 through Figure 7.40. The pitch attitude angle (Figure 7.40) is bounded and behaves as expected. A climb produces an increase in pitch attitude angle and a descent produces a negative value. The pitch rate behaviour seen in Figure 7.37 agrees with the commanded trajectory. The initial transient of pitch rate are continuous as seen in Figure 7.38. Note that the controller without actuator state feedback also generates the same internal state trajectories. This is because these solutions were determined assuming the pitch-attitude angle and pitch-rate respond fast and which holds true for the aircraft. In comparison with results published in Reference [109], this exact internal state trajectory was obtained using the technique proposed in [107]. The complete two-dimensional trajectory is shown in Figure 7.41. Notice that difference in thrust completely alters the performance of control design without actuator state feedback. The three-dimensional trajectory for the aircraft model with actuator state feedback is shown in Figure 7.42.

7.4.5 Summary

A control formulation for output tracking of a general class of nonlinear non-minimum phase aircraft was developed. The desired internal-state reference and feedback control to stabilize the unstable internal dynamics were posed as an asymptotic slow tracking problem for singularly perturbed systems. Based on the results presented, the following conclusions are drawn. The perfect output tracking was a result of perfect internal state tracking that was achieved by the nonlinear feedback law. The tracking error was within $|0.002|$ for the forward velocity and $|0.049|$ for

the vertical velocity. The controller demonstrated asymptotic tracking irrespective of the desired reference trajectory. The controller was causal and did not require any preview of the desired reference. Owing to the nonlinear nature of (7.95) the controller is not real-time implementable and requires offline computation.

7.5 Closing Remarks

Applications of the general nonlinear control design procedure developed in Section 6 to three benchmark non-minimum phase systems was presented. Starting from the open-loop analysis, this section detailed step by step procedure for determining the inherent time scale properties of the system and representing the dynamical equations in singularly perturbed form. Block diagrams along with control synthesis procedure for real-time implementation was presented.

Based on the results and theoretical developments presented, the following conclusions are drawn. First, the control technique is applicable to several class of non-minimum phase problems. The beam and ball experiment is an example of a system with no well-defined relative degree and Lyapunov stable internal dynamics. The helicopter and aircraft systems are examples of systems with unstable internal dynamics. Moreover, exact input-output linearization for these systems is not desirable and approximate input-output linearization does not guarantee desired performance. Second, the sequential procedure is not dependent upon the underlying controller for the reduced-order models. Any feedback control methodology can be used. Back-stepping, Lyapunov-based control, proportional feedback control and dynamic inversion were some techniques used in the examples presented. Third, owing to the sequential nature of the design, determination of the internal state trajectory is independent of the operating condition. Fourth, the hover control example proves that the interconnection conditions are not an artifact of the design procedure. This

was shown through use of dynamical model instead of the singularly perturbed model to prove stability. Fifth, the aircraft example demonstrates that better performance is guaranteed by the developed control laws for systems that have slow actuator dynamics and are difficult to control. The benefits and limitations of the approach are detailed below:

7.5.1 Benefits

1. First, the control laws developed apply to several class of non-minimum phase systems ranging from those that do not have well-defined relative degree to those that have unstable internal dynamics. Physical examples with two, three and four inherent time scales were shown.

2. Second, the sequential nature of the design procedure guarantees asymptotic output stabilization for a large operating regime since desired internal state trajectory computation is causal and does not require knowledge of reference trajectory beforehand.

3. The control development is independent of the underlying nonlinear control technique. This means that the design procedure is applicable to a large class of continuous time dynamical systems.

4. Fourth, the controller demonstrates better performance for systems with slow actuators over other time scale design procedures that require fast actuator dynamics.

5. Fifth, as a byproduct the time scale procedure justifies the stability guarantees of approximate input-output linearization and provides quantitative reasons for its low performance.

7.5.2 Limitations

1. As mentioned in Section 6, determination of the manifold, or in this case the internal state trajectory depends upon a non-affine control technique. Due to limited availability of these procedures, sometimes the desired internal state reference is forced to be computed beforehand. In this section, the desired pitch-attitude angle for the nap-of-the-earth was computed offline.

2. Verification of interconnection conditions becomes cumbersome with higher dimensions.

8. CONCLUSIONS AND RECOMMENDATIONS

This dissertation investigated feedback control methodologies and developed rigorous techniques to address the stabilization problem for non-affine in control, non-standard multiple time scale systems. Toward this end, novel control law procedures were synthesized to address the three major open challenges identified in Section 1. Applications of the developed methodologies were shown for several examples from science and engineering. This section reviews the contributions made by this work, conclusions drawn from the theoretical developments as well as numerical simulations and details recommendations for future work.

8.1 Contributions of Research

This research is novel and makes the following nine major contributions to the field of nonlinear control theory:

1. The result given in Theorem 3.1 gives a generalization of the famous Kalman-Yakubovich-Popov lemma for non-affine systems under mild restrictions. This new result helps to determine whether or not an input-output description of a nonlinear system is passive. It is expected that this generalization will play a vital role in developing adaptive control laws for nonlinear systems based on Lyapunov's direct method analogous to its linear counterpart.

2. Theorem 3.6 extends the powerful feedback passivation approach for non-affine systems. This static compensation technique provides conditions under which a nonlinear system can be made passive through state-feedback and forms the basis for stabilization of general non-affine systems.

3. Theorem 3.7 presents for the first time, a general control law design procedure for asymptotic stabilization of non-affine systems using memoryless state-feedback without making any assumptions regarding the control influence or nature of nonlinearities present in the dynamical model. This result along with constructive control law given in Theorem 3.9 asymptotically stabilizes a class of single-input systems.

4. Two new hierarchical control design procedures, presented in Section 4 and Section 6, accomplish slow state tracking for non-standard singularly perturbed systems without imposing any assumptions about the solution of the transcendental equations or the effect of the control variables. As discussed in Section 2.3 construction of manifolds for non-standard systems is difficult and the cause of local bounded results.

5. The sequential design procedures of Section 4 and Section 6 are Lyapunov-based designs because of which the global or local nature of the closed-loop results are relaxed from the complexities of analytic construction of the manifold and entirely a consequence of underlying controllers for reduced-order models. This contribution provides the control engineer the freedom to choose a desired state-feedback technique that is suitable for the nonlinear system under study.

6. The asymptotic tracking approach for multiple time scale systems given in Theorem 6.1 addresses systems with controllers that have different speeds of response. This is an advance over the composite control technique and was verified in simulation (Section 7.4) to demonstrate better steady-state time-response compared to other time scale procedures.

7. Theorem 5.1 outlines a procedure for simultaneous slow and fast state track-

ing for non-standard singularly perturbed systems for the first time using the reduced-order model approach and without making any assumptions about construction of the manifold.

8. The control law design procedures for both two and multiple time scale systems developed in Sections 4, 5 and 6 of this dissertation are not a function of the singular perturbation parameter, nor require any knowledge of it. This is an important contribution for aerospace applications, where quantifying this parameter is extremely difficult.

9. Finally, the results given in Theorem 6.1 for control of multiple time scale systems have been shown to guarantee real-time implementable exact output tracking for a class of non-minimum phase systems. This is an advance over the exact output tracking approach known in literature that requires immense offline processing and is dependent upon the desired reference trajectory.

8.2 Conclusions

Based on the theoretical developments and numerical simulation results presented in this dissertation, the following conclusions are drawn:

1. A universal construction formula for non-affine control systems similar to Sontag's formula for affine systems is not possible due to inherent nonlinear dynamic behaviour. Theorem 3.7 gives a unified construction procedure for design of static-feedback for all class of non-affine systems.

2. Application of Theorem 3.7 to non-affine dynamical systems (See Section 3.5) shows that stiffness function $\alpha(\mathbf{x})$ is the solution of a nonlinear inequality and is consequently obtained to be discontinuous in nature. This behaviour is

consistent with the result given in [Corollary 5.8.8][3] that proves that open-loop unstable systems cannot be C^1 stabilizable.

3. The sequential design procedure developed here for asymptotic stabilization of multiple time scale systems essentially converts the open-loop non-standard form into a closed-loop standard form (See example given in Section 4.4.3.4). This ensures that all conclusions from singular perturbation methods remain valid and reduced-order models can be employed for design.

4. Numerical simulation results presented in Sections 4, 5 and 6 indicate that the upper-bound estimate for the singular perturbation parameter is conservative and overall stability is guaranteed to hold even for higher values of the perturbation parameter.

5. Control of non-minimum phase examples presented in Section 7 indicates that inherent multiple time scale behaviour is the cause of unstable internal dynamics in some systems and is the reason for stability guarantees of approximate input-output linearizations proposed in the past.

6. Several singularly perturbed system examples presented in this dissertation conclude that interaction conditions due to composite Lyapunov approach for stability are difficult to verify as the dimension of the system model increases. However, the hover control for a helicopter discussed in Section 7.3 indicates that these conditions are not dependent on composite Lyapunov approach and are in fact an artifact of multiple time scale systems. The stability conclusions drawn from this example indicate that as long as the closed-loop gains chosen maintain sufficient time scale separation between the slow and fast modes of the system, these conditions are satisfied.

8.3 Recommendations

Several recommendations are made here based on the research presented in this dissertation:

1. *Stabilization of singularly perturbed systems with control constraints:* Control design procedures developed in this dissertation assume the control variables can take any value in the real vector space. In order for these control methods to be applicable for a larger class of physical systems, control constraints need to be imposed in the synthesis procedure. This can be done by employing available constrained control techniques as the underlying controllers to satisfy the conditions of the hierarchical procedure given in Theorem 6.1.

2. *Constructive control algorithm for large class of non-affine systems:* Investigation of static feedback control developed in Section 3 demonstrates that the desired control is the solution of a nonlinear inequality. This inequality was further separated to determine the specific conditions upon the magnitude and the direction of the desired input signal. Theorem 3.9 provides a constructive control law for a class of single input non-affine systems that satisfy these conditions. These results can be extended to a larger class of single-input non-affine systems by developing quantitative relationships between different vector norms and using this information for satisfying the inequalities.

3. *Optimal control for non-standard singularly perturbed systems:* The reduced-order model approach has been extensively used in the past to remove stiffness and reduce the order of optimal control problems for standard singularly perturbed systems. This was done by restricting the fast states on the isolated manifold. For non-standard systems, the reduced-order models can still be re-

tained by employing the fast states as intermediate level controls for optimizing the slow states. It is expected that modified composite control and Approach II detailed in this dissertation can be used to approximate the optimal solution to an accuracy of $O(\epsilon)$.

4. *Pure output feedback control of nonlinear systems:* The techniques developed in this dissertation for continuous-time dynamical systems require complete state information for feedback. This assumption is quite restrictive and output feedback methodologies need to be explored. This can be done by introduction of an observer in the dynamical model under consideration. It is expected that the stability guarantees of the developed control laws will be valid as long as additional observability conditions are met and the observer responds faster than the fastest state of the physical system.

5. *Multiple time scale approach for propulsion-controlled aircraft:* As mentioned in the introduction the control techniques presented in this dissertation can be used to address the slow times of response of throttle. Better performance of the proposed methods compared to conventional approach was demonstrated for the nap-of-the-earth maneuver with slow engine response in Section 7.4. The developed techniques can be extended to address the propulsion-control problem by inclusion of an adaptive outer loop to address the uncertainties arising in the system due to control surface failure.

REFERENCES

[1] G. F. Franklin, J. D. Powell, and A. Emami-Naeini, *Feedback Control of Dynamic Systems*. Upper Saddle River, NJ: Pearson Prentice Hall, 2006.

[2] S. P. Bhattacharyya, A. Datta, and L. H. Keel, *Linear Control Theory: Structure, Robustness and Optimization*. Boca Raton, FL: CRC Press, 2009.

[3] E. D. Sontag, *Mathematical Control Theory: Deterministic Finite Dimensional Systems*. New York, NY: Springer, 2nd ed., 1998. ISBN 0-387-984895.

[4] A. Isidori, *Nonlinear Control Systems*. London: Springer-Verlag, 3rd ed., 1995. ISBN 3-540-19916-0.

[5] N. Fenichel, "Geometric singular perturbation theory for ordinary differential equations," *Journal of Differential Equations*, vol. 31, no. 1, pp. 53–98, 1979.

[6] A. Siddarth and J. Valasek, "Output tracking of non-minimum phase dynamics," in *AIAA Guidance, Navigation and Control Conference*, (Portland, Oregon), August 2011. AIAA-2011-6487.

[7] A. Siddarth and J. Valasek, "Tracking control for a non-minimum phase autonomous helicopter," in *AIAA Guidance, Navigation and Control Conference*, (Minneapolis, Minnesota), August 2012.

[8] K. Rompala, R. Rand, and H. Howland, "Dynamics of three coupled van der pol oscillators with application to circadian rhythms," *Communications in Nonlinear Science and Numerical Simulation*, vol. 12, no. 5, pp. 794–803, 2007.

[9] P. Kokotović, H. K. Khalil, and J. O'Reilly, *Singular Perturbation Methods in Control: Analysis and Design.* Orlando, FL: Academic Press, 1986.

[10] P. Menon, M. E. Badgett, and R. Walker, "Nonlinear flight test trajectory controllers for aircraft," *Journal of Guidance*, vol. 10, no. 1, pp. 67–72, 1987.

[11] V. Saksena, J. O'Reilly, and P. Kokotović, "Singular perturbations and time-scale methods in control theory: Survey 1976-1983," *Automatica*, vol. 20, no. 3, pp. 273–293, 1984.

[12] P. V. Kokotović, "Applications of singular perturbation techniques to control problems," *SIAM Review*, vol. 26, no. 4, pp. 501–550, 1984. Society for Industrial and Applied Mathematics.

[13] D. Naidu and A. J. Calise, "Singular perturbations and time scales in guidance and control of aerospace systems: A survey," *Journal of Guidance, Control and Dynamics*, vol. 24, no. 6, pp. 1057–1078, 2001.

[14] D. S. Naidu, "Singular perturbations and time scales in control theory and applications: Overview," *Dynamics of Continuous, Discrete and Impulsive Systems Series B: Applications & Algorithms*, vol. 9, no. 2, pp. 233–278, 2002.

[15] A. N. Tikhonov, "On the dependence of the solutions of differential equations on a small parameter," *Mat. Sb.*, vol. 22, pp. 193–204, 1948. In Russian.

[16] M. Suzuki and M. Miura, "Stabilizing feedback controllers for singularly perturbed linear constant systems," *IEEE Transactions on Automatic Control*, vol. 21, no. 1, pp. 123–124, 1976.

[17] M. Vidyasagar, "Robust stabilization of singularly perturbed systems," *Systems and Control Letters*, vol. 5, no. 6, pp. 413–418, 1985.

[18] R. G. Phillips, "A two-stage design of linear feedback controls," *IEEE Transactions on Automatic Control*, vol. 25, no. 6, pp. 1220–1283, 1980.

[19] B. S. Heck, "Sliding mode control for singularly perturbed systems," *International Journal of Control*, vol. 53, no. 4, pp. 985–1001, 1991.

[20] A. Saberi and H. Khalil, "Stabilization and regulation of nonlinear singularly perturbed systems-composite control," *IEEE Transactions on Automatic Control*, vol. 30, no. 4, pp. 739–747, 1985.

[21] L. T. Grujic, "On the theory and synthesis of nonlinear non-stationary tracking singularly perturbed systems," *Control Theory and Advanced Technology*, vol. 4, no. 4, pp. 395–409, 1988.

[22] H.-L. Choi and J.-T. Lim, "Gain scheduling control of nonlinear singularly perturbed time-varying systems with derivative information," *International Journal of Systems Science*, vol. 36, no. 6, pp. 357–364, 2005.

[23] J. Chow and P. Kokotović, "Two-time-scale feedback design of a class of nonlinear systems," *IEEE Transactions on Automatic Control*, vol. 23, no. 3, pp. 49–54, 1978.

[24] L. Li and F. C. Sun, "An adaptive tracking controller design for nonlinear singularly perturbed systems using fuzzy singularly perturbed model," *IMA Journal of Mathematical Control and Information*, vol. 26, no. 4, pp. 395–415, 2009.

[25] H. K. Khalil, "Feedback control of nonstandard singularly perturbed systems," *IEEE Transactions on Automatic Control*, vol. 34, no. 10, pp. 1052–1060, 1989.

[26] S. A. Snell, D. F. Enns, and W. L. G. Jr., "Nonlinear inversion flight control for a supermaneuverable aircraft," *Journal of Guidance, Control and Dynamics*, vol. 15, no. 4, pp. 976–984, 1992.

[27] S. S. Mulgund and R. F. Stengel, "Aircraft flight control in wind shear using sequential dynamic inversion," *Journal of Guidance, Control and Dynamics*, vol. 18, no. 5, pp. 1084–1091, 1995.

[28] G. Avanzini and G. de Matteis, "Two time-scale inverse simulation of a helicopter model," *Journal of Guidance, Control and Dynamics*, vol. 24, no. 2, pp. 330–339, 2001.

[29] E. Fridman, "A descriptor system approach to nonlinear singularly perturbed optimal control problem," *Automatica*, vol. 37, no. 4, pp. 543–549, 2001.

[30] Z. Artstein and A. Vigodner, "Singularly perturbed ordinary differential equations with dynamic limits," *Proceedings of the Royal Society of Edinburgh*, vol. 126, no. 3, pp. 541–569, 1996.

[31] K. Hashtrudi and K. Khorasani, "An integral manifold approach to tracking control for a class of non-minimum phase linear systems using output feedback," *Automatica*, vol. 32, no. 11, pp. 1533–1552, 1996.

[32] L. Glielmo and M. Corless, "On output feedback control of singularly perturbed systems," *Applied Mathematics and Computation*, vol. 217, no. 3, pp. 1053–1070, 2010.

[33] A. Balakrishnan, "On the controllability of a nonlinear system," *Proceedings of the National Academy of Sciences of the United States of America*, vol. 55, no. 3, pp. 465–468, 1966.

[34] F. L. Lewis and V. L. Syrmos, *Optimal Control*. New York, NY: John Wiley & Sons Inc, 2nd ed., 1995. ISBN 0-471-03378-2.

[35] Z. Artstein, "Stabilization with relaxed controls," *Nonlinear Analysis, Theory, Methods & Applications*, vol. 7, no. 11, pp. 1163–1173, 1983.

[36] B. Jayawardhana, "Noninteracting control of nonlinear systems based on relaxed control," in *Proceedings of 49th IEEE Conference on Decision and Control*, (Atlanta), December 2010.

[37] E. Moulay and W. Perruquetti, "Stabilization of nonaffine systems: A constructive method for polynomial systems," *IEEE Transactions on Automatic Control*, vol. 50, no. 4, pp. 520–526, 2005.

[38] W. Lin, "Feedback stabilization of general nonlinear control systems: A passive system approach," *Systems & Control Letters*, vol. 25, no. 1, pp. 41–52, 1995.

[39] W. Lin, "Global asymptotic stabilization of general nonlinear systems with stable free dynamics via passivity and bounded feedback," *Automatica*, vol. 32, no. 6, pp. 915–924, 1996.

[40] N. Hovakimyan, E. Lavretsky, and C. Cao, "Dynamic inversion for multivariable non-affine-in-control systems via time-scale separation," *International Journal of Control*, vol. 81, no. 12, pp. 1960–1967, 2008.

[41] J. Teo, J. P. How, and E. Lavretsky, "Proportional-integral controllers for minimum-phase nonaffine-in-control systems," *IEEE Transactions on Automatic Controls*, vol. 55, no. 6, pp. 1477–1482, 2010.

[42] R. Ghasemi, M. Menhaj, and A. Afsar, "Output tracking controller for non-affine nonlinear systems with nonlinear output: Fuzzy adaptive approach," in *Proceedings of the 7th Asian Control Conference*, pp. 1073–1078, IEEE, 2009.

[43] C. C. Chen, "Global exponential stabilization for nonlinear singularly perturbed systems," *IEEE Proceedings of Control Theory and Applications*, vol. 145, no. 4, pp. 377–382, 1998.

[44] J. D. Bošković, L. Chen, and R. K. Mehra, "Adaptive control design for non-affine models arising in flight control," *Journal of Guidance, Control and Dynamics*, vol. 27, no. 2, pp. 209–217, 2004.

[45] N. Hovakimyan, E. Lavretsky, and A. Sasane, "Dynamic inversion for non-affine-in-control systems via time-scale separation: part i," *Journal of Dynamical and Control Systems*, vol. 13, no. 4, pp. 451–465, 2007.

[46] J. Xiang, Y. Li, and W. Wei, "Stabilization of a class of non-affine systems via modelling error compensation," *IET Control Theory and Applications*, vol. 2, no. 2, pp. 108–116, 2008.

[47] E. D. Sontag, "A 'universal' construction of artstein's theorem on nonlinear stabilization," *Systems & Control Letters*, vol. 13, no. 2, pp. 117–123, 1989.

[48] R. Burridge, A. Rizzi, and D. Koditschek, "Sequential composition of dynamically dexterous robot behaviours," *The International Journal of Robotics Research*, vol. 18, no. 6, pp. 534–555, 1999.

[49] A. Leonessa, W. M. Haddad, and V. Chellaboina, "Nonlinear system stabilization via hierarchical switching control," *IEEE Transactions on Automatic Control*, vol. 46, no. 1, pp. 17–28, 2001.

[50] G. S. Ladde and D. D. Šiljak, "Multiparameter singular perturbations of linear systems with multiple time scales," *Automatica*, vol. 19, no. 4, pp. 385–394, 1983.

[51] D. Naidu, "Analysis of non-dimensional forms of singular perturbation structures for hypersonic vehicles," *Acta Astronautica*, vol. 66, no. 3, pp. 577–586, 2010.

[52] V. Gaitsgory, "Suboptimization of singularly perturbed control," *SIAM Journal of Control and Optimization*, vol. 30, no. 5, pp. 1228–1249, 1992.

[53] H. J. Kelley, "Aircraft maneuver optimization by reduced-order approximations," in *Control and Dynamic Systems* (C. T. Leonides, ed.), pp. 131–178, Orlando, FL: Academic Press, 1973.

[54] K. Mease, "Multiple time-scales in nonlinear flight mechanics: diagnosis and modeling," *Applied Mathematics and Computation*, vol. 164, no. 2, pp. 627–648, 2005.

[55] A. J. Calise, N. Markopoulos, and J. E. Corban, "Non dimensional forms for singular perturbation analyses of aircraft energy climbs," *Journal of Guidance, Control and Dynamics*, vol. 17, no. 3, pp. 584–590, 1994.

[56] M. Ardema and N. Rajan, "Slow and fast state variables for three-dimensional flight dynamics," *Journal of Guidance*, vol. 8, no. 4, pp. 532–535, 1985.

[57] M. D. Ardema, "Computational singular perturbation method for dynamic systems," *Journal of Guidance*, vol. 14, no. 3, pp. 661–664, 1991.

[58] C. I. Brynes, A. Isidori, and J. C. Willems, "Passivity, feedback equivalence, and the global stabilization of minimum phase nonlinear systems," *IEEE Transactions on Automatic Control*, vol. 36, no. 11, pp. 1228–1240, 1991.

[59] M. Larsen and P. V. Kokotović, "On passivation with dynamic output feedback," *IEEE Transactions on Automatic Control*, vol. 46, no. 6, pp. 962–967, 2001.

[60] H. K. Khalil, *Nonlinear Systems*. Upper Saddle River, NJ: Prentice Hall, 3 ed., December 2001.

[61] D. Hill and P. Moylan, "The stability of nonlinear dissipative systems," *IEEE Transactions on Automatic Control*, vol. 21, no. 5, pp. 708–711, 1976.

[62] D. Hill and P. Moylan, "Stability results for nonlinear feedback systems," *Automatica*, vol. 13, no. 4, pp. 377–382, 1977.

[63] R. Sepulchre, M. Janković, and P. Kokotović, *Constructive nonlinear control*. Communications and control engineering, New York, NY: Springer, 1997.

[64] J. Slotine and W. Li, *Applied nonlinear control*. Upper Saddle River, NJ: Prentice Hall, 1991.

[65] P. Ioannou and J. Sun, *Robust Adaptive Control*. Upper Saddle River, NJ: Prentice Hall Inc., 2003.

[66] H. Sira-Ramirez, "Sliding regimes in general non-linear systems: a relative degree approach," *International Journal of Control*, vol. 50, no. 4, pp. 1487–1506, 1989.

[67] A. S. Shiriaev and A. L. Fradkov, "Stabilization of invariant sets for nonlinear non-affine systems," *Automatica*, vol. 36, no. 11, pp. 1709–1715, 2000.

[68] S. Ge, C. Hang, and T. Zhang, "Nonlinear adaptive control using neural networks and its application to cstr systems," *Journal of Process Control*, vol. 9, no. 4, pp. 313–323, 1999.

[69] S. S. Ge and J. Zhang, "Neural-network control of nonaffine nonlinear system with zero dynamics by state and output feedback," *IEEE Transactions on Neural Networks*, vol. 14, no. 4, pp. 900–918, 2003.

[70] O.Bethoux, T. Floquet, and J. Barbot, "Advanced sliding mode stabilization of a levitation system." presented at the European Control Conference, Cambridge, U.K., 2003.

[71] J. Carr, *Applications of Centre Manifold Theory*, vol. 35. New York, NY: Applied Mathematical Sciences, 1981.

[72] T. J. Kaper, "An introduction to geometric methods and dynamical systems theory for singular perturbation problems," in *Analyzing Multiscale Phenomena Using Singular Perturbation Methods: Proceedings of Symposia in Applied Mathematics* (J. Cronin and R. E. O. Jr., eds.), pp. 85–131, American Mathematical Society, 1986.

[73] A. Siddarth and J. Valasek, "Kinetic state tracking for a class of singularly perturbed systems," *Journal of Guidance, Control and Dynamics*, vol. 34, no. 3, pp. 734–749, 2011.

[74] Y. Fan, F. H. Lutze, and E. M.Cliff, "Time-optimal lateral maneuvers of an aircraft," *Journal of Guidance,Control and Dynamics*, vol. 18, no. 5, pp. 1106–1112, 1995.

[75] D. Ito, J. Georgie, and J. Valasek, "Re-entry vehicle flight control design guidelines: Dynamic inversion," tech. rep., 2002. NASA TP-2002-210771.

[76] A. Siddarth and J. Valasek, "Tracking control design for non-standard nonlinear singularly perturbed systems," in *Proceedings of American Control Conference*, (Montreal, Canada), June 2012.

[77] A. Siddarth and J. Valasek, "Global tracking control structures for nonlinear singularly perturbed aircraft systems," in *Advances in Aerospace Guidance, Navigation and Control* (F. Holzapfel and S. Theil, eds.), pp. 235–246, Berlin: Springer, 2011.

[78] A. J. Calise, "Singular perturbation methods for variational problems in aircraft flight," *IEEE Transactions on Automatic Control*, vol. 21, no. 3, pp. 345–353, 1976.

[79] H. Schaub and J. L. Junkins, *Analytical Mechanics of Space Systems*. Reston, VA: AIAA Education Series, 2003.

[80] F. Hoppensteadt, "Properties of solutions of ordinary differential equations with small parameters," *Communication on Pure and Applied Mathematics*, vol. XXIV, pp. 807–840, 1971.

[81] J. R. Sesak and T. Coradetti, "Decentralized control of large space structures via forced singular perturbation," in *17th Aerospace Sciences Meeting*, no. 79-0195, (New Orleans, LA), 1979.

[82] P. V. Kokotović, "The joy of feedback: nonlinear and adaptive," *IEEE Control Systems Magazine*, vol. 12, no. 3, pp. 7–17, 1992.

[83] T. Kane, *Dynamics*. New York: McGraw-Hill Book Company, 1968.

[84] J. Hauser, S. Sastry, and P. Kokotović, "Nonlinear control via approximate input-output linearization: The ball and beam example," *IEEE Transactions on Automatic Control*, vol. 37, no. 3, pp. 392–398, 1992.

[85] H. Sussman and P. Kokotović, "The peaking phenomenon and the global stabilization of nonlinear systems," *IEEE Transactions on Automatic Control*, vol. 36, no. 4, pp. 424–440, 1991.

[86] T. Koo, F. Hoffman, H. Shim, and S. Sastry, "Control design and implementation of autonomous helicopter," in *Invited Session in Conference on Decision & Control*, (Tampa, Florida), 1998.

[87] R. Mahony, T. Hamel, and A. Dzul, "Hover control via lyapunov control for an autonomous model helicopter," in *Proceedings of the 38th Conference on Decision & Control*, pp. 3490–3495, 1999. Phoenix, Arizona.

[88] E. Frazzoli, M. A. Dahleh, and E. Feron, "Trajectory tracking control design for autonomous helicopters using a backstepping algorithm," in *Proceedings of the American Control Conference*, pp. 4102–4107, 2000. Chicago, Illinois.

[89] H. Zhou, H. Pei, and Y. Zhao, "Trajectory tracking control of a small unmanned helicopter using mpc and backstepping," in *Proceedings of the American Control Conference*, pp. 1583–1589, 2011. San Francisco, CA.

[90] E. N. Johnson and S. K. Kannan, "Adaptive trajectory control for autonomous helicopters," *AIAA Journal of Guidance, Control, and Dynamics*, vol. 28, no. 3, pp. 524–538, 2005.

[91] C.-T. Lee and C.-C. Tsai, "Improved nonlinear trajectory tracking using rbfnn for a robotic helicopter," *International Journal of Robust and Nonlinear Control*, vol. 20, no. 10, pp. 1079–1096, 2010.

[92] A. Gonzalez, R. Mahtani, M. Bejar, and A. Ollero, "Control and stability analysis of an autonomous helicopter," in *Proceedings of the 2004 World Automation Congress*, pp. 399–404, 2004.

[93] S. Esteban, J. Aracil, and F. Gordilli, "Lyapunov based asymptotic stability analysis of a three-time scale radio/control helicopter model," in *AIAA Atmospheric Flight Mechanics Conference and Exhibit*, (Honolulu, Hawaii), August 2008. AIAA-2008-6566.

[94] S. Devasia, "Output tracking with nonhyperbolic and near nonhyperbolic internal dynamics: Helicopter hover control," *Journal of Guidance, Control and Dynamics*, vol. 20, no. 3, pp. 573–580, 1997.

[95] R. W. Prouty, *Helicopter Performance, Stability and Control*. Boston, MA: PWS Publishers, 1986.

[96] L. Benvenuti, M. D. D. Benedetto, and J. W. Grizzle, "Approximate output tracking for nonlinear nonminimum phase systems with an application to flight control," *Journal of Nonlinear Robust Control*, vol. 4, pp. 397–414, 1994.

[97] J. Hedrick and S. Gopalswamy, "Nonlinear flight control design via sliding manifolds," *Journal of Guidance*, vol. 13, no. 5, pp. 850–858, 1990.

[98] F. J. Doyle, F. Allgöwer, and M. Morari, "A normal form approach to approximate input-output linearization for maximum phase nonlinear siso systems," *IEEE Transactions on Automatic Control*, vol. 41, no. 2, pp. 305–309, 1996.

[99] I. A. Shkolnikov and Y. B. Shtessel, "Non-minimum phase tracking in mimo systems with square input-output dynamics via dynamic sliding manifolds," *Journal of Franklin Institute*, vol. 337, no. 1, pp. 43–56, 2000.

[100] I. A. Shkolnikov and Y. B. Shtessel, "Aircraft nonminimum phase control in dynamic sliding manifolds," *Journal of Guidance, Control and Dynamics*, vol. 24, no. 3, pp. 566–572, 2001.

[101] B. Zhu, X. Wang, and K.-Y. Cai, "Approximate trajectory tracking of input-disturbed pvtol aircraft with delayed attitude measurements," *International Journal Robust Nonlinear Control*, vol. 20, no. 14, pp. 1610–1621, 2010.

[102] J. Lee and I. Ha, "Autopilot design for highly maneuvering stt missiles via singular perturbation-like technique," *IEEE Transactions on Control System Technology*, vol. 7, no. 5, pp. 527–541, 1999.

[103] J.-I. Lee and I.-J. Ha, "A novel approach to control of nonminimum-phase nonlinear systems," *IEEE Transactions on Automatic Control*, vol. 47, no. 9, pp. 1480–1486, 2002.

[104] R. Sepulchre, "Slow peaking and low-gain designs for global stabilization of nonlinear systems," *IEEE Transactions on Automatic Control*, vol. 45, no. 3, pp. 453–461, 2000.

[105] A. R. Teel, "A nonlinear small gain theorem for the analysis of control systems with saturation," *IEEE Transactions on Automatic Control*, vol. 41, no. 9, pp. 1256–1270, 1996.

[106] W. Lin and X. Li, "Synthesis of upper-triangular nonlinear systems with marginally unstable free dynamics using state-dependent saturation," *International Journal of Control*, vol. 72, no. 12, pp. 1078–1086, 1999.

[107] S. Devasia, D. Chen, and B. Paden, "Nonlinear inversion-based output tracking," *IEEE Transactions on Automatic Control*, vol. 41, no. 7, pp. 930–942, 1996.

[108] Q. Zoua and S. Devasia, "Precision preview-based stable-inversion for nonlinear nonminimum-phase systems: The vtol example," *Automatica*, vol. 43, no. 1, pp. 117–127, 2007.

[109] S. A. Al-Hiddabi, "Trajectory tracking control and maneuver regulation control for the ctol aircraft model," in *Proceedings of the 38th Conference on Decision & Control*, pp. 1958–1963, 1999. Phoenix, Arizona.

[110] A. H. Nayfeh, *Introduction to Perturbation Techniques*. New York: Wiley-Interscience, 1993.

[111] C. A. Desoer and S. M. Shahruz, "Stability of nonlinear systems with three time scales," *Circuits Systems Signal Process*, vol. 5, no. 4, pp. 449–464, 1986.

[112] J. H. Chow, "Asymptotic stability of a class of nonlinear singularly perturbed systems," *Journal of Franklin Institute*, vol. 305, no. 5, pp. 275–281, 1978.

[113] L. T. Grujic, "Uniform asymptotic stability of nonlinear singularly perturbed and large scale systems," *International Journal of Control*, vol. 33, no. 3, pp. 481–504, 1981.

[114] A. Saberi and H. Khalil, "Quadratic-type lyapunov functions for singularly perturbed systems," *IEEE Transactions on Automatic Control*, vol. 29, no. 6, pp. 542–550, 1984.

APPENDIX A

REVIEW OF GEOMETRIC SINGULAR PERTURBATION THEORY

Singular perturbation theory is a tool used to obtain the reduced-order approximations of the full-order equations of motion which are difficult to analyze. The theory is valid so long as the singular perturbation parameter remains sufficiently small and the time-scale behaviour is preserved. The Method of Matched Asymptotic Expansions[110] and its variation, the Method of Composite Expansions[110] have been the foremost methods employed to develop these reduced-order models. The alternative geometric approach describes the motion of the full-order system using the concept of invariant manifolds. Both approaches produce the exact same reduced-order models, but with different assumptions about the system. Asymptotic methods assume that the dynamical system possesses isolated roots, while the geometric approach is more general and takes into consideration multiple non-isolated roots of nonlinear systems.

To introduce the necessary concepts of geometric singular perturbation theory, consider the nonlinear autonomous open-loop dynamical system

$$\dot{\mathbf{x}} = \mathbf{f}(\mathbf{x}, \mathbf{z}) \tag{A.1a}$$

$$\epsilon\dot{\mathbf{z}} = \mathbf{l}(\mathbf{x}, \mathbf{z}) \tag{A.1b}$$

with $\mathbf{x} \in \mathbb{R}^m$ and $\mathbf{z} \in \mathbb{R}^n$. Note that the following results also apply to non-autonomous systems. The model in (A.1) can be rewritten in the fast time-scale $\tau = \frac{(t-t_0)}{\epsilon}$ as

$$\mathbf{x}' = \epsilon \mathbf{f}(\mathbf{x}, \mathbf{z}) \tag{A.2a}$$

$$\mathbf{z}' = \mathbf{l}(\mathbf{x}, \mathbf{z}) \tag{A.2b}$$

The independent variables t and τ are referred as the *slow* and the *fast* time-scales respectively and (A.1) and (A.2) (referred as the slow and the fast systems respectively) are equivalent whenever $\epsilon \neq 0$. This is not the case in the limit $\epsilon \to 0$. The fast system reduces to n dimensions with variables $\mathbf{x}$ as constant parameters producing the *reduced fast system*:

$$\mathbf{x}' = \mathbf{0} \tag{A.3a}$$

$$\mathbf{z}' = \mathbf{l}(\mathbf{x}, \mathbf{z}) \tag{A.3b}$$

On the other hand, the order of the slow system reduces to m dimensions and results in a set of differential-algebraic equations, producing the *reduced slow system*:

$$\dot{\mathbf{x}} = \mathbf{f}(\mathbf{x}, \mathbf{z}) \tag{A.4a}$$

$$\mathbf{0} = \mathbf{l}(\mathbf{x}, \mathbf{z}) \tag{A.4b}$$

The reduced slow system appears to be a locally flattened vector space of the complete slow system. Thus the set of points $(\mathbf{x}, \mathbf{z}) \in \mathbb{R}^m \times \mathbb{R}^n$ is expected to have a C^r smooth manifold $\mathcal{M}_0$ of dimension m inside the zero set of function $\mathbf{l}(.)$, provided the functions $\mathbf{f}(.)$ and $\mathbf{l}(.)$ are assumed to be C^r.

Assumption A.1. *The functions* $\mathbf{f}(\mathbf{x}, \mathbf{z})$ *and* $\mathbf{l}(\mathbf{x}, \mathbf{z})$ *are sufficiently smooth so that* C^r *with* $r \geq 1$.

The requirement to be continuous and at least once differentiable assures smooth-

ness of the manifold $\mathcal{M}_0$. The flow on this manifold evolves as

$$\dot{\mathbf{x}} = \mathbf{f}(\mathbf{x}, \mathbf{h}_0(\mathbf{x})) \tag{A.5}$$

where $\mathbf{h}_0(\mathbf{x})$ is the solution of the algebraic part in (A.4) that defines the manifold

$$\mathcal{M}_0 : \mathbf{z} = \mathbf{h}_0(\mathbf{x}); \quad \mathbf{x} \in \mathbb{R}^m, \mathbf{z} \in \mathbb{R}^n. \tag{A.6}$$

When viewed from the perspective of the reduced fast system, the manifold $\mathcal{M}_0$ is the set of fixed points $(\mathbf{x}, \mathbf{h}_0(\mathbf{x}))$ and therefore $\mathcal{M}_0$ is trivially invariant. If every fixed point $(\mathbf{x}, \mathbf{h}_0(\mathbf{x}))$ of the reduced fast system is assumed to be hyperbolic, then starting from arbitrary initial conditions the flow will exponentially fast settle down onto the manifold after which the flow evolves according to (A.5). Equivalently, the flow normal to the manifold is faster than that tangential to it. Such a manifold is said to be *normally hyperbolic*. Furthermore, a normally hyperbolic invariant manifold has local, C^r smooth, stable and unstable manifolds: $\mathcal{W}^S_{loc}(\mathcal{M}_0)$ and $\mathcal{W}^U_{loc}(\mathcal{M}_0)$. These manifolds are unions over all $(\mathbf{x})$ in $\mathcal{M}_0$ of the local stable and unstable manifolds of the reduced fast system's hyperbolic fixed points $(\mathbf{x}, \mathbf{h}_0(\mathbf{x}))$.

To show these concepts consider the following example. Let

$$\dot{x} = -x + xz \tag{A.7a}$$

$$\epsilon\dot{z} = x - z - z^3 \tag{A.7b}$$

so that the reduced slow system is

$$\dot{x} = -x + x^2 \tag{A.8a}$$

$$z = x \tag{A.8b}$$

defined for $|x| < 1$ and the reduced fast system is

$$x' = 0 \tag{A.9a}$$

$$z' = x - z - z^3 \tag{A.9b}$$

The solution of the algebraic equation in (A.8) is $z = x$ which is also the fixed point of (A.9) for small values of the slow state. The invariant manifold is given by $\mathcal{M}_0 : z = x$. The origin is the stable hyperbolic equilibrium of the reduced slow system so any trajectory starting on the manifold approaches the origin in forward time as seen in Figure A.1. Studying the reduced fast system suggests that for any point with non-zero initial condition $z(0)$, the flow approaches normal to the manifold. Intuitively one may conclude that for initial conditions not on the manifold the reduced fast system describes the transition to the manifold, after which the system evolves according to the reduced slow system (see in Figure A.2). Furthermore, since only points in the domain $|x| < 1$ approach the manifold at an exponential rate forward in time, the complete space is not the stable manifold $\mathcal{W}^S(\mathcal{M}_0)$.

For the full-order system, similar inferences can be made. The presence of ϵ in A.1 indicates that the fast variables grow relatively faster than the other states of the system. If their open-loop system is stabilizing, these states quickly settle down to their equilibrium. The other variables continue to evolve in time with the fast variables fixed by an equilibrium hypersurface. Mathematically, $\exists t^* : t^* > t_0$, after which the solutions $\mathbf{x}(t, \epsilon)$ and $\mathbf{z}(t, \epsilon)$ lie on a distinct m dimensional-invariant manifold $\mathcal{M}_\epsilon$:

$$\mathcal{M}_\epsilon : \mathbf{z} = \mathbf{h}(\mathbf{x}, \epsilon); \quad \mathbf{x} \in \mathbb{R}^m, \mathbf{z} \in \mathbb{R}^n \tag{A.10}$$

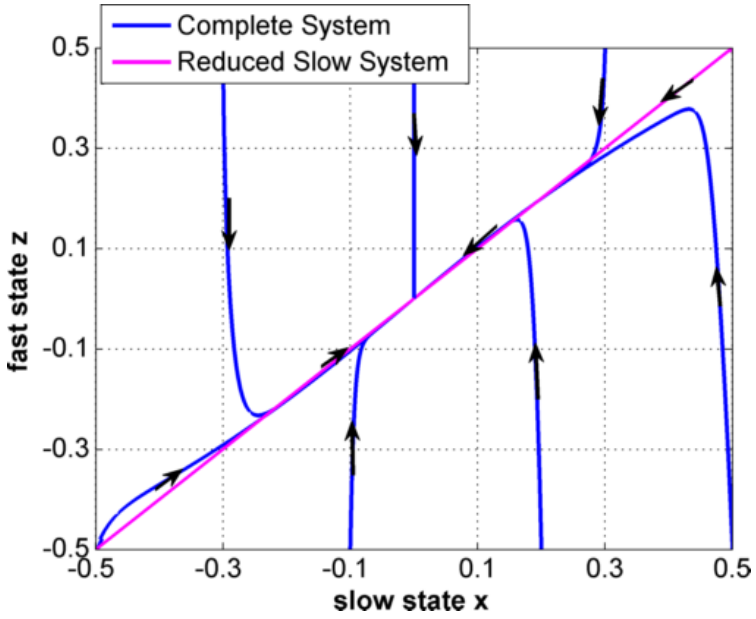

Figure A.1: Trajectories of singularly perturbed slow system given in (A.7) (blue lines) compared with reduced slow system (A.8) (pink lines)

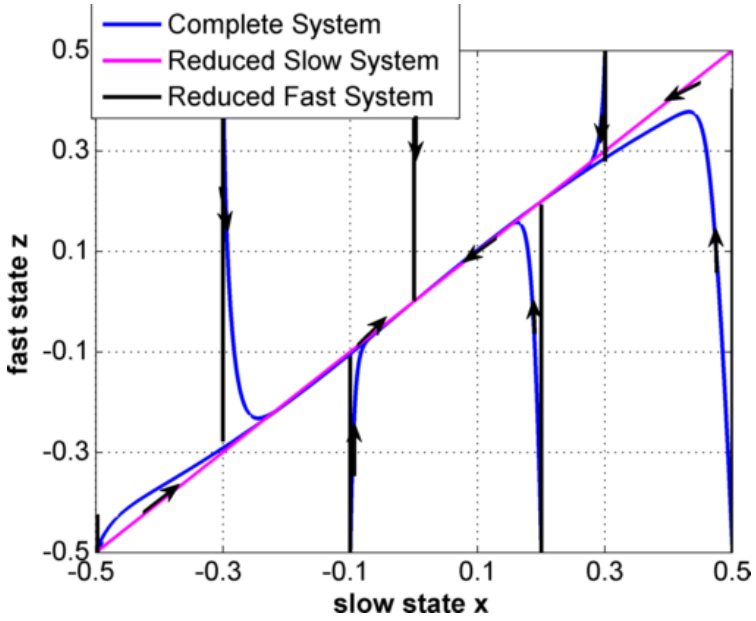

Figure A.2: Trajectories of singularly perturbed slow system given in (A.7) (blue lines) compared with reduced slow system (A.8) (pink lines) and reduced fast system (A.9) (black lines)

For the system in (A.7) the manifold varies with the singular perturbation parameter. Consider Figure A.2 to study this behaviour. To generate this figure, ϵ was chosen to be 0.05. For a fixed initial condition the flow evolves in two parts: one component along the manifold $\mathcal{M}_\epsilon$ which is governed by the reduced slow system and the other component in the normal direction whose flow is governed by the reduced fast system. Points that are already on the manifold are seen to evolve similar to the flow sketched in Figure A.1. Thus the reduced-order models provide good insight into the behaviour of the full-order system. It is apparent that if the reduced fast system were unstable then an initial condition not on the manifold would move farther away in time. Additionally, since the manifold $\mathcal{M}_0$ is defined for small values of the slow state, the dynamics of the reduced slow system closely approximate the dynamics of the complete system only for the restricted state domain. This fact is illustrated in Figure A.3.

The geometric constructs discussed above are formal statements of Fenichel's persistence theory [5] which assumes the slow system given in (A.1) satisfies

Assumption A.2. *There exists a set $\mathcal{M}_0$ that is contained in $\{(\mathbf{x}, \mathbf{z}) : \mathbf{l}(\mathbf{x}, \mathbf{z}) = \mathbf{0}\}$ such that $\mathcal{M}_0$ is a compact boundary-less manifold.*

Assumption A.3. *$\mathcal{M}_0$ is normally hyperbolic relative to the reduced fast system and in particular, it is required that for all points $\mathbf{z} \in \mathcal{M}_0$, there are k (respectively l) eigenvalues of $D_{\mathbf{z}}\mathbf{l}(0, \mathbf{z})$ with positive (respectively negative) that real parts are bounded away from zero, where $k + l = n$.*

Under these conditions the following theorem due to Fenichel [5] for compact boundary-less manifolds

Definition A.0.1. Let the slow system satisfy Assumption A.1, Assumption A.2 and Assumption A.3. If $\epsilon > 0$ is sufficiently small, then there exists a manifold $\mathcal{M}_\epsilon$

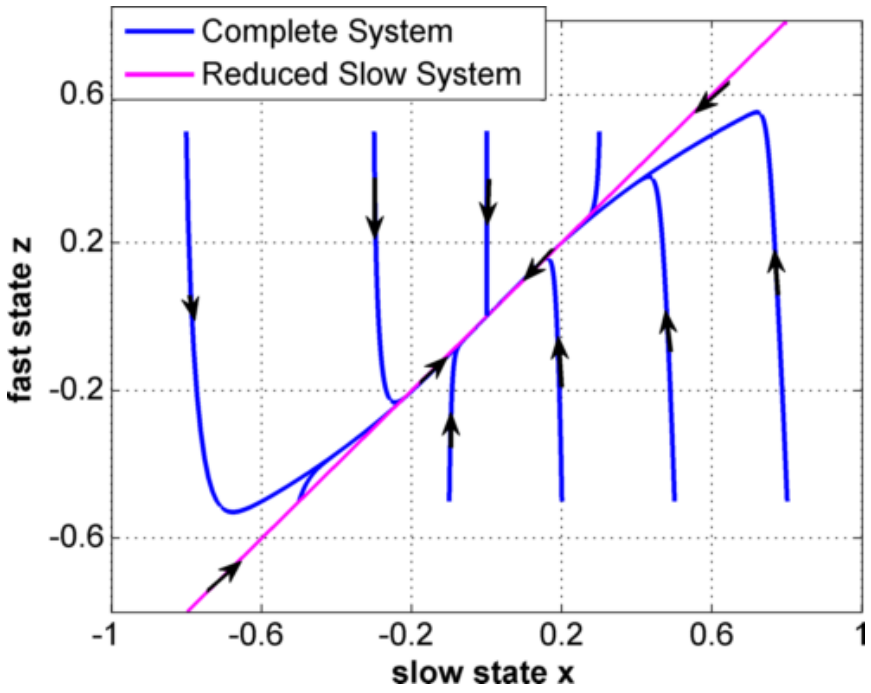

Figure A.3: Trajectories of singularly perturbed slow system given in (A.7) (blue lines) compared with reduced slow system (A.8) (pink lines) for large state values

that is C^{r-1} smooth locally invariant under the fast system and C^{r-1} $O(\epsilon)$ close to $\mathcal{M}_0$. In addition, there exist perturbed local stable and unstable manifolds of $\mathcal{M}_\epsilon$ and they are C^r $O(\epsilon)$ close, for all $r < \infty$, to their unperturbed counterparts.

The above results by Fenichel apply to more general singularly perturbed systems than the slow system (A.1) discussed in this appendix. The reader is referred to [72] for further details. Additionally, these concepts have been extended for systems with multiple inherent time scales and [80], [111] present insightful discussions.

APPENDIX B

COMPOSITE LYAPUNOV APPROACH FOR STABILITY ANALYSIS OF SINGULARLY PERTURBED SYSTEMS

Stability properties of a standard singularly perturbed system are concluded by studying the underlying geometric constructs of the reduced-order models. These conclusions provide qualitative insights regarding the nature of the response in forward time. In order to *quantify* these results, researchers use Lyapunov's direct method to determine the nature of stability (such as uniform, asymptotic or exponential) and the domains of attraction. The main idea is to use a combination of the Lyapunov functions of the lower-order models to study the stability of the complete singularly perturbed system. This composite Lyapunov function approach has been extensively used in literature to develop different sufficiency conditions for studying stability of different class of singularly perturbed systems [23], [112], [113]. This dissertation follows closely the developments for general class of nonlinear systems given in [114].

To present the necessary concepts, consider the following nonlinear standard singularly perturbed system

$$\dot{\mathbf{x}} = \mathbf{f}(\mathbf{x}, \mathbf{z}) \tag{B.1a}$$

$$\epsilon\dot{\mathbf{z}} = \mathbf{g}(\mathbf{x}, \mathbf{z}, \epsilon) \tag{B.1b}$$

where $\mathbf{x} \in D_x \subset \mathbb{R}^m$ is the vector of slow variables and $\mathbf{z} \in D_z \subset \mathbb{R}^n$ is the vector of fast variables. Assume that origin is the unique equilibrium in the domain D_x and D_z. The objective is to analyze the stability properties of the origin in

this domain. Toward this end, develop the reduced-order models for the singularly perturbed system. Following developments of geometric singular perturbation theory (see Appendix A for details) the reduced-order slow system is defined by setting $\epsilon = 0$ in (B.1) to get

$$\dot{\mathbf{x}} = \mathbf{f}(\mathbf{x}, \mathbf{z}) \tag{B.2a}$$

$$\mathbf{0} = \mathbf{g}(\mathbf{x}, \mathbf{z}, 0) \tag{B.2b}$$

Assume $\mathbf{z} = \mathbf{h}(\mathbf{x})$ is the unique solution of the algebraic equation of (B.2) in the domain D_x and D_z. Then the reduced system can be expressed as

$$\dot{\mathbf{x}} = \mathbf{f}(\mathbf{x}, \mathbf{h}(\mathbf{x})) \tag{B.3}$$

Assume that the reduced-order system (B.3) satisfies:

(i) Suppose there exists a positive-definite Lyapunov function $V(\mathbf{x})$ such that

$$\frac{\partial V}{\partial \mathbf{x}} \mathbf{f}(\mathbf{x}, \mathbf{h}(\mathbf{x})) \leq -\alpha_1 \Psi^2(\mathbf{x})$$

with $\alpha_1 > 0$ and $\Psi(\mathbf{x})$ is a continuous scalar function in the domain $\mathbf{x} \in B_x$ that satisfies $\Psi(\mathbf{0}) = 0$.

This assumption ensures that origin of the reduced slow system is asymptotically stable over the domain $\mathbf{x} \in B_x$.

The reduced fast system is represented in the time scale $\tau = \frac{t - t_0}{\epsilon}$

$$\mathbf{x}' = 0 \tag{B.4a}$$

$$\mathbf{z}' = \mathbf{g}(\mathbf{x}, \mathbf{z}, 0) \tag{B.4b}$$

Note the solution $\mathbf{z} = \mathbf{h}(\mathbf{x})$ is also the equilibrium of the reduced fast system. Define error $\tilde{\mathbf{z}} := \mathbf{z} - \mathbf{h}(\mathbf{x})$ and rewrite (B.4) in error coordinates

$$\tilde{\mathbf{z}}' = \mathbf{g}(\mathbf{x}, \tilde{\mathbf{z}} + \mathbf{h}(\mathbf{x}), 0) \tag{B.5}$$

with $\mathbf{x}$ as a parameter. Assume the origin of the reduced fast system (B.5) is asymptotically stable.

(ii) Suppose there exists a positive-definite Lyapunov function $W(\mathbf{x}, \tilde{\mathbf{z}})$ such that

$$\frac{\partial W}{\partial \tilde{\mathbf{z}}} \mathbf{g}(\mathbf{x}, \tilde{\mathbf{z}} + \mathbf{h}(\mathbf{x}), 0) \leq -\alpha_2 \Phi^2(\tilde{\mathbf{z}})$$

with $\alpha_2 > 0$ and $\Phi(\tilde{\mathbf{z}})$ is a continuous scalar function in the domain $\tilde{\mathbf{z}} \in B_z$ that satisfies $\Phi(\mathbf{0}) = 0$.

Note condition (ii) is stronger than condition (i) as origin $\tilde{\mathbf{z}} = \mathbf{0}$ is required to asymptotically stable *uniformly for all values of* $\mathbf{x}$.

The central idea in analyzing stability for (B.1) is to consider the complete singularly perturbed model as an interconnection of the reduced-order models. In order to do see this, rewrite (B.1) in error coordinates

$$\dot{\mathbf{x}} = \mathbf{f}(\mathbf{x}, \tilde{\mathbf{z}} + \mathbf{h}(\mathbf{x})) \tag{B.6a}$$

$$\epsilon \dot{\tilde{z}} = \mathbf{g}(\mathbf{x}, \tilde{\mathbf{z}} + \mathbf{h}(\mathbf{x}), \epsilon) - \epsilon \frac{\partial \mathbf{h}}{\partial \mathbf{x}} \mathbf{f}(\mathbf{x}, \tilde{\mathbf{z}} + \mathbf{h}(\mathbf{x})) \tag{B.6b}$$

Clearly the reduced-order models are systems obtained from (B.6) in the limit $\epsilon \to 0$. In order to make use of the stability properties of the reduced-order models given in conditions (i) and (ii) to analyze (B.6) a weighted sum of the Lyapunov functions is

constructed. Let this function be defined as

$$\nu(\mathbf{x},\tilde{\mathbf{z}}) = (1-d)V(\mathbf{x}) + dW(\mathbf{x},\tilde{\mathbf{z}}); \quad 0 < d < 1 \tag{B.7}$$

where V and W are as defined in conditions (i) and (ii) and d is a free parameter. The derivative of this composite Lyapunov function along (B.6) gives

$$\begin{aligned}
\dot{\nu} =&(1-d)\frac{\partial V}{\partial \mathbf{x}}\mathbf{f}(\mathbf{x},\tilde{\mathbf{z}}+\mathbf{h}(\mathbf{x})) + d\frac{\partial W}{\partial \mathbf{x}}\mathbf{f}(\mathbf{x},\tilde{\mathbf{z}}+\mathbf{h}(\mathbf{x})) \\
&+ \frac{d}{\epsilon}\frac{\partial W}{\partial \tilde{\mathbf{z}}}\Big[\mathbf{g}(\mathbf{x},\tilde{\mathbf{z}}+\mathbf{h}(\mathbf{x}),\epsilon) - \epsilon\frac{\partial \mathbf{h}}{\partial \mathbf{x}}\mathbf{f}(\mathbf{x},\tilde{\mathbf{z}}+\mathbf{h}(\mathbf{x}))\Big] \\
=&(1-d)\frac{\partial V}{\partial \mathbf{x}}\mathbf{f}(\mathbf{x},\mathbf{h}(\mathbf{x})) + \frac{d}{\epsilon}\frac{\partial W}{\partial \tilde{\mathbf{z}}}\mathbf{g}(\mathbf{x},\tilde{\mathbf{z}}+\mathbf{h}(\mathbf{x}),0) \\
&+ (1-d)\frac{\partial V}{\partial \mathbf{x}}\Big[\mathbf{f}(\mathbf{x},\tilde{\mathbf{z}}+\mathbf{h}(\mathbf{x})) - \mathbf{f}(\mathbf{x},\mathbf{h}(\mathbf{x}))\Big] \\
&+ \frac{d}{\epsilon}\frac{\partial W}{\partial \tilde{\mathbf{z}}}\Big[\mathbf{g}(\mathbf{x},\tilde{\mathbf{z}}+\mathbf{h}(\mathbf{x}),\epsilon) - \mathbf{g}(\mathbf{x},\tilde{\mathbf{z}}+\mathbf{h}(\mathbf{x}),0)\Big] \\
&+ d\Big[\frac{\partial W}{\partial \mathbf{x}} - \frac{\partial W}{\partial \tilde{\mathbf{z}}}\frac{\partial \mathbf{h}}{\partial \mathbf{x}}\Big]\mathbf{f}(\mathbf{x},\tilde{\mathbf{z}}+\mathbf{h}(\mathbf{x}))
\end{aligned} \tag{B.8}$$

The derivative of the composite Lyapunov function is represented as sum of five terms. The first two terms are the derivatives of V and W along the reduced slow and fast systems respectively. These terms are negative from conditions (i) and (ii). The third term represents the difference between the singularly perturbed model and reduced slow system. This error occurs because of arbitrary initial conditions for the fast variables which do not lie on the solution $\mathbf{h}(\mathbf{x})$. The fourth term captures the effect of neglecting the singular perturbation parameter ϵ. Finally, the fifth term in (B.8) is the difference between the fast dynamics of the complete singularly perturbed model (B.6) and the reduced fast system given in (B.5). Suppose these error terms satisfy with $\beta_i \geq 0$ and $\gamma_i \geq 0$:

(iii) $$\frac{\partial V}{\partial \mathbf{x}}\Big[\mathbf{f}(\mathbf{x},\tilde{\mathbf{z}}+\mathbf{h}(\mathbf{x})) - \mathbf{f}(\mathbf{x},\mathbf{h}(\mathbf{x}))\Big] \leq \beta_1\Psi(\mathbf{x})\Phi(\tilde{\mathbf{z}})$$

(iv) $$\frac{\partial W}{\partial \tilde{\mathbf{z}}}\Big[\mathbf{g}(\mathbf{x},\tilde{\mathbf{z}}+\mathbf{h}(\mathbf{x}),\epsilon)-\mathbf{g}(\mathbf{x},\tilde{\mathbf{z}}+\mathbf{h}(\mathbf{x}),0)\Big]\leq \epsilon\gamma_1\Phi^2(\tilde{\mathbf{z}})+\epsilon\beta_2\Psi(\mathbf{x})\Phi(\tilde{\mathbf{z}})$$

(v) $$\Big[\frac{\partial W}{\partial \mathbf{x}}-\frac{\partial W}{\partial \tilde{\mathbf{z}}}\frac{\partial \mathbf{h}}{\partial \mathbf{x}}\Big]\mathbf{f}(\mathbf{x},\tilde{\mathbf{z}}+\mathbf{h}(\mathbf{x}))\leq \beta_3\Psi(\mathbf{x})\Phi(\tilde{\mathbf{z}})+\gamma_2\Phi^2(\tilde{\mathbf{z}})$$

Using conditions (i) through (v), (B.8) becomes

$$\begin{aligned}\dot{\nu} =& -(1-d)\alpha_1\Psi^2(\mathbf{x})+\left[(1-d)\beta_1+d\beta_2+d\beta_3\right]\Psi(\mathbf{x})\Phi(\tilde{\mathbf{z}})\\ &-d\left[\frac{\alpha_2}{\epsilon}-(\gamma_1+\gamma_2)\right]\Phi^2(\tilde{\mathbf{z}})\end{aligned} \tag{B.9}$$

or rearrange to get

$$\dot{\nu}=-\Gamma^T(\mathbf{x},\tilde{\mathbf{z}})\mathbb{K}\Gamma(\mathbf{x},\tilde{\mathbf{z}}) \tag{B.10}$$

where

$$\Gamma(\mathbf{x},\tilde{\mathbf{z}})=\begin{bmatrix}\Psi(\mathbf{x})\\ \Phi(\tilde{\mathbf{z}})\end{bmatrix} \tag{B.11}$$

and

$$\mathbb{K}=\begin{bmatrix}(1-d)\alpha_1 & -\frac{1}{2}\left[(1-d)\beta_1+d\beta_2+d\beta_3\right]\\ -\frac{1}{2}\left[(1-d)\beta_1+d\beta_2+d\beta_3\right] & d\left[\frac{\alpha_2}{\epsilon}-(\gamma_1+\gamma_2)\right]\end{bmatrix} \tag{B.12}$$

The inequality (B.10) is quadratic in $\Gamma(\mathbf{x},\tilde{\mathbf{z}})$ and thus negative definite whenever the determinant of matrix $\mathbb{K}$ is positive. This implies

$$d(1-d)\alpha_1\left[\frac{\alpha_2}{\epsilon}-(\gamma_1+\gamma_2)\right]>\frac{1}{4}\left[(1-d)\beta_1+d\beta_2+d\beta_3\right]^2 \tag{B.13}$$

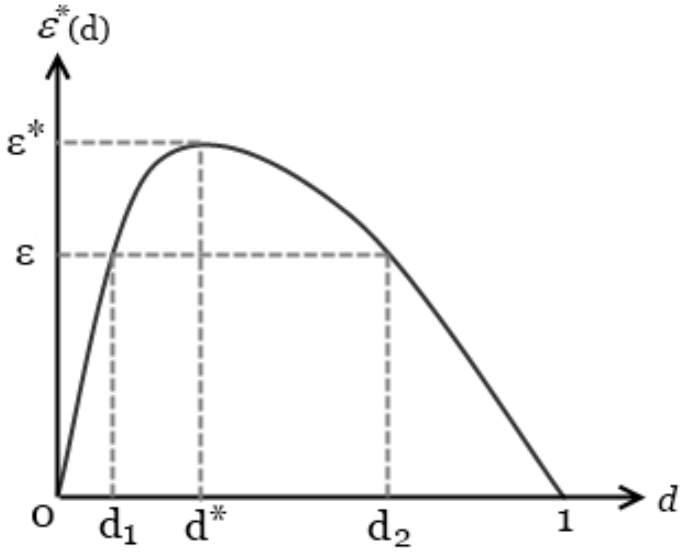

Figure B.1: Sketch of the upper-bound ϵ^* as a function of the parameter d

or whenever

$$\epsilon < \frac{\alpha_1\alpha_2}{(\gamma_1+\gamma_2)\alpha_1 + \frac{1}{4d(1-d)}\left[(1-d)\beta_1 + d\beta_2 + d\beta_3\right]^2} = \epsilon^*(d) \tag{B.14}$$

The upper bound $\epsilon^*(d)$ depends on the free parameter d and this dependence is sketched in Figure B.1. The bound takes on maximum value

$$\epsilon^* = \frac{\alpha_1\alpha_2}{\gamma_1+\gamma_2)\alpha_1 + \beta_1(\beta_2+\beta_3)} \tag{B.15}$$

for $d = \frac{\beta_1}{\beta_1+\beta_2+\beta_3}$. This condition implies that for all $\epsilon < \epsilon^*$ the origin of the singularly perturbed model (B.6) or equivalently (B.1) is *asymptotically stable* in the domain $\mathbf{x} \in D_x$ and $\mathbf{z} \in D_z$ and for $d_1 < d < d_2$.

Finally, it must be mentioned conditions (iii) through (v) are generally called the interconnection or interaction conditions. These conditions will be satisfied if the

underlying Lyapunov functions V and W are quadratic that is their partials satisfy

$$\left\| \frac{\partial V}{\partial \mathbf{x}} \right\| \leq k_1 \Psi(\mathbf{x}) \tag{B.16a}$$

$$\left\| \frac{\partial W}{\partial \mathbf{x}} \right\| \leq k_2 \Phi(\tilde{\mathbf{z}}) \tag{B.16b}$$

$$\left\| \frac{\partial W}{\partial \tilde{\mathbf{z}}} \right\| \leq k_3 \Phi(\tilde{\mathbf{z}}) \tag{B.16c}$$

Furthermore, the vector fields are Lipschitz

$$\|\mathbf{f}(\mathbf{x}, \tilde{\mathbf{z}} + \mathbf{h}(\mathbf{x})) - \mathbf{f}(\mathbf{x}, \mathbf{h}(\mathbf{x}))\| \leq k_4 \Phi(\tilde{\mathbf{z}}) \tag{B.17a}$$

$$\|\mathbf{f}(\mathbf{x}, \mathbf{h}(\mathbf{x}))\| \leq k_5 \Psi(\mathbf{x}) \tag{B.17b}$$

$$\|\mathbf{g}(\mathbf{x}, \tilde{\mathbf{z}} + \mathbf{h}(\mathbf{x}), \epsilon) - \mathbf{g}(\mathbf{x}, \tilde{\mathbf{z}} + \mathbf{h}(\mathbf{x}), 0)\| \, k_6 \Phi(\tilde{\mathbf{z}}) \tag{B.17c}$$

For an exhaustive discussion about quadratic Lyapunov functions and their use for stability, the reader is referred to texts [9] and [60].

APPENDIX C

NONLINEAR F/A-18 HORNET AIRCRAFT MODEL

The nonlinear mathematical model of the aircraft are represented by the following dynamic and kinematic equations:

$$\dot{M} = \frac{1}{mv_s}\left[T_m\eta\cos\alpha\cos\beta - \frac{1}{2}C_D\left(\alpha,q,\delta e\right)\rho {v_s}^2 M^2 S - mg\sin\gamma\right] \quad \text{(C.1a)}$$

$$\dot{\alpha} = q - \frac{1}{cos\beta}\left\{(p\cos\alpha + r sin\alpha)\, sin\beta\right\} \quad \text{(C.1b)}$$

$$- \frac{1}{\cos\beta}\Big\{\frac{1}{mv_s M}\Big[T_m\eta\sin\alpha + \frac{1}{2}C_L(\alpha,q,\delta e)\rho {v_s}^2 M^2 S$$

$$- mg\cos\mu\cos\gamma\Big]\Big\}$$

$$\dot{\beta} = \frac{1}{mv_s M}\left[-T_m\eta\cos\alpha\sin\beta + \frac{1}{2}C_Y\left(\beta,p,r,\delta e,\delta a,\delta r\right)\rho {v_s}^2 M^2 S\right. \quad \text{(C.1c)}$$

$$+ \left. mg\sin\mu\cos\gamma\right] + (p\sin\alpha - r\cos\alpha)$$

$$\dot{p} = \frac{I_y - I_z}{I_x}qr + \frac{1}{2I_x}\rho {v_s}^2 M^2 SbC_l\left(\beta,p,r,\delta e,\delta a,\delta r\right) \quad \text{(C.1d)}$$

$$\dot{q} = \frac{I_z - I_x}{I_y}pr + \frac{1}{2I_y}\rho {v_s}^2 M^2 ScC_m(\alpha,q,\delta e) \quad \text{(C.1e)}$$

$$\dot{r} = \frac{I_x - I_y}{I_z}pq + \frac{1}{2I_z}\rho {v_s}^2 M^2 SbC_n(\beta,p,r,\delta e,\delta a,\delta r) \quad \text{(C.1f)}$$

$$\dot{\phi} = p + q\sin\phi\tan\theta + r\cos\phi\tan\theta \quad \text{(C.1g)}$$

$$\dot{\theta} = q\cos\phi - r\sin\phi \quad \text{(C.1h)}$$

$$\dot{\psi} = (q\sin\phi + r\cos\phi)\sec\theta \quad \text{(C.1i)}$$

Wind axes orientation angles μ and γ are defined as follows:

$$\sin\gamma = \cos\alpha\cos\beta\sin\theta - \sin\beta\sin\phi\cos\theta - \sin\alpha\cos\beta\cos\phi\cos\theta \quad \text{(C.2a)}$$

$$\sin\mu\cos\gamma = \sin\theta\cos\alpha\sin\beta + \sin\phi\cos\theta\cos\beta - \sin\alpha\sin\beta\cos\phi\cos\theta \quad \text{(C.2b)}$$

$$\cos\mu\cos\gamma = \sin\theta\sin\alpha + \cos\alpha\cos\phi\cos\theta \quad \text{(C.2c)}$$

In order to write the equations in the form of (4.65a) and (4.65b),

$$\mathbf{f_{11}}(\mathbf{x}, M, \theta, \phi) = \begin{bmatrix} -\frac{1}{mv_s M \cos\beta}\left[\frac{1}{2}C_L(\alpha)\rho {v_s}^2 M^2 S - mg\cos\mu\cos\gamma\right] \\ \frac{1}{mv_s M}\left[\frac{1}{2}C_Y(\beta)\rho {v_s}^2 M^2 S + mg\sin\mu\cos\gamma\right] \\ 0 \end{bmatrix} \tag{C.3}$$

$$\mathbf{f_{12}}(\mathbf{x}, \theta, \phi) = \begin{bmatrix} -\cos\alpha\tan\beta & 1 & -\sin\alpha\tan\beta \\ \sin\alpha & 0 & -\cos\alpha \\ 0 & \sec\theta\sin\phi & \cos\phi\sec\theta \end{bmatrix} \tag{C.4}$$

$$\mathbf{f_2}(\mathbf{x}, M) = \begin{bmatrix} -\frac{1}{2m\cos\beta}\rho v_s MSC_{L_{\delta_e}} & 0 & 0 \\ 0 & \frac{1}{2m}C_{Y_{\delta_a}}\rho v_s MS & \frac{1}{2m}C_{Y_{\delta_r}}\rho v_s MS \\ 0 & 0 & 0 \end{bmatrix} \tag{C.5}$$

$$\mathbf{g_{11}}(\mathbf{z}) = \begin{bmatrix} \frac{I_y - I_z}{I_x}qr \\ \frac{I_z - I_x}{I_y}pr \\ \frac{I_x - I_y}{I_z}pq \end{bmatrix} \tag{C.6}$$

$$\mathbf{g_{12}}(\mathbf{x}, M) = \begin{bmatrix} \frac{1}{2I_x}\rho {v_s}^2 M^2 SbC_l(\beta) \\ \frac{1}{2I_y}\rho {v_s}^2 M^2 ScC_m(\alpha) \\ \frac{1}{2I_z}\rho {v_s}^2 M^2 SbC_n(\beta) \end{bmatrix} \tag{C.7}$$

$$\mathbf{g_{13}}(\mathbf{x}, M) = \begin{bmatrix} \frac{1}{2I_x}\rho {v_s}^2 M^2 SbC_{l_p} & 0 & \frac{1}{2I_x}\rho {v_s}^2 M^2 SbC_{l_r} \\ 0 & \frac{1}{2I_y}\rho {v_s}^2 M^2 ScC_{m_q} & 0 \\ \frac{1}{2I_z}\rho {v_s}^2 M^2 SbC_{n_p} & 0 & \frac{1}{2I_z}\rho {v_s}^2 M^2 SbC_{n_r} \end{bmatrix} \quad \text{(C.8)}$$

$$\mathbf{g_2}(\mathbf{x}, M) = \begin{bmatrix} 0 & \frac{1}{2I_x}\rho {v_s}^2 M^2 SbC_{l_{\delta_a}} & \frac{1}{2I_x}\rho {v_s}^2 M^2 SbC_{l_{\delta_r}} \\ \frac{1}{2I_y}\rho {v_s}^2 M^2 ScC_{m_{\delta_e}} & 0 & 0 \\ 0 & \frac{1}{2I_z}\rho {v_s}^2 M^2 SbC_{n_{\delta_a}} & \frac{1}{2I_z}\rho {v_s}^2 M^2 SbC_{n_{\delta_r}} \end{bmatrix} \quad \text{(C.9)}$$